



# D5.2 Impact analyses for bridges and viaducts

# Final evaluation report on bridges and viaducts; Impact Analyses

Probabilistic analyses for determining the impact on the structural safety of bridges and viaducts

**July 15, 2022** 



# **DOCUMENT INFORMATION**

#### **Authors**

NAME	ORGANISATION
B. Cerar MSc	TNO
Dr.Ir. D.L. Allaix	TNO
Dr.Ir. A.H.J.M. Vervuurt	TNO

## **Distribution**

DATE	VERSION	DISSEMINATION
March 15, 2022	Version 1	
May 27, 2022	Version 2	
July 15, 2022	Version 3	

## **Additional information**

TNO report number	TNO-2022-R10012	
Signature	Project manager	
		Dr.Ir. A.H.J.M. Vervuurt
	Research Manager	
		Ir. A.D. Pikaart



TNO report

#### TNO 2022 R10012

Ursa Major neo Truck Platooning Trial

# D5.2: Impact analyses Super EcoCombi and Truck Platooning scenarios

Final evaluation report on bridges and viaducts; Impact Analyses

Date July 15, 2022

Author(s) B. Cerar, MSc

Dr.Ir. D.L. Allaix

Dr.Ir. A.H.J.M. Vervuurt

Project name Truck Platooning Trial - Ursa Major neo 6.2
Project number 060.37962 – Ursa Major neo Truck Platooning

060.42563 - Impact measurements bridges and viaducts

All rights reserved.

No part of this publication may be reproduced and/or published by print, photoprint, microfilm or any other means without the previous written consent of TNO.

In case this report was drafted on instructions, the rights and obligations of contracting parties are subject to either the General Terms and Conditions for commissions to TNO, or the relevant agreement concluded between the contracting parties. Submitting the report for inspection to parties who have a direct interest is permitted.

© 2022 TNO

Molengraaffsingel 8 2629 JD Delft P.O. Box 155 2600 AD Delft The Netherlands

www.tno.nl

T +31 88 866 20 00



# **PREFACE**

An important aspect towards commercial introduction of new (heavy) vehicle concepts such as Truck Platooning (TP) is managing the potential impact on civil infrastructures like bridges and viaducts. At the moment there is no sufficient quantitative insight into the expected impact of such heavy vehicle concepts on the structural safety and service life of bridges and viaducts.

In this deliverable a method is presented for determining the impact on the structural safety of bridges and viaducts due to the introduction of new vehicle concepts such as TP. For that purpose a probabilistic model is developed and the results of the analyses of the load effects due to investigated new vehicle concepts are compared with the measurements performed at a steel and a concrete bridge. The two bridges that are selected are based on a risk analysis considering most of the bridges in the corridor Maasvlakte-Venlo. The risk analysis led to the understanding that vehicle concepts such as TP may have impact on these type of bridges. The measurement results are presented in deliverable D5.1A [1] and D5.1B [2] respectively. The method for determining the impact on the structural safety is applied for the SuperEco Combi (SEC) vehicle concept that is assumed to be a special type of Truck Platoon driving at a constant distance of about 2 m.

The work reported here is part of the research project 'Truck Platooning Trial' which is carried out by TNO on behalf of Rijkswaterstaat (the Ministry of Infrastructure and Water Management, RWS), as part of the Ursa Major neo program. It includes the first real real-life truck platooning trial on Dutch public roads, investigating the impact on motorway traffic, and assessing the expected impact on structural safety and service life of bridges and viaducts.



# **TABLE OF CONTENTS**

Do	ocument Information	2
Pr	eface	4
Та	ble of Contents	5
1	Introduction	8
	1.1 Background	8
	1.2 Approach	8
2	Methodology of impact analyses	11
	2.1 Safety requirements	11
	2.2 Research questions	12
	2.3 Calculation methodology	12
	2.3.1 Overview	12
	2.3.2 Evaluation of the structural reliability on annual basis	13
	2.3.3 Measuring impact	14
	2.4 Impact analysis for ULS conditions	15
	2.4.1 Overview of limit state functions and stochastic variables	
	2.4.2 Assessment of the resistance	16
	2.5 Impact analysis for FLS conditions	
	2.5.1 Overview of limit state functions and stochastic variables	
	2.5.2 Calibration of load spectrum	18
3	Scenarios for safety assessments	20
	3.1 Load conditions	20
	3.2 Structural behavior	20
	3.2.1 Introduction	20
	3.2.2 Bridge characteristics	21
	3.3 Current vehicle and traffic characteristics	23
	3.3.1 Introduction	23
	3.3.2 Current traffic composition	24
	3.3.3 Inter-vehicle distance	28
	3.4 Starting points for the impact analyses	28
	3.4.1 Introduction	28
	3.4.2 Inter-vehicle distance	28
	3.4.3 Number of TP and SEC vehicles	29
	3.4.4 Vehicles weight and axle loads	31
	3.5 Other assumptions	31
	3.6 Assessment scenarios	32
4	Assessment of traffic load effects in bridges	34



	4.1	Introdu	uction	34
	4.2	Traffic	load effects in bridges for ULS verification	35
		4.2.1	Assessment of load effects induced by regular vehicles (reference scenario)	35
		4.2.2	Assessment of load effects induced by SEC vehicles	36
		4.2.3	Assessment of load effects induced by Truck Platooning	41
		4.2.4	Comparison between the traffic load effects induced by regular vehicles, vehicles, Truck Platooning and LM1 of NEN-EN1991-2	
		4.2.5	Comparison between the impact of SEC vehicles based on simulation and measurement campaigns on the Moerdijk bridge and Geldrop viaduct	
	4.3	Traffic	load effects in bridges for FLS verification	48
		4.3.1	Design S-N curve according to NEN-EN 1993 1-9	48
		4.3.2	Assessment of the stress histogram for traffic with regular vehicles	49
		4.3.3	Assessment of the stress histogram for traffic with SEC vehicles	50
		4.3.4	Comparison of fatigue damage SEC versus 2xT11O3	51
5	Rei	nforce	d concrete bridge - ULS conditions	54
	5.1	Introdu	uction	54
	5.2	Calcul	ation methodology	54
		5.2.1	Limit state function	54
		5.2.2	Stochastic variables	55
	5.3	Result	S	59
		5.3.1	Calculations based on the calibrated resistance	59
		5.3.2	Calculations based on the resistance calculated with the old Dutch standards .	60
6	Ste	el brid	ge - ULS conditions	63
	6.1	Introdu	uction	63
	6.2	Calcul	ation methodology	63
			Limit state function	
		6.2.2	Stochastic variables	63
	6.3	Result	S	64
7	Ste	el brid	ge - fatigue limit state (FLS)	67
	7.1	Introdu	uction	67
			ation methodology	
			Limit state function	
			Stochastic variables	
	7.3		S	
8	Coi	nclusio	ons	71
_				



Appendix 1	WIM characteristics	77
Appendix 1A	WIM-NL vehicle subclasses	77
	Traffic composition	
Appendix 1C	Distribution of vehicle and axle weight	80
Appendix 2	Procedure for Simulating traffic load effects in bridges	85
Appendix 2A	Filtering of the WIM database	85
Appendix 2B	Generation of a stream of axles from the WIM database	85
Appendix 2C	Numerical simulation of traffic load effects	86
Appendix 3	Generation of WIM databases including SEC vehicles AND TP	87
Appendix 3A		
Appendix 3B	Generation of SEC vehicles from T11O3 vehicles	90
Appendix 3C	Generation of Truck Platoons from T11O3 vehicles	94
Appendix 4	Traffic load effects in bridges	95
Appendix 4A	Traffic load effects induced by regular traffic	
Appendix 4B	Traffic load effects induced by SEC vehicles	99
Appendix 4D	Comparison between the load effects induced by individual SEC vehicles	107
Appendix 5	Assessment of design load effects based on Load Model 1 of NEN-EN 199	)1-2
	for new and existing structures and old Dutch standards	111
Appendix 5A	Design traffic load effects according to NEN-EN 1991-2 and NEN 8701	111
Appendix 5B	Traffic load effects based on the old Dutch standards	114
Appendix 6	Results concrete bridge (ULS conditions)	118
Appendix 6A	Calibrated resistance and reliability indices	118
Appendix 6B	Comparison between the reference, full replacement and gradual replacement	
	scenarios	125
Appendix 6C		
	scenarios based on old Dutch standards	157
Appendix 7	Results steel bridge (ULS conditions)	189
Appendix 8	Results steel bridge (Fatigue limit state)	192



# 1 INTRODUCTION

## 1.1 Background

In Europe, the developments in robotization for transport and mobility are directed towards connected and cooperative automation as well as improving sustainability. The same developments can be observed in the Netherlands. There are many potential technologies associated with automation and robotization in transport and logistics. For CO2-reduction Truck Platooning (TP)¹ is considered a high potential scenario in cooperative automation in transport and logistics. With truck platooning heavy-duty trucks drive in convoy formation with short time-gaps between them. An important aspect towards commercial introduction of truck platooning is managing the potential impact on civil infrastructure like bridges and viaducts. At the moment Rijkswaterstaat lacks sufficient quantitative insight into the expected impact of truck platooning (and other new heavy vehicle concepts) on the structural safety and service life of bridges and viaducts. It is therefore important to gain this insight, so that the road authority is able to formulate mitigation strategies (if considered necessary).

Rijkswaterstaat is active within the Ursa Major neo (UMneo) program together with other road operators from Germany, Austria and Italy (<a href="www.its-platform.eu">www.its-platform.eu</a>). Under contract with RWS, TNO is performing a research project in which different aspects are studied, such as the impact on traffic safety, fuel consumption and emissions, traffic throughput, human driver acceptance and C-ITS communication. In this research report, the impact on the structural safety of bridges and viaducts is studied.

# 1.2 Approach

In this report the impact of new vehicle concepts such as Truck Platooning (TP)<sup>1</sup> and Super EcoCombi (SEC)<sup>2</sup> on the structural safety of bridges and viaducts is investigated. The impact is calculated as the effect on the calculated normative service life (in years) of bridges and viaducts.

In the approach of the project different steps can be distinguished. These steps are presented schematically in Figure 1 and explained in detail thereafter.

In this report Truck Platooning and the corresponding abbreviation TP are used for indicating automated truck platooning where multiple vehicles drive in a convoy while they are connected using connectivity technology and automated driving support systems

The SuperEco Combi may be considered as a special type of platoon where two truck trailer combinations are combined to one single vehicle. For this reason the intervehicle distance is constant and rather small compared to a truck platoon. Therefore SEC may be considered as conservative to TP.



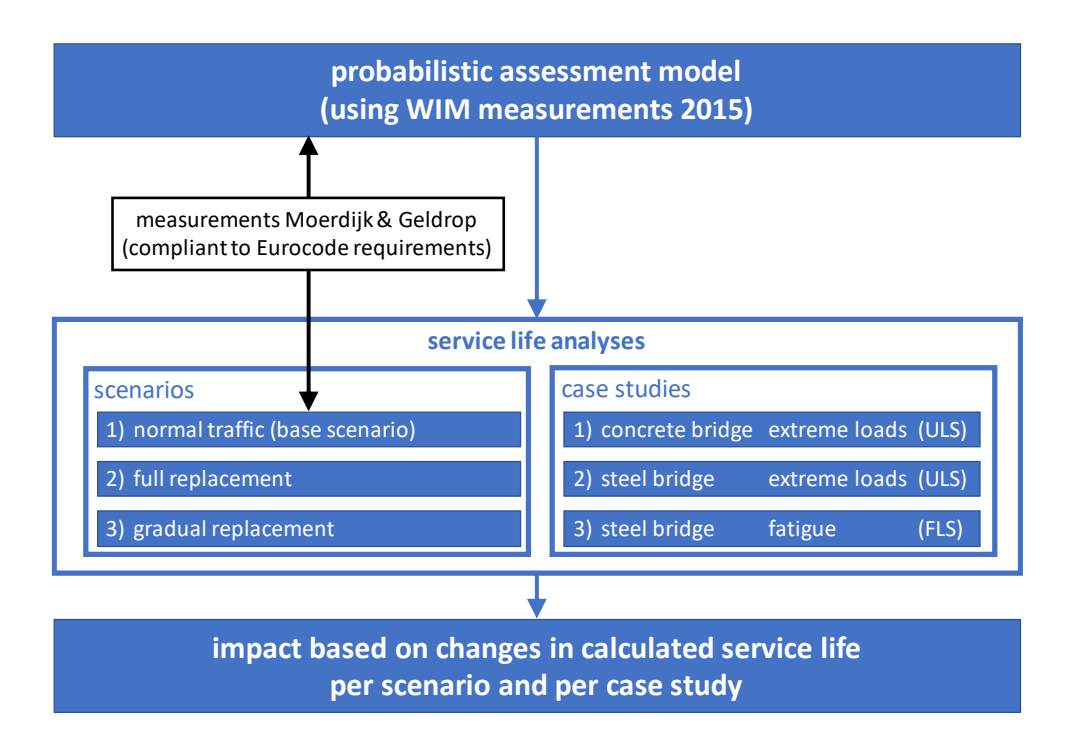


Figure 1: Graphical presentation of the adopted approach for determining the impact on bridges and viaducts

A reliability-based methodology accounting for the uncertainties of loads and resistance governing the safety of bridges and viaducts is developed to assess the structural reliability in each year of the normative service life. For this purpose, a probabilistic assessment of the traffic effects in bridges is performed, as explained in chapter 4, by using simplified models of the structural behaviour and Weigh in Motion (WIM) data. For the load characteristics of the normal traffic the assessment model uses Motion (WIM) measurements of 2015 as provided by Rijkswaterstaat.

The results of the assessment of the traffic load effects induced by a truck platoon are compared with the measurements at the following two typical bridges in the by Rijkswaterstaat and TNO selected Rotterdam-Venlo corridor (A15-A16-A58-A2-A67 in the Dutch highway network):

- a steel bridge consisting of 10 separate spans, each with a length of about 100 m (Moerdijk bridge, A16).
- a concrete box girder viaduct near Geldrop with three continuous spans of 22 m, 36 m and
   22 m respectively

Details of the bridges considered and the measuring results are reported in [1] and [2]. Based on two trials in 2021, the effect of a single truck platoon on the structural behaviour of the bridges was studied. These results are reported in [1] and [2] as well. For 2022, a pilot trial of a number of TP compositions is being prepared for the same corridor.

 The model is applied to for different scenarios comprising the introduction of the vehicle concept considered. As mentioned before, for this purpose, the SEC vehicle scenario is considered as a worst case truck platoon since the intervehicle distance is quite small (constant axle distance between the first and the second trailer).



In total three different scenarios were studied. The starting points for the scenarios studied are given in chapter 3. The three scenarios are:

- The base scenario, that includes the current (normal) traffic (based on the WIM measurements of 2015). No multi-trailer vehicles are included
- 2) A full replacement scenario in which couples of specific 5-axle truck trailer combinations are replaced by a single vehicle comprising multiple trailers and where replacement at t=0 is assumed. This is a conservative approach when determining the impact on the structural reliability.
- 3) A gradual replacement scenario in which a limited number of the couples of truck trailer combinations from the second scenario is replaced by a single multi-trailer vehicle. Moreover, it is assumed that the replacement will take place gradually in time.
- Based on the expected failure mechanisms for steel and concrete bridges and viaducts, the
  normative service life is calculated for the selected scenarios and for three case studies,
  representing typical bridge structures and design or assessment situations in the Netherlands.
  The cases are according to the current codes for design and assessment and comprise bending
  and shear under extreme and frequent load conditions.
  - 1) Extreme load (ultimate limit state) conditions for concrete bridges
  - 2) Extreme load (ultimate limit state) conditions for steel bridges
  - Fatigue load conditions (FLS) for steel bridges.

The results of the analyses are presented in chapter 5, 6 and 7 respectively and give the calculated normative service life (in years)

• Finally, the impact of the introduction of the new vehicle concept is determined by comparing the calculated normative service life for the base scenario to the calculated service life for the two replacement scenarios. These results are summarized in the conclusions (chapter 8).



# 2 METHODOLOGY OF IMPACT ANALYSES

## 2.1 Safety requirements

The requirements for the structural safety of bridges and viaducts are defined in the Dutch Building Decree, which is a governmental decree of the Dutch Housing Act. Moreover, in the Building Decree a reference to NEN-EN 1990 (Eurocode: basis of structural design) is made for new structures and additionally to NEN 8700 for existing structures.

In these standards it is stated that a structure must satisfy a certain level of safety, denoted as the reliability index ( $\beta$ ) and depends, among others, on the consequences of structural failure (Consequence Classes). The reliability index is a measure of the probability of failure during the (remaining) service life (or reference period) of the structure<sup>3</sup>. In order to determine the probability of failure all traffic that is to be expected during the service life must be taken into account, including possible changes in loads due to trends with respect to the amount of traffic and traffic loads (see section 3.1).

It may be obvious that for predicting the probability of failure of a structure during its service life many uncertainties must be taken into account. Both the strength of a structure and the effect of traffic loading on the structure have a stochastic nature. This is shown graphically in Figure 2. In the figure on the horizontal axes the service life is given and the structural strength (R) and the effect of loading on the structure (solicitation S) is given on the vertical axis. Both R and S are uncertain and vary in time. The structure fails when the load effect exceeds the structural strength (S>R). The assumed changes in the service life due to the introduction of new vehicle concepts are indicated in the figure in grey. In Figure 2 the required reliability is indicated as  $\beta_{target}$  and the corresponding probability of failure is denoted as  $P_{f,target}(\beta_{target})$ .

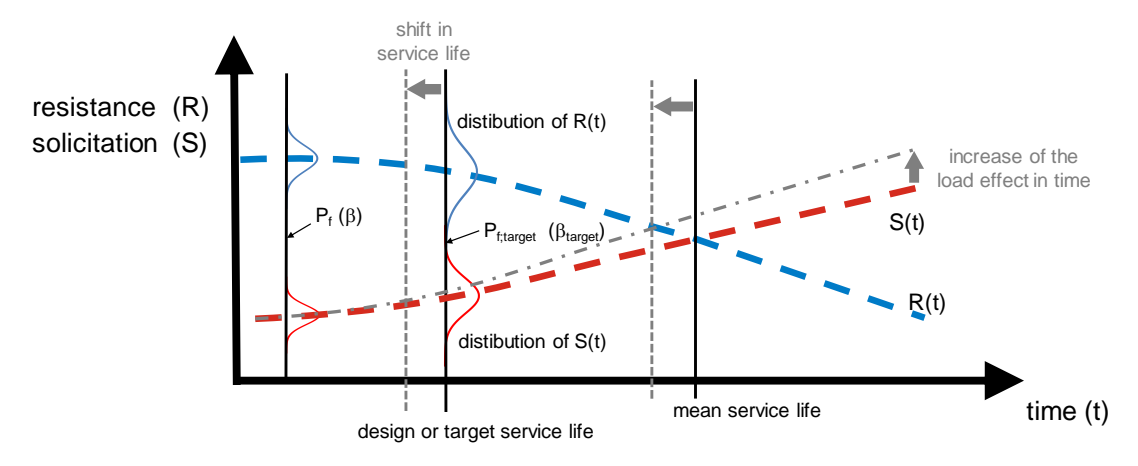


Figure 2: Schematization of the failure probability (related to  $\beta$ ) in time, depending on the structural strength (R) and the load effect on the structure (S).

\_

Failure occurs when the structures is not able to fulfil the functions for which it was designed. For the ultimate limit state this is generally associated with structural collapse



For structures in the Dutch road network Reliability Class 3 must be assumed when determining the impact of new vehicle concepts (e.g. TP and SEC) on the structural safety of bridges and viaducts. The Dutch National Annex of EN 1990 additionally requires that for Reliability Class 3 a minimum reference period of 100 years for the design of bridges is adopted. Consequently, according to NEN-EN 1990 [3], the target cumulative reliability level  $\beta_{target}$  = 4.3 applies for structures that are designed (new structures). The reliability requirements for existing structures are taken from RBK (Richtlijnen Beoordeling Kunstwerken [4]), which proposes that the minimum cumulative reliability level  $\beta_{target}$  = 3.3 is selected with a reference period of 30 years for the "utilisation level" ("gebruiksniveau" in Dutch).

#### 2.2 Research questions

The goal of this study is to evaluate the impact of truck platooning (TP) on the structural safety of new and existing steel and concrete bridges with respect to the Ultimate Limit State (ULS) and Fatigue Limit State FLS conditions. The approach presented in this chapter aims to answer the following questions (research question 1-3):

- given that new structures are designed for a design service life of 100 years and the design load models cover the current loading conditions and future trends, would TP lead to a shorter design life?
- 2. if an existing structure fulfils exactly the reliability requirements of the current standards under normal traffic conditions, would TP lead to a shorter remaining life?
- 3. given that existing structures have been designed according to old standards, what would be the effect of TP on the change in time of safety compared to regular traffic?

In this chapter the calculation procedure of the probabilistic impact analyses used to address the questions listed above is presented. The term probabilistic expresses the fact that the resistance and the load effects in structures resulting from the self-weight of the structure and traffic are uncertain parameters and described with probabilistic distributions instead of deterministic point-values.

#### 2.3 Calculation methodology

#### 2.3.1 Overview

To answer the questions listed in the introduction to this chapter, a reliability-based approach is resorted to for the following reasons:

- the design load model given in the standards, such as NEN-EN 1991-2 with the adjustment factors for existing structures defined in NEN 8701, are calibrated with respect to normal traffic conditions and do not account for innovative transport concepts
- the semi-probabilistic approach implemented in the current standards for design and assessment
  allows to check the compliance of structures with the safety requirements given in the standards
  for the specified reference periods (100 years for new structures and 30 years for existing
  structures), but it is not suited for assessing at which point in time in the future structures are not
  safe enough.



In order to overcome these limitations of the current semi-probabilistic approach to structural safety, the reliability-based approach presented in this report consists of the following steps:

- 1) assessment of the probabilistic model of the traffic load effects in bridges: the probability distributions of the traffic load effects due to regular traffic and due to new heavy vehicle concepts are estimated based on simulations. This is addressed in chapter 4 of this report.
- 2) **evaluation of the structural reliability on annual basis**: the reliability index and the failure probability are evaluated in each year of the assumed design service life (new structures) and residual service life (existing structures) in case of regular traffic and new heavy vehicle concepts.
- 3) calculation of the impact of TP: the impact analysis is based on evaluating the difference in terms of service life of bridges and viaducts and in terms of development in time of the reliability index between regular traffic and the TP concept considered\.

Aiming to simplify the problem, a generic approach based on the following assumptions is taken:

- the investigation focuses only on relevant and recurrent bridge typologies of the Dutch highway network rather than on real specific bridges. Therefore, idealized structures, such as the simplysupported and continuous bridges, are considered.
- the resistance of the structure (ULS case studies, chapter 5 and 6) and the stress histogram (FLS case study, chapter 7) are calibrated such that the structures fulfil exactly reliability requirements of the current Dutch standards for the design of new structures and the assessment of existing structures
- furthermore, for existing concrete structures an additional analysis is performed where the resistance is determined based on the load models and design rules of the old Dutch standards.

#### 2.3.2 Evaluation of the structural reliability on annual basis

Structural reliability is understood as the probability that a structure will not exceed specified limit states (ULS and FLS in this investigation) during a specified reference period. In practice, structural reliability is quantified by the probability of the complementary event, i.e. the probability of failure. In the simple case of two random variables R and E representing, respectively, the resistance and the load effect of a cross-section of a structure, the failure probability is defined as:

$$P_f = P(R < E) \tag{2.1}$$

The resistance R and the load effect E are generally functions of time. Therefore, the period of time to which the failure probability refers has to be defined. The choice of the period of time is of relevance for two aspects. The first aspect is related to the statistical assessment of variable loads when investigating ULS conditions, since the extreme loads in the chosen period of time are generally considered in the analysis. The second aspect concerns the verification against reliability requirements, which is performed by comparing the estimated probability of failure (or reliability index) with the target values given in the standards which refer to a period of time, called reference period T<sub>ref</sub>. As an example, target reliability levels for ULS conditions are given in EN 1990 [3] for the reference periods of 1 year and 50 years and in NEN 8700 for a reference period of 15 and 30 years.



A reliability assessment performed for a reference period longer than 1 year enables only to draw conclusions about the compliance of the structure with the target reliability levels for the specified reference period. If the probability of failure in the reference period is larger than the target value, it is not possible to assess in which year the structure does not fulfil anymore the requirements of the standards. For this purpose, it is necessary to perform the reliability assessment on annual basis (e.g. with the 1 year reference period).

The failure probability in year *i* of the design lifetime of new structures is defined as the probability that the structure fails in that year and has survived until the previous year:

$$P_{\text{fannual,i}} = P(F_i \cap S_1 \cap S_2 \cap ... \cap S_{i-1})$$
(2.2)

where:

- F<sub>i</sub> denotes the failure event in year i
- $S_1$ ,  $S_2$  and  $S_{i-1}$  represent the survival events from year 1 to year i-1

The annual failure probability is estimated in this report as the difference between the failure probabilities  $P[failure\ in\ (0,\ t_i)]$  and  $P[failure\ in\ (0,\ t_{i-1})]$ . These two probabilities are referred to in the following as "cumulative" failure probabilities:

$$P_{f,\text{annual,i}} = P_{f[0,i]} - P_{f[0,i-1]}$$
(2.3)

where:

- $P_{f[0,i]}$  is the cumulative probability of failure up to year i
- $P_{f[0,i-1]}$  is the cumulative probability of failure up to year *i-1*

The annual reliability index  $\beta_{annual,i}$  for year i is then calculated as follows:

$$\beta_{annual,i} = -\Phi^{-1}(P_{f,annual,i}) \tag{2.4}$$

where  $\Phi^{-1}$  is the inverse standard normal distribution function.

The failure probability for a reference period  $T_{ref}$  longer than 1 year can be determined as follows based on the annual failure probabilities in each year of the reference period:

$$P_{f,T_{ref}} = \sum_{i=1}^{n} P_{f,\text{annual,i}}$$
 (2.5)

where n is the number of years in T<sub>ref</sub>.

The calculations of the reliability index are based on the First Order Reliability Method (FORM) as implemented in the TNO Prob2B tool [5].

#### 2.3.3 Measuring impact

Three traffic scenarios are considered in the present report: normal traffic, gradual replacement of multiple truck trailer combinations by a single vehicle and full replacement. The normal traffic is the reference scenario, i.e. the current traffic conditions, to which the replacement scenario are



compared in order to assess the impact of TP. For further description of traffic scenarios considered see chapter 4.

Impact is measured in terms of the decrease in normative service life. Consider a fictitious example, as shown in Figure 3. This figure shows annual reliability index ( $\beta_{annual}$ ), which was calculated for a particular structure. The annual reliability index was calculated for normal traffic (blue line) and full replacement (red line) scenarios, including the trends in the traffic loads leading to a reduction of the reliability index over time. The value of the annual reliability index for the normal traffic scenario in the last year of the reference period is denoted as  $\beta_{annual,ref}$ . The scenario with full replacement leads to lower annual reliability levels over the considered time period in comparison to the normal traffic scenario, meaning that the failure probability is higher. In the full replacement scenario, the annual reliability index reaches  $\beta_{annual,ref}$  at time  $T_{end-of-service life with SEC}$ , meaning that the annual reliability is reached earlier compared to the normal traffic scenario. Consequently, the impact of full replacement is estimated as the time difference  $T_{ref}$  -  $T_{end-of-service life with SEC}$ .

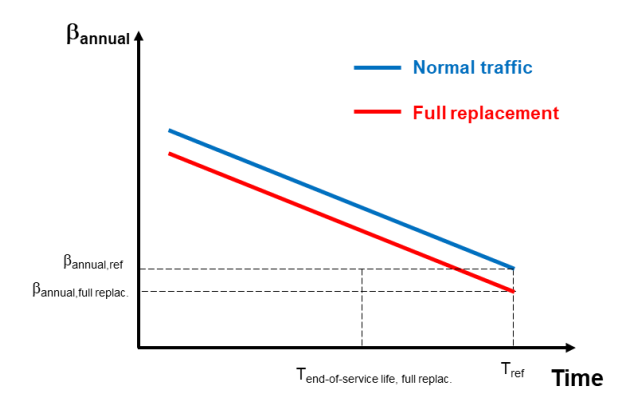


Figure 3: An Illustration of the difference in annual reliability index values between the normal traffic (blue) and full replacement scenario (red).

#### 2.4 Impact analysis for ULS conditions

#### 2.4.1 Overview of limit state functions and stochastic variables

The reliability assessment based on the partial factor method under ULS conditions is performed by using the following inequality:

$$R_d > E_d \tag{2.6}$$

where:

- R<sub>d</sub> is the design value of the resistance R
- E<sub>d</sub> is the design value of the load effect E

The following limit-state function, that describes the threshold between safe and unsafe state of the structure and is associated with Eq. (2.6), is used to calculate the probability of failure (and the corresponding reliability index):



$$Z = R - E = R - (\theta_G \cdot G + \theta_{trend} \cdot \theta_{spat.var.} \cdot \theta_{DAF} \cdot \theta_T \cdot T)$$
 (2.7)

where the random variables:

- R is the random variable representing resistance of the structure to the load effect E;
- *G* is the random variable representing permanent load effect acting on the structure;
- T is the random variable representing traffic load effect acting on the structure;
- $\theta_G$  is the random variable representing model uncertainty, reflecting the uncertainty in the structural model used to estimate evaluate the load effect G induced by permanent actions:
- $\theta_{trend}$  is the random variable representing uncertainty about the development of future traffic trends:
- $\theta_{\text{spat.var}}$  is the random variable representing uncertainty about spatial variability of traffic loads in the Netherlands:
- $\theta_{DAF}$  is the random variable representing uncertainty regarding the dynamic interaction between the bridge and the vehicles;
- $\theta_T$  is the random variable representing the uncertainty of the structural model (influence lines) used to evaluate the traffic load effect T.

The probabilistic model and the description of random variables used in the ULS case studies are further elaborated in section 5.2.

#### 2.4.2 Assessment of the resistance

In the ULS case studies, the resistance R is considered to be a random variable. The distribution function and the coefficient of variation are chosen in agreement with previous studies, as explained in section 5.2. The mean value  $\mu_R$  of the resistance R is determined as follows:

- new structures: the mean value μ<sub>R</sub> is calibrated to fulfil the safety requirements for new structures (target reliability level btarget equal to 4.3 for the reference period of 100 years)
- existing structures:
  - $_{\odot}$  the mean value  $\mu_R$  is calibrated to fulfil the safety requirements for the assessment of existing structures with respect to the assessment level "gebruiksniveau" (target reliability level  $\beta_{target}$  equal to 3.3 for the reference period of 30 years)
  - $_{\odot}$  for concrete structures only, the mean value  $\mu_R$  is also derived from the design equations of the old Dutch standards VOSB 1938 GBV 1950, VOSB 1963 GBV 1962, VB 1974 and VBB 1995

#### 2.4.2.1 Calibration of the resistance to fulfil exactly the reliability requirements of the standards

The mean value of the resistance is calculated so that cumulative reliability index  $\beta$  in the reference traffic scenario (normal traffic), representing the current traffic conditions, is approximately equal to the target reliability  $\beta_{\text{target}}$  for given a limit state function Z:

$$\beta(\mu_R) \cong \beta_{target}$$
 (2.8)



The calibration procedure is a root-finding problem, which is iteratively solved in this project by using the bisection method.

# 2.4.2.2 Assessment of the resistance based on the old Dutch standards for design of concrete bridges

The standards VOSB 1938 – GBV 1950, VOSB 1963 – GBV 1962, VB 1974 and VBB 1995 are based on the concept of global safety factor relating the characteristic value of the resistance to the characteristic value of the load effects as follows:

$$\gamma_{global} = \frac{R_k}{E_k} = \frac{R_k}{G_k + T_k} \tag{2.9}$$

where:

- R<sub>k</sub> is the characteristic value (5% fractile) of the resistance
- E<sub>k</sub> is the characteristic value of the load effects
- Gk is the characteristic value of the load effects due to permanent actions
- $\bullet$   $T_k$  is the characteristic value of the traffic load effects

The mean value  $\mu_R$  of the resistance is determined as follows:

- the characteristic value T<sub>k</sub> of the traffic load effects, including the amplification and the reduction factors is calculated using the load model and rules of the standard (the results are listed in Appendix 5B)
- the characteristic value  $G_k$  of the load effects due to permanent actions is determined from the ratio between the traffic load effects and the total load effects:

$$\chi = \frac{T_k}{G_k + T_k} \tag{2.10}$$

where the following values are assumed [6]:

 $\circ$  L = 20 m:  $\chi = 0.55$   $\circ$  L = 50 m:  $\chi = 0.50$   $\circ$  L = 100 m:  $\chi = 0.42$  $\circ$  L = 200 m:  $\chi = 0.25$ 

The  $\chi$  value is obtained by interpolation for other length of the influence line.

- the characteristic value  $R_k$  of the resistance is determined from Eq.(2.9) based on the value of the global factor  $\gamma_{alobal}$  given in the standard
- the mean value  $\mu_R$  of the resistance is determined assuming that the resistance is modelled by a lognormal distribution with coefficient of variation  $V_R = 10\%$ :

$$\mu_R = R_k \cdot exp(1.645 \cdot V_R) \tag{2.11}$$



# 2.5 Impact analysis for FLS conditions

#### 2.5.1 Overview of limit state functions and stochastic variables

The assessment of the structural reliability based on the partial factor method under FLS conditions is performed by using the following inequality:

$$\sum_{i=1}^{m} \frac{n_i}{5 \cdot 10^6 \cdot \max\left[\left(\frac{\Delta \sigma_D}{\gamma_{M,fat} \cdot \gamma_{F,fat} \cdot \Delta \sigma_i}\right)^{m_1}, \left(\frac{\Delta \sigma_D}{\gamma_{M,fat} \cdot \gamma_{F,fat} \cdot \Delta \sigma_i}\right)^{m_2}\right]} \le 1$$
(2.12)

#### where:

- m is the number of stress range bins of the stress spectrum with  $\Delta \sigma_i$  larger than the cut-off stress  $\sigma_L = 32.4$  MPa;
- $\Delta \sigma_i$  is the stress range of bin *i* in the stress histogram;
- $n_i$  is the number of stress reversals (cycles) in stress range bin  $l_i$
- $m_1 = 3$  is a constant representing the slope of the first branch of the S-N curve in the logarithmic scale;
- $m_2 = 5$  is a constant representing the slope of the second branch of the S-N curve in log-log scale:
- $\Delta\sigma_D = 59$  MPa is a constant representing the stress range of the knee-point of the S-N curve (according to NEN-EN 1993-1-9 this corresponds to  $0.737 \cdot \Delta\sigma_C$  (80 MPa);
- $\gamma_{M,fat}$  (=1.35) is the partial factor for fatigue strength;
- $\gamma_{F,fat}$  (=1.00) is the partial factor on the load side.

The following limit-state function associated with Eq. (2.12) is used to calculate the probability of failure and the corresponding reliability index:

$$Z = X_d - \sum_{i=1}^m \frac{n_i}{5 \cdot 10^{(6+X_{SN})} \cdot \max\left[\left(\frac{\Delta \sigma_D}{X_U \cdot \Delta \sigma_i}\right)^{m_1}, \left(\frac{\Delta \sigma_D}{X_U \cdot \Delta \sigma_i}\right)^{m_2}\right]} \le 1$$
(2.13)

#### where:

- ullet  $X_d$  is the random variable representing the uncertainty of the Miner's rule;
- $X_{SN}$  is the random variable representing the uncertainty of the  $log_{10}(N)$  of the S-N curve;
- $X_U$  is the random variable representing the uncertainty load effect.

The probabilistic model and the description of random variables are further elaborated in sections 7.2.1 and 7.2.2, respectively.

#### 2.5.2 Calibration of load spectrum

In the fatigue case study, a similar calibration approach as for ULS case studies is taken, except the calibrated parameter  $\alpha$  is now a multiplicative, deterministic factor, which is used to scale the values of bins  $\Delta \sigma_i$  of the stress histogram in order obtain accumulated fatigue damage that leads to the



prescribed target reliability  $\beta_{target}$  over the prescribed reference period. The following limit-state function is used for calibration:

$$Z = X_d - N_{years} \sum_{i=1}^{m} \frac{n_i}{5 \cdot 10^{(6+X_{SN})} \cdot \max\left[\left(\frac{\Delta \sigma_D}{X_U \cdot (\alpha \cdot \Delta \sigma_i)}\right)^{m_1}, \left(\frac{\Delta \sigma_D}{X_U \cdot (\alpha \cdot \Delta \sigma_i)}\right)^{m_2}\right]} \le 1$$
(2.14)

#### where:

- N<sub>years</sub> is the reference period being considered;
- $\alpha$  is a multiplicative calibration factor to be calibrated to meet the reliability requirements.



# 3 SCENARIOS FOR SAFETY ASSESSMENTS

#### 3.1 Load conditions

For assessing the safety of the structure, all possible loads that are expected during the service life of the structure are important. In the Netherlands, the legally permissible vehicle and axle loads are 50 ton Gross Vehicle Weight GVW, excluding some special vehicles like crane vehicles and EMS1. The maximum axle load is 10 t, excluding some exceptions. A full description of vehicles and loads that are allowed on the Dutch road network is given in the <a href="Dutch vehicles regulations">Dutch vehicles regulations</a> according to the Dutch Traffic Act.

Because all traffic that may be present must be taken into account, also the effect of overloaded vehicles need to be taken into account, as well as trends and accompanying uncertainties that may be expected in the future. Such trends concern the growth of traffic (in frequency, weight) and developments in the field of mobility, such as new vehicle concepts, and the effects of new developments on the structural behavior.

At the same time, measures may also be taken into consideration, including their effectiveness, which depend, among others, on the enforcement of these measures. Examples of such measures are: physical restrictions such as (partial) road blocks or traffic signs or regulations for special transports for which a one-time exemption is granted by the RDW (the Dutch Vehicle Authority). For these vehicles a special procedure is followed where the transport is accompanied by a special vehicle [6] that can affect the behavior of other vehicles in traffic, for example by preventing overtaking the special transport and/or a relatively low speed of the special transport when passing the bridge.

It may be obvious that the effectiveness of physically blocking the road is higher than for example the use of signs that do not allow for overtaking. With respect to the structural safety of bridges where a failure probability of about 10<sup>-4</sup> during the service life of the structure is considered, signs are considered hardly effective [7].

#### 3.2 Structural behavior

#### 3.2.1 Introduction

As explained in the previous section, for the assessment of structural safety of bridges and viaducts the expected traffic loads need to be taken into account. The probability of failure, however, depends on the effect of the loading on the structure (the load effect, for example expressed in terms as stresses, strains, bending moment or shear force) and the strength of the structure. The load effect can be determined with appropriate structural models that are validated on the basis of measurements. The safety is then estimated by comparing the load effect with the resistance of the structure and by verifying if the probability of failure during the (remaining) service life is less than required.

For estimating the resistance of bridges and viaducts it is important to consider all possible failure mechanisms and the locations on the structure where the possible failure might occur. The failure



mechanisms depend on the type of structure and are material-dependent [8]. For that reason, in this study, steel and concrete bridges are both considered.

For civil structures the most common failure mechanisms are failure in bending, failure in shear and failure due to (in)stability and due to buckling. In particular for steel structures, fatigue of the material under variable loading conditions is often decisive for the structural safety. Generally for fatigue, frequently passing and rather heavy loads are important factors for structural safety. The order of magnitude depends strongly on the type of bridge (detail) and corresponding influence line, as will be explained in the next section. For concrete structures, variable loads are generally less important and the extreme (quasi-static) loads with a low probability of occurrence tend to be more important. Because concrete structures are in general significantly less slender than steel structures, the mechanisms such as buckling and stability tend to be less important.

Other civil engineering structures, like tunnels and hydraulic structures, are out of scope of this study as the effect of traffic loads has no or a less significant role on these structures.

#### 3.2.2 Bridge characteristics

For civil structures like bridges and viaducts different types of structures can be distinguished, each with a different way of load transfer at the global level (the main load-bearing structure) and at the local level (details and components of the structure). The type of bridge depends on the material: steel, concrete or the combination of both [8].

The effect of the load on a considered component of the structure is characterized by the influence line. The influence line represents the effect of the load at a specific point at the bridge, for example the bending moment at mid span or the shear force near the support. For simplicity a parallel can be drawn with the bridge span: the shorter the span, the greater the effect of a SEC or TP, but also the greater the effect of other vehicles on the bridge. This is illustrated in Figure 4.

For short span bridges (e.g. Figure 4a or Figure 4e) it can be imagined that the effect is only determined by the SEC, whereas for longer spans (e.g. Figure 4c and Figure 4d) the effect is also affected by other cars and trailer combinations on the bridge. It may be obvious that for bridges with multiple lanes also the effect of passing of vehicles contributes to the load effect. In general the load effect can be divided into several ranges, depending on the span length or the length of the influence line. This is explained in Table 1.

Table 1: Effect of loading a bridge structure, depending on the influence length

Influence length	Effect
less than 1 to 2 m (short)	These are structural details that primarily experience the effect of a passing axle, wheel, or tire, such as trough details in steel bridges. These are especially important for the assessment of fatigue resistance. The weight of the vehicle hardly plays a role for such details.
between 5 and 10 m	These influence lengths can be expected for example at cross-girders in steel structures. For such structural components especially the load of axles, tandems and tridems is important. The vehicle weight is hardly of any importance



Influence length	Effect			
up to 20 m	These include the main load-bearing structure of statically determined, double-supported bridges and viaducts with a span that just fits a truck-trailer vehicle combination of 18 m length with 4 to 6 axles. Especially the total vehicle (or tandem/tridem) weight is important for such structures.			
between 20 and 50 m	For (main bearing) structures with such an influence length several vehicle types are of importance, such as short trucks or (generally only in a traffic jam situation) two trucktrailer combinations that are together on the bridge. Axle of tandem loads are of less importance.			
	For such influence lines also long and heavy vehicles with lengths from 25 m upwards, or Super EcoCombi vehicles with lengths up to 32 m are important to consider,.			
between 50 and 100 m	These influence lines relate often to the main bearing structure and for those types of influence lengths especially vehicle weights are of importance, but also the probability of occurrence of several heavy vehicles within the influence zone.			
	The load of a single axle is hardly of any importance for such influence lengths.			
between 100 and 200 m (large)	These are mainly related to the main load-bearing systems of bridges with large spans, such as arches on arched bridges, cables on cable-stayed bridges or the load-bearing system of large span concrete <a href="box girder bridges">box girder bridges</a> . For these lengths the vehicle weight is importance, including the probability of several heavy vehicles passing the bridge simultaneously. The effect of single axles is negligible.			

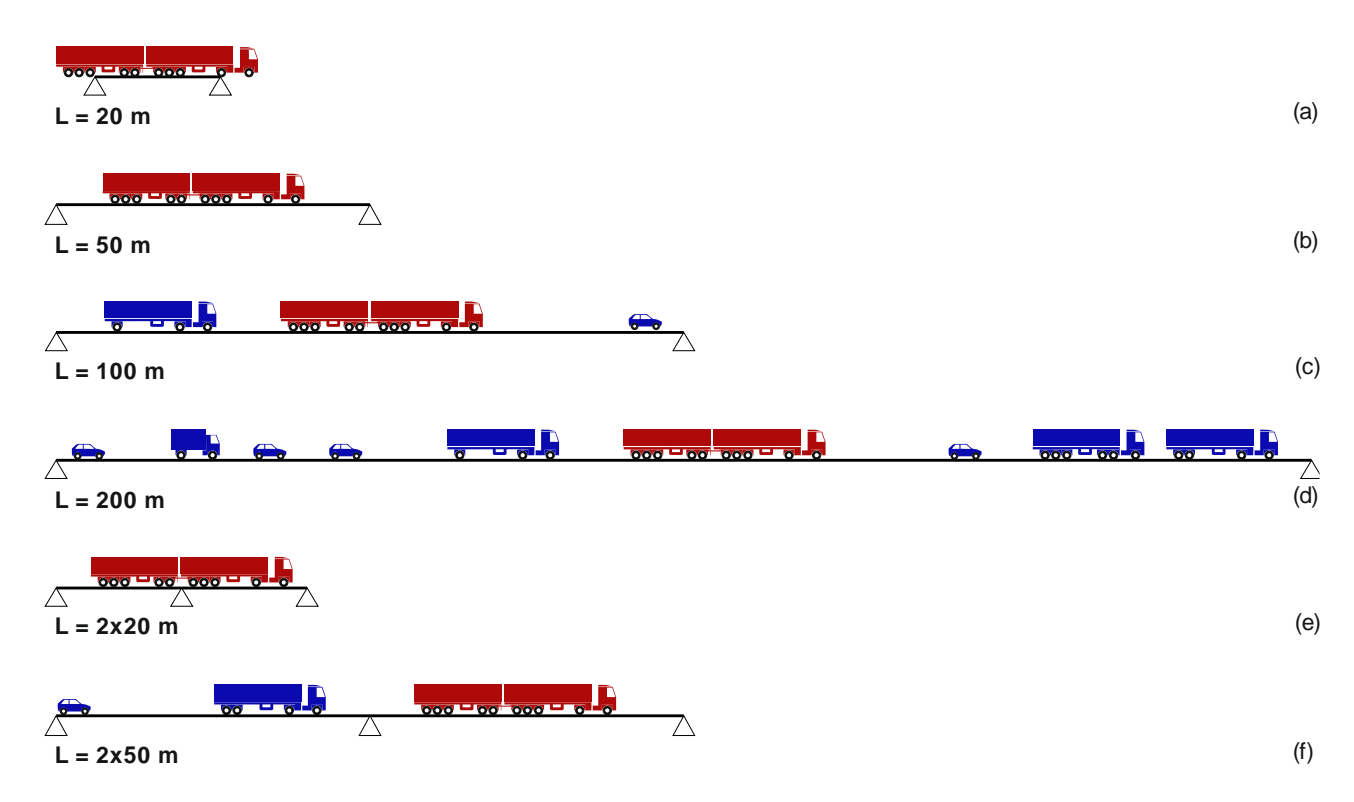


Figure 4: Different vehicle configurations, including a SEC vehicles, at bridges with a different span

In EN 1991 [9], for Load Model 1 (LM1), a distinction is made between four influence lengths (L = 20, 50, 100 and 200 m). Short influence lines where wheel, axle and tandem loads are dominant, are taken into account in NEN-EN 1991 with load models LM2 and FLM4 for fatigue. Because it is assumed that the legally-permissible axle and tandem loads will not change in the future and



because it is assumed that the trends towards the future is similar for all scenarios, it is questionable whether short influence lengths are relevant for TP and SEC vehicles.

For the impact analyses with respect to the structural safety of bridges and viaducts, a summary of the considered influence lines in this research is given in Table 2. Structural elements with an influence length shorter that a single vehicle no effect is expected because the axle loads do not change. Nevertheless, for completeness also a short influence line with L=20 m will be taken into account. Further distinction is made between the bending moment (M) and the shear force (V) in the middle of the span or next to the middle support in accordance with [10]

Table 2: Considered ranges of influence line according to the length of the influence line, internal force and number of spans.

No. of spans	Interi	nal force	Influence length	
One	M <sub>05L</sub>	(moment at mid-span)	L = 20 m	
		L = 50 m		
			L = 100 m	
			L = 200 m	
Two	Ms	(moment above support)	L = 2 x 20 m	
			L = 2 x 50 m	
	Vs	(shear force)	L = 2 x 20 m	
			L = 2 x 50 m	

From the above it may be obvious that the load effect also depends on the vehicle configuration (axle distances, axle load distribution) and other vehicles on the bridge. In this respect, for short influence lines, the axle configuration is relevant, whereas for long influence lines the distance between different vehicles is of importance (the inter-vehicle distance, see section 3.3.3).

Apart from influence lengths, other aspects are also important for determining the effect of traffic loading on bridges, such as the dynamic amplification factor. Since it is assumed that these do not differ for regular traffic and new transport concepts such as TP and SEC, these aspects will not be considered differently in the different scenarios.

#### 3.3 Current vehicle and traffic characteristics

#### 3.3.1 Introduction

For the assessment of structural safety of bridges and viaducts it is important to take into account all relevant traffic parameters that may be present during the (remaining) service life of the structure. As explained previously the load effect depends on the influence length of the considered load effect and cross section in the structure along with the vehicle configuration. Within this scope, axle loads and vehicle weights are two important characteristics, but also the configuration of the axles and the associated weights of multiple axes (tandems, tridems).

Because the structural safety is evaluated by the probability of failure (collapse) also the probability that several heavy vehicles pass the structure simultaneously must be considered. This is relevant especially for long span bridges. For this purpose insight is needed in:



- expected developments of traffic growth (in terms of numbers and weight)
- expected developments the traffic composition, including the inter-vehicle distance and the probability of traffic jams since that is related to the inter-vehicle distance.
- Actual axle and vehicle loads (including possible overloading and depending on measures that might be taken)

A consideration of the current traffic composition at the corridor that is considered is given in the following section. From earlier research it may be concluded that this is representative for the Dutch highway network [7]. Possible changes in the traffic composition that may be expected in the future are given in section 3.4, followed by the assumptions for the impact analyses with respect to the structural safety of bridges and viaducts.

#### 3.3.2 Current traffic composition

#### 3.3.2.1 Number of vehicles

Measurements of a number of Weight-in-Motion (WIM) systems have been analyzed in order to gain an insight in the current traffic composition on the Dutch highway network. For this purpose a database of traffic data originating from 2015, that was made available to TNO, has been analyzed. For the probabilistic analyses these results are considered sufficiently reliable and up to date<sup>4</sup>.

The WIM measurements include the individual axle loads and axle distances as well as the vehicle speed for all vehicles heavier than 3.5 t, as well as the axle configuration per vehicle. Moreover, the vehicle type is represented using the codes as used by the WIM system (see Appendix 1A)<sup>5</sup>.

Figure 5 shows the distribution of vehicle types detected in the slowest lane by seven WIM stations on the highway network in 2015. The results are also presented in tabular form in Appendix 1B (including the raw counts). From the figure, it can be observed that more than half of the vehicles are the so-called Truck Trailer Combination (TOC, in Dutch "*Trekker Oplegger Combination*"). This mainly concerns vehicles of the subclass T11O3 and T1102, but to a lesser extent T11011, T1203, and T1101<sup>6</sup>. These TOCs account for more than 63% of passages. Additionally, a relatively large proportion of trucks V11 was observed.

It is noted that mobility is subject to lots of developments that depend on various aspects, including the economic situation. On the other hand, these uncertainties do not necessarily imply that the design value of the traffic loads for analyzing the structural safety during the service life of structures will change as well.

It is noted that the results of the strain measurements at the Moerdijk bridge and the bridge near Geldrop have not been used for analyzing the traffic volume composition, because they don't provide direct information about the number and type of vehicles.

Vehicles of type T11O11 have almost identical axle configuration as T11O2, except that the distance between the two rear axles in a T11O11 is larger so that these two axles are not identified as a tandem but as two single axles. A vehicle of type T11O1 can also be a vehicle of type T11O2 with one rear axle raised and is usually a vehicle with a lower vehicle weight. The relevant types are illustrated in Figure 5b. A complete overview is given in Appendix 1A



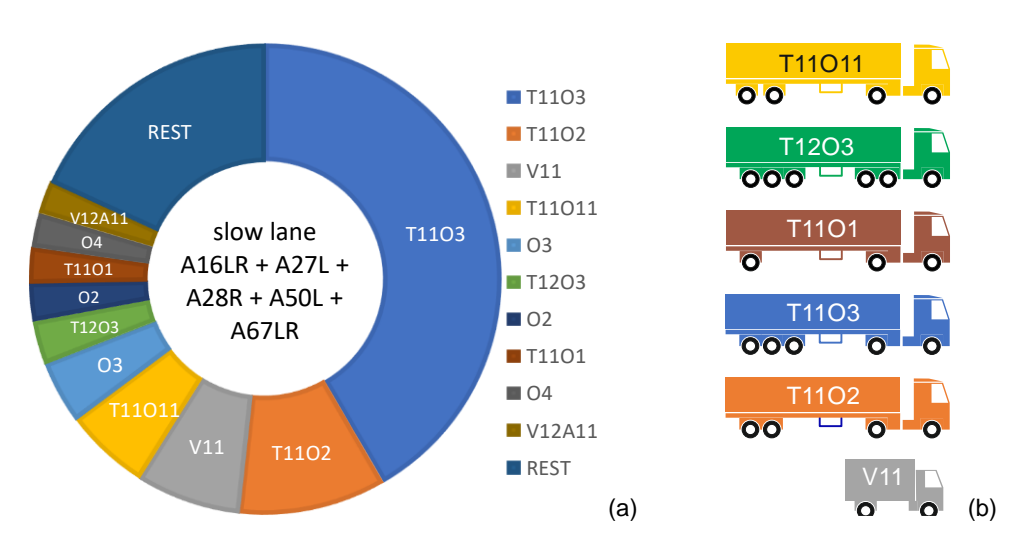


Figure 5: Distribution of the number of (freight) vehicles on the Dutch highway network, subdivided into different subclasses according to Appendix 1A (a). The configurations of a number of frequent vehicle subclasses is shown in (b).

It may be assumed that the distribution of vehicles given in Figure 5a provides a representative estimation of the freight vehicle distribution on the Dutch highway network. Table 18 in Appendix 1B shows that the largest number of TOCs (T11... and T12...) is observed on the A16 and A67 which are both part of the Maasvlakte-Venlo traffic corridor. On both highways (A16 and A67) the share of TOCs is 70%-73%. For A27, A28 and A50 this share is 60-65%. The distribution of the number of freight vehicles on the A16 and A67 is illustrated in Figure 6.

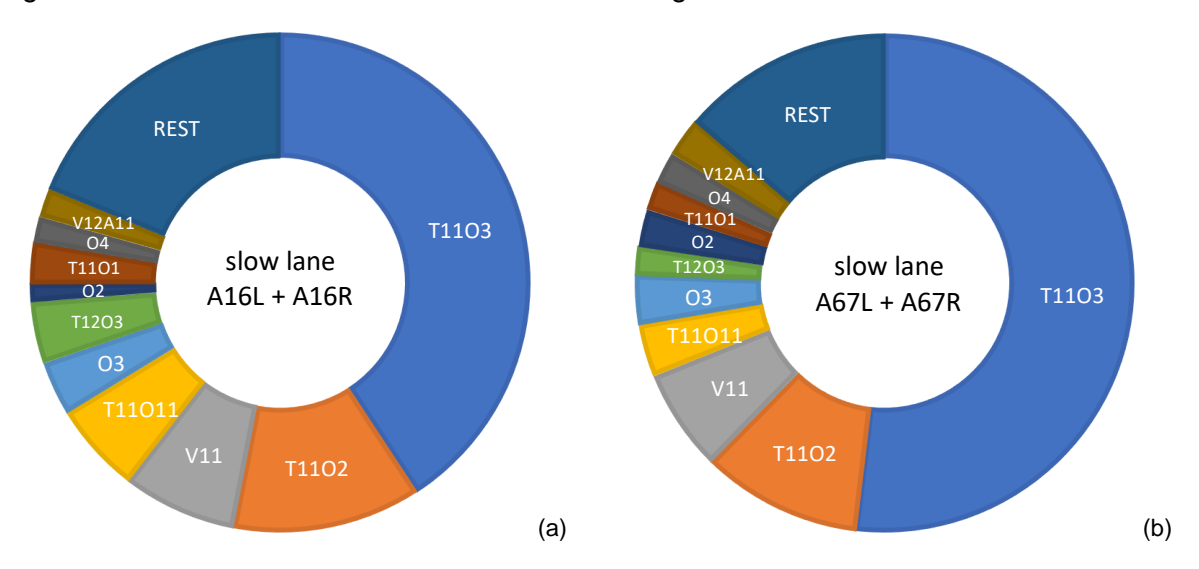


Figure 6: Distribution of the number of freight vehicles on the A16 (a) and A67 (b), subdivided into several WIM subclasses.

Both from Figure 5 and Figure 6 it can be seen that there is a relatively large number of lorries of subclass V11. These are generally less heavy compared to the TOCs. The number of lorries of subclass V11 averages about 7% of the total number of passages.

The traffic composition presented in Figure 6 reasonably matches an earlier study where the WIM data from the A16 from 2018 was analyzed in [22], despite in that report a distinction was made by



the number of vehicle axes per vehicle rather than the type of vehicle. This would imply that the composition of heavy vehicles has not substantially changed in recent years.

#### 3.3.2.2 Loads

In order to obtain insight in the present loads by the different vehicles, in this section the results are presented that relate to the vehicle and axle loads as observed on the A67 (based on WIM data, A67L+R, April to June 2015, slow lane and fast lane combined)<sup>7</sup>.

#### **Gross Vehicle Weight**

The distribution of the Gross Vehicle Weight (GVW) is given in Figure 7. From the figure it is observed that the majority of TOCs have a weight of 15 to 20 t or around 40 t. Figure 7 is based on the results given in Appendix 1C from which it can be concluded that the vehicles with a weight of about 40 t mainly consist of trucks with 3 trailer axles (T1103 and T1203) that are maximum loaded. Trucks with 2 or 1 trailer axles (T1102, T11011, T1101) can be characterized generally as volume transports and weigh around 20 t.

Based on Figure 7a, the cumulative probability of exceeding a certain vehicle load is illustrated in Figure 7b. The probability of exceedance is presented on a logarithmic scale for providing insight in the tail of the frequency distribution. Since the design value of the traffic load for bridges is governed by the extreme load events, the tail of the distribution function is most decisive (at least for long influence lines).

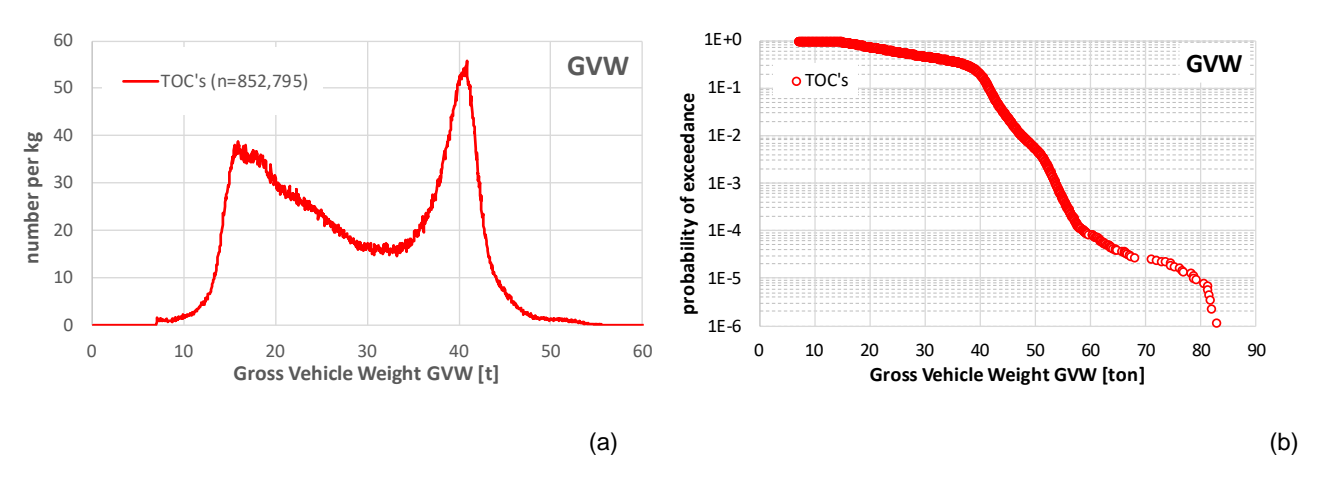


Figure 7: Distribution of GVW of TOC's (a). Cumulative probability of exceedance is given in (b). The distribution of other subclasses is given in in Appendix 1C.

From Figure 7b that approximately 0.5% of the TOC vehicles have a weight of more than 50 t. Those are overloaded vehicles or vehicles that were granted an (annual) exemption [11], and mainly consist of trucks with 3 trailer axles (T11O3 and T12O3, see Appendix 1C). The maximum observed vehicle weight is almost 83 t with a corresponding probability of exceedance 10<sup>-6</sup>.

The Dutch vehicle regulation can be found on wetten.overheid.nl (in Dutch)



#### Axle loads

The distribution of the weight of the individual axles and tandems of the truck of the truck trailer combinations is given in Figure 8. The distributions per subclass are given in Appendix 1C (Figure 51 to Figure 53). Figure 8a shows the distributions for the first and the second axle of the truck of the truck trailer combinations with two rear axles (T11O3, T11O2, T11O11, and T11O1). The truck of the subclass T12O3 has a double second axle (tandem 1). The weight distribution for tandem 1 is given in Figure 8b.

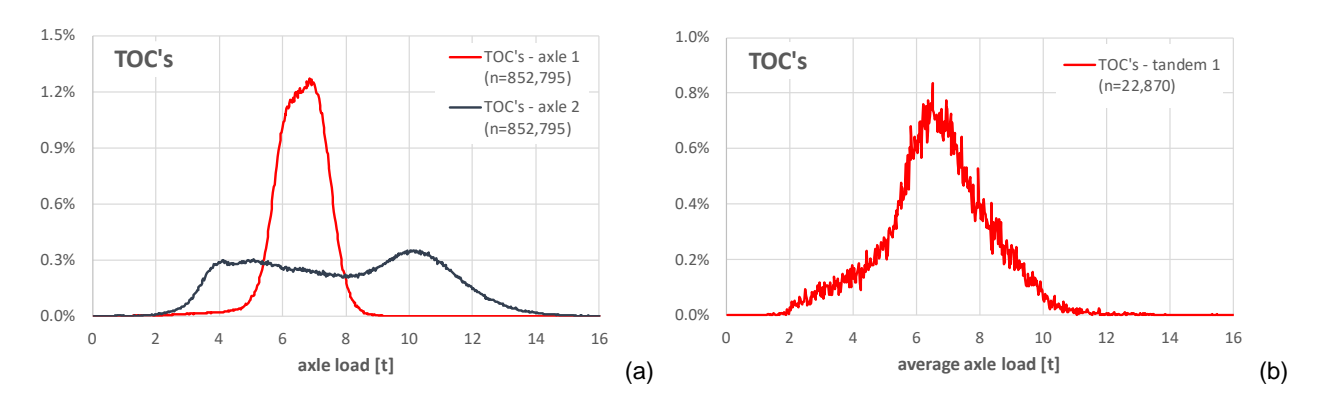


Figure 8: Distribution of the axle load for axle 1 (a) and axle 2 (b) for all trucks or truck-trailer combinations.

Figure 8a shows that especially the first axle has a single, narrow distribution with a relatively small spread. This makes sense because the weight on the first axle is mainly determined by the weight of the tractor. The second axle seems to be characterized by a multimodal distribution, which can be explained by the fact that the vehicle can be loaded or unloaded. The average axle load distribution for the tandem shows a more or less normal distribution as well. This may be explained that these results mainly apply to the fully loaded vehicles because for less loaded vehicles the one of these axles may be lifted. In that case T12O3 is recognized by the WIM system as T11O3.

The cumulative probability of exceedance for axles, tandems and tridems are given in Figure 9. For the tandems and tridems the axle loads in the figure refers to the average load of two (tandems) or three (tridems) axles. It is noticeable that overloading occurs particularly on the second axle of the trucks with two rear axles. Assuming a legally allowed maximum axle load of 10, depending on the type of axle, it appears that around 15% of the observed axles are overloaded. For the first axle the percentage of overloading is only marginal (2·10-5).

For a tandem a lower average allowed axle load applies (depending on the distance between the axles and whether one of the axles is a driven-axle). When an average allowed axle load of 10 t is assumed for a tandem, overloading amounts up to 2% (based on the average axle load). For tandem 2 and tridem an overloading between 0,1% and 1% is noticed.



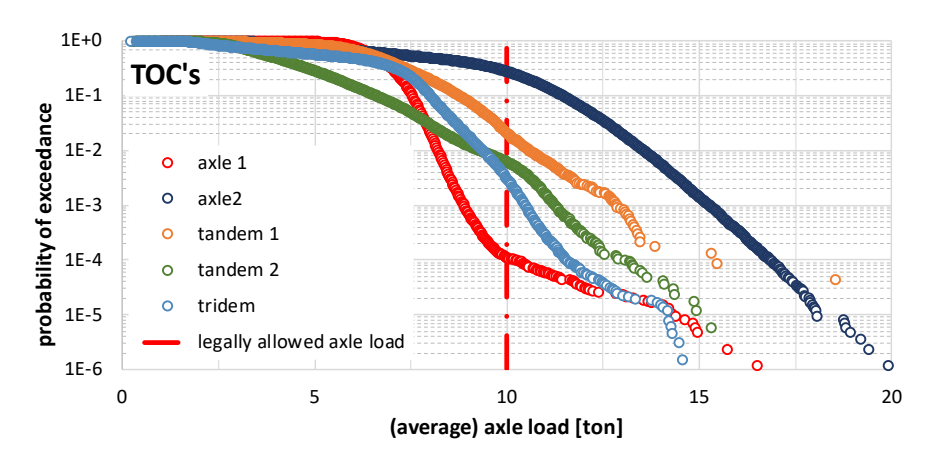


Figure 9: Distribution of the (average) axle load for individual axles, tandems and tridems for all truck-trailer combinations.

#### 3.3.3 Inter-vehicle distance

For the impact analyses considering the SEC vehicles, the inter-vehicle distance for the normal traffic is calculated from the tracking time of the vehicle(s) in the WIM measurements, the axle distances and the corresponding vehicle speed of the different vehicles.

Because vehicles with a GVW less than 3.5 t are excluded from the measurements, the intervehicle distances equals the distance between the vehicles available in the WIM database. Vehicles with a GVW less than 3.5 t may be neglected for determining the design values.

#### 3.4 Starting points for the impact analyses

#### 3.4.1 Introduction

In order to study the impact on the structural safety due to the introduction of new vehicle concepts, scenarios need to be developed in which possible changes and traffic characteristics are incorporated. In this respect it needs to be taken into account that the service life for structures may be up to 100 years or sometimes even larger, contrary to most predictions of vehicle developments such as in [12] where a prospect of 10 years is taken into account. A prediction on long notices will lead to larger uncertainties which must be taken into account in the structural analyses. Alternatively a conservative approach may be assumed. For existing structures a minimum remaining service life of 15 years must be taken into account.

In the following section the starting points for the analyses are given with respect to the inter-vehicle distance (section 3.4.2), the assumed number of SEC vehicles and TP during the service life of the structure (section 3.4.3) and the vehicle weights and axle loads (section 3.4.4).

#### 3.4.2 Inter-vehicle distance

For truck platooning several vehicles will follow the platoon leader, where the control algorithm typically aims to realize a certain (constant) time gap. Moreover it affects the traffic compositions because the probability that several TOC vehicles drive in a platoon equals one.



For the distance between the vehicles as part of a platoon it may be assumed that the gap varies between 0.3 and 1.5 seconds. In example the ENSEMBLE EU project [13] has defined two Platooning Levels: the Platooning Support Function (PSF) and the Platooning Autonomous Function (PAF). The Support function aims for quick deployment and assumes a gap of 1.5s. For a vehicle speed varying between 70-90 km/h a vehicle distance between 9.7 m (70 km/h, 0.5 s) and 37.5 m (90 km/h, 1.5 s) may be expected.

The PAF, as a future vision on a more automated platooning level, foresees a driver in the first truck followed by maximum two trucks with the driver out of the loop. Moving the responsibility from the driver to the system also offers the opportunity to potentially reduce the time gap (up to 0.3S depending on the braking capacities of the individual vehicles). The PAF would yield a distance gap of 5.8 m to 7.5 m in the 70-90 km/h speed range. It is noted that these are all bumper to bumper distances. For the axle to axle distance about 4 m must be added.

The SuperEco Combi may be considered as a special type of platoon where two TOC vehicles are combined to one single TOC vehicle. In the analyses for the different scenarios the intervehicle distance kept constant at about 5 m between the two semitrailers. The intervehicle distance is constant and does not depend on the vehicle speed. Compared to truck platooning this is considered conservative for analysing the structural safety. For that reason the results of analyses may also be used for estimating the effect of TP.

For the scenarios that are examined it is assumed that the intervehicle distance of the normal traffic is not changed.

#### 3.4.3 Number of TP and SEC vehicles

The structural safety is determined, among others, by the probability of several vehicles simultaneously passing a bridge. For that reason also the number of vehicles that will be present in the future is of importance. For truck platooning this depends on the expected match and adoption rate during the (remaining) service life of the structures considered. For SEC vehicles the number of vehicles that is equipped for coupling and will be coupled to a single vehicle, is of importance.

The number of TPs and SEC vehicles in the coming 100 years is hard to estimate. Since the T11O3 vehicle is by far the most common vehicle (about 50% of all vehicles with a GVW of 3.5 t and higher and 75% of all truck trailer combinations) on the A67, see Appendix 1B and section 3.3.2) and because the vehicle weight of the T11O3 vehicles is quite large), it may be assumed that it a conservative approach for assessing the structural safety if all these vehicles drive in platoons of 2 or 3 vehicles and that the platoons drive randomly and uncorrelated in the normal traffic. This also applies to the SEC scenarios where a combination of only two trailers applies.

Another conservative approach for assessing the structural safety is when it is furthermore assumed that this replacement will occur instantaneously in time (at t=0). In practice this replacement will evolve gradually over time and the number of replacements may be capped.





Figure 10: Assumed replacement scenarios for TP (top) and SEC (bottom).

Next to the scenario where the replacement of T11O3 vehicles is assumed instantaneously in time (at t=0), a less conservative scenario is considered in which the number of replacements increases gradually over the years. Experiences with the introduction EcoCombi (EC) show that after 20 years the number of EC vehicles was about 4% of the TOC vehicles [14].

In an exploratory study performed by CE-Delft & Buck Consultants International [12] the expected number of rides per day with a Super EcoCombi (SEC) in the Netherlands is forecasted for the period 2021-2030. The results are shown in Figure 11. In the figure it is shown that in the first ten years after introduction a quadratic growth is predicted.

Because for assessing the structural reliability a time frame of 30 to 100 years is taken into account, the predictions according to [12] are too limited in time. For that reason an extrapolation is required. Assuming the 4% growth according to [14] and a quadratic growth over the years according to [12], it can be calculated that in 30 years this percentage is 9% and in 80 years 64%8. Furthermore it may be assumed that the growth will be capped after a certain period. In the current study it is assumed that this cap is about 70% after >100 year. No literature was found estimating for such a long period.

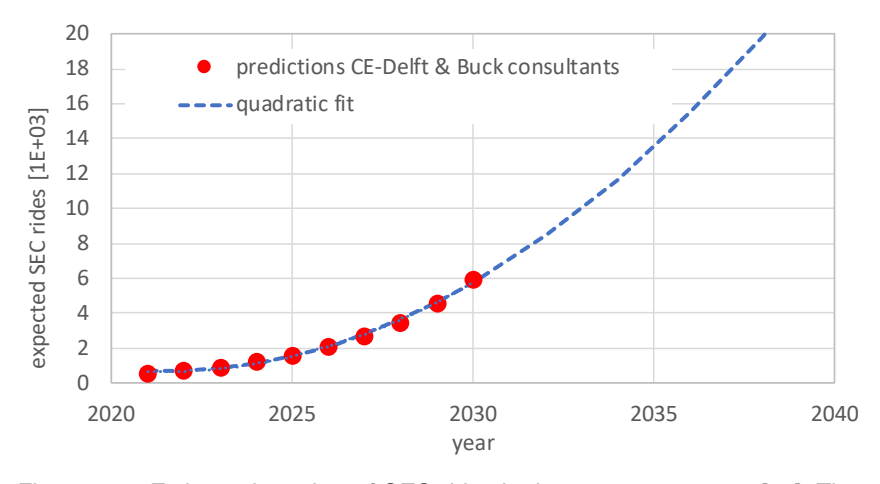


Figure 11: Estimated number of SEC rides in the years 2020-2030 [12]. The quadratic fit also shows the extrapolated results until 2040.

A replacement scenario of 64% of the truck trailer combinations of type T11O3 corresponds to a replacement scenario's of about 40% of all truck trailer combinations (all vehicles of type T11O... and T12O...).



Based on the above, the assumed growth in the gradual replacement scenario is illustrated Figure 12 by the dashed black line and the schematized solid blue line. As mentioned before, it may be clear that there is a great deal of uncertainty about this replacement scenario, particularly about the percentage cap and its development in time. Despite these values are quite arbitrary, insight in the sensitivity for this parameters is given. For completeness the full replacement scenario is illustrated in Figure 12 by the dashed red line (100% from t=0 onwards).

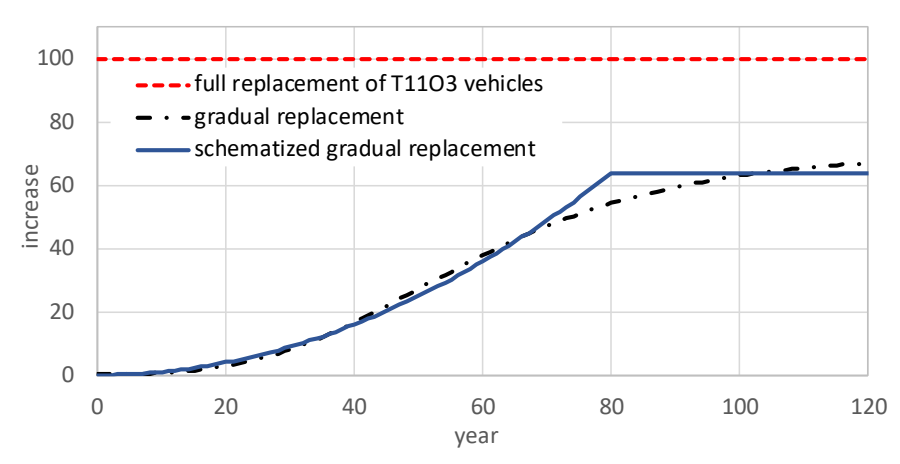


Figure 12: Scenarios for the replacement of vehicles (as a % of the number of TO1103 vehicles) in the full replacement scenario (red, dashed), theoretical gradual replacement of SECs (dash-dot) and replacement percentage scenario taken into account for the probabilistic impact analyses (blue).

#### 3.4.4 Vehicles weight and axle loads

In the analyses it is assumed that a SEC vehicle is formed by randomly joining two TOCs, but that the combination is limited to 76 t. For the TP such a limit is assumed to be not applicable.

It is unclear if the requirements for maximum GVW of SEC vehicles will remain the same in the future. Moreover it is unclear whether the maximum vehicle weight and/or axle loads will be enforced for both the TPs and the SECs, for example by on-board measurements [15]. For now, both aspects are not taken into account in the analyses.

#### 3.5 Other assumptions

To determine the impact on the structural safety of bridges and viaducts the reference scenario is formed by the current traffic composition. The starting points for the different scenarios that are studied are given in the previous section. In order to avoid that different changes in the future give a blurred view of the effect of the TP or SEC, other changes that affect the traffic composition and/or weight distributions are neglected. This concerns, for example, changes due to the introduction of multiple transport concepts (e.g. TP together with SEC), consequential model shifts (e.g. from ship to road or shift due to the use of freight hubs), degree of loading, weight distributions or altering requirements for axle loads and vehicle weights. This implies that also the growth in freight transport is the same for the different scenarios, including the reference scenario.



#### 3.6 Considered structures and assessment scenarios

#### 3.6.1.1 Introduction

In total three cases, depending on the type of structure and reference time that is taken into account) are studied for determining the impact of new vehicle concepts such as SEC and TP on the structural safety of bridges and viaducts. These cases are described in the following sections.

#### 3.6.1.2 Case 1: Reinforced concrete bridge under ultimate limit state (ULS) conditions

In the calculation for the reinforced concrete bridge (case study 1), two idealized representative structural schemes are considered: a simply-supported beam (Figure 13) and a two-span continuous beam (Figure 14).

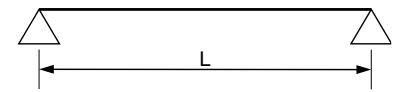


Figure 13: Simply supported beam.

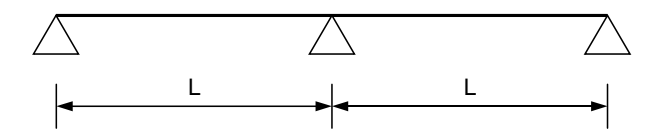


Figure 14: Two-span continuous beam.

Influence lines, corresponding to the simply supported beam (Figure 15) and continuous bridge (Figure 16 and Figure 17), respectively, for the bending moment and shear force were used in the calculation of the traffic load effect and consequently the traffic load effect probabilistic model.

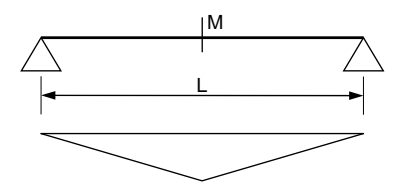


Figure 15: Influence line for the bending moment (midspan, moving point load) for the simply supported beam.

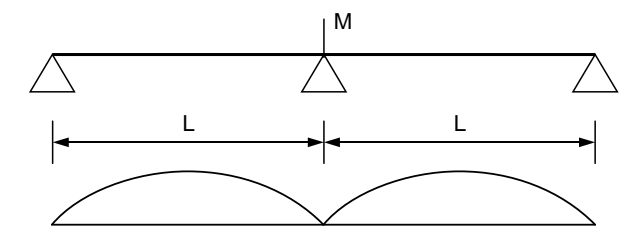


Figure 16: Influence lines for the bending moment (internal support, moving point load) for the two-span continuous structure.



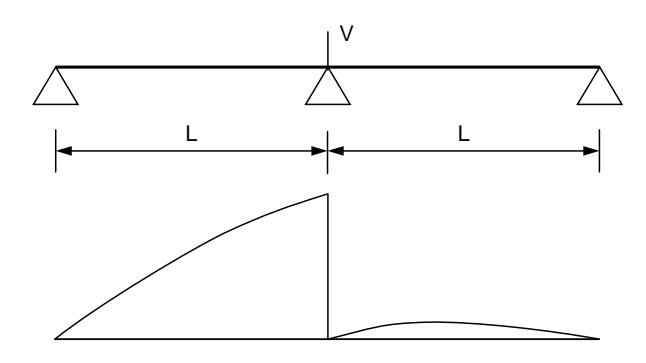


Figure 17: Influence line for the shear force (internal support, moving point load) for the two-span continuous structure.

In accordance with the types of structures that are given in the Eurocode, four influence lengths are defined: L = 20, 50, 100, and 200 m based on the assessment of critical bridge spans in section 3.2.2. For the continuous beam model, shorter lengths of each span are considered: L = 20 and 50 m. The following assessment situations were considered:

- 1) new structure.
- 2) existing structure elapsed service life  $t_0$  = 30 years,
- 3) existing structure elapsed service life  $t_0 = 50$  years,
- 4) existing structure elapsed service life  $t_0 = 70$  years.

#### 3.6.1.3 Case 2: Steel bridge under ultimate limit state (ULS) conditions

In the analysis of the steel bridge under ULS conditions, a simply-supported beam (Figure 13) was considered with an influence line as shown in Figure 15 and span length L = 50 m based on the following assessment situations:

- 1) new structure,
- 2) existing structure elapsed service life  $t_0 = 30$  years.

#### 3.6.1.4 Case 3: Steel bridge under fatigue limit state (FLS) conditions

In the analysis of the steel bridge under FLS conditions, a simply-supported beam (Figure 13) was considered with an influence line as shown in Figure 15 and two span length of L = 100 m based on the following assessment situations:

- 1) new structure,
- 2) existing structure elapsed service life  $t_0 = 30$  years,
- 3) existing structure elapsed service life  $t_0 = 50$  years,
- 4) existing structure elapsed service life  $t_0 = 70$  years.



# 4 ASSESSMENT OF TRAFFIC LOAD EFFECTS IN BRIDGES

#### 4.1 Introduction

This chapter focuses on the analyses of the traffic load effects induced in bridges at the ultimate limit state (ULS) and fatigue limit state (FLS) conditions. The goals of the analyses are:

- to assess the distribution of the extreme traffic load effects to be used for the reliability analysis of concrete and steel bridges with respect to the ULS conditions (chapters 5 and 6)
- to assess the stress histogram required for the reliability assessment of steel bridges with respect to the FLS conditions (chapter 7)

The traffic load effects for both ULS and FLS are evaluated based on the theoretical influence lines described in section 3.6 of simply supported and two-span continuous bridges and the 2015 Weigh-In-Motion (WIM) database of the highway A67R, which is part of the Maasvlakte-Venlo traffic corridor. The evaluation of the traffic load effects comprises of the following steps:

- filtering of the WIM database
- generation of a stream of axles from the WIM database
- · simulation of the traffic load effects
- postprocessing of the traffic load effects

The filtering of the WIM database aims to remove erroneous measurements (e.g. double registration of the same vehicle, incorrect registration of arrival time at the WIM station, "NaN" values of axle loads or axle distances, etc.). The criteria used in this project for removing erroneous records are presented in Appendix 2A "Filtering of the WIM database".

Once the WIM data has been cleaned, the records of the database are transformed into an array of axles that is ran afterwards on the influence line of the load effect under investigation (numerical simulation of traffic load effects). The procedure used for the second and third steps of the bullet list above are described in Appendix 2B "Generation of a stream of axles from the WIM database" and Appendix 2C "Numerical simulation of traffic load effects".

The postprocessing of the simulation results is the step leading to the distribution of the extreme traffic load effects and the stress histogram, which are used, respectively, for the reliability analyses with respect to the ULS and FLS conditions. The postprocessing of the simulation results are presented in section 4.2.2 and 4.3.2.

In this section, the results of the analyse of the load effects in bridges due to regular vehicles, SEC vehicles and truck platooning (TP) are presented. In addition, the load effects in the reference scenario (regular traffic) and the full replacement scenarios based on SEC vehicles and TP are compared with the design values of the load effects calculated based on load model LM1 of NEN-EN1991-2 and the partial factors given in RBK [4] and NEN 8701:2011 [16] is provided.



# 4.2 Traffic load effects in bridges for ULS verification

The reliability assessment of bridges with respect to ULS conditions is based on the probability distribution of the extreme traffic load effects over a certain reference period (e.g. 1 year or 30 years for the assessment level "gebruiksniveau" for existing structures or 100 years for new structures). In this project, the distribution of the extreme annual load effects is the result of the analysis of the traffic load effect simulations with respect to ULS conditions. The procedure explained in Appendix 2C "Numerical simulation of traffic load effects" leads to the distribution of the maximum load effects for each load event (defined by the simultaneous presence of one or more trucks on the bridge) based on Weight-In-Motion (WIM) data and the influence lines of the load effects under investigation. Two traffic lanes in one direction, the slow and the fast lane, are considered in the simulations of the traffic load effects. The results of the simulations are post-processed using the block-maxima method to assess the distribution of extreme annual load effects:

- the extreme daily load effects are calculated as the maximum load effects of the load events occurring in each day
- the obtained values of the extreme daily traffic load effects (usually referred to as the empirical distribution of the load effects) are fitted by a Gumbel maximum distribution with mean value  $\mu_{daily}$  and standard deviation  $\sigma_{daily}$ . In principle, also other extreme value distributions, like the Weibull, the Frechet and the Generalized Extreme Value distribution could be considered as probabilistic models of the extreme daily traffic load effects. However, the goodness-of-fit of the Gumbel distribution is considered sufficient for the purpose of this project.
- the mean value  $\mu_{annual}$  and the standard deviation  $\sigma_{annual}$  of the Gumbel maximum distribution modelling the extreme annual traffic load effects are obtained using the following expressions:

$$\mu_{annual} = \mu_{daily} + 0.78 \cdot ln(365) \cdot \sigma_{daily} \tag{4.1}$$

$$\sigma_{annual} = \sigma_{daily} \tag{4.2}$$

# 4.2.1 Assessment of load effects induced by regular vehicles (reference scenario)

The probability of exceedance of the empirical distribution of the extreme traffic load effects, the fitted Gumbel distribution and the Gumbel distribution of the annual extreme traffic load effects for each structural system and influence length are shown in Appendix 4A. The parameters of the Gumbel distribution of the annual extreme traffic load effects considered in this project are given in Table 3.

Table 3: Parameters of the Gumbel distribution of the maximum annual traffic load effect with normal traffic conditions (one slow and one fast lane in one direction).

Structural system and load			Mean value	Coefficient of
effect	Unit	L [m]	$\mu_T$	variation [-]
Simply-supported bridge,	kNm	20	4,404	0.08
bending moment at		50	15,055	0.08
mid-span		100	34,949	0.07
		200	92,454	0.06



Structural system and load			Mean value	Coefficient of
effect	Unit	L [m]	$\mu_T$	variation [-]
Continuous bridge, bending	kNm	2.20	2,543	0.08
moment at middle support		2.50	8,921	0.07
Continuous bridge, shear force	kN	2.20	956	0.08
at middle support		2.50	1,288	0.08

#### 4.2.2 Assessment of load effects induced by SEC vehicles

The analysis of the load effects induced by SEC vehicles when they are mixed with regular traffic consists of the following steps:

- the selection of the T11O3 vehicles for replacement
- the generation of SEC vehicles from pairs of T11O3 vehicles
- the assessment of the probabilistic model of the extreme daily and annual traffic load effects. The first two steps are addressed in Appendix 3A and Appendix 3B, while the third one is the same as for regular traffic (section 4.2). The evaluation of the load effects induced by SEC vehicles and the conclusions presented in the following concern the "full replacement" scenario, where all T11O3 vehicles in the 2015 WIM database are replaced by SEC vehicles.

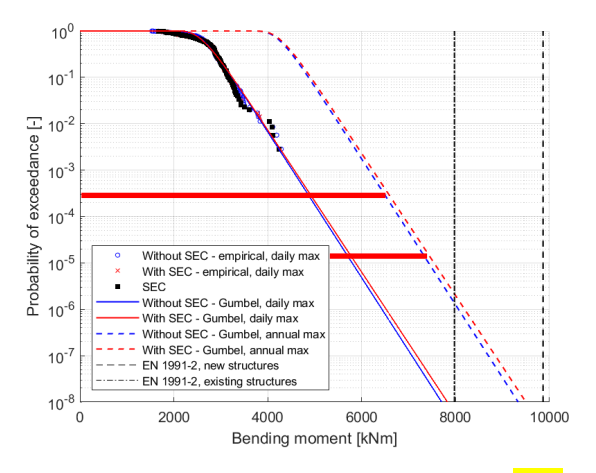
Based on the influence lines for each bridge considered in the investigation, the load effect exerted on the structure was calculated. By performing the same procedure as for the reference scenario, the Gumbel maximum distribution was fitted to the values of the maximum daily traffic load effect obtained by simulation. The probability of exceedance of the extreme daily traffic load effects for the scenarios "normal traffic" and "full replacement" for few cases concerning short-, medium- and long-span bridges. The whole set of plots is reported in Appendix 4B for the bridges and influence lines considered in this project.

The following distributions are plotted in **Error! Reference source not found.** to **Error! Reference so urce not found.**:

- the empirical distribution for the scenario "normal traffic" (blue circles),
- the empirical distribution for the scenario "full replacement" (red crosses),
- the points of the empirical distribution for the scenario "full replacement" that are caused by the load events comprising one SEC vehicle and eventually other regular vehicles (black squares),
- the fitted Gumbel distribution of the daily extreme load effects for the scenario "normal traffic" (red continuous line),
- the fitted Gumbel distribution of the daily extreme load effects for the scenario "full replacement" (blue continuous line),
- the Gumbel distribution of the yearly extreme load effects for the scenario "normal traffic" (red dashed line),
- the Gumbel distribution of the yearly extreme load effects for the scenario "full replacement" (blue dashed line),
- the design value of the traffic load effects for new structures based on the Load Model 1 of NEN-EN 1991-2 [9] (black dashed line),
- the design value of the traffic load effects for existing structures based on the Load Model 1 of NEN-EN 1991-2 (black dash-dotted line).



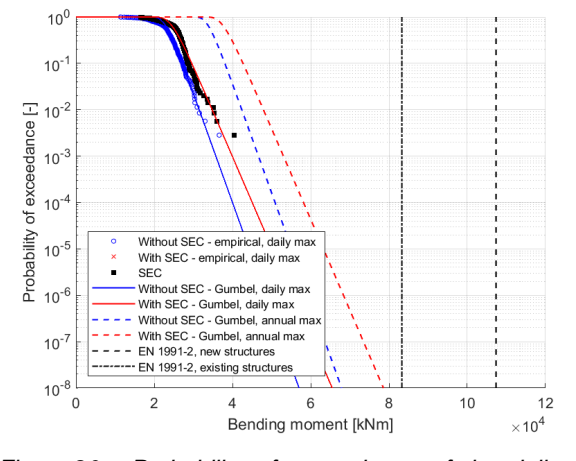
The design values of the traffic load effects for new and existing structures based on NEN-EN 1991-2 are listed in Appendix 5A for all static schemes, influence lengths and load effects considered in this project.



10<sup>0</sup> 10 of exceedance [-] 10-10 Probability Without SEC - empirical, daily ma 10<sup>-</sup> With SEC - empirical, daily max Without SEC - Gumbel, daily max 10 With SEC - Gumbel, daily max
Without SEC - Gumbel, annual m
With SEC - Gumbel, annual max
EN 1991-2, new structures 10<sup>-7</sup> EN 1991-2, existing structures 10 2 2.5 Bending moment [kNm]

Figure 18: Probability of exceedance of the daily and annual extreme bending moment in the midspan section of a simply supported bridge with length L equal to 20 m. The requirements are indicated by the solid red line

Figure 19: Probability of exceedance of the daily and annual extreme bending moment in the midspan section of a simply supported bridge with length L equal to 50 m.



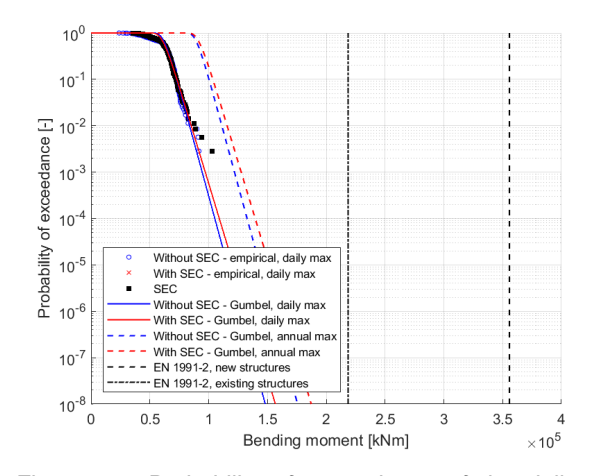


Figure 20: Probability of exceedance of the daily and annual extreme bending moment in the midspan section of a simply supported bridge with length L equal to 100 m.

Figure 21: Probability of exceedance of the daily and annual extreme bending moment in the midspan section of a simply supported bridge with length L equal to 200 m.

The design values of the traffic load effects according to the Dutch standards for new and existing structures are provided only as reference. The sound comparison between the design values based on the Dutch standards and the design values based on the probabilistic analysis of the traffic load effects should include, in addition to the Gumbel distributions of the annual extremes, also the additional uncertainties listed in section 2.4.1, such as the uncertainties about future trends, spatial variability of traffic loads, dynamic interaction between the bridge and the vehicles and the structural



model. Therefore, an explicit comparison is not performed in this chapter, but the reader is provided with guidance on the how to quantify the design values of the traffic load effects based on only the uncertainty of these load effects. The additional uncertainties listed above lead approximately to an increase of 15% of the design value of the traffic load effects.

Given a probabilistic model of the traffic load effects is available, the design value  $E_d$  to be compared with the design value of the standards is defined in probabilistic terms as follows [3]:

$$P(E > E_d) = \Phi(\alpha_E \beta) \tag{4.3}$$

where:

- E is the distribution of the extreme traffic load effects for the reference period T<sub>ref</sub>
- $\Phi(\cdot)$  is the cumulative distribution function of the standard normal random variable
- $\alpha_E$  = -0.7 is the sensitivity factor for dominant load variables
- $\beta$  is the target reliability index associated with the reference period  $T_{ref}$

The Gumbel distribution of the extreme annual traffic load effects is plotted in the figures above instead of the distribution of the extreme traffic load effects for the reference period. Under the assumption of independence of the extreme traffic load effects in subsequent years of the lifetime, the cumulative distribution function of the extreme values for the reference period  $F_{E,T_{ref}}$  is written as:

$$F_{E,T_{ref}}(e) = \left[F_{E,annual}(e)\right]^{T_{ref}} \tag{4.4}$$

where  $F_{E,annual}(\cdot)$  is the cumulative distribution function of the Gumbel distribution of the annual extremes and the numerical value of the reference period in  $T_{ref}$  years. From Eq.(4.3) and Eq.(4.4) the design value  $E_d$  can be written as:

$$P(E > E_d) = 1 - F_{E,T_{ref}}(E_d) = \Phi(\alpha_E \beta) = 1 - [F_{E,annual}(E_d)]^{T_{ref}}$$
 (4.5)

Therefore, the design value  $\mathcal{E}_d$  for the reference period can be estimated as follows:

$$E_d = F_{E,annual}^{-1} \left[ 1 - \frac{\Phi(\alpha_E \beta)}{T_{ref}} \right] \tag{4.6}$$

where  $F_{E,annual}^{-1}(\cdot)$  is the inverse of the cumulative distribution function of the Gumbel distribution of the annual extremes. The design value  $E_d$  can be read on the plots of the probability of exceedance as the value of the traffic load effects corresponding to the probability of exceedance

$$1 - \left[1 - \frac{\Phi(\alpha_E \beta)}{T_{ref}}\right] = \frac{\Phi(\alpha_E \beta)}{T_{ref}} .$$

This annual probability of exceedance can be calculated as follows:

new structures (consequence class CC3):

$$\frac{\Phi(\alpha_E \beta)}{T_{ref}} = \frac{\Phi(-0.7 \cdot 4.3)}{100} = \frac{1.31 \cdot 10^{-3}}{100} = 1.31 \cdot 10^{-5}$$
 (4.7)

existing structures (assessment level "gebruiksniveau"):



$$\frac{\Phi(\alpha_E \beta)}{T_{ref}} = \frac{\Phi(-0.7 \cdot 3.3)}{30} = \frac{1.04 \cdot 10^{-2}}{30} = 3.48 \cdot 10^{-4}$$
 (4.8)

From the analyses, the following conclusions are drawn:

- SEC vehicles are present in most of the load events leading to the maximum daily load effect, as shown by the black dots in the figures above.
- The difference between the maximum load effects induced by regular vehicles or SEC in combination with other regular vehicles is small for short span bridges, because the interaxle distance and the axle loads govern the load effects in these bridges. The last points of the curve are due to load events with one vehicle per lane.
- In case of medium span bridges, a significant effect of SEC vehicles on the bending moment in the midspan section of simply supported bridges with span length of 50 m and two-span bridges with total length of 40 m can be observed. The frequency of load events with one or more vehicles simultaneously on the bridge leading to the extreme daily load effects is given in Table 4 and Table 5 for regular traffic and the "full replacement" scenario, respectively. As an example, 29% and 71% of the load events in the simulations of 20 m long simply supported bridges in the "reference" scenario are characterised by one truck and two trucks, respectively. It can be observed that the frequency of load events with more than two vehicles is higher in the "regular traffic" scenario compared to the "full replacement" scenario. However, the axle configuration of SEC vehicles and their GVW in combination with another heavy truck on the other lane leads to higher values of the load effects. In addition, the effect of SEC vehicles on the shear force to the left of the inner support of two-span bridges is less than the effect on the bending moment, because the shear force is mainly governed by vehicles on the first span.
- In case of bridges with span length of 100 m, the increase of extreme daily load effects depends on the shape of the influence line. An increase of the bending moment in the midspan section of simply supported bridges and in two-span continuous bridges in case of shear due to SEC vehicles is observed. The increase of bending moment is explained by the fact that the largest part of load events is characterized by two or three vehicles. The higher values of the shear force are due to the higher frequency of combinations of one SEC vehicle with other heavy trucks on the first span, as for simply supported bridges with the same span length. On the contrary, there is a small effect of SEC vehicles on the bending moment in the inner support of two-span bridges. As listed in in Table 4 and Table 5, load events with more than three vehicles are more frequent in the "regular traffic" scenario compared to the "full replacement" scenario. As a result, combinations of regular vehicles lead to load effects comparable with those of SEC vehicles.
- Almost no effect of SEC vehicles on the bending moment in the midspan section of 200 m long simply supported bridges is observed. In this case the bending moment is governed by the total traffic load applied to the bridge. Therefore, load events with several regular vehicles



on the bridge lead to similar values of the bending moment caused by SEC vehicles in combination with other regular vehicles.

Table 4: Frequency of number of vehicles leading the extreme traffic load effects – regular traffic.

Structural system				Number of vehicles							
and load effect	Span	Load effect		1	2	3	4	5	6	7	8
Simply-supported bridge	L= 20 m	M <sub>midspan</sub>	(bending)	0.29	0.71	0.00	0.00	0.00	0.00	0.00	0.00
Simply-supported bridge	L= 50 m	M <sub>midspan</sub>	(bending)	0.14	0.71	0.15	0.01	0.00	0.00	0.00	0.00
Simply-supported bridge	L= 100 m	M <sub>midspan</sub>	(bending)	0.03	0.27	0.38	0.26	0.05	0.01	0.00	0.00
Simply-supported bridge	L= 200 m	M <sub>midspan</sub>	(bending)	0.00	0.10	0.16	0.18	0.22	0.20	0.10	0.04
Continuous bridge	L= 2x20 m	M <sub>mid support</sub>	(bending)	0.24	0.45	0.28	0.03	0.00	0.00	0.00	0.00
Continuous bridge	L= 2x50 m	M <sub>mid support</sub>	(bending)	0.01	0.19	0.31	0.40	0.08	0.01	0.00	0.00
Continuous bridge	L= 2x20 m	V <sub>mid support</sub>	(shear)	0.22	0.72	0.05	0.01	0.00	0.00	0.00	0.00
Continuous bridge	L= 2x50 m	V <sub>mid support</sub>	(shear)	0.10	0.40	0.34	0.13	0.03	0.00	0.00	0.00

Table 5: Frequency of number of vehicles leading the extreme traffic load effects - full SEC replacement.

Structural system				Number of vehicles							
and load effect	Span	Load effect		1	2	3	4	5	6	7	8
Simply-supported bridge	L= 20 m	M <sub>midspan</sub>	(bending)	0.37	0.63	0.00	0.00	0.00	0.00	0.00	0.00
Simply-supported bridge	L= 50 m	M <sub>midspan</sub>	(bending)	0.10	0.85	0.04	0.01	0.00	0.00	0.00	0.00
Simply-supported bridge	L= 100 m	M <sub>midspan</sub>	(bending)	0.03	0.53	0.34	0.08	0.01	0.00	0.00	0.00
Simply-supported bridge	L= 200 m	M <sub>midspan</sub>	(bending)	0.01	0.17	0.21	0.25	0.21	0.12	0.02	0.01
Continuous bridge	L= 2x20 m	M <sub>mid support</sub>	(bending)	0.11	0.82	0.07	0.00	0.00	0.00	0.00	0.00
Continuous bridge	L= 2x50 m	M <sub>mid support</sub>	(bending)	0.01	0.29	0.48	0.20	0.02	0.01	0.00	0.00
Continuous bridge	L= 2x20 m	V <sub>mid support</sub>	(shear)	0.23	0.75	0.02	0.00	0.00	0.00	0.00	0.00
Continuous bridge	L= 2x50 m	V <sub>mid support</sub>	(shear)	0.08	0.65	0.23	0.04	0.00	0.00	0.00	0.00

The calculated parameters of the Gumbel distribution of the annual extreme traffic load effects for the "full replacement" scenario are listed in Table 6.

Table 6: Parameters of the Gumbel distribution of the maximum annual traffic load effect with full SEC replacement.

Structural system		L	Mean value	Coefficient of
and load effect	Unit	[m]	$\mu_T$	variation [-]
Simply-supported bridge,	kNm	20	4,437	0.08
bending moment at		50	16,551	0.08
mid-span		100	38,257	0.07
		200	94,480	0.07
Continuous bridge, bending	kNm	2-20	2,681	0.08
moment at middle support		2.50	8,971	0.07
Continuous bridge, shear force	kN	2-20	1,000	0.08
at middle support		2.50	1,396	0.08



# 4.2.3 Assessment of load effects induced by Truck Platooning

The analysis of the load effects induced by TPs mixed with regular traffic concerns only the "full replacement" scenario, where groups of three T11O3 vehicles are replaced by one TP. Two values of the intervehicle gap are considered, 0.3 s and 1.5 s as discussed in section 3.4.2. These two gap values are considered as lower and upper bounds of the gap between two trucks of the same platoon. By considering an average speed of 80 km/h, the intervehicle distance is, respectively, approximately equal to 6.5 m and 33 m. For the sake of comparison with SEC vehicles, the distance between the articulated truck (first part of the vehicle) and the semi-trailer (second part of the vehicle) is estimated about 2 m, which corresponds to a gap of less than 0.1 s.

The minimum intervehicle gap estimated from the 2015 WIM database of the A67R highway is 0.16 s, which corresponds approximately to an intervehicle distance of 3.5 m. The probability density function (PDF) and the cumulative distribution function (CDF) of the intervehicle gap up to 3 s are shown in Figure 22. The graph of the CDF (red curve) shows that the probability of observing gaps less than or equal to 0.3 s in the WIM database is negligible, while almost 45% of the gaps do not exceed 1.5 s. The graph of the PDF (blue curve) shows that the most probable gap is between 1.15 and 1.3 s, where the curve has a maximum.

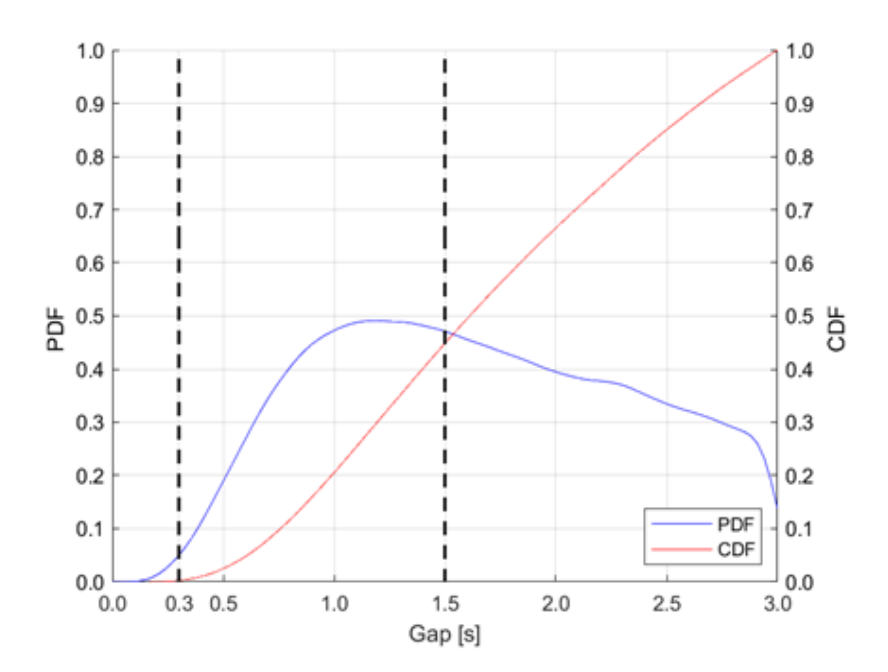


Figure 22: Probability density function and cumulative distribution function of the intervehicle gap up to 3 s.

The probability of exceedance of the extreme daily traffic load effects for the scenarios "normal traffic" and "full replacement" for few cases concerning short-, medium- and long-span bridges. The whole set of plots is reported in Appendix 4D for the bridges and influence lines considered in this project. The following distributions are plotted in each figure:

- the empirical distribution for the scenario "normal traffic" (blue crosses),
- the empirical distribution for the scenario "full replacement by SEC" (red crosses),
- the empirical distribution for the scenario "full replacement by Truck Platooning" with intervehicle gap of 0.3 s (green circles),



- the empirical distribution for the scenario "full replacement by Truck Platooning" with intervehicle gap of 1.5 s (black squares),
- the design value of the traffic load effects for new structures based on the Load Model 1 of NEN-EN 1991-2 (black dashed line),
- the design value of the traffic load effects for existing structures based on the Load Model 1 of NEN-EN 1991-2 (black dash-dotted line).

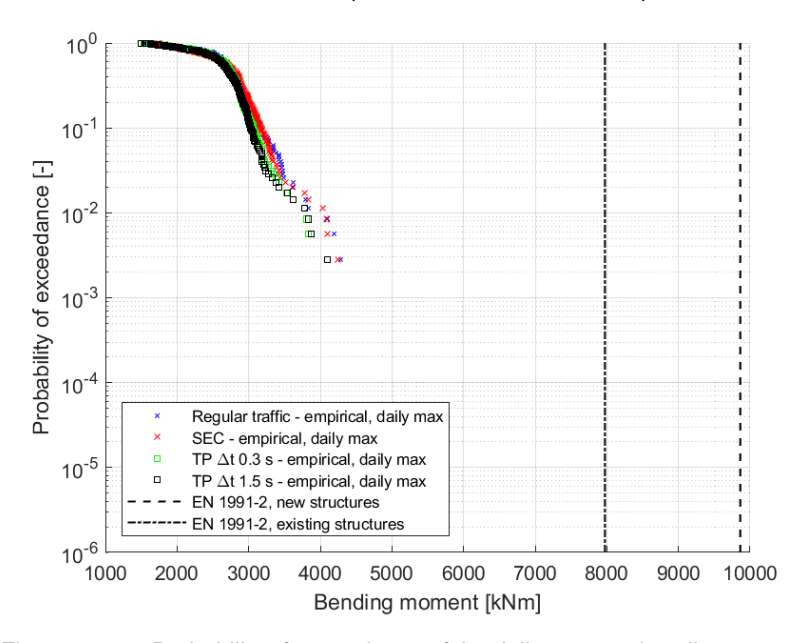


Figure 23: Probability of exceedance of the daily extreme bending moment in the midspan section of a simply supported bridge with length L equal to 20 m. The dashed lines indicate the design values for new and existing structures, calculated according to Appendix 5A.

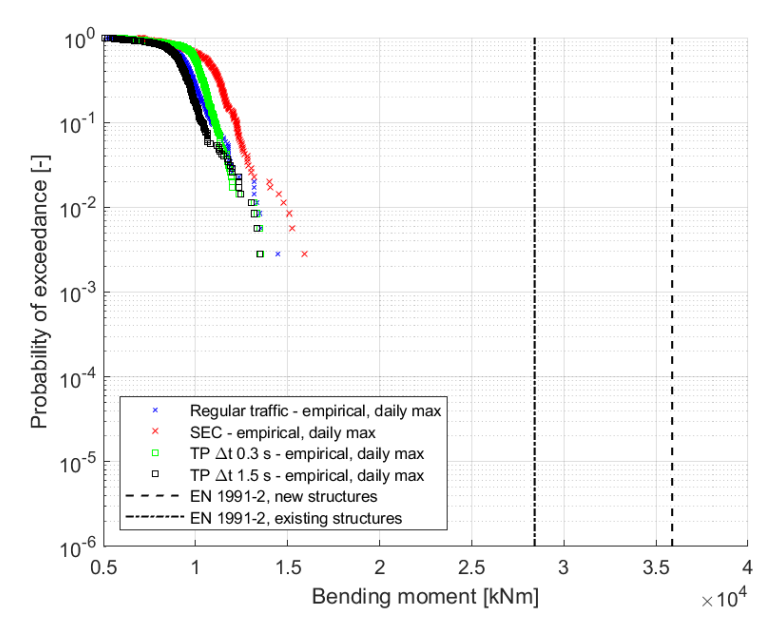


Figure 24: Probability of exceedance of the daily extreme bending moment in the midspan section of a simply supported bridge with length L equal to 50 m. The dashed lines indicate the design values for new and existing structures, calculated according to Appendix 5A.



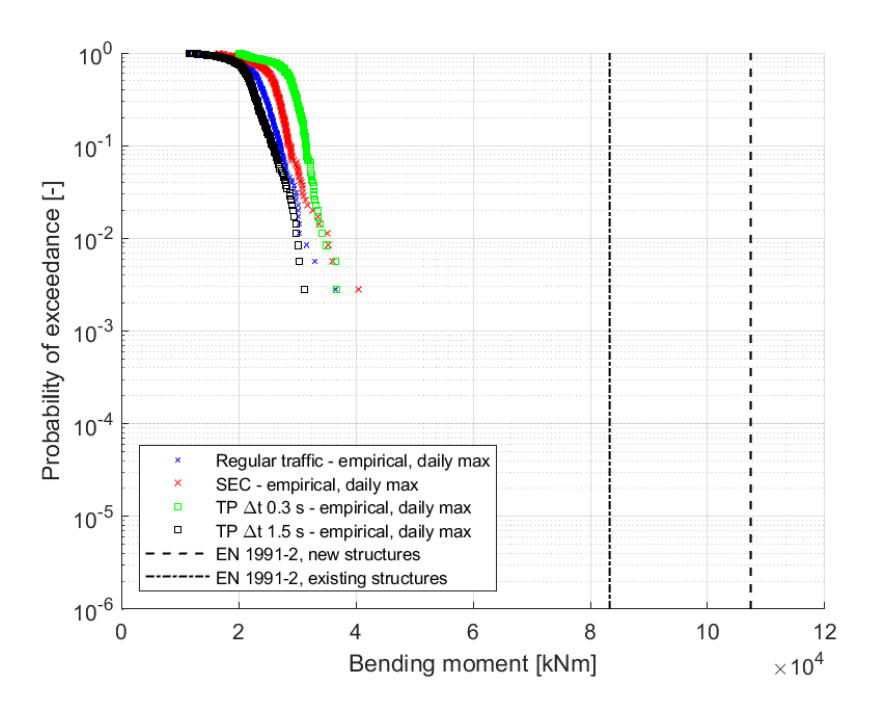


Figure 25: Probability of exceedance of the daily extreme bending moment in the midspan section of a simply supported bridge with length L equal to 100 m.

The following conclusions can be drawn from the analysis:

- truck platooning with an intervehicle gap of 1.5 s leads to load effects not higher than those induced by regular traffic.
- the effect of TP on the right tail of the distribution of the extreme daily load effects is negligible for simply supported short span bridges (e.g. span length of 20 m) because the inter-axle distance and the axle loads govern the load effects in these bridges.
- for simply supported medium span bridges (e.g. span length of 50 m), TP is less severe than SEC vehicles, because of the higher intervehicle distance of TPs compared to SEC vehicles.
- TP with an intervehicle gap of 0.3 s has a significant effect for long span bridges (e.g. simply supported bridge with 100 m and 200 m span length), due to the occurrence of load events characterized by the simultaneous presence on the bridge of the three T11O3 vehicles forming the platoon and other regular vehicles.
- TP with an intervehicle gap of 0.3 s has also a remarkable effect on the bending moment in the inner support of two-span continuous bridges with total length of 40 and 100 m), due to the occurrence of load events characterized by the simultaneous presence on the bridge of at least two T11O3 vehicles forming the platoon and other regular vehicles.
- the effect of TP on the maximum shear force in the section to the left to the intermediate support of a two-span continuous bridge depends on the length of the bridge. No significant difference between truck platooning and regular traffic was observed in the simulations for the 40 m long bridge, because the extreme load effects are governed by the presence of one or two vehicles on the first span of the bridge. In case that the bridge has a total length of 100 m, truck platooning with a gap of 0.3 s leads to similar effects as SEC vehicles (except



for the last part of the tail) due to the presence of two of the three vehicles of the platoon on the first span of the bridge.

The frequency of load events with one or more vehicles simultaneously on the bridge leading to the extreme daily load effects is given in Table 4, Table 7 and Table 8 for TPs with gap of 0.3 s and 1.5 s, respectively. By comparison with the "full replacement" scenario (Table 5), it can be observed that the frequency of load events with only one vehicle on the bridge in case of TP is higher than the corresponding value for SEC. This is caused by considering in the simulation program a TP as one single vehicle comprising three groups of five axles each one.

When comparing Table 4, Table 7 and Table 8, it can be observed that the values are approximately the same for short span bridges (length of 20 m) because the load events are characterized by one or two vehicles on the bridge. In case of simply supported bridges with longer spans, the frequency of events with one TP and one or more regular vehicles simultaneously on the bridge increases and the difference between the two gaps scenarios reduces as the span length increases. Regarding the two-span bridges, the values given in the tables depend on the considered load effect. In case of bending, the difference between the two gap scenarios decreases as the span length increases, while it is the opposite for shear because the shear force is governed by vehicles only on one span of the bridge.

Table 7: Frequency of number of vehicles leading the extreme traffic load effects – full TP replacement (0.3 s gap).

Structural system			Number of vehicles								
and load effect	Span	Load effe	ct	1	2	3	4	5	6	7	8
Simply-supported bridge	L= 20 m	M <sub>midspan</sub>	(bending)	0.40	0.60	0.00	0.00	0.00	0.00	0.00	0.00
Simply-supported bridge	L= 50 m	M <sub>midspan</sub>	(bending)	0.13	0.81	0.05	0.00	0.00	0.00	0.00	0.00
Simply-supported bridge	L= 100 m	M <sub>midspan</sub>	(bending)	0.10	0.62	0.25	0.03	0.00	0.00	0.00	0.00
Simply-supported bridge	L= 200 m	M <sub>midspan</sub>	(bending)	0.05	0.24	0.32	0.29	0.07	0.02	0.01	0.00
Continuous bridge	L= 2x20 m	M <sub>mid support</sub>	(bending)	0.14	0.77	0.08	0.00	0.00	0.00	0.00	0.00
Continuous bridge	L= 2x50 m	M <sub>mid support</sub>	(bending)	0.07	0.45	0.38	0.10	0.00	0.00	0.00	0.00
Continuous bridge	L= 2x20 m	V <sub>mid support</sub>	(shear)	0.29	0.70	0.01	0.00	0.00	0.00	0.00	0.00
Continuous bridge	L= 2x50 m	V <sub>mid support</sub>	(shear)	0.09	0.69	0.19	0.03	0.00	0.00	0.00	0.00

Table 8: Frequency of number of vehicles leading the extreme traffic load effects – full TP replacement (1.5 s gap).

Structural system		Number of vehicles									
and load effect	Span	Load effe	ct	1	2	3	4	5	6	7	8
Simply-supported bridge	L= 20 m	M <sub>midspan</sub>	(bending)	0.39	0.61	0.00	0.00	0.00	0.00	0.00	0.00
Simply-supported bridge	L= 50 m	M <sub>midspan</sub>	(bending)	0.21	0.70	0.08	0.01	0.00	0.00	0.00	0.00
Simply-supported bridge	L= 100 m	M <sub>midspan</sub>	(bending)	0.10	0.44	0.35	0.09	0.02	0.00	0.00	0.00
Simply-supported bridge	L= 200 m	M <sub>midspan</sub>	(bending)	0.06	0.26	0.36	0.22	0.07	0.02	0.00	0.00
Continuous bridge	L= 2x20 m	M <sub>mid support</sub>	(bending)	0.36	0.49	0.14	0.01	0.00	0.00	0.00	0.00
Continuous bridge	L= 2x50 m	M <sub>mid support</sub>	(bending)	0.07	0.46	0.34	0.11	0.02	0.00	0.00	0.00
Continuous bridge	L= 2x20 m	V <sub>mid support</sub>	(shear)	0.31	0.66	0.03	0.00	0.00	0.00	0.00	0.00
Continuous bridge	L= 2x50 m	V <sub>mid support</sub>	(shear)	0.20	0.52	0.23	0.05	0.01	0.00	0.00	0.00



# 4.2.4 Comparison between the traffic load effects induced by regular vehicles, SEC vehicles and LM1 of NEN-EN1991-2

The analysis of the load effects induced by SEC vehicles in bridges is performed in two steps:

- step 1: comparison of the load effects of individual SEC vehicles with the load effects due to regular traffic,
- step 2: comparison of the extreme daily load effects due to SEC vehicles and other vehicles with the extreme daily load effects due regular traffic.

The first step provides the reader with conclusions on the aggressiveness of individual SEC vehicles compared to the current traffic conditions as recorded in the WIM database. The second step enables the evaluation of the impact of permitting the transit of SEC vehicles in combination with regular traffic on the extreme load effects and, as shown in the sections 5 and 6, on the reliability of bridges.

The load effects of individual SEC vehicles are compared in Figure 26 (short influence lines), Figure 27 (medium span bridges) and Figure 28 (long span bridges) with the load effects due regular traffic. The full set of figures can be found in Appendix 3C. Three curves are plotted in each figure:

- the green curve represents the probability of exceedance of the maximum load effect per load event due to regular traffic, where a load event is defined here as an event characterised by one or more vehicles on the bridge
- the red curve refers to the maximum load effect due to SEC vehicles travelling alone on the bridge
- the blue curve concerns the extreme daily load effects due to regular vehicles only.

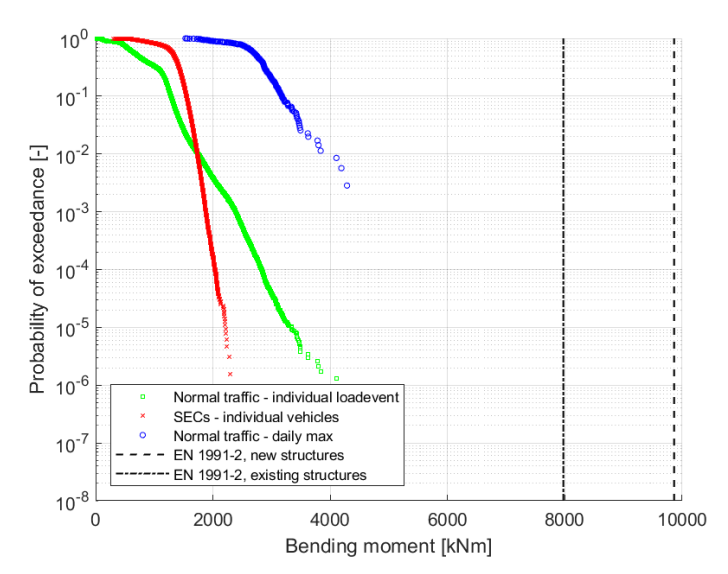


Figure 26: Probability of exceedance of the extreme bending moment in the midspan section of a simply supported bridge with length L equal to 20 m.



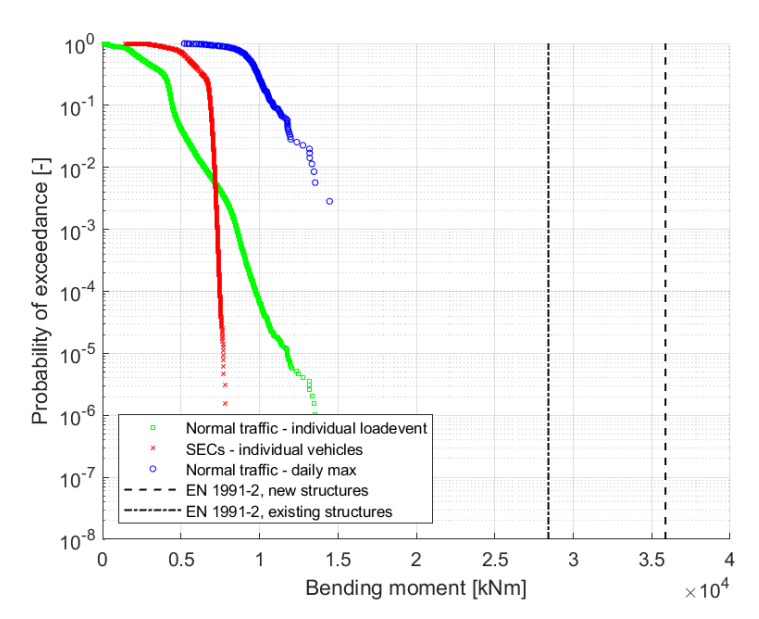


Figure 27: Probability of exceedance of the extreme bending moment in the midspan section of a simply supported bridge with length L equal to 50 m.

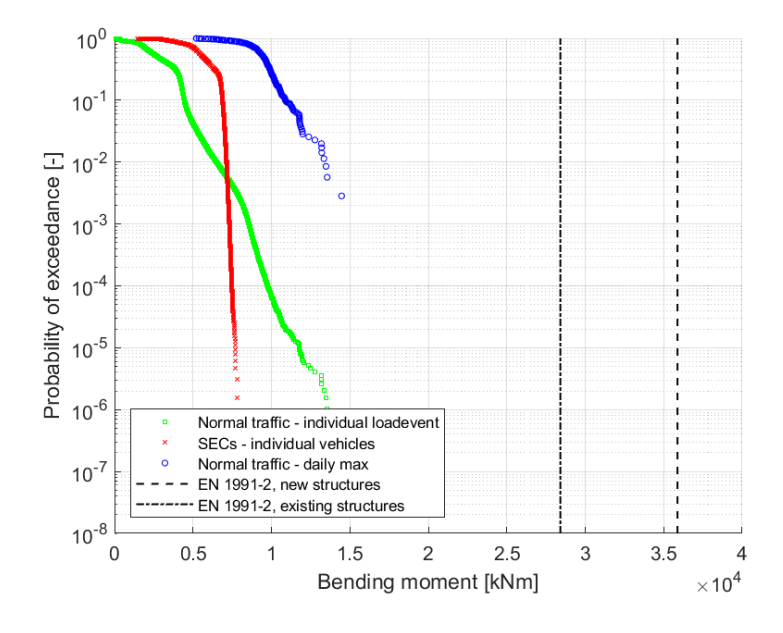


Figure 28: Probability of exceedance of the extreme bending moment in the midspan section of a simply supported bridge with length L equal to 100 m.

The following conclusions can be drawn from the figures above:

• SEC vehicles alone are not critical for the safety of the bridges considered in this investigation: the load effects of individual SEC vehicles do not exceed the knickpoint between the first and the second branch of the extreme daily traffic load effects (blue curve). In addition, the comparison of the green curve with the red one shows that there exist regular vehicles or combinations of regular vehicles leading to higher load effects than the most loaded SEC vehicles: the maximum load effects due to one SEC vehicle are about 50% of the maximum load effects induced in by regular traffic;



the maximum GVW of 76 t considered for SEC vehicles influences the maximum load
effects only for medium- to long-span bridges: in case of influence lengths equal to or
higher than 50 m the second branch of the red curve (SEC vehicles) tends to be vertical. This
is not surprising, because the longer the influence length, the higher the effect of the GVW
and number of vehicles travelling simultaneously on the bridge.

# 4.2.5 Comparison between the impact of SEC vehicles based on simulation and the measurement campaigns on the Moerdijk bridge and Geldrop viaduct

The analysis of strain measurements performed during the trails campaigns of SEC vehicles on the Moerdijk bridge and Geldrop viaduct is documented in [1] and [2]. The probability of exceedance of the minute, hourly and daily extreme stresses at the locations of the sensors are plotted in Figure 29 (Moerdijk bridge) and Figure 30 (Geldrop viaduct) as well as the measured stresses due to the SEC vehicle (vertical dashed lines).

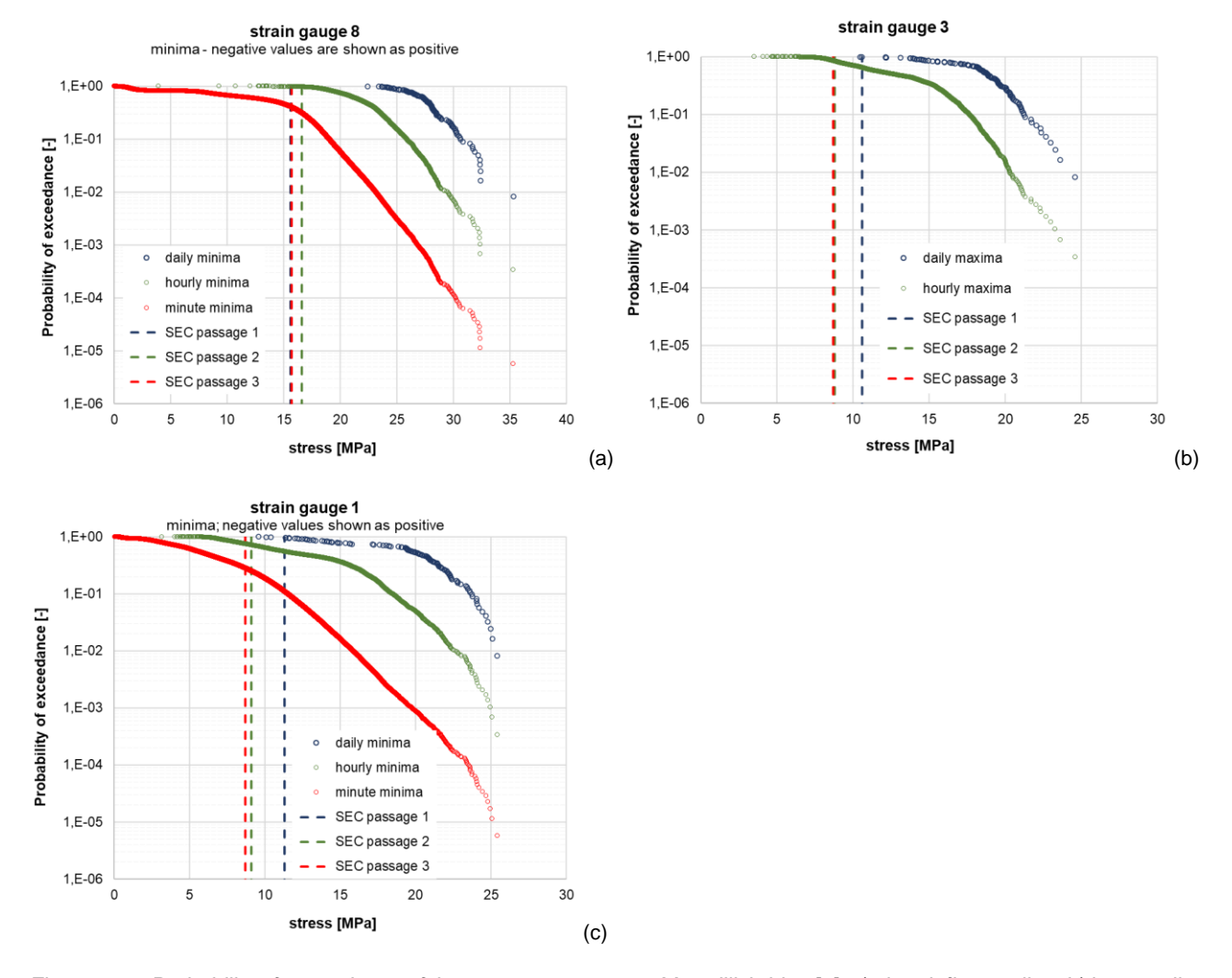


Figure 29: Probability of exceedance of the extreme stresses at Moerdijk bridge [1]: a) short influence line; b) intermediate influence line; c) long influence line.



In both Figure 29 and Figure 30 it can be observed that the single SEC vehicle leads to small load effects compared to the extreme daily load effects. Even though the full comparison between the measured strains on the Moerdijk bridge and Geldrop viaduct and the corresponding values from the simulations has not been reported in this document, the conclusions of the simulations regarding the effect of individual SECs on the extreme daily load effects are qualitatively confirmed by the measurement campaign. The load effects induced by the SEC vehicle used in the trial campaign in the short, medium and long bridges considered in this report can be summarized as follows:

short influence line (20 m long simply supported bridge): 1,373 kNm,
intermediate influence line (50 m long simply supported bridge): 6,383 kNm,

long influence line (100 m long simply supported bridge):
 15,667 kNm

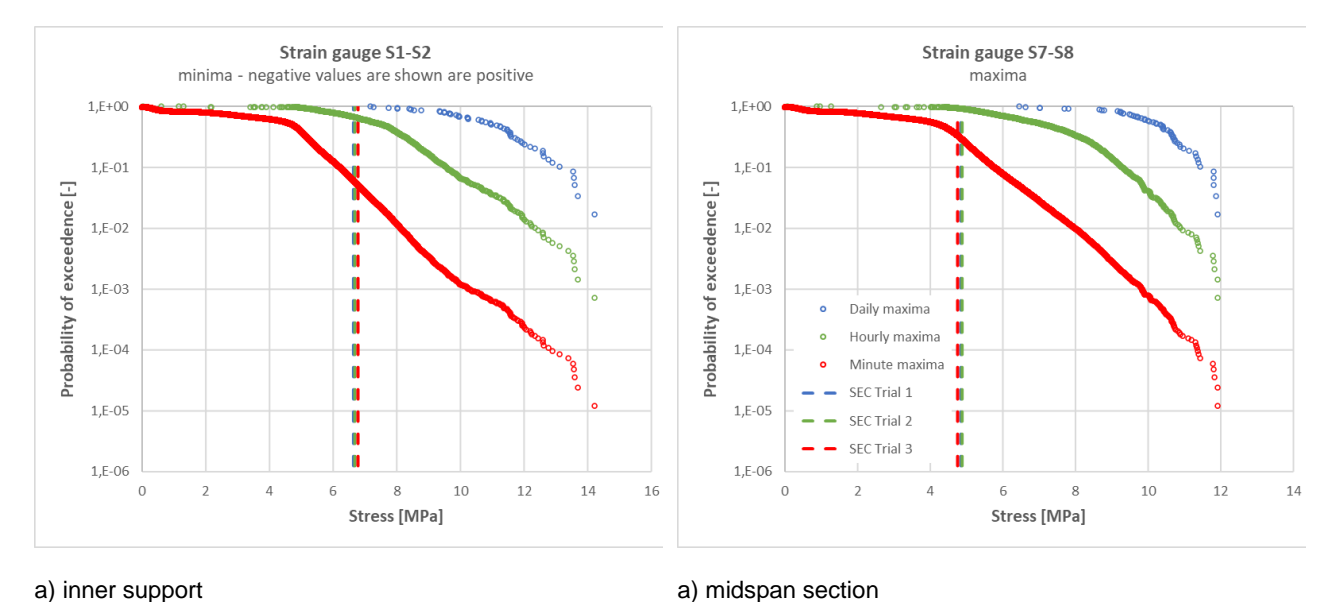


Figure 30: Probability of exceedance of the extreme stresses at Geldrop viaduct [2].

It can be observed in Figure 26 (short span bridges), Figure 27 (medium span bridges) and Figure 28 (long span bridges) that the values listed above are comparable with the values of the left tail of the distribution of the extreme daily load effects due to regular traffic. This is in agreement with the conclusions of the measurement campaign on the Moerdijk bridge and Geldrop viaduct.

# 4.3 Traffic load effects in bridges for FLS verification

## 4.3.1 Design S-N curve according to NEN-EN 1993 1-9

Damage due to fatigue is in this study calculated based on S-N curves, which are defined in NEN-EN 1993-1-9 [17]. The characteristic curve used for fatigue limit state verification is shown in Figure 31 and is defined by three distinct points:

- 1) the detail category defines the stress range for  $N_C = 2.10^6$  cycles (in this case  $\Delta \sigma_C = 80$  MPa);
- 2) the constant amplitude fatigue limit (knee point) at  $N_D = 5.10^6$  and  $\Delta \sigma_D = 58.9$  MPa and;



3) the cut-off limit at  $N_L = 1.10^8$  and  $\Delta \sigma_L = 32.4$  MPa, below which fatigue damage is not taken into account.

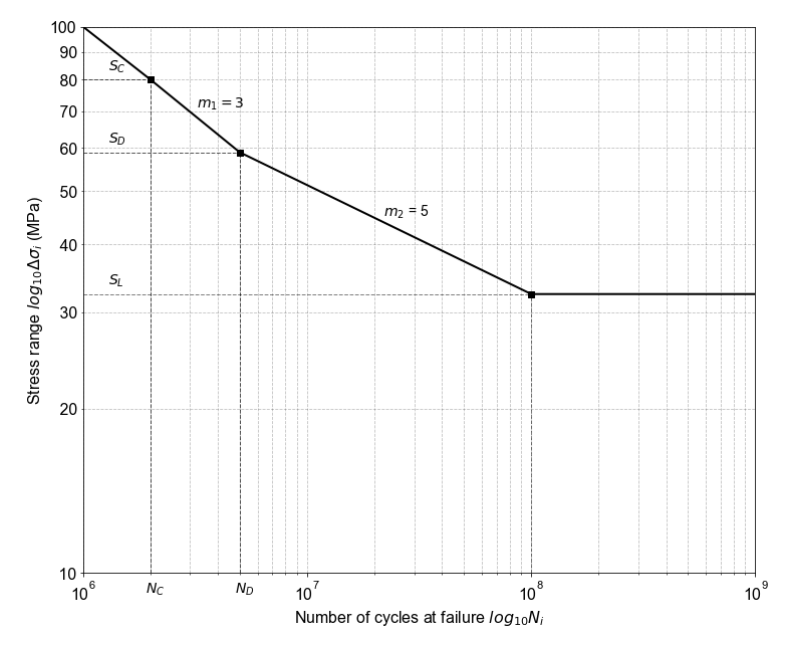


Figure 31: The characteristic S-N curve used in case study 3.

The design S-N curve is then obtained by reducing the three stress points:  $\Delta \sigma_{\rm C}/\gamma_{Mfat}$ ,  $\Delta \sigma_{\rm D}/\gamma_{Mfat}$  and  $\Delta \sigma_{\rm L}/\gamma_{Mfat}$ , where  $\gamma_{Mfat} = 1.35$  is the partial factor for fatigue strength as defined in NEN-EN 1993-1-9 [17].

The cumulative fatigue damage is calculated based on the performed fatigue analysis, which results in a stress histogram containing the number of stress reversals caused by the continuously variable vehicle load being exerted on the structure leading to fatigue. The accumulated fatigue damage D is calculated using Miner's rule, as the sum of the ratio between the counted number of stress reversals  $n_i$  in each stress range bin  $\Delta \sigma_i$  and the number of stress reversals  $N_i$  at failure specified in the design S-N diagram as follows:

$$D = \sum_{i=1}^{m} \frac{n_i}{N_i}$$
 (4.9)

# 4.3.2 Assessment of the stress histogram for traffic with regular vehicles

The stress histogram is calculated based on Weight-In-Motion (WIM) data. Based on the influence lines presented in section 3.6.1.4, stress due a specific vehicle in the WIM database can be calculated at certain locations along the length of the structure. The rainflow counting method is the used to count the number of stress reversals  $n_i$  for a particular stress range (bins)  $\Delta \sigma_i$ .

The stress histogram for regular vehicles (under normal traffic conditions) is presented Figure 32. In the figure, the design S-N curve is also shown (solid black line), as well as the cut-off limit (dashed



vertical line). The fatigue damage caused by regular vehicles in 1 year based on the design S-N curve is calculated to be D = 0.043.

From the stress histogram for regular vehicles it can be concluded that most of the stress histogram bins are under the cut off limit – neglected in the fatigue damage calculation, hence the 1-year fatigue damage is low.

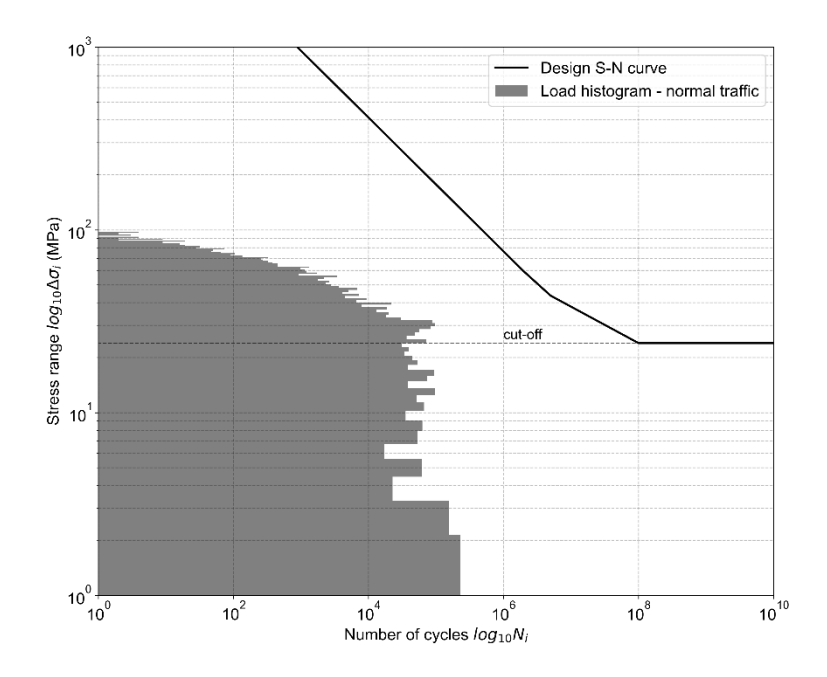


Figure 32: Yearly stress histogram for the structure with span L = 100 based on normal traffic conditions, and the design S-N curve.

# 4.3.3 Assessment of the stress histogram for traffic with SEC vehicles

The stress histogram for traffic with SEC vehicles (full replacement) is calculated based on modified Weight-In-Motion (WIM) data, where all pairs of T11O3 were replaced with a SEC vehicle. Based on the influence lines presented in section 3.6.1.4, stress due a specific vehicle in the WIM database can be calculated at certain locations along the length of the structure. The rainflow counting method is used to count the number of stress reversals  $n_i$  for a particular stress range (bins)  $\Delta \sigma_i$ .

The stress histograms for traffic with SEC vehicles (full replacement) are presented for a structure with span L = 100 m in Figure 33. In the figure, the design S-N curve is also shown (solid black line), as well as the cut-off limit (dashed vertical line). The fatigue damage caused by traffic under full replacement with SEC vehicles accumulated in 1 year and based on the design S-N curve is calculated to be D = 0.1372.

From the stress histograms for regular vehicles it can be concluded that for the influence line considered (L = 100 m) more stress reversals above the cut-off limit calculated in case of full replacement with SEC, which leads to higher fatigue damage in comparison to normal traffic conditions.



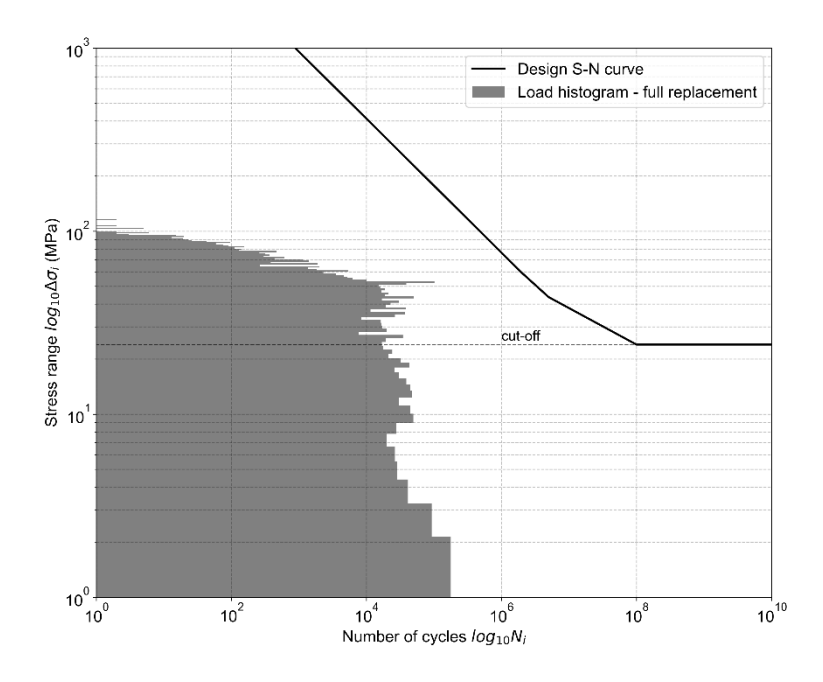


Figure 33: Yearly stress histogram for the structure with span L = 100 m based on the full replacement with SEC vehicles and the design S-N curve.

# 4.3.4 Comparison of fatigue damage SEC versus two T1103 vehicles

In order to further investigate the cause of the significant difference of the calculated reliability values between full SEC replacement and normal traffic as well as gradual replacement scenario, the fatigue damage of each pair of T11O3 vehicles driving on the bridge at the same time was compared to a single SEC, which is made up from the exact same T11O3 vehicles.

To this end, two possible ranges of the inter-vehicle distances between the T11O3s were considered:

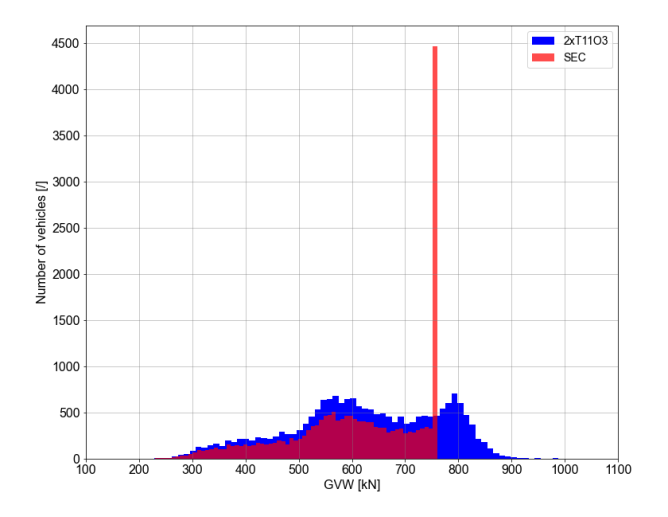
- 1) less than 10 meters.
- 2) between 10 and 20 meters.

These inter-vehicle distances were chosen in order to study how the distance between two T1103 vehicles affects the accumulated fatigue damage and how does the fatigue damage cause by pairs of T1103 vehicles compare to SECs. For the first range, 19.705 pairs of T1103s (and SECs) that meet the requirement were filtered from the WIM database from 2015, while for the second range 1.456 pairs of T1103s (and SECs) were found. Here, only the results a fatigue analysis on the vehicles corresponding to inter-vehicle distance less than 10 meters are presented since the results for both ranges are identical.

In Figure 34 the histogram presenting the number of T11O3 pairs and SECs according to their gross vehicle weight (GVW) is shown. It can be observed that the WIM system detected T11O3 pairs matching the inter-vehicle distance filter where the sum of the weight of both vehicles was higher than 76 t. In the case of SECs it was assumed that maximum allowed GVW is observed, meaning that more than 20% of filtered SECs had a weight of 76 t. In Figure 35, a comparison between the cumulative histograms for the T11O3 pairs and SECs is presented, showing for every stress reversal value  $\Delta \sigma_i$  the number of cycles (stress reversals)  $N_i$  less than or equal to  $\Delta \sigma_i$ . It can be seen that for



each stress reversal value under 50 MPa the SEC vehicles cause a higher number of stress reversals, meaning that more fatigue damage is inflicted on the structure.



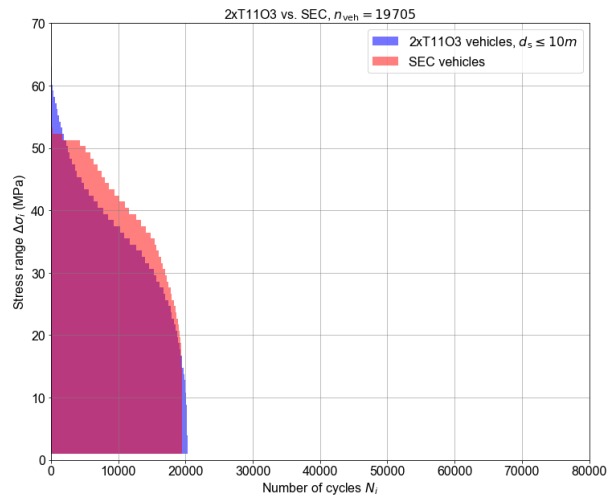
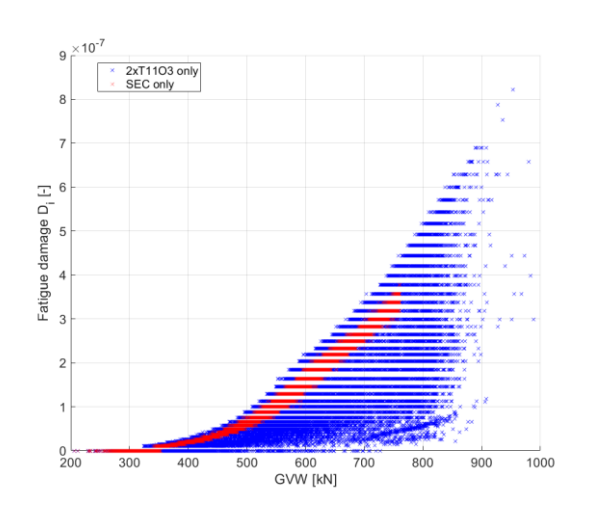


Figure 34: Number of SEC (red) and T1103 pairs (blue) for each recorded GWV considering intervehicle distance ≤ 10m.

Figure 35: Cumulative stress histogram for SEC vehicles (red) and T11O3 pairs (blue) considering inter-vehicle distance ≤ 10m.

In Figure 36 the fatigue damage caused by a single T11O3 pair and SEC vehicle  $D_i$  is shown in terms of its GWV. SECs seem to show a consistently higher level of fatigue damage per vehicle, while for the T11O3 pair the level of individual vehicle fatigue damage varies considerably.



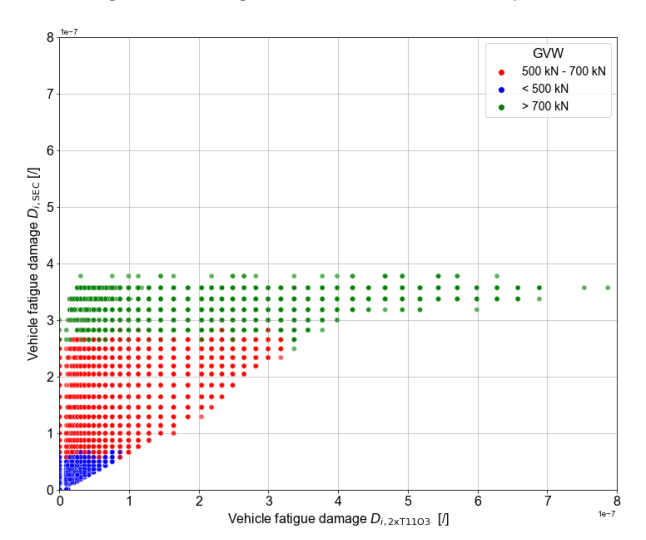


Figure 36: Fatigue damage caused by each SEC (red) and T11O3 (blue) vehicle as a function of its GVW considering inter-vehicle distance ≤ 10m.

Figure 37: Comparison of the fatigue damage caused by each SEC vehicle and the corresponding T1103 pair considering inter-vehicle distance ≤ 10m.

Similar can be observed in Figure 37, which shows the individual damage of each SEC in comparison to the individual fatigue damage to the pair of T11O3 it replaced. This figure would be linear in case that each SEC causes the exact same amount of fatigue damage as its corresponding T11O3 pair. But since a majority of points are above the diagonal, the fatigue damage of each SEC is larger



compared to the corresponding T11O3. This results in a higher cumulative annual fatigue damage due to SECs in comparison to T11O3 pairs when considering inter-vehicle distance ≤ 10m, as shown in Figure 38. Since the fatigue damage of each SEC vehicle has been compared with the fatigue damage of the corresponding T11O3 vehicles in absence of other vehicles, it is not possible to draw conclusions about the effects of SEC vehicles on the remaining lifetime of steel bridges based on Figure 38. The investigation of the change of remaining lifetime due to the introduction of SEC vehicles is presented in chapter 7 of this report.

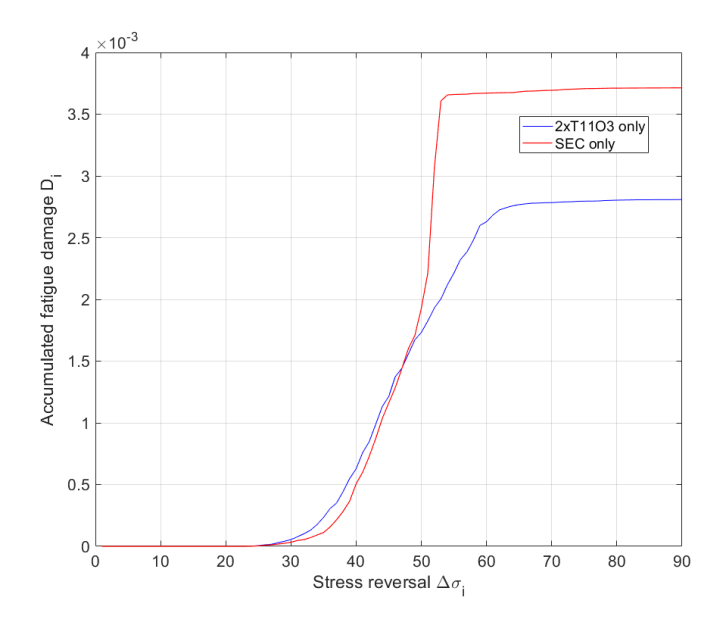


Figure 38: Cumulative annual fatigue damage for SEC vehicles (red) and T11O3 pairs (blue) as a function of GVW considering inter-vehicle distance ≤ 10m.



# 5 REINFORCED CONCRETE BRIDGE - ULS CONDITIONS

## 5.1 Introduction

In the consideration of reinforced concrete bridge under ULS, the reliability analysis is performed for two bridge models: simply-supported structure and a continuous structure with various span length and the calibration of resistance is consequently performed for different assessment situations (new or existing structure, see section 3.6). The limit state functions, probabilistic models and results are presented in the following section.

Additionally, reliability analyses are performed on the basis of the values of the resistance of the structure calculated based on older normative documents. This calculation procedure is described in Appendix 5B. These reliability analyses are performed on the basis of the same probabilistic model as the analyses based on the calibrated value of the resistance.

# 5.2 Calculation methodology

## 5.2.1 Limit state function

For the study of the resistance of a reinforced concrete bridge the following limit-state function is used:

$$Z = R - E = R - (\theta_G \cdot G + \theta_{trend} \cdot \theta_{snat,var} \cdot \theta_{DAF} \cdot \theta_T \cdot T)$$
 (5.1)

where:

- R is the resistance of the structure to the load effect E;
- E is the load effect acting on the structure.

Furthermore, the load effect is considered as a combination of the permanent load effect G and traffic load effect T. The following uncertainties are taken into account for the two considered load effects:

- $\theta_G$  is the random variable representing model uncertainty, reflecting the uncertainty in the structural model used to estimate evaluate the load effect G induced by permanent actions:
- $\theta_{trend}$  is the random variable representing uncertainty about the development of future traffic trends:
- θ<sub>spat.var</sub>. is the random variable representing uncertainty about spatial variability of traffic loads in the Netherlands;
- $\theta_{DAF}$  is the random variable representing uncertainty regarding the dynamic interaction between the bridge and the vehicles;
- $\theta_T$  is the random variable representing the uncertainty of the structural model (influence lines) used to evaluate the traffic load effect T.



# 5.2.2 Stochastic variables

#### 5.2.2.1 Traffic load effect

#### Reference scenario

In the reference scenario (normal traffic conditions without SEC vehicles), the traffic load effect model is obtained based on Weight-In-Motion (WIM) data. The traffic data from the A67 motorway in The Netherlands from the whole of 2015 was analysed. Based on vehicle weight identified by the WIM system and the influence lines presented earlier, the load effect on the structure was calculated and consequently the empirical distribution function of the daily maxima was constructed. This sample distribution was fitted with a Gumbel maximum distribution and the yearly maximum traffic load effect was consequently obtained expressed with the mean  $(\mu_T)$  and variance  $(\sigma_T^2)$  of its distribution. The calculated sample parameters for a specific structural system and influence length are given in Table 9.

In the probabilistic calculation, the reliability analysis is performed to obtain the reliability index of the structure for a certain time period, for example for the next 100 years for new structures and 30 years for existing structures. Therefore, the distribution of the extreme load effects for the relevant time period (e.g. N years) has to be determined. If the distribution of the annual maximum traffic load effect model is modelled by the Gumbel distribution with mean value  $\mu_T$  and standard deviation  $\sigma_T$ , the parameters of the Gumbel distribution of the extreme load effects for a period of N years are calculated

$$\mu_{T,N} = \mu_T + 0.78 \cdot ln(N) \cdot \sigma_T \tag{5.2}$$

$$\sigma_{T.N} = \sigma_T \tag{5.3}$$

Where  $\mu_{T,N}$  and  $\sigma_{T,N}$  are the mean and standard deviation of the traffic load effect distribution, scaled to year N.

Table 9: Mean and CoV of the annual maximum traffic load effect distribution under normal traffic conditions (one slow and one fast lane in one direction).

Structural system	L [m]	Mean $\mu_T$ [kNm]	CoV¹ [-]
Simply-supported beam,	20	4,404	0.08
bending moment at	50	15,055	0.08
mid-span	100	34,949	0.07
	200	92,454	0.06
Continuous beam, bending	2.20	2,543	0.08
moment at middle support	2.50	8,921	0.07
Continuous beam, shear force	2.20	956	0.08
at middle support	2.50	1,288	0.08

<sup>&</sup>lt;sup>1</sup>Standard deviation is calculated as:  $\sigma_T = CoV \cdot \mu_T$ 

## SEC scenario - full replacement

The full replacement scenario traffic load effect parameters presented in Table 10 were obtained by modifying the original WIM database from 2015 and replacing each pair of T11O3 vehicles with one SEC vehicle. Based on the influence lines for each of the assessment scenarios, the load effect



exerted on the structure was calculated. By performing the same procedure as for the reference scenario, the Gumbel maximum distribution was used to fit the maximum annual traffic load effect. The calculated parameters are shown in Table 10.

Table 10: Mean and CoV of the annual maximum traffic load effect distribution under full SEC replacement (one slow and one fast lane in one direction).

Structural system	L [m]	Mean $\mu_T$ [kNm or kN]	CoV <sup>1</sup> [-]
Simply-supported beam,	20	4,437	0.08
bending moment at	50	16,551	0.08
mid-span	100	38,257	0.07
	200	94,480	0.07
Continuous beam, bending	40	2,681	0.08
moment at middle support	100	8,971	0.07
Continuous beam, shear force	40	1,000	0.08
at middle support	100	1,396	0.08

<sup>&</sup>lt;sup>1</sup>Standard deviation is calculated as:  $\sigma_T = CoV \cdot \mu_T$ 

# SEC scenario – gradual replacement

The traffic load effect scenarios presented in chapter 3 represents two extreme cases with either no adoption of SECs or with 100% replacement of T11O3 vehicles from the first year of consideration onwards. A gradual replacement scenario as presented in Figure 12 in chapter 3 is assumed to be more realistic. In this scenario, the share of replacement is capped at 64%, which is reached after 80 years.

The growth models is taken into account in the probabilistic analyses by calculating the maximum annual traffic load effect mean and variance for each considered year by interpolating between the mean and variance values for reference (0% replacement) and full replacement scenarios given the percentage of replaced SEC corresponding to that year. The Gumbel maximum distribution with the interpolated annual mean and variance is then sampled to obtain the parameters of the traffic load effect random variable distribution that corresponds to the year of calculation.

#### 5.2.2.2 Permanent load effect

In the calculation, the mean value of the permanent load effect  $\mu_G$  is calculated based on the load ratio  $\chi$ , which expresses the share of the traffic load effect in the total load effect:

$$\chi = \frac{\mu_{T,1year}}{\mu_G + \mu_{T,1year}} \tag{5.4}$$

#### where

- μ<sub>T,1year</sub> is the mean value of the distribution of the annual maximum of the traffic load effect T listed in Table 9;
- μ<sub>G</sub> is the mean value of the distribution of the permanent load effect G.

Based on known load ratio and traffic load effect model, the mean value of the permanent load effect model is calculated as follows:



$$\mu_G = \frac{1 - \chi}{\chi} \,\mu_{T,1year} \tag{5.5}$$

The following values of  $\chi$ , are used in the calculation depending on the total length L of the considered structure:

Table 11: Load ratios  $\chi$  based on total structure span L (op basis van [6]).

<i>L</i> [m]	χ [-]
20	0.5
40	0.45
50	0.4
100	0.3
200	0.1

# 5.2.2.3 Traffic trend uncertainty model

The traffic trend stochastic variable expresses the uncertainty of future development of traffic. In the calculations it is considered as a multiplicative factor on the traffic load effect. It is assumed that the trend is a time-dependent random variable, with the parameters of its distribution depending on the span length of the structure L, and on the year of service t. Additionally, the assumptions made are different for new and for existing structures, where for the latter the elapsed service life  $\tau$  is taken in the calculation of trend model parameters.

For new structures, it is assumed that both the traffic load as well as the uncertainty about the growth of traffic will linearly increase from construction throughout the considered time period of 100 years.

For existing structures, it is again assumed that the traffic load effect and its uncertainty increase during the considered time period. A distinction from new structures is made in that the growth begins from the year of elapsed service life of the structure. An example of such growth is given in Figure 39 (new structure) and Figure 40 (existing structure).

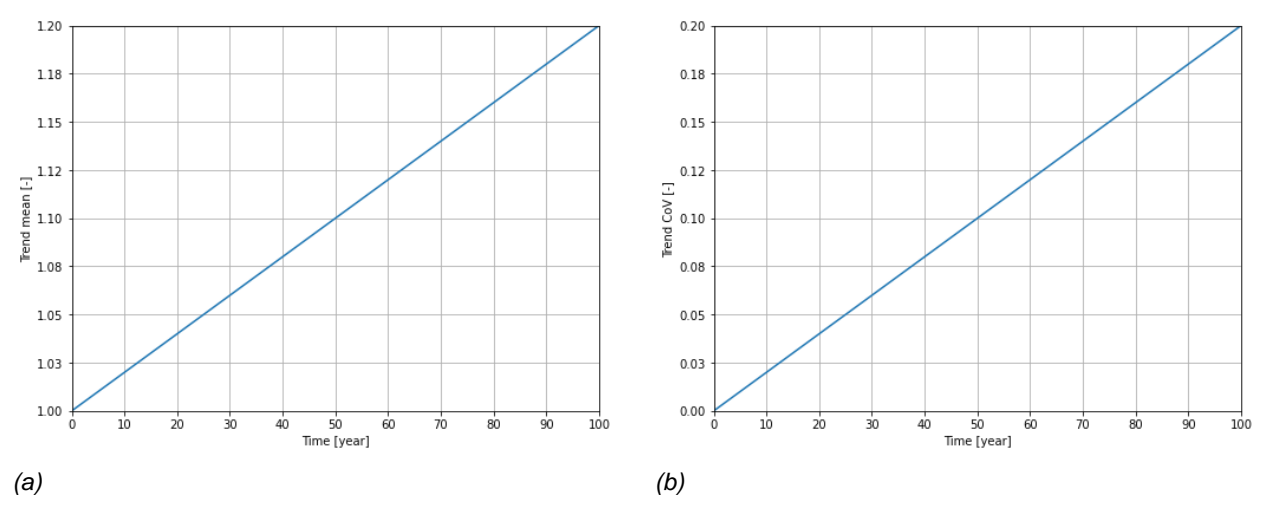
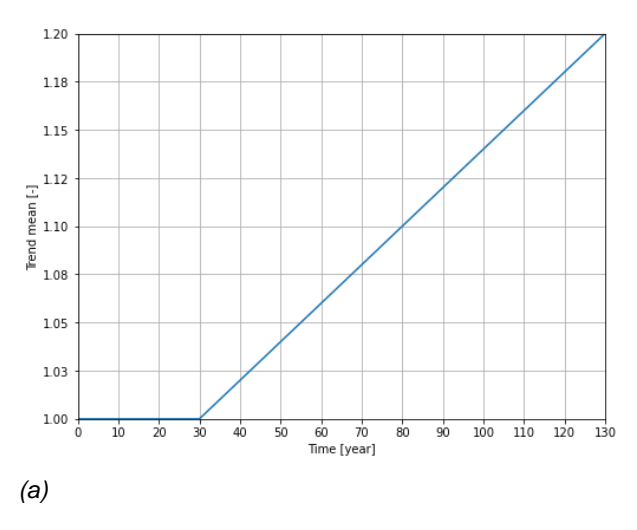


Figure 39: Mean (a) and coefficient of variation (b) of the trend stochastic variable  $\theta_{trend}$  as a function of time for a new structure with influence length L = 50 m.





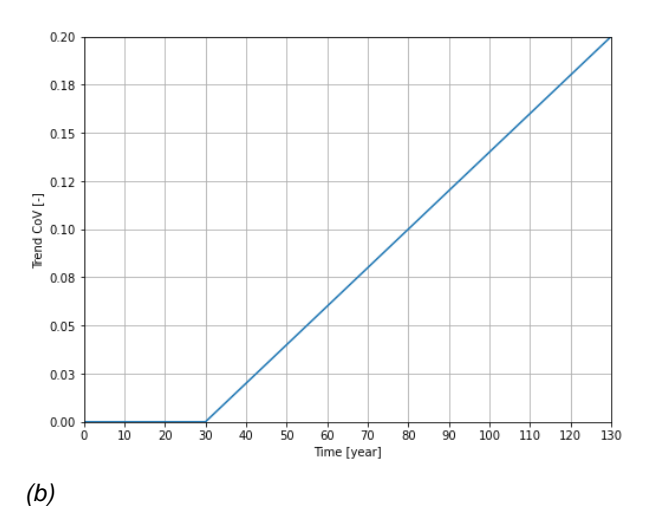


Figure 40: Mean (a) and coefficient of variation (b) of the trend stochastic variable  $\theta_{trend}$  as a function of time for an existing structure with influence length L = 50 m and elapsed service life 30 years.

Table 12 presents the equations of the trend model parameters depending on the span length of the structure L, year t and elapsed service life  $t_0$ .

Table 12: Equations for calculating the time-dependent parameters of the trend uncertainty stochastic random variable  $\theta_{trend}$ .

	L <sup>*</sup> [m]	Mean value [-]	CoV [-]
New structure	20 – 50	$1 + \frac{0.10 \cdot t}{50}$	$\frac{0.10 \cdot t}{50}$
	100	$1 + \frac{0.25 \cdot t}{50}$	$\frac{0.12 \cdot t}{50}$
	200	$1 + \frac{0.30 \cdot t}{50}$	$\frac{0.15 \cdot t}{50}$
Existing structure (for $t > t_0$ )	20 – 50	$1 + \frac{0.10 \cdot (t - t_0)}{50}$	$\frac{0.10 \cdot (t - t_0)}{50}$
	100	$1 + \frac{0.25 \cdot (t - t_0)}{50}$	$\frac{0.12 \cdot (t - t_0)}{50}$
	200	$1 + \frac{0.30 \cdot (t - t_0)}{50}$	$\frac{0.15 \cdot (t - t_0)}{50}$

<sup>\*</sup>span length of the structure.

## 5.2.2.4 Other stochastic variables

Stochastic variables presented in section 5.2.1, their distributions and the selection of parameters of distribution is presented in Table 13.

Table 13: Parameters of the stochastic variables in the distributions used in the reinforced concrete bridge under ULS conditions.

Variable	Distribution	Mean	CoV	Reference	
R	L-N	calibrated	0.10	TNO R11640	[18]
G	N	see 5.2.2.2	0.07	TNO R11640	[18]
T	GUM	varies, see Table 9.	varies, see Table 9.	-	
$ heta_{ ext{trend}}$	N	see 5.2.2.3	see 5.2.2.3	TNO R1814	[7]
θ <sub>spat.var.</sub>	N	0.86	0.07	TNO R1814	[18]

t - year in consideration.

 $t_0$  – elapsed service life.



Variable	Distribution	Mean	CoV	Reference	
$ heta_{DAF}$	N	1.10	0.05	TNO R11640	[18]
$\theta_{ ext{stat}}$	N	1.00	0.05	TNO R1814	[7]
<b>∂</b> <sub>G</sub>	N	1.00	0.07	TNO R11640	[18]
$\theta_{T}$	N	1.00	0.10	TNO R1814	[7]

N - normal distribution

GUM - Gumbel distribution of the maximum

#### 5.3 Results

#### 5.3.1 Calculations based on the calibrated resistance

The results for the concrete bridge under extreme load conditions are given in Appendix 6. The calibrated resistance based on the reference scenario is given in Table 24 in Appendix 6A. From Table 24 it can be observed that the value of the calibrated resistance is the highest in the case of new structures. This is due to higher value of reliability being demanded for a longer period of time (reference period) as highlighted in section 3.6.

In Table 26 to Table 28 the calculated cumulative and annual reliability for new and existing structures are given at the begin and the end of the assessment period. A comparison between the normal traffic, full replacement and gradual replacement scenario is given Appendix 6B where the cumulative and annual reliability indices of all three scenarios are graphically presented as a function of time. By comparing the different assessment scenarios, it is clear that the impact of SEC varies depending on the structure span.

In Figure 41 the calculated reduction of the normative service life for the analyses regarding the concrete bridge (ULS). In the figures the calculated years of reduction of the (normative) service life is given on the vertical axes for both replacement scenarios (full and gradual replacement, Figure 41a and b respectively). In the figures, the vertical dashed lines indicate the different analyses and depend on the type of structure and load effect that is considered, as indicated on the horizontal axes.

For both new and existing structure meeting exactly the reliability requirements of the Dutch standards, the simply-supported structure with span L = 50 m appears to be critical in the scenario of full replacement. For the new structure the reliability requirement is reached after 81 years (i.e. 19 year reduction), while for the existing structures full replacement with SEC vehicles would mean that the end of normative service equals the reference period (i.e. 30 years), regardless of the elapsed service life.

For the remaining simply-supported (new) structures, the end of normative service life is reached after 98, 87 and 92 years for spans L = 20 m, 100 m and 200 m, respectively. For continuous new structures, the end of normative service life is reached after 11 and 1 year (bending moment), and 9 and 12 years (shear force at middle support) for spans L = 2.20 m and 2.50 m, respectively.

For simply-supported existing structures with a span of L = 20 m, 100 m and 200 m, regardless of elapsed service life, the reliability requirement is reached after 28, 16 and 19 years respectively. For continuous existing structures, regardless of elapsed service life, the reliability requirement is

L-N - log-normal distribution



reached after 17 and 29 years (bending moment), and 19 and 18 years (shear force at middle support) for spans L = 2.20 m and 2.50 m, respectively.

When comparing Figure 41b to Figure 41a it can be seen clearly that a significantly lower impact is observed for the case of gradual replacement with SEC. For the simply-supported new structures the reliability requirement is achieved after year 99, 92, 95 and 97 for spans L = 20 m, 50 m, 100 m and 200 m, respectively. For the continuous (new) structures the reliability requirement is achieved after year 96, 99 (bending moment) and after year 97 and 95 (shear force at the middle support) for spans L = 2.20 m and 2.50 m, respectively. For the simply-supported existing structures, regardless of elapsed service life, the reliability requirement is achieved after year 29, 28, 29 and 29 for spans L = 20 m, 50 m, 100 m and 200 m, respectively (i.e. less than 2 year reduction). For continuous new structure the reliability requirement is achieved after year 29 for both bending and shear at middle support.

It is concluded from the above that for the gradual replacement scenario, again, simply-supported structures with L = 50 m appear to be the most impacted. Nevertheless, in all cases, the reduction is less than 10 years. The difference in the impact between the new and existing structure can be explained by the shorter reference period and the percentage of replacement since after 30 years only 9% pairs of T11O3 vehicles are to be replaced by SEC vehicles, while after 80 years 64% of T11O3 pairs are assumed to have been replaced.

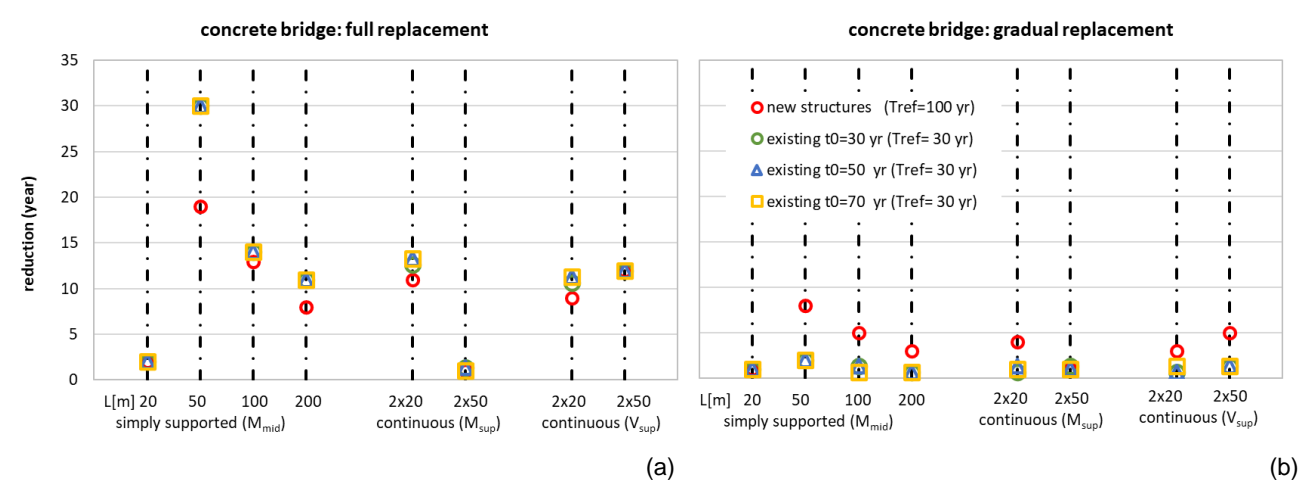


Figure 41: Calculated reduction of the normative service life for the analyses regarding the concrete bridge (ULS) for different types of structures and different scenarios based on calibration of the structural resistance to fulfill exactly the reliability requirements of the current Dutch standards.

#### 5.3.2 Calculations based on the resistance calculated with the old Dutch standards

In **Appendix 6**C the results of the reliability analysis based on resistance, which was calculated for the existing structures with elapsed service life of 30, 50, 60 and 70 on the basis of four standards: VOSB 1938 – GBV 1950, VOSB 1963 – GBV 1962, VB 1974 and VBB 1995. With these standards, structures with different elapsed service life were considered:

- VOSB 1938-GBV 1950: elapsed 70 years,
- VOSB 1963-GBV 1962: elapsed 60 years,



- VB 1974: elapsed 50 years,
- VBB 1995: elapsed 30 years.

Table 25 presents the calculated mean value of the resistance of a particular structural system (simple or continuous beam) with varying span length. It can be observed that the resistances are on average higher in comparison to those values of the resistance that were calibrated (shown in Table 24) based on the reliability requirements given in the current Dutch standards. The higher resistance is reflected in the impact of full replacement with SEC vehicles. In Table 30, the results of the reliability analysis for the full replacement scenario are shown. The reliability requirements for existing structures of the current standards are fulfilled in all scenarios when the resistance is calculated according to the provisions of old Dutch standards. Therefore, the decrease in time to reach the annual reliability index corresponding to the reference scenario (regular traffic only) at the end of the 30-year reference period is calculated instead of the reduction of the normative service life.

In Figure 42 the calculated reduction of the time to reach the annual reliability index at the end of the 30-year reference period in the reference scenario for existing concrete bridges (ULS) with the resistance calculated based on old Dutch standards. In the figures the calculated years of reduction of the (normative) service life is given on the vertical axes for both replacement scenarios (full and gradual replacement in Figure 42a and Figure 42b respectively). The vertical dashed lines indicate the different analyses and depend on the type of structure and load effect that is considered, as indicated on the horizontal axes.

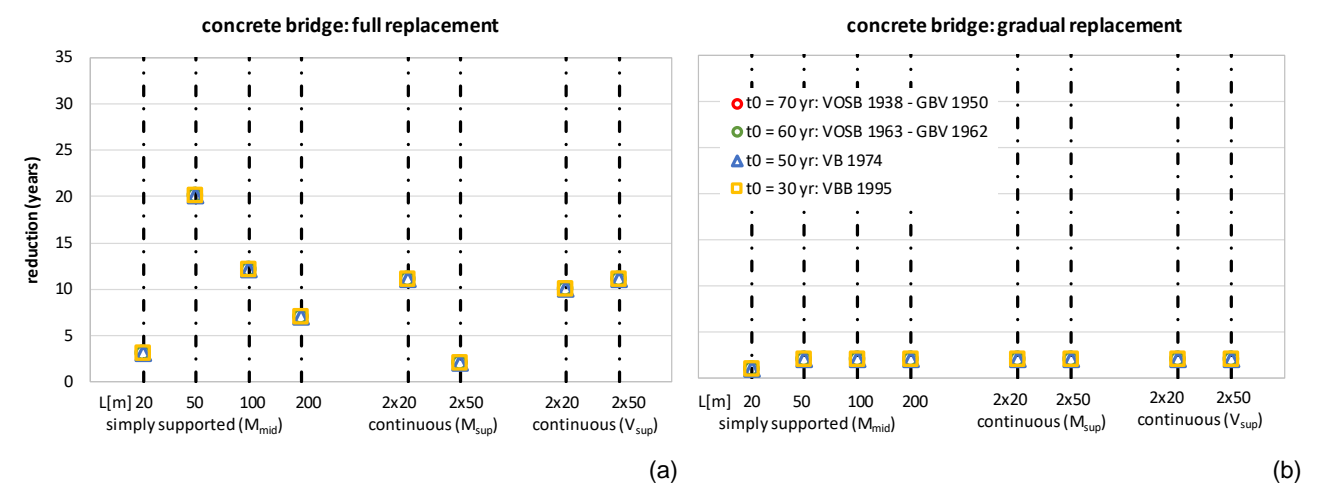


Figure 42: Calculated reduction of time to reach the annual reliability index at the end of the 30-year reference period in the reference scenario for existing concrete bridges (ULS) for different types of structures and different scenarios based on the structural resistance calculated on the basis of old Dutch standards.

The simply-supported beam with span  $L=50\,\mathrm{m}$  is again the most critical case: for this structure, the decrease of the time to reach the annual reliability index corresponding to the reference scenario at the end of the 30-year reference period is equal to 20 years in the full replacement scenario. In contrast, for structures with shorter ( $L=20\,\mathrm{m}$ ) and longer influence lines ( $L=200\,\mathrm{m}$ ), the full replacement with SECs appears to only have a limited impact; there the decrease of the time to



reach the annual reliability index corresponding to the reference scenario at the end of the 30-year reference period is 3 and 7 years, respectively. These values were observed for all of the calculations irrespective of the standard used to calculate the resistance.

The gradual replacement scenario appears to have a significantly lower impact: for all of the considered structures the decrease of the time to reach the annual reliability index corresponding to the reference scenario at the end of the 30-year reference period is 2 years. A similarly limited impact in the gradual replacement scenario was also observed in the impact analysis of existing structures based on calibrated values of the resistance.



# 6 STEEL BRIDGE - ULS CONDITIONS

## 6.1 Introduction

In the consideration of steel bridge under ULS, the reliability analysis is performed by considering a single bridge model: a simply-supported structure with the length  $L=50\,\text{m}$ . Here the calculation methodology is almost identical to the RC bridge under ULS conditions with an exception of a higher load ratio used to calculate the mean permanent load effect.

# 6.2 Calculation methodology

#### 6.2.1 Limit state function

The limit state function taken into consideration is identical to the limit state function for the reinforced concrete bridge, presented in section 5.2.1.

#### 6.2.2 Stochastic variables

#### 6.2.2.1 Traffic load effect

The same parameters of the annual Gumbel maximum distribution, which is used to represent the traffic load effect, are used as for the case study of the strength of the reinforced concrete bridge. The mean and coefficient of variation of the yearly maximum load effect are shown in Table 9 for the reference scenario and in Table 10 for the full replacement scenario. The mean and coefficient of variation for the gradual replacement are calculated by interpolating between the reference and full replacement scenarios assuming quadratic growth of SEC vehicles as described in section 3.4.3.

#### 6.2.2.2 Permanent load effect

In contrast to the reinforced concrete bridge under ULS conditions (case study 1), a higher and constant load ratio  $\chi$  is assumed, as given in TNO Report R11640 [18]:

$$\chi = \frac{\mu_{T,1year}}{\mu_G + \mu_{T,1year}} = 0.7 \tag{6.1}$$

Based on the load ratio, the mean of the permanent load effect distribution is calculated as follows:

$$\mu_G = \frac{1-\chi}{\chi} \mu_{T,1year} = 0.43 \mu_{T,1year}$$
 (6.2)

## 6.2.2.3 Traffic trend uncertainty model

Identical traffic trend was taken into consideration as for the reinforced concrete bridge under ULS conditions (case study 1). See section 5.2.2.3.

#### 6.2.2.4 Other stochastic variables

The stochastic variables, their distributions and parameters of distributions, taken into consideration for the reliability analysis in case study 2 are presented in Table 14



Table 14: Parameters of the stochastic variables in the distributions used for the steel bridge under extreme load conditions (case study 2).

Variable	Distribution	Mean	CoV	Reference	
R	L-N	calibrated	0.10	TNO R11640	[18]
G	N	see 6.2.2.2	0.07	TNO R11640	[18]
T	GUM	varies, see 6.2.2.1	varies, see 6.2.2.1	-	
$ heta_{ ext{trend}}$	N	see 5.2.2.3	see section 5.2.2.3	TNO R1814	[7]
θ <sub>spat.var.</sub>	N	0.86	0.07	TNO R1814	[18]
$ heta_{DAF}$	N	1.10	0.05	TNO R11640	[18]
$ heta_{ ext{stat}}$	N	1.00	0.05	TNO R1814	[7]
$ heta_{ m G}$	N	1.00	0.07	TNO R11640	[18]
$\theta_{T}$	N	1.00	0.10	TNO R1814	[7]

N - normal distribution

L-N - log-normal distribution

GUM - Gumbel distribution of the maximum

#### 6.3 Results

The results for the steel bridge under extreme load conditions are given in Appendix 7. The calibrated resistance for the reference scenario is given in Table 32 in the appendix. As for the case of the reinforced concrete structure, a higher value of calibrated resistance was observed for the new structure. Here again, this is connected to the higher value of the reliability index being required over a longer period of time (reference period) for the new structure in comparison to the existing structure.

In Table 33 the calculated cumulative and annual reliability for the considered scenarios (reference scenario and the full and gradual replacement scenario. Following in the appendix, the results are graphically presented. For each type of structure that is considered the annual and cumulative reliability index is given as a function of the time.

In Figure 43 and Figure 44 the cumulative and annual reliability index are respectively shown for the structure with span L=50 m and elapsed service life 30 years. A significant decrease in both cumulative and annual reliability can be observed for the full replacement scenarios in comparison to the normal traffic scenario. The value of annual reliability after 60 years (the reference period for a structure with elapsed service life 30 years) in the normal traffic scenario is equal to 3.94. The same annual reliability index value is in the full replacement scenario reached after 9 years, while for the gradual replacement scenario the stated annual reliability value is reached after approximately 28 years.



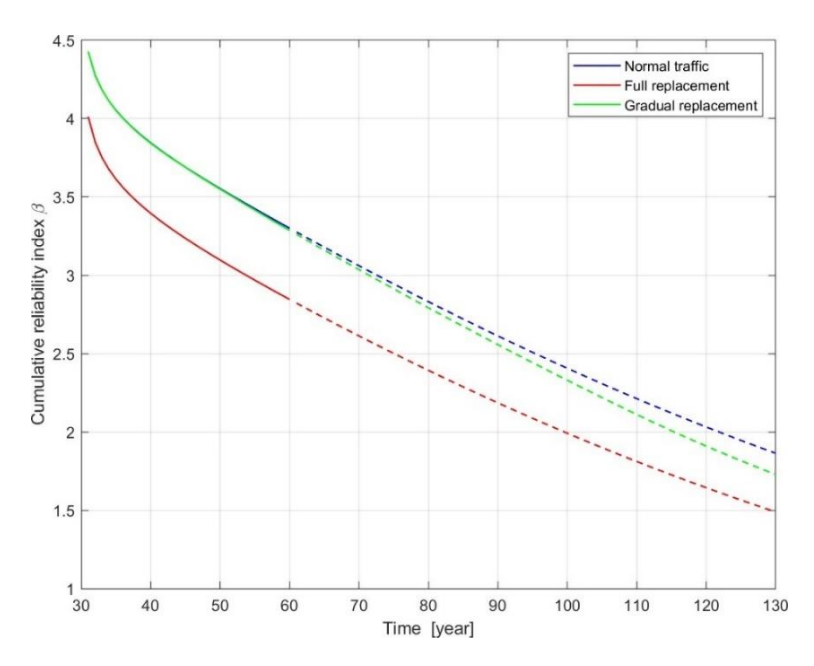


Figure 43: Cumulative reliability for the existing structure (L = 50 m) with elapsed 30 years under normal traffic conditions (blue), full replacement with SEC (red), and gradual replacement with SEC (green).

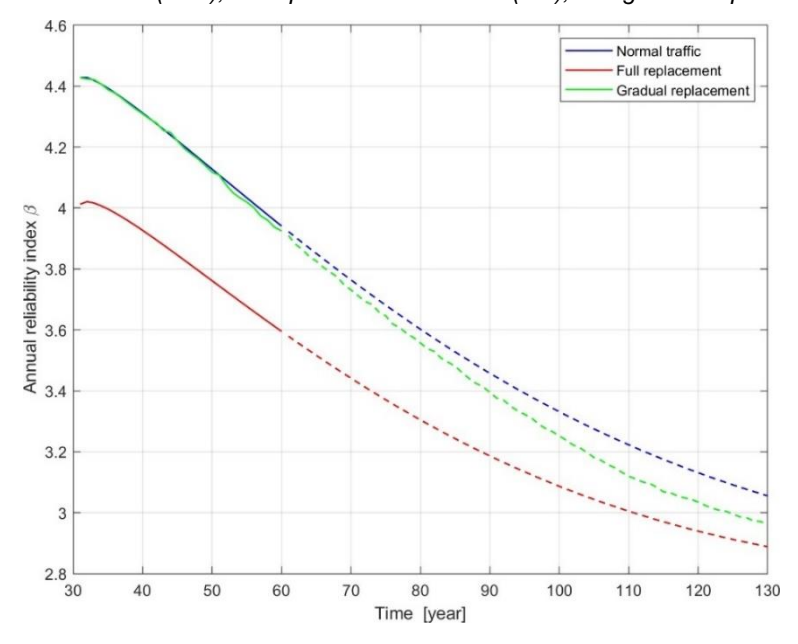


Figure 44: Annual reliability for the new structure (L = 50 m) with elapsed 30 years under normal traffic conditions (blue), full replacement with SEC (red), and gradual replacement with SEC (green).

The calculated reduction in the normative service life is graphically shown Figure 45. In the figure the calculated years of reduction of the (normative) service life is given on the vertical axes for both replacement scenarios (full and gradual replacement). The vertical dashed lines indicates the different analyses and depend on the type of structure and load effect that is considered, as indicated on the horizontal axes. From the figure it can be seen that the impact of the full replacement scenario is about 20 year reduction. For the gradual replacement scenario very limited less than 10 year reduction in service life is calculated. This is explained by the fact that in the gradual replacement model only 9% of T11O3 pairs have been replaced by SECs after 30 years. The impact of SECs in



the case of the new structures is larger due to a higher percentage of replacement in comparison to the existing structure. The difference in calculated cumulative and annual reliability values for the two replacement scenarios is therefore also less significant in comparison to the existing structure. The annual reliability for the new structure after 100 years is equal 4.3, in the full replacement case this value is obtained after 82 years (meaning a reduction of 18 years), while for the gradual replacement scenario after about 93 years (reduction of 7 years).

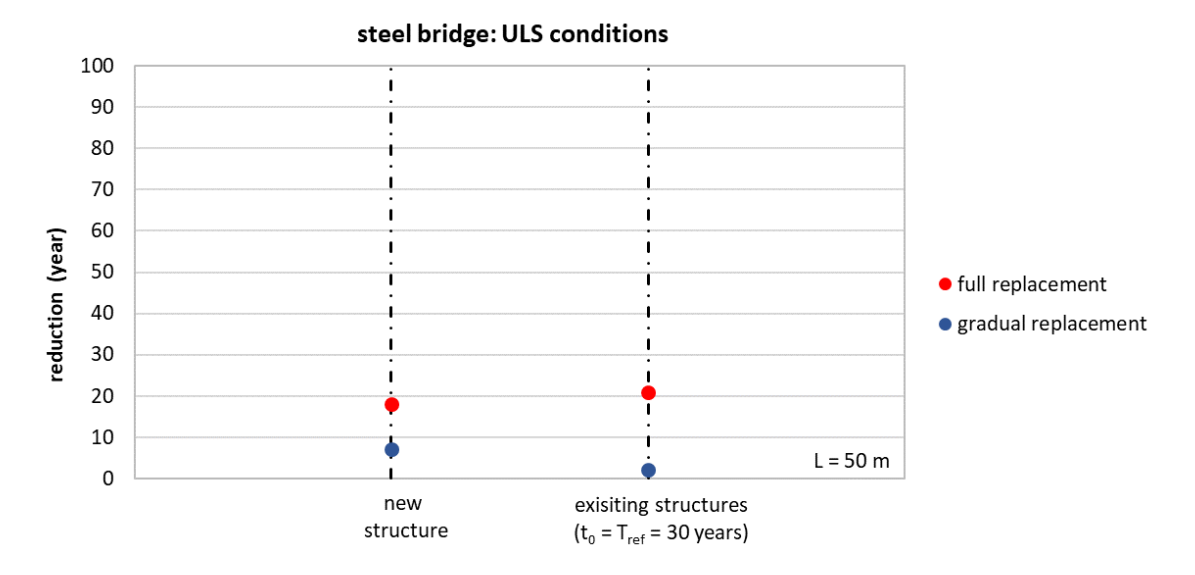


Figure 45: Calculated reduction of the normative service life for the analyses for the steel bridge under ULS conditions.



# 7 STEEL BRIDGE - FATIGUE LIMIT STATE (FLS)

#### 7.1 Introduction

In the consideration of fatigue, the reliability analysis is performed by considering a bridge model of a simply-supported structures with a length of L = 100 m. The vehicles are considered as moving point loads and a triangular shape of the influence line is used. Both new and existing structures are considered. The fatigue analyses are performed based on the WIM database A67 from 2015 and the accumulated fatigue damage is calculated using the design S-N curve from NEN-EN 1993-1-9 [17]. The cumulative and annual reliability indices are calculated by taking into account the uncertainties of the S-N curve, Miner's rule, and load effect. A calibration of the stress histogram is performed based on the normal traffic conditions scenario in order to enable the comparison between the normal traffic and SEC replacement scenarios.

# 7.2 Calculation methodology

#### 7.2.1 Limit state function

For the reliability analysis, the following limit state function was used:

$$Z = X_d - X = X_d - \sum_{i=1}^m \frac{n_i}{5 \cdot 10^{(6+X_{SN})} \cdot \max\left[\left(\frac{\Delta \sigma_D}{X_U \cdot \Delta \sigma_i}\right)^{m_1}, \left(\frac{\Delta \sigma_D}{X_U \cdot \Delta \sigma_i}\right)^{m_2}\right]}$$
(7.1)

where:

 $X_d$  is the random variable representing the uncertainty of the Miner's rule;

m is the number of stress range bins of the stress spectrum with  $\Delta \sigma_i$  larger

than the cut-off stress  $\sigma_L = 32.4$  MPa;

 $X_{SN}$  is the random variable representing the uncertainty of the  $log_{10}(N)$  of the S-

N curve;

 $X_U$  is the random variable representing the uncertainty load effect;

 $\Delta \sigma_i$  is the stress range of bin *i*;

 $n_i$  number of stress reversals (cycles) in stress range bin i;

 $m_1 = 3$  is the slope of the first branch of the S-N curve in the logarithmic scale;

 $m_2 = 5$  is the slope of the second branch of the S-N curve in log-log scale;

 $\Delta \sigma_D = 59 \, MPa$  is the stress range of the knee-point of the S-N curve (according to NEN-

EN 1993-1-9 this corresponds to  $0.737 \cdot \Delta \sigma_C$  (80 MPa).

## 7.2.2 Stochastic variables

The stochastic variables considered in case study 3, their probabilistic distributions and the selection of parameters of the distributions are presented in Table 15.



Table 15: Parameters of the stochastic variables in the distributions used for the steel bridge under fatigue load conditions (case study 3).

Variable	Distribution	Mean	Standard deviation	Reference
$X_d$	L-N	1.0	0.30	Maljaars [19]
$X_{SN}$	N	0.33	0.20	Maljaars [19]
$X_U$	L-N	1.0	0.12	Maljaars [19]

N - normal distribution

L-N - log-normal distribution

#### 7.3 Results

The results for the steel bridge under fatigue load conditions are given in Appendix 8. In order to perform reliability analyses and to make a comparison between the traffic scenarios, the stress spectrum obtained from the fatigue analysis needs to calibrated. The process of calculating the calibration factor  $\alpha$  is presented in section 2.5.2. The values of the  $\alpha$  factors are then given in Table 34 in the Appendix 8. It can be observed that the value of the calibrated value  $\alpha$  is the lowest for the new structure scenario. Since  $\alpha$  is a multiplicative factor, this represents the fact that the stress bins of the stress histogram have to be in the case of new structures scaled more in comparison to existing structures in order to reach the prescribed reliability requirements.

In

Table 35 the calculated cumulative and annual reliability are given for the considered scenarios (reference, full and gradual SEC replacement scenario. For each type of structure that is considered, the cumulative and annual reliability index is shown as a function of the time are presented graphically.

In Figure 46 and Figure 47 the cumulative and annual reliability, respectively, are shown for the structure with span L = 100 m and elapsed service life of 50 years. A significant reduction of cumulative and annual reliability index for the considered time period can be observed when comparing the normal traffic and full replacement scenarios. For the gradual replacement, the cumulative and annual reliability index are lower in comparison to the normal traffic conditions, the reduction depending on length of the time period considered: since for the existing structure, only 30 years are considered, the reduction in reliability index is not as high as for the new structure, since for gradual replacement we assume that only 9% (see section 3.4.3) of T11O3s will be replaced with SECs, compared to 65% over the coming 100 years. The large reduction of cumulative and annual reliability index in replacement scenarios compared to normal traffic scenario is mainly due to SEC vehicles leading to more accumulation of fatigue damage compared to a pair of T11O3 vehicles, as shown section in 4.3.4.



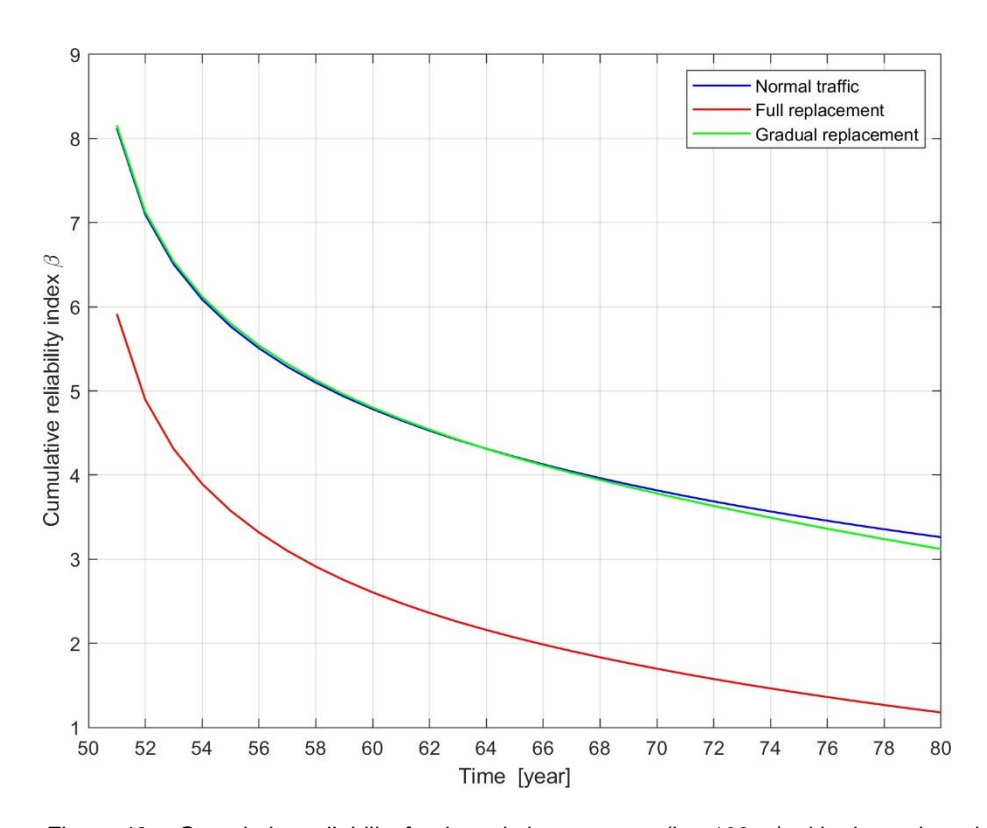


Figure 46: Cumulative reliability for the existing structure (L = 100 m) with elapsed service life 50 years with normal traffic conditions (blue), gradual replacement with SEC (green) and full replacement with SEC (red).

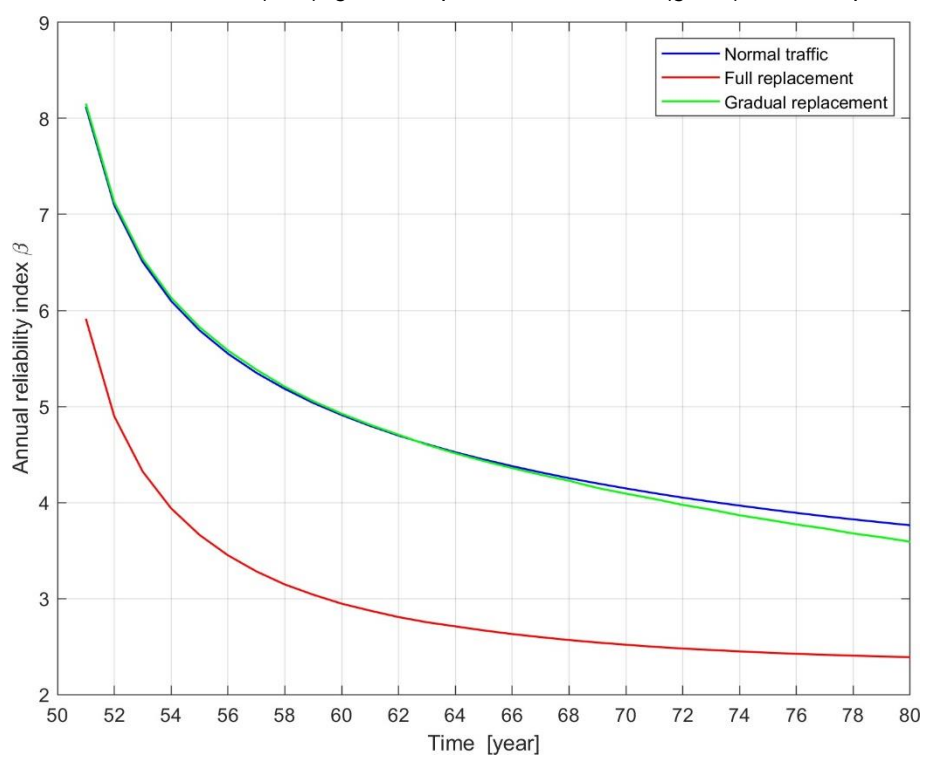


Figure 47: Annual reliability for the existing structure (L = 100 m) with elapsed service life 50 years with normal traffic conditions (blue), gradual replacement with SEC (green) and full replacement with SEC (red).



Note that the annual reliability index in the full replacement scenario is theoretically increasing after the considered reference period (shown with the dashed red line in Figure 47). This is due to a negative cumulative reliability index being calculated, meaning the probability of failure that is higher than 50%, calculated over that period of time (for example, cumulative reliability index shown in year 100 indicates the probability of failure between years 50 and 100).

The significant difference in the annual reliability index values between the traffic scenarios leads to a significant impact on the normative service life when considering a full or gradual replacement scenario. This is illustrated in Figure 48 in which the calculated years of reduction of the (normative) service life (on the vertical axis) is given for the different analyses (on the horizontal axis and indicated by the vertical dashed lines. Considering new structures, the full replacement scenario leads to a reduction of normative service life of 89 years, while the gradual replacement scenario leads to a reduction of 50 years. For the existing structures (regardless of elapsed service life), the full replacement scenario leads to a reduction of normative service life of 26 years, while the gradual replacement scenario to 4 years.

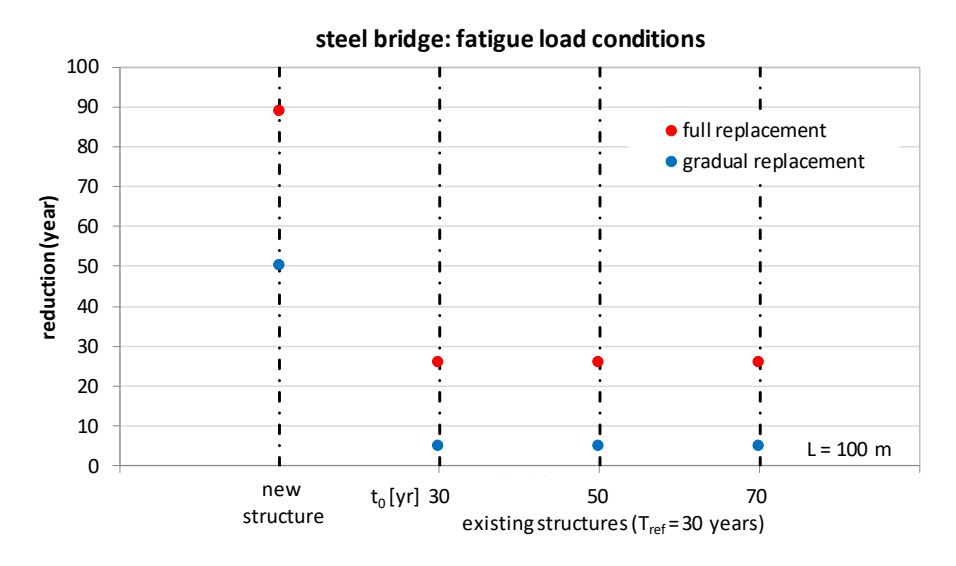


Figure 48: Calculated reduction of the normative service life for the analyses of the steel bridge under FLS conditions.



# 8 CONCLUSIONS

In this report a method is presented for determining the impact on the expected (normative) service life of bridges and viaducts due to the introduction of new vehicle concepts. The service life is defined in this report as the period of time for which a structure or part of it fulfils the reliability requirements of the current Dutch standards for the design of new structures or the assessment of existing structures. The normative service life is assumed equal to 100 years for new structures and 30 years for existing structures (assessment level "gebruiksniveau" of RBK [4]). The method is based on a probabilistic approach with which the annual reliability index over a certain number of years is calculated, depending on the scenario that is considered. The method is applied for the SuperEco Combi (SEC) vehicle concept, which is considered to be a special type of Truck Platoon (TP) where two trailer combinations are driving at a constant (front-to-back) distance of about 2 m from each other.

From the assessment of the load effects induced by SEC vehicles it appears that SEC vehicles alone are not critical for the safety of the bridges considered in this investigation. There are regular vehicles or combinations of regular vehicles that lead to higher load effects than the heaviest SEC vehicles. This is confirmed by the measurements at the (steel) Moerdijk bridge [1] and the concrete box girder viaduct near Geldrop [2]. Moreover, it is concluded that limitations to the GVW of SEC vehicles (i.e. 76 t) effects the maximum load effects only for medium- to long-span bridges (>50 m).

# Analyses and explanation of the results

In total three scenarios have been studied: 1) normal traffic conditions (no replacements, also noted as the reference scenario), 2) full replacement of all truck-trailer combinations of type T11O3 by SEC vehicles and 3) a gradual replacement over a certain number of years of a limited amount of T11O3 vehicles with SEC vehicles.

For each scenario the impact is calculated for different types of structures and influence lines, which represent typical concrete and steel bridges in the Dutch road network. Three distinct cases are considered: a reinforced concrete bridge and a steel bridge under extreme load conditions in the Ultimate Limit State (ULS) conditions, and a steel bridge under fatigue load conditions (Fatigue Limit State, FLS).

In the analyses the impact is calculated in terms of reduction of the service life that is calculated as the difference between the reference period (100 years for new structures and 30 years for existing structures) and the year in which the reliability index in the last year determined according to the reference traffic scenario is reached. With respect to research question 1 and 2 (section 2.2), regarding the ULS conditions, an analysis has been performed after calibrating the resistance to reach the target reliability levels of the current Dutch standards at the end of the reference period (new structures:  $\beta_{target} = 4.3$  for  $T_{ref} = 100$  years, existing structures:  $\beta_{target} = 3.3$  for  $T_{ref} = 30$  years). An additional analysis has been performed for existing concrete structures where the parameters of the resistance have been evaluated based on the old Dutch standards VOSB 1938, VOSB 1963, VB 1974 and VBB 1995 (presented in section 5.3.2, addressing research question 3 from section 2.2).



Regarding the FLS conditions, the analysis is based on the calibration of the stress spectrum to reach the target reliability levels of the current Dutch standards at the end of the reference period (new structures:  $\beta_{target} = 4.3$  for  $T_{ref} = 100$  years, existing structures:  $\beta_{target} = 3.3$  for  $T_{ref} = 30$  years).

The results of the analyses are summarized in Figure 49 for concrete bridges (ULS) and Figure 50 for steel bridges (ULS and FLS) and are based on the results given in Table 26 to Table 28 from Appendix 6 (ULS concrete bridge) and for steel bridges in Table 33 from Appendix 7 (ULS) and Table 35 from Appendix 8 (FLS).

In the figures the calculated years of reduction of the (normative) service life is given on the vertical axes for both replacement scenarios (full and gradual replacement). The vertical dashed lines indicate the different analyses and depend on the type of structure and load effect that is considered, as indicated on the horizontal axes.

# Results concrete bridges (ULS)

The results for concrete bridges (Figure 49) are based on calibration of the structural resistance to fulfill exactly the reliability requirements of the current Dutch standards (according to section 5.3.1).

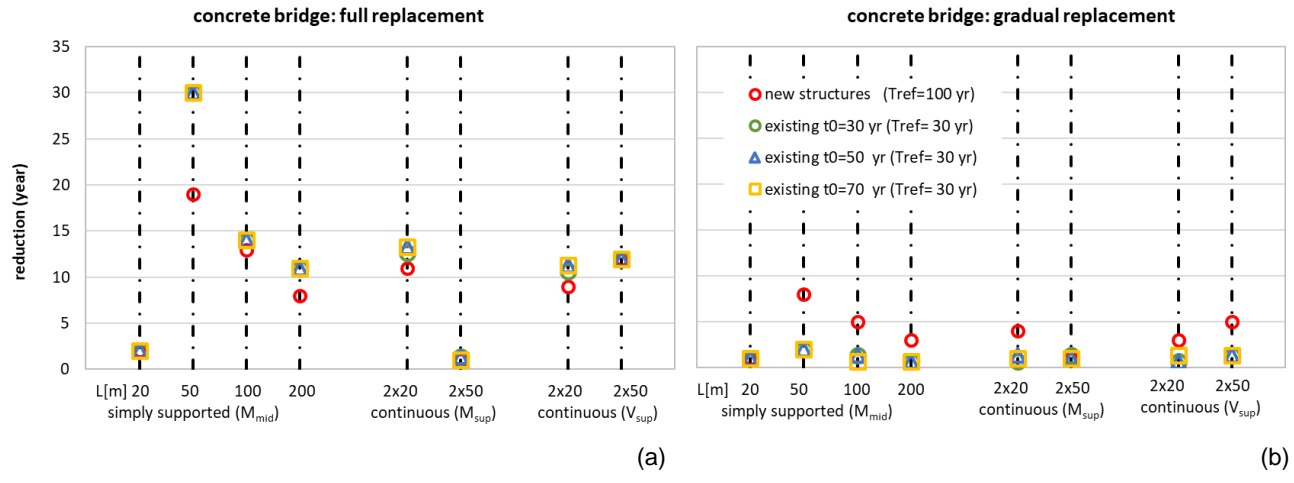


Figure 49: Calculated reduction of the normative service life for the analyses regarding the concrete bridge (ULS) for different types of structures and different scenarios based on calibration of the structural resistance to fulfill exactly the reliability requirements of the current Dutch standards.

With respect to the results in Figure 49 the following conclusions are drawn:

- The calculated reduction of the normative service life is marginal for all cases considering structures with a short influence length (20 m).
- For new structures with a larger influence length, the calculated reduction in service life is up to 20 years for the full replacement scenario. The largest reduction is observed for an influence length of 50 m. For larger influence lengths the reduction is less significant. It can be seen from the figure that for the full replacement scenario considering L = 50 m, remarkably, the reduction is larger for existing structures compared to new structures.
- In alle cases, the gradual replacement scenario shows less reduction compared to the full replacement scenario.



• For existing structures with different elapsed service life  $t_0$ , the reduction of the service life is identical for all cases, regardless the elapsed service life  $t_0$  or span length.

In section 5.3.2 of this report it is explained that the reliability requirements for existing structures are fulfilled in all scenarios when the resistance is calculated according to the provisions of old Dutch standards (VOSB 1938, VOSB 1963, VB 1974, VBB 1995). Therefore, the decrease in time to reach the annual reliability index at the end of the 30-year reference period in the reference scenario (regular traffic only) is calculated instead of the reduction of the normative service life. From the analyses it appears that the reliability requirements at the end of the reference period of 30 years are fulfilled in all scenarios. A negligible difference in the decrease of normative service life is observed for all structural cases. This result agrees well with the results based on the calibrated resistance shown in Figure 49 for existing structures. In the case of assessed impact based on the old standards, the simply-supported structure with L = 50 m seems to be the most critical

#### Results steel bridges (ULS and FLS)

With respect to the results considering steel bridges, it can be concluded that the full replacement scenario leads to a reduction of the calculated normative service life of about 20 years for ULS loading conditions for both new and existing structures (Figure 50a).

Considering the Fatigue Limit State (FLS) it can be seen from Figure 50b that the reduction of the normative service life for new structures is almost 90 years in the full replacement scenario. As explained in section 4.3.4, this is due to a SEC vehicle causing a larger accumulation of fatigue damage in a year in comparison to a pair of T11O3 vehicles. For existing structures the reduction is less (about 25 years).

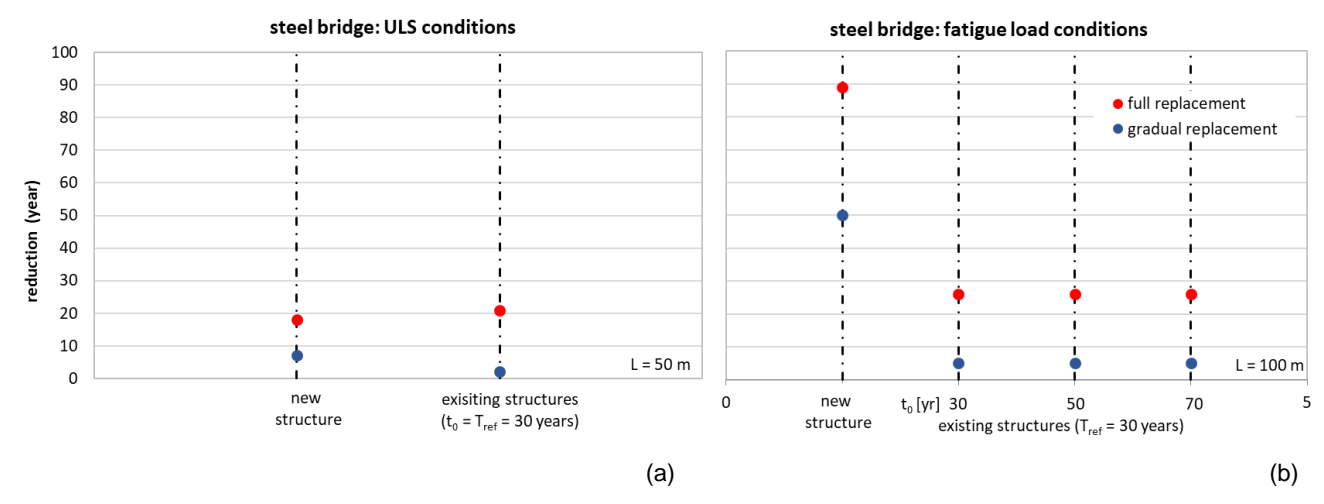


Figure 50: Calculated reduction of the normative service life for the analyses regarding the steel bridge under ULS (a) and FLS (b) conditions.

As may be expected, for the gradual replacement scenario the reduction in service life is considerably smaller compared to the full replacement scenario. In almost all situations studied the reduction of the service life is less than about 10 year. For new structures the reduction of the normative service life when considering the gradual replacement scenario under FLS conditions is



still 50 years, this being mainly a consequence of the assumed replacement with time (64% after 100 years).

#### Concluding remarks

From the results it can be concluded that the estimated reduction of the normative service life is highly affected by the chosen gradual replacement scenario. In this scenario considered in the analyses, a growth of the SEC vehicles over the years is assumed where the percentage of replacement was capped at 64% after 80 years<sup>9</sup>. As mentioned in section 3.4.3, the capped value is an arbitrary chosen value, as well the growth in time.

Furthermore, no distinction is made as to which T11O3 vehicles have been replaced. If the SEC is primarily a volume transport (rather than mass), the gross vehicle weight for SEC vehicles may be expected to be smaller compared to regular truck trailer combinations. This will have a positive effect on the vehicle weight distribution, leading to a smaller reduction in the normative service life. Finally, in the analyses the effect of SEC and/or TP on other traffic trends, the corresponding traffic load distributions and load effects are not taken into account. Possible other effects such as an expected modal shift are explained in detail in section 2.2. of the CATALYST report TNO-2021-R12277 [14].

A replacement of 64% of all T11O3 vehicles equals 48% of all truck trailer combinations and 32% of all vehicles with a GVW greater than 3.5 tons



### 9 REFERENCES

- [1] Braendstrup, C. Verdenius, S. and Vervuurt, A. Load effect measurements at the Moerdijk bridge in the A16, report D 5.1A Ursa Major Truck Platooning, December, 15 2021
- [2] Load effect measurements at the box girder bridge near Geldrop in the A67, report D 5.1B Ursa Major Truck Platooning, December 24, 2021.
- [3] NEN-EN 1990:2002. Eurocode Basis of structural design, CEN, 2002.
- [4] RBK 1.1, Richtlijnen Beoordeling Kunstwerken, Rijkswaterstaat, 2013.
- [5] Prob2B variables, expression and Excel® Installation and Getting Started. TNO Report 2007-D-R0887/A, 2007.
- [6] Vervuurt, A.H.J.M., Hellebrandt, L., Dieteren, G.G.A. en Steenbergen, R.D.J.M. Invloed van permanente en éénmalige vergunningen op de constructieve veiligheid van bestaande bruggen. TNO-rapport TNO-2014-R11680 (InfraQuest report IQ-2014-24), December 29, 2014 (in Dutch)
- [7] Steenbergen, R.D.J.M., Morales Napoles, O. en Vrouwenvelder, A.C.W.M. Algemene veiligheidsbeschouwing en modellering van wegverkeerbelasting voor brugconstructies (update van TNO Rapport 98-CON-R1813). TNO rapport TNO-060-DTM-2011-03695-1814, 17 juli 2012 (in Dutch)
- [8] Nicoreac, M., Hellebrandt, L., Lent, D. van en Giezen, C. Effect vrachtverkeer op levensduur infrastructuur. TNO rapport TNO 2015 R11804, 23 december 2015 (in Dutch)
- [9] NEN-EN 1991-2+C1:2015/NB:2019. National Annex to NEN-EN 1991-2+C1: Eurocode 1: Actions on structures Part 2: Traffic loads on bridges, NEN, 2019.
- [10] Nicoreac, M.P., Maljaars, J. en Vervuurt, A.H.J.M. Uniform Vermoeiingsbelastingmodel. Belastingeffectmodel op basis van invloedsvlakken en voor meerdere rijstroken (IQ-2015-02a). TNO rapport TNO-2015-R11590, 11 februari 2016 (in Dutch)
- [11] Steenbergen, R.D.J.M, Allaix, D.L., Gasse, L.C. la en Vervuurt, A.H.J.M.. Verkeersbelasting-model voor wegverkeersbruggen in het onderliggend wegennet zonder jaarontheffingen. TNO-report TNO-2017-R10614, 25 januari 2018 (in Dutch)
- [12] Verweij, K. et al. Super EcoCombi. Verkenning van kansen en verwachte effecten. Report of CE-Delft & Buck Consultants International on behalf of the Topsector Logistiek, July 2020 (in Dutch)
- [13] Willemsen, D., et al., (2020) V2 Platooning use cases, scenario definition and Platooning Levels (Version A) D2.2 (Version A) of H2020 project ENSEMBLE, (www.platooningensemble.eu)
- [14] Meerveld, H. van and Swaalf, F.E.M.. CATALYST | Verkenning naar de mogelijke impact van de Super EcoCombis op de Nederlandse infrastructuur, TNO report TNO-2021-R12277 November 30, 2021 (in Dutch).
- [15] Meerveld, H. van Paulissen, J.H., Oudenes, L. en Vervuurt, A.H.J.M.. Scenarios for determining strategies for traffic weight measurements in The Netherlands, TNO report TNO-2020-R10679A, july 2020



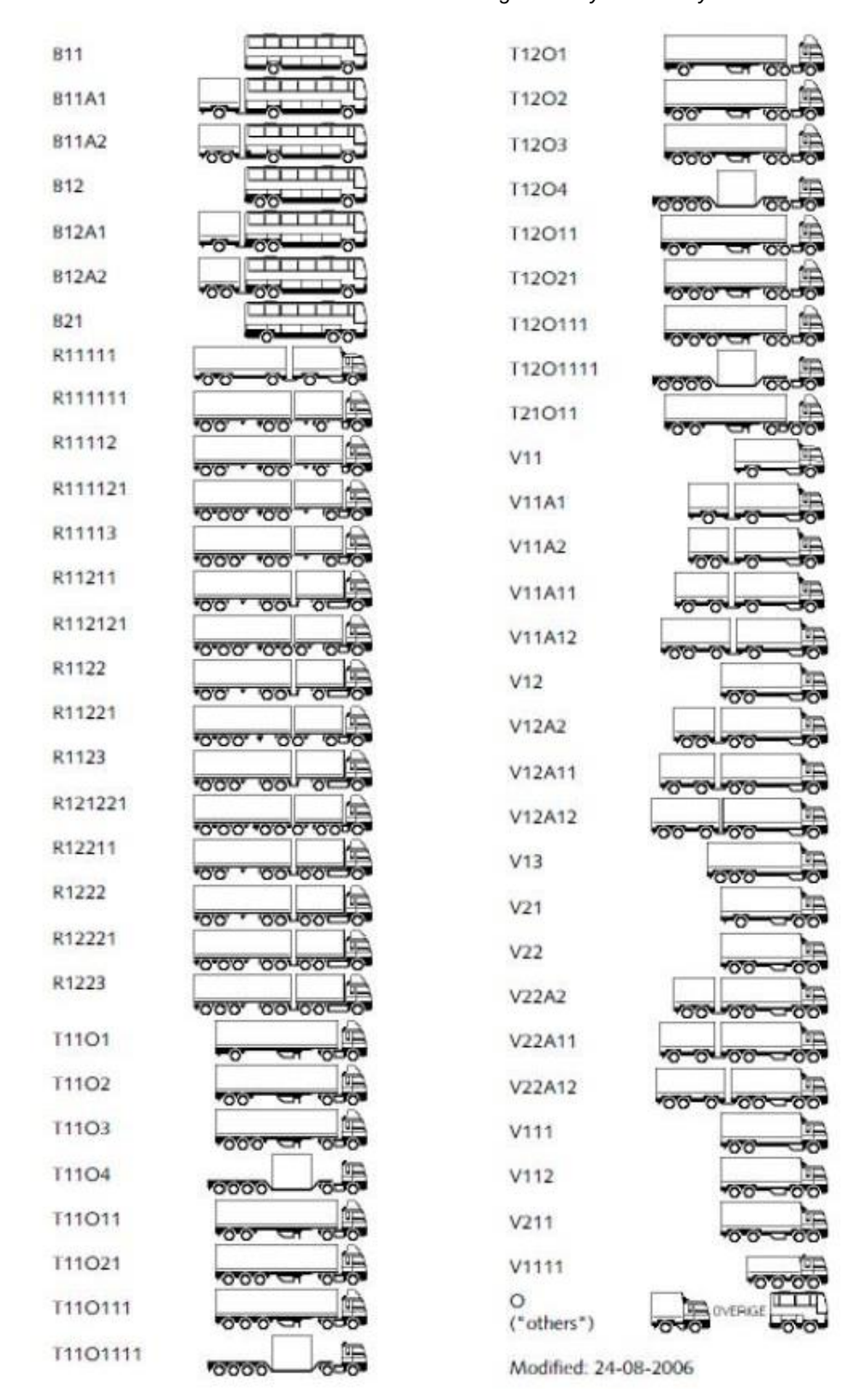
- [16] NEN 8701:2011+A1:2020. Beoordeling van de constructieve veiligheid van een bestaand bouw bij verbouwen en afkeuren Belastingen, NEN, 2020.
- [17] NEN-EN 1993-1-9:2006. Eurocode 3: Design of steel structures Part 1-9: Fatigue, CEN, 2006.
- [18] De Vries, R., Steenbergen, R. D. J. M., Maljaars, J. Reliability analysis on an annual basis applied to bridges in The Netherlands. TNO Report R11640, 2019.
- [19] Maljaars, J. Evaluation of traffic load models for fatigue verification of European road bridges. Engineering Structures; 225: 111326, 2020.
- [20] Mascalchi, E. & Willemsen, D. (2022). *ENSEMBLE Platooning Autonomous Function: high level description* (ENSEMBLE website, 19 Jan 2022). <u>ENSEMBLE project</u>.
- [21] Van Ark, E.J., Duijnisveld, M., Van Eijk, E., Hendrickx, N., Janssen, G.R., Malone, K., Van Ommeren, C., Soekroella, A. (2017). Value Case Truck Platooning an early exploration of the value of large-scale truck platooning deployment, TNO Report TNO-2017-R11299, TNO Den Haag, pp. 1-107, 2017.
- [22] Miraglia, S., Maljaars, J., Steenbergen, R.D.J.M. en Vervuurt, A.H.J.M. Fatigue load model for structures in motorways based on WIM measurements in The Netherlands. Phase 1b: elaboration of WIM measurements. TNO report TNO-2013-R11419, 5 December 2013.



### **APPENDIX 1 WIM CHARACTERISTICS**

#### Appendix 1A WIM-NL vehicle subclasses

Table 16: Overview of subclasses of vehicles as registered by the WIM systems.





#### Appendix 1B Traffic composition

Following, an overview is given of the measured amount of vehicles according to a number of the WIM systems in the Dutch road network. The measurements refer to vehicles with a vehicle weight larger than 3.5 t that were measured in 2015. Table 17 refers to the absolute numbers, the second table (Table 18) shows the percentage distribution.

Table 17: Total number of vehicles divided into vehicle subclasses as detected by a number of WIM systems.

SUB	15,704,801	2,517,473	2,344,407	2,084,235	1,968,637	2,177,771	2,228,149	2,384,129
CLASS	TOTAL	A16L1	A16R1	A27L1	A28R1	A50L1	A67L1	A67R1
T11O3	6,536,052	1,028,599	953,761	740,348	625,810	794,455	1,161,915	1,231,164
T11O2	1,587,329	331,743	264,992	179,348	137,975	192,416	241,866	238,989
V11	1,130,889	189,000	169,881	152,855	144,216	169,927	143,583	161,427
T11O11	925,182	128,638	156,242	129,023	172,022	181,049	75,093	83,115
О3	679,793	81,758	87,976	110,480	128,969	123,982	68,567	78,061
T12O3	469,769	88,098	105,858	66,393	70,967	53,788	44,708	39,957
O2	405,473	19,908	38,375	113,185	70,009	52,825	51,689	59,482
T11O1	388,563	73,470	57,474	47,890	60,215	65,233	39,701	44,580
O4	368,222	36,989	43,299	65,641	64,568	61,500	41,967	54,258
V12A11	355,362	44,301	46,937	42,123	48,848	55,637	58,703	58,813
T11O111	336,637	29,546	43,972	47,420	85,281	69,851	29,383	31,184
V11A11	308,083	47,339	44,039	35,935	50,935	56,218	32,087	41,530
T11O21	259,598	42,900	39,998	34,771	53,299	46,104	20,661	21,865
V11A2	258,917	34,413	26,903	42,053	28,775	32,115	45,862	48,796
V12	212,893	43,628	36,972	28,032	31,346	27,921	21,953	23,041
B11	146,604	16,025	14,364	68,383	13,172	8,604	12,250	13,806
V112	126,372	26,208	21,209	12,585	12,259	14,166	13,829	26,116
V12A2	120,290	20,955	13,931	11,792	8,685	15,041	25,981	23,905
V12A12	102,464	15,767	16,126	16,334	17,999	20,264	9,428	6,546
T12O111	74,991	12,818	10,703	13,113	15,101	14,116	4,814	4,326
B12	64,025	8,928	7,660	10,491	7,301	6,624	11,004	12,017
T12O2	59,472	10,165	8,893	10,358	8,838	6,122	6,436	8,660
V11A1	49,345	4,436	4,363	4,398	4,608	7,166	11,296	13,078
V11A12	47,241	7,406	5,203	7,079	6,673	9,011	5,039	6,830
REST	691,235	174,435	125,276	94,205	100,766	93,636	50,334	52,583



Table 18 Distribution of the total number of vehicles per subclass as detected by a number of WIM systems.

A16R1 A27L1	A16R1 A27L1 A28R1	A16R1 A27L1 A28R1 A50L1	A16R1 A27L1 A28R1 A50L1 A67L1
40.7% 35.5%	40.7% 35.5% 31.8%	40.7% 35.5% 31.8% 36.5%	40.7% 35.5% 31.8% 36.5% 52.1%
11.3% 8.6%	11.3% 8.6% 7.0%	11.3% 8.6% 7.0% 8.8%	11.3% 8.6% 7.0% 8.8% 10.9%
7.2% 7.3%	7.2% 7.3% 7.3%	7.2% 7.3% 7.3% 7.8%	7.2% 7.3% 7.3% 7.8% 6.4%
6.7% 6.2%	6.7% 6.2% 8.7%	6.7% 6.2% 8.7% 8.3%	6.7% 6.2% 8.7% 8.3% 3.4%
3.8% 5.3%	3.8% 5.3% 6.6%	3.8% 5.3% 6.6% 5.7%	3.8%         5.3%         6.6%         5.7%         3.1%
4.5% 3.2%	4.5% 3.2% 3.6%	4.5% 3.2% 3.6% 2.5%	4.5%     3.2%     3.6%     2.5%     2.0%
1.6% 5.4%	1.6% 5.4% 3.6%	1.6% 5.4% 3.6% 2.4%	1.6% 5.4% 3.6% 2.4% 2.3%
2.5% 2.3%	2.5% 2.3% 3.1%	2.5% 2.3% 3.1% 3.0%	2.5% 2.3% 3.1% 3.0% 1.8%
1.8% 3.1%	1.8% 3.1% 3.3%	1.8% 3.1% 3.3% 2.8%	1.8%     3.1%     3.3%     2.8%     1.9%
2.0% 2.0%	2.0% 2.5%	2.0% 2.5% 2.6%	2.0% 2.5% 2.6% 2.6%
1.9% 2.3%	1.9% 2.3% 4.3%	1.9% 2.3% 4.3% 3.2%	1.9%     2.3%       4.3%     3.2%       1.3%
1.9% 1.7%	1.9% 1.7% 2.6%	1.9% 1.7% 2.6% 2.6%	1.9% 1.7% 2.6% 2.6% 1.4%
1.7%	1.7% 1.7% 2.7%	1.7%   1.7%   2.7%   2.1%	1.7%         1.7%         2.7%         2.1%         0.9%
1.1% 2.0%	1.1% 2.0% 1.5%	1.1% 2.0% 1.5% 1.5%	1.1% 2.0% 1.5% 1.5% 2.1%
1.6% 1.3%	1.6% 1.3% 1.6%	1.6%         1.3%         1.6%         1.3%	1.6%         1.3%         1.6%         1.3%         1.0%
0.6% 3.3%	0.6% 3.3% 0.7%	0.6% 3.3% 0.7% 0.4%	0.6% 3.3% 0.7% 0.4% 0.5%
0.6%	0.6% 0.6%	0.9% 0.6% 0.6% 0.7%	0.9% 0.6% 0.6% 0.7% 0.6%
0.6%	0.6% 0.4%	0.6% 0.4% 0.7%	
0.8%	0.7% 0.8% 0.9%	0.7% 0.8% 0.9% 0.9%	0.7% 0.8% 0.9% 0.9% 0.4%
0.6%	0.6% 0.8%	0.6% 0.8% 0.6%	0.6% 0.8% 0.6% 0.2%
0.5%	0.5% 0.4%	0.5% 0.4% 0.3%	0.5% 0.4% 0.3% 0.5%
.4% 0.5%	.4% 0.5% 0.4%	.4% 0.5% 0.4% 0.3%	.4% 0.5% 0.4% 0.3% 0.3%
% 0.2%	% 0.2% 0.2%	% 0.2% 0.2% 0.3%	% 0.2% 0.2% 0.3% 0.5%
0.3%	0.3% 0.3%	0.3% 0.3% 0.4%	0.3% 0.3% 0.4% 0.2%
4.5%	4.5% 5.1%	4.5% 5.1% 4.3%	4.5% 5.1% 4.3% 2.3%
	31.8% 7.0% 7.3% 8.7% 6.6% 3.6% 3.6% 3.1% 3.3% 2.5% 4.3% 2.6% 2.7% 1.6% 0.7% 0.6% 0.4% 0.9% 0.8% 0.4% 0.9% 0.4% 0.2% 0.3%	31.8%         36.5%           7.0%         8.8%           7.3%         7.8%           8.7%         8.3%           6.6%         5.7%           3.6%         2.5%           3.6%         2.4%           3.1%         3.0%           3.3%         2.8%           2.5%         2.6%           4.3%         3.2%           2.6%         2.1%           1.5%         1.5%           1.6%         1.3%           0.7%         0.4%           0.6%         0.7%           0.4%         0.9%           0.8%         0.6%           0.4%         0.3%           0.2%         0.3%           0.3%         0.4%	31.8%         36.5%         52.1%           7.0%         8.8%         10.9%           7.3%         7.8%         6.4%           8.7%         8.3%         3.4%           6.6%         5.7%         3.1%           3.6%         2.5%         2.0%           3.6%         2.4%         2.3%           3.1%         3.0%         1.8%           3.3%         2.8%         1.9%           2.5%         2.6%         2.6%           4.3%         3.2%         1.3%           2.6%         2.4%         2.1%           1.5%         1.5%         2.1%           1.5%         1.5%         2.1%           1.6%         1.3%         1.0%           0.7%         0.6%         0.5%           0.6%         0.7%         0.6%           0.4%         0.3%         0.5%           0.4%         0.3%         0.5%           0.4%         0.3%         0.5%           0.4%         0.3%         0.5%           0.4%         0.3%         0.5%           0.4%         0.3%         0.5%           0.3%         0.5%           0



#### Appendix 1C Distribution of vehicle and axle weight

In this appendix, an overview is given of the measured vehicle weights and axle loads based on the measurement data from April to June 2015 (A67 left and right, slow lane and fast lane together). The measurements relate to vehicles with a vehicle weight larger than 3.5 tonne.

## Gross Vehicle Weight

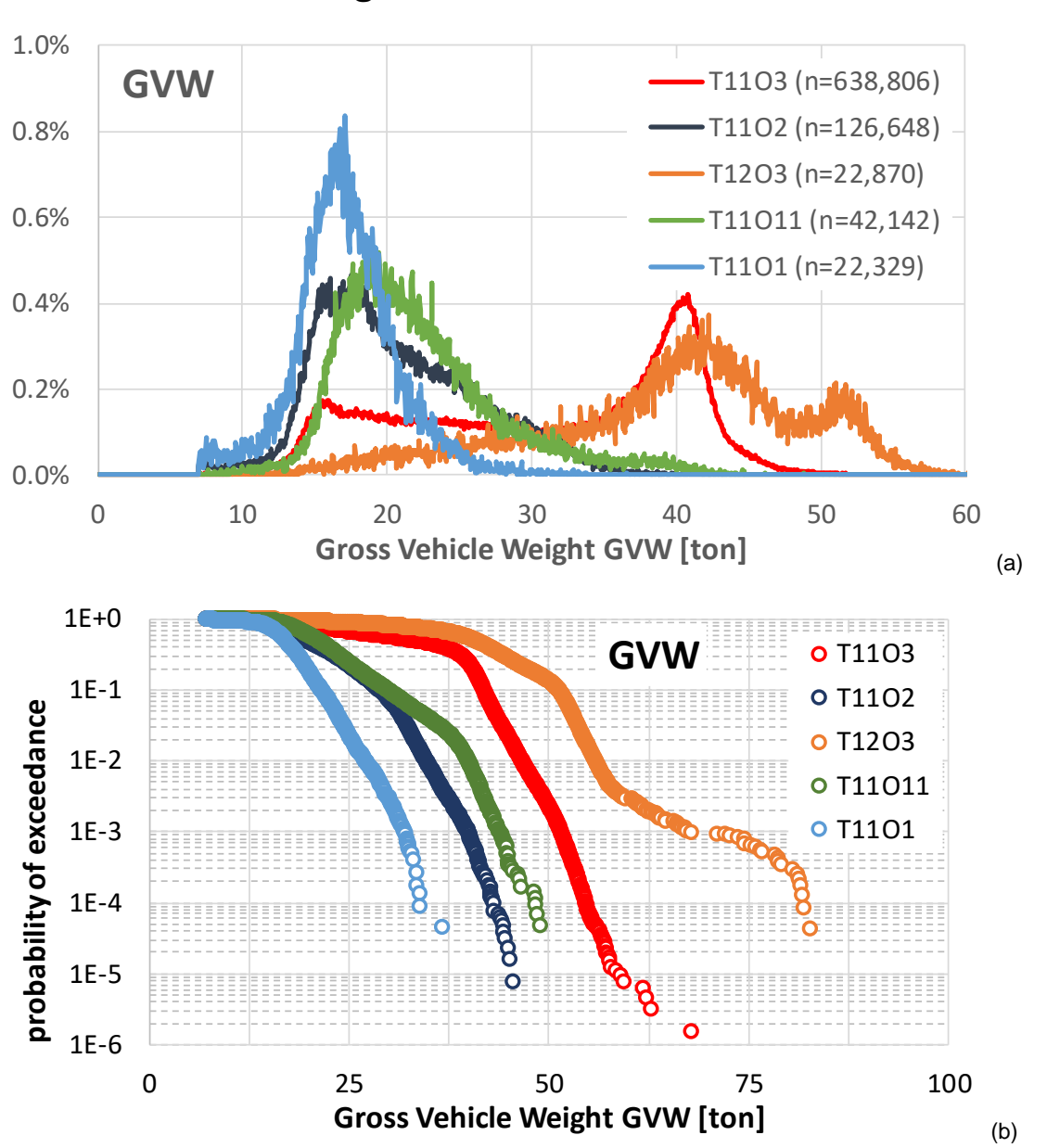


Figure 51 Distribution of weight for different vehicle subclasses (a). The cumulative probability of exceedance is given in (b).



# Axle loads and weights

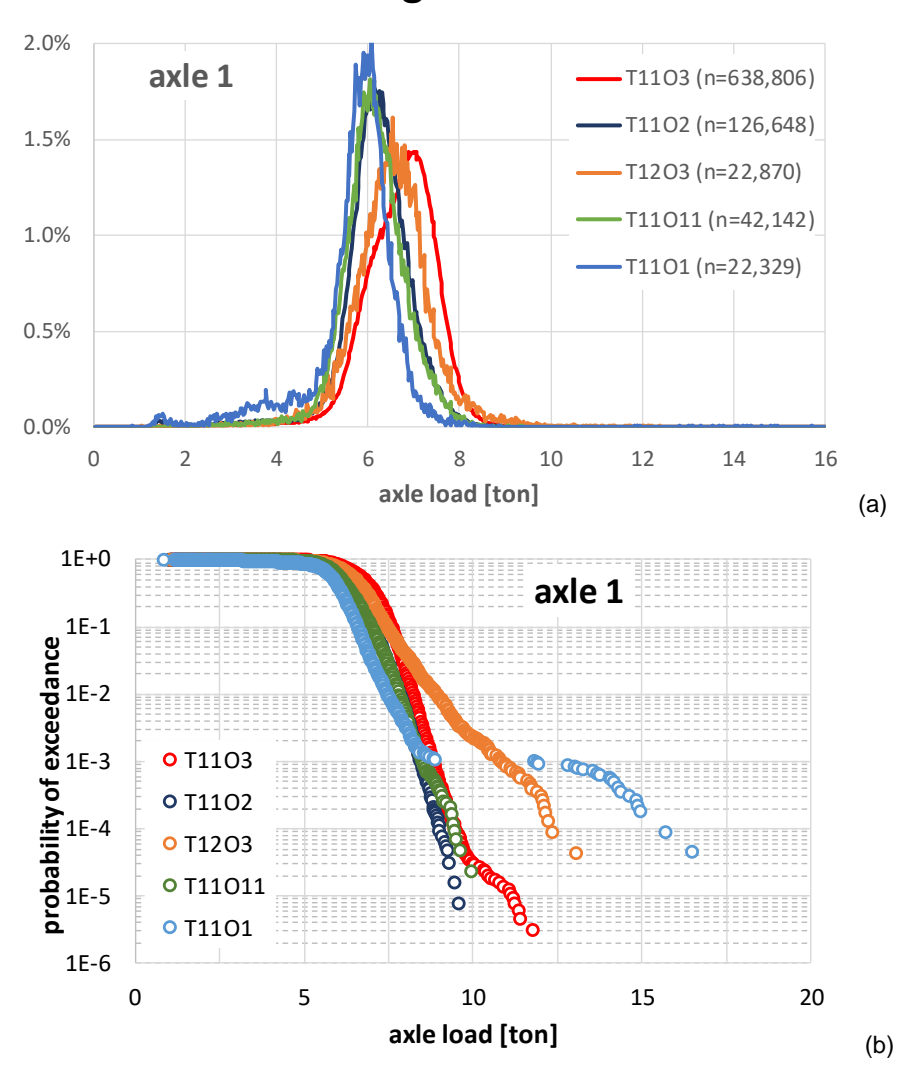


Figure 52 Distribution of the weight on the front axle for different TOCs (a). The cumulative probability of exceedance is given in (b).



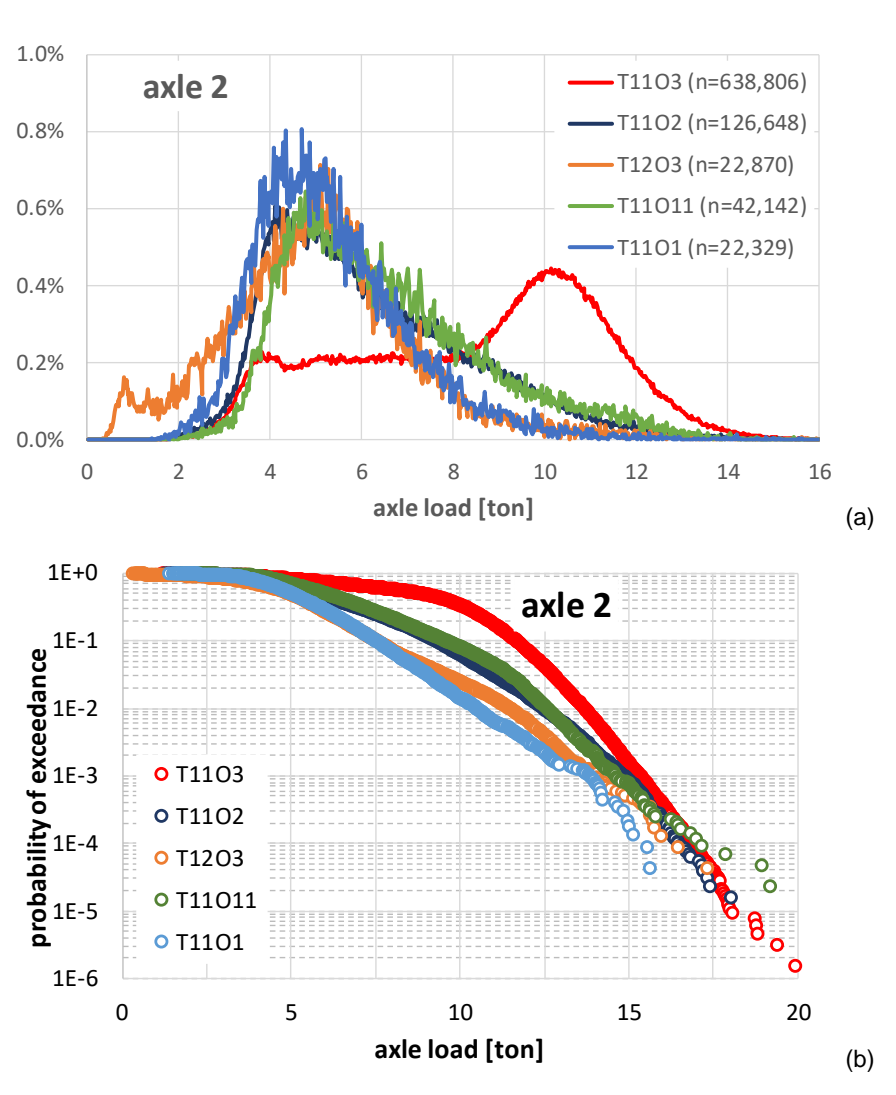


Figure 53 Distribution of the load on the second axle for different TOCs (a). The cumulative probability of exceedance is given in (b).



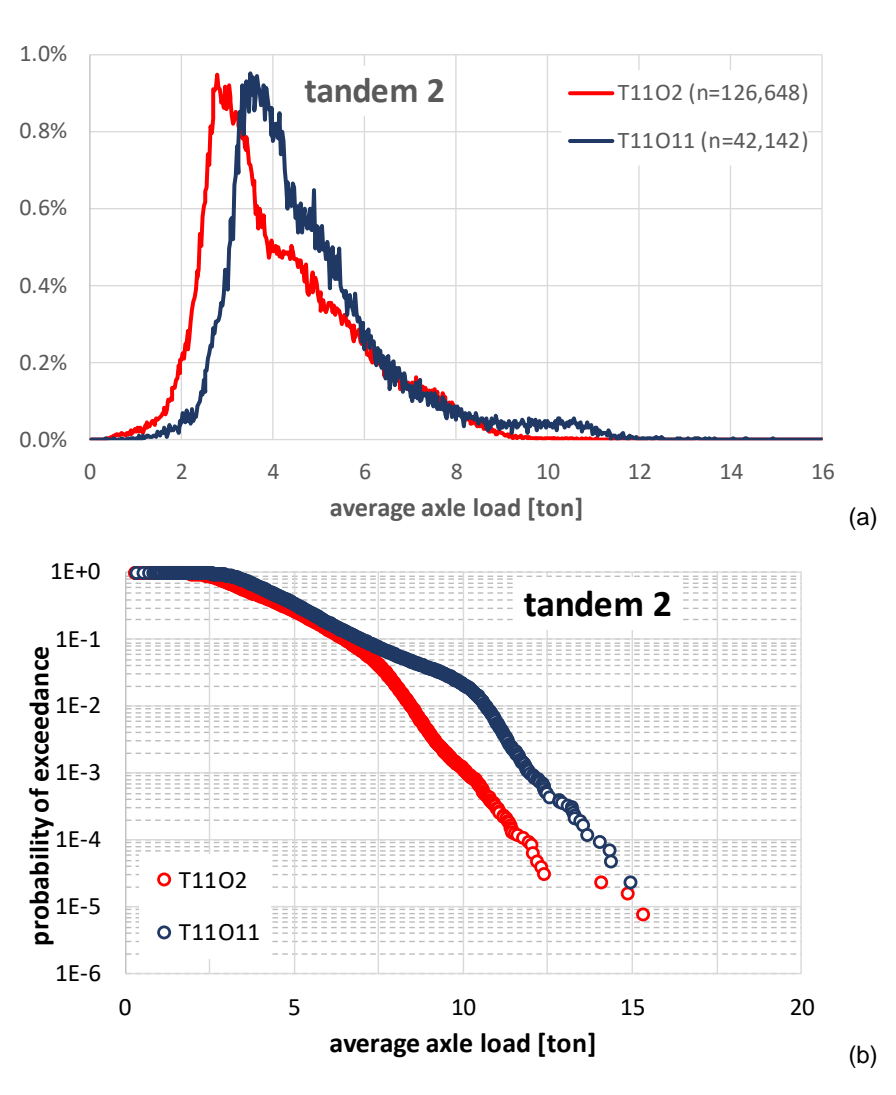


Figure 54 Distribution of the load on the tandem for different TOCs (a). The given load is the mean of the two axle loads. The probability of exceedance is given in (b).



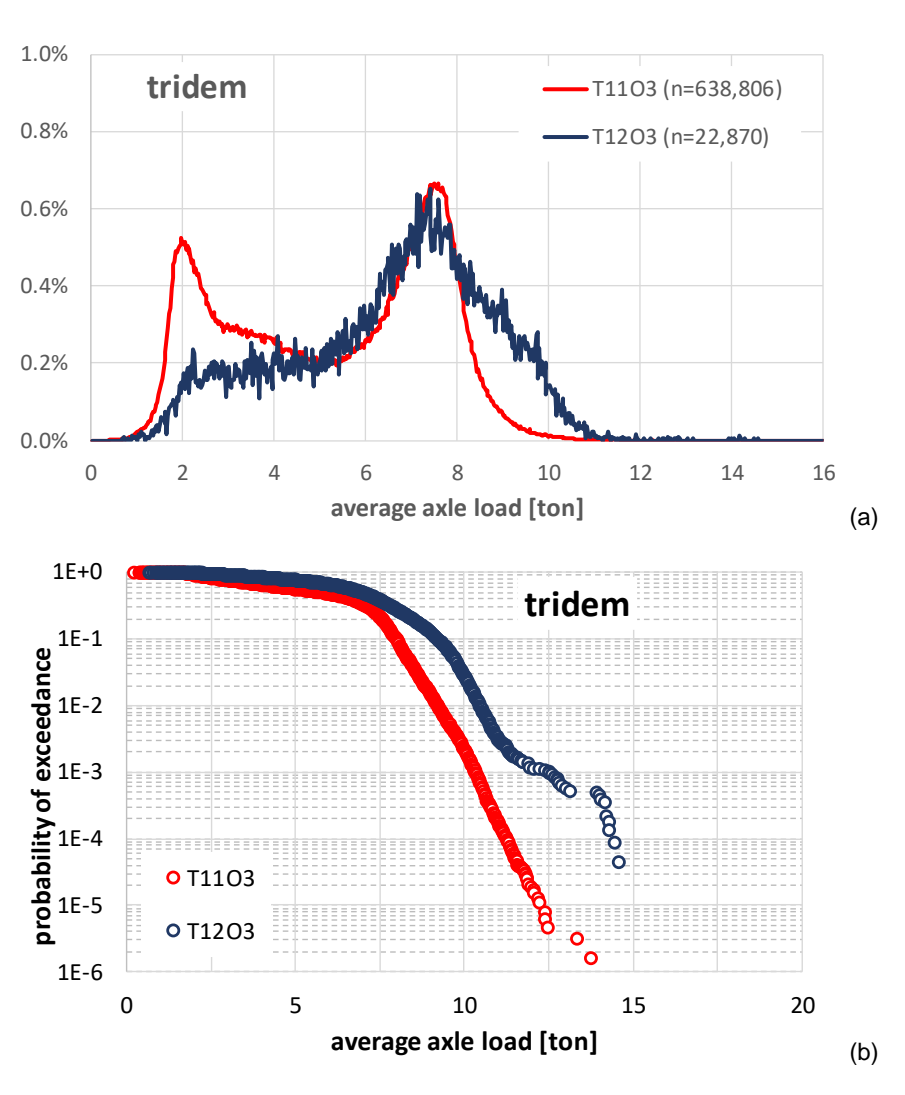


Figure 55 Distribution of the load on the tridem for different TOCs (a). The given load is the mean of the three axles. The probability of exceedance is given in (b).



# APPENDIX 2 PROCEDURE FOR SIMULATING TRAFFIC LOAD EFFECTS IN BRIDGES

#### Appendix 2A Filtering of the WIM database

The 2015 database of the highway A67R has been filtered according to the following criteria:

- vehicles with GVW > 110 tonne are removed: vehicles above the 100 tonne are subjected to
  a one-off permit per journey. However, a margin of 10% is assumed here, because heavy
  trucks without need of one-off permit might be overloaded [8],
- vehicles with erroneous registration of axles loads or inter-axle distances ('Nan' values),
- vehicles registered multiple times (e.g. vehicles with the same axle configuration, axle loads and time of passage at the WIM station).

#### Appendix 2B Generation of a stream of axles from the WIM database

The WIM dataset consist of a large number of records, one for each vehicle registered at the WIM station. The following information are provided for each vehicle:

- date and time when the vehicle passes by the WIM station
- speed
- lane
- truck type (according to the categories given in Appendix 1A "WIM-NL vehicle subclasses")
- total vehicle length (measured by inductive loop detectors)
- individual axle loads
- · axle spacings

The WIM database is translated into a sequence of axles as follows. Starting from the first vehicle of the database, the interaxle distances stored in the WIM dataset are used to define the position of the each axle load with respect to the first axle. The front-to-front distance between two vehicles is estimated as follows:

$$d = v_i \Delta t = v_i (t_{i+1} - t_i)$$

#### where:

- v<sub>i</sub> is the speed of the leading vehicle
- t<sub>i</sub> and t<sub>i+1</sub> are the arrival times of two consecutive vehicles at the WIM station

The distance d' between the front axles of two subsequent vehicles is of interest for the purpose of generating a sequence of axle loads. The distance d' is approximated by the front-to-front distance, as shown in Figure 56, without introducing significant errors.



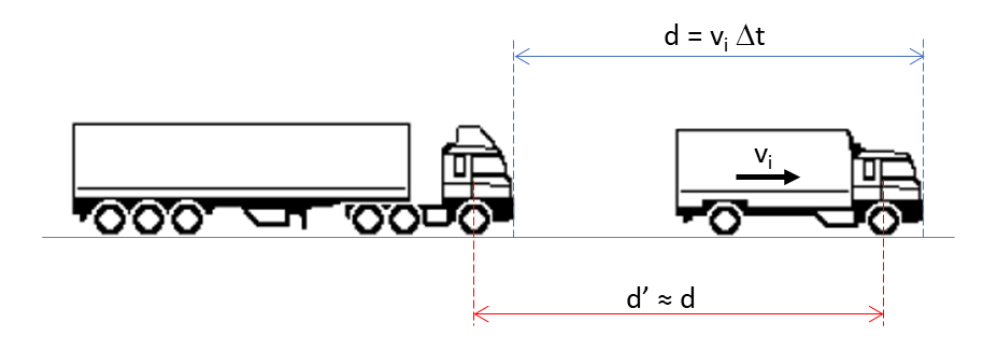


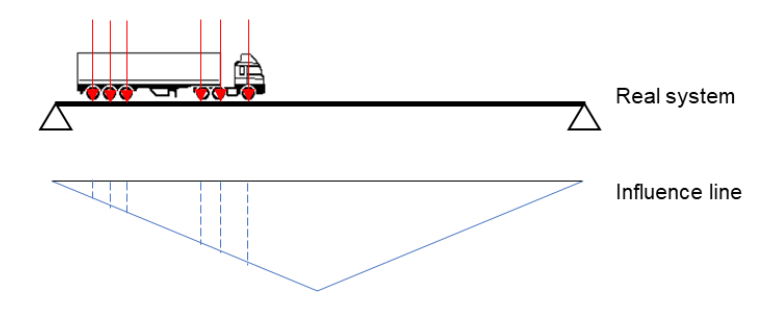
Figure 56 Intervehicle distance

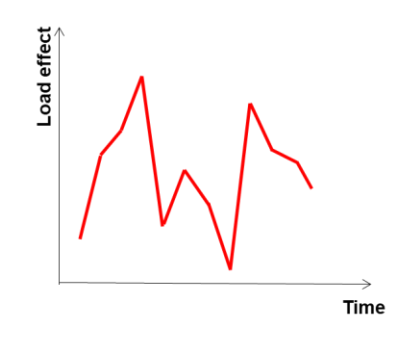
#### Appendix 2C Numerical simulation of traffic load effects

A computer code has been written for simulating the load effects of vehicles in prescribed crosssections of the bridge. The simulation consists of moving the sequence of axles previously determined on the bridge and evaluating the load effects by using a structural model of the bridge. In this project, the structural model consists of influence lines of the load effects in certain crosssections of the bridge. The following steps are performed, aiming to speed up the analysis of the load effects:

- identification of load events
- evaluation of the load effects per load event

One load events is defined by the presence of one or more vehicles on the bridge. Given the length of the bridge, the sequence of axles previously generated is analysed to identify groups of vehicles that can be on the bridge at the same time. Then, the axles loads are moved on the chosen influence lines and the load effects are evaluated for each position of the trucks (Figure 57a) by multiplying the intensity of each axle load by the corresponding value of the influence line. The time series of the load effects (Figure 57b) is obtained by storing the value of the load effect for each position of the axle loads on the bridge.





a) evaluation of the load effects

b) time series of the load effects

Figure 57 Results of the traffic load effects simulation



# APPENDIX 3 GENERATION OF WIM DATABASES INCLUDING SEC VEHICLES AND TP

#### Appendix 3A Criteria for selecting T1103 vehicles to be replaced by SEC vehicles and TP

As outlined in section 4, the effect of replacing 5-axle articulated vehicles (Figure 58) with SEC vehicles is investigated in the report. The main characteristics of the considered 5-axle vehicles have been summarized in a previous TNO study [22]:

- the distance between the first two axles ranges between 3.65 m and 3.80 m,
- the distance between second and third axles ranges between 3.0 m and 6.0 m,
- the distances between the axles in the tridem ranges between 1.34 m and 1.4 m.



Figure 58: T1103 vehicle.

The subclass "T11O3" registered by the WIM systems contains the 5-axle vehicles of interest, according to the WIM-NL classification reported in Annex 1 "WIM characteristics". However, the analysis of the interaxle distances of the vehicles registered as "T11O3" in the WIM database shows that this subcategory comprises different types of vehicles. The scatterplot of the interaxle distance between the first two axles and the axles 2 and 3 is shown in Figure 59. It can be observed that a large amount of vehicles is characterised by an inter-axle distance between axles 1 and 2 between approximately 3.5 m and 4.2 m. Nevertheless, the scatterplot shows also the presence of vehicles with inter-axle distance less than 2 m or above 5 m. The latter might be due to 5-axle vehicles consisting of a 3-axle lorry with a 2-axle trailer (Figure 60). It can be also observed that the distance between the second and the third axle ranges from 2 m to more than 14 m.

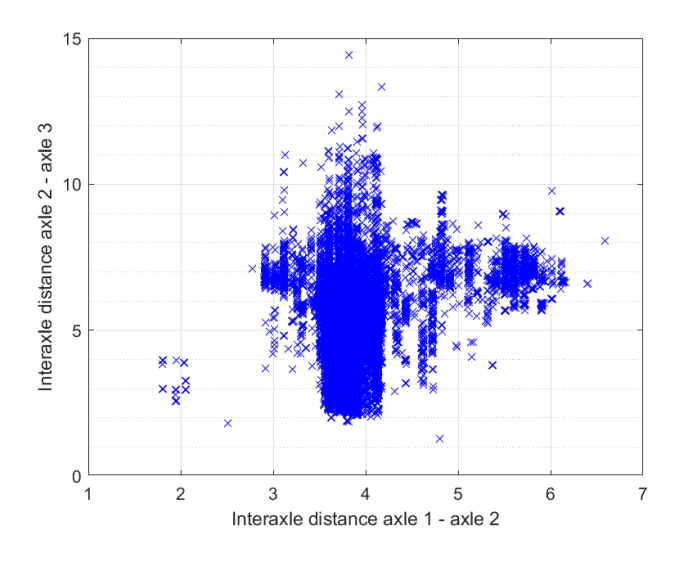


Figure 59: Interaxle distances (in m) between axle 1 and axle 2 and between axle 2 and axle 3.





Figure 60: Three-axle lorry with a two-axle trailer [22].

The scatterplot of the interaxle distances between the tyres of the tridem axle is shown in Figure 61. Even though most of the data are in the range between 1.3 m and 1.4 m, there exist tridem axles with interaxle distance less than 1 m. These axles can be seen in the lower part of Figure 62 showing the scatterplot of the inter-axle distances between axle 1 and axle 2 and between the first two axles of the tridem axles. It can be observed that vehicles with interaxle distances between axle 3 and axle 4 less than 1 m are also characterized by an interaxle distances between axle 1 and axle 2 ranging from approximately 3 m to 6.5 m. Therefore, it seems that a subset of these vehicles may comprise the five-axle vehicles shown in Figure 60

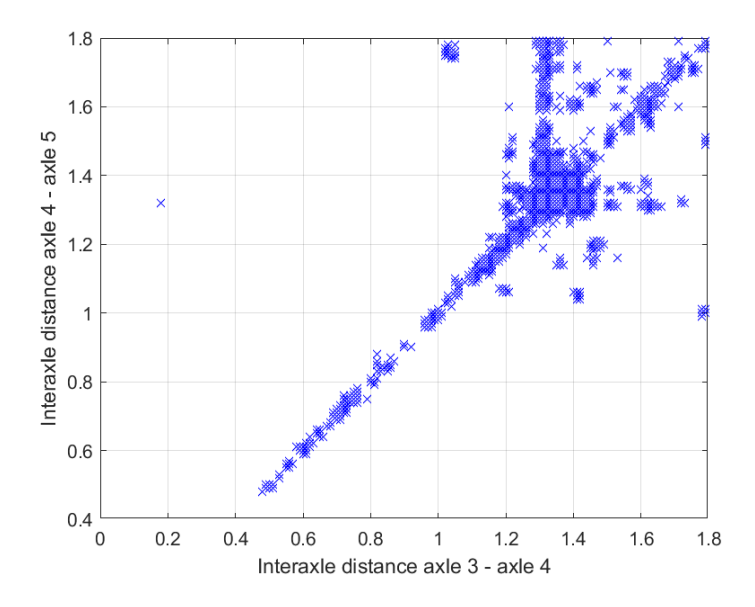


Figure 61: T1103 vehicles – inter-axle distances between axle 3 and 4 and between axle 4 and axle 5.



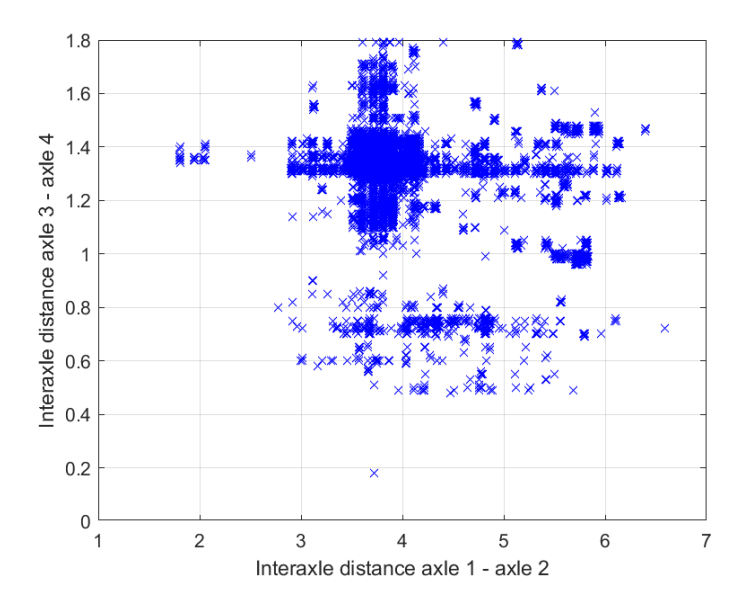


Figure 62: T1103 vehicles – inter-axle distances between axle 1 and axle 2 and between axle 3 and axle 4.

Aiming to replace only the five-axle articulated vehicles shown in Figure 58 by SEC vehicles, the following criteria for the selection of T11O3 vehicles have been defined:

- first axle load ≥ 5 t,
- inter-axle distance between the first and second axle between 3 m and 4 m,
- inter-axle distance between the second and third axle between 3 m and 7 m,
- inter-axle distance of the tridem axle larger than 1.2 m.



#### Appendix 3B Generation of SEC vehicles from T1103 vehicles

The SEC vehicles considered in this project are assumed to be ten-axle vehicles as shown in Figure 63 and they are generated from pairs of T11O3 vehicles as follows. The pairs of T11O3 vehicles are randomly selected but in chronological order of passage at the WIM station. The first part of the SEC vehicle consists of the 5 axles of the first T11O3. The axle loads and interaxle distances for the first 5 axles are exactly the same as those given in the WIM database. The interaxle distance between the fifth and the sixth axle of the SEC vehicle is assumed equal to 4 m. The configuration of the axles of the trailer of the SEC vehicle is generally different from the one of the axle of T11O3 vehicles, because the first and the second axle of these vehicles are single axle and not part of a tandem. Therefore, the WIM database was analysed to find vehicles with a trailer consisting of one tandem axle and one tridem axle. This axle configuration was found in the R1223 vehicles (Figure 64), consisting of a truck and a trailer connected by a dolly.



Figure 63: SEC vehicle.



Figure 64: R1223 vehicle.

The WIM database contains 544 records of R1223 vehicles. The scatterplots of the interaxle distances of the trailer (Figure 65 and Figure 66) show that low variability of the interaxle distances of the tandem and tridem axles. Furthermore, the distance between the second and third axle of the trailer is between 5m and 6 m, which is consistent with the filtering criterion used for the selection of the T11O3 vehicles. Therefore, it can be concluded that the axle configuration of the trailer of the R1223 vehicles is suited for SEC vehicles.



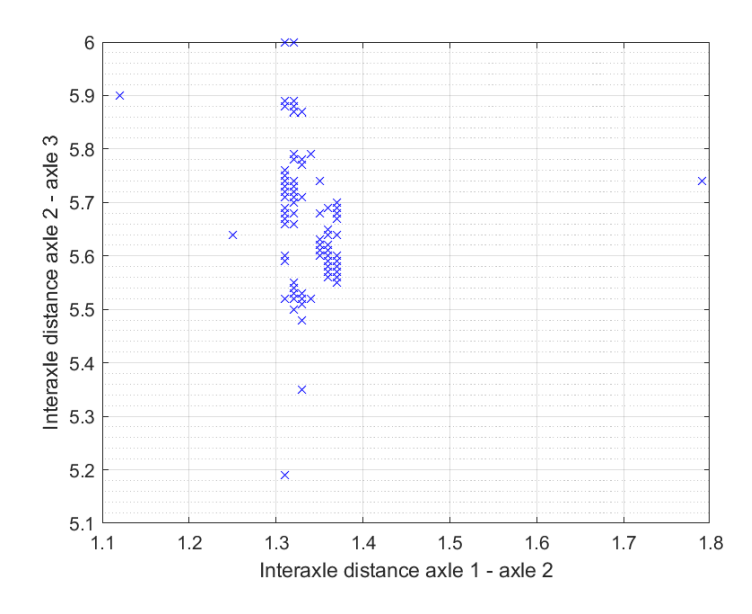


Figure 65: Trailer of R1223 vehicles - Interaxle distances (in m) between axle 1 and 2 and between axle 2 and axle 3.

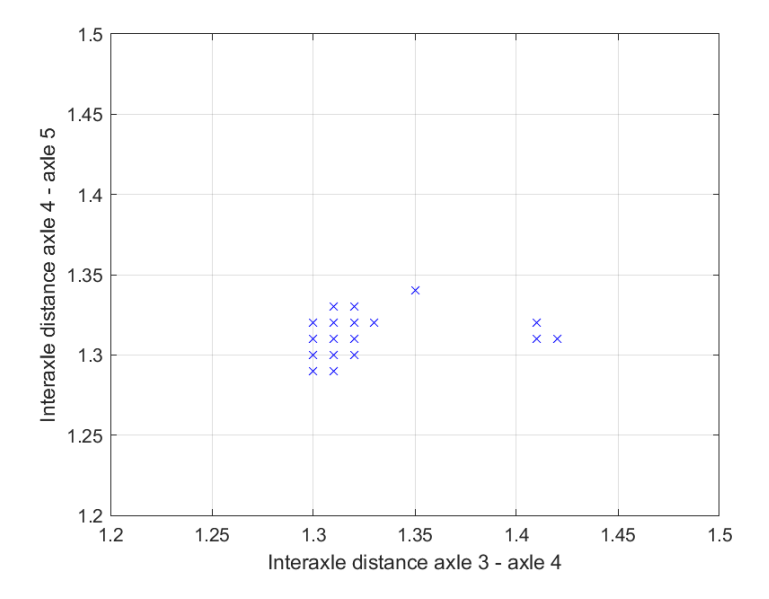


Figure 66: Trailer of R1223 vehicles - Interaxle distances (in m) between axle 1 and 2 and between axle 2 and axle 3.

The values of each axle load of the trailer of R1223 vehicles are plotted in Figure 67 against the gross weight of the trailer itself. A linear trend is visible for each axle load, although more scatter can be observed for the tandem axle (axles 1 and 2) than for the tridem axle (axles 3, 4 and 5).



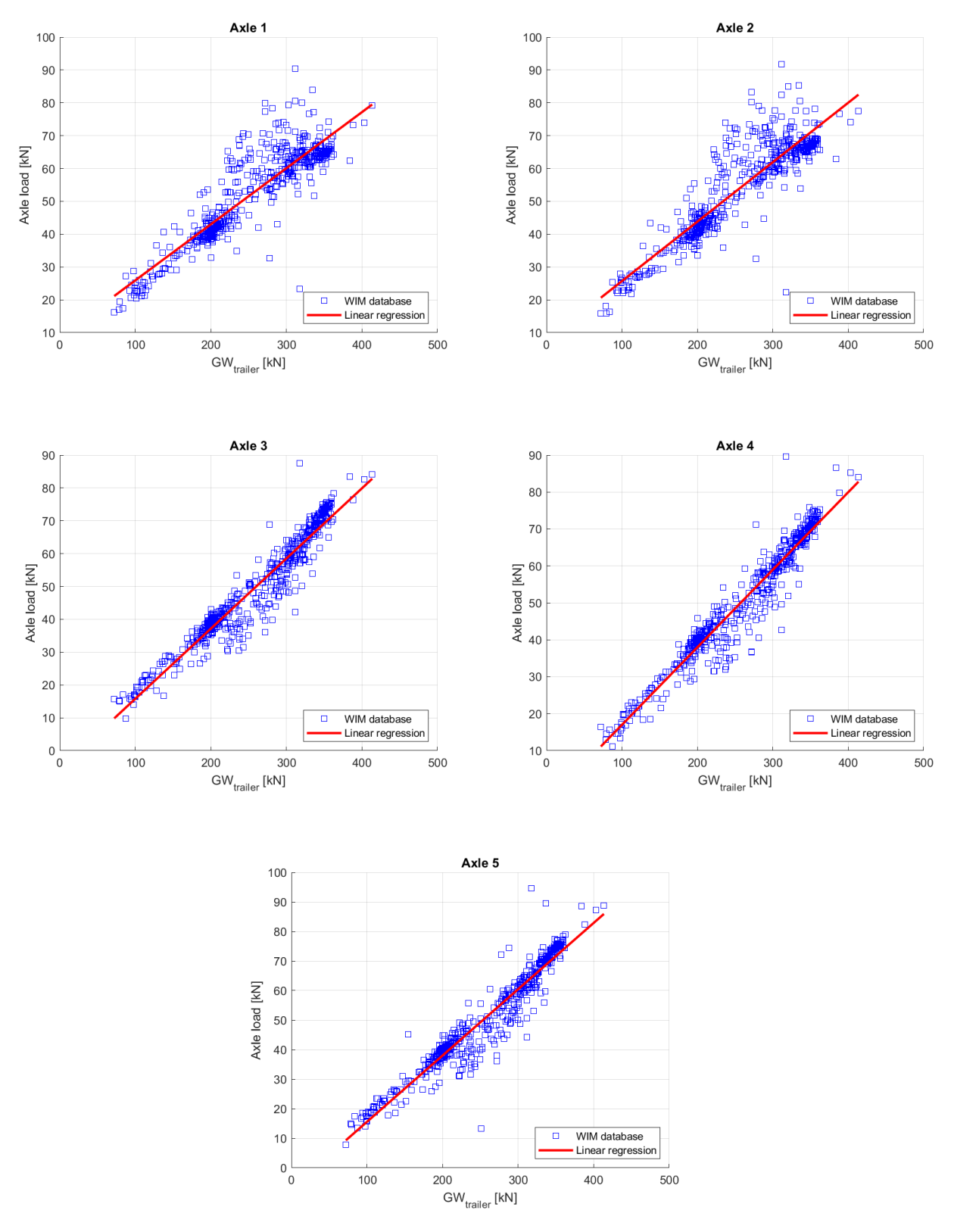


Figure 67: Trailer of R1223 vehicles – Axle loads vs gross weight of the trailer.



The procedure for generating SEC vehicles is summarized as follows:

- two T11O3 vehicles are selected from the WIM database and their gross vehicle weights GVW<sub>1</sub> and GVW<sub>2</sub> are computed,
- one R1223 vehicle is randomly selected from the WIM database and the weight of the trailer GVW<sub>trailer</sub> is computed,
- the first five axles loads and their interaxle distances of the SEC vehicle are set equal to those of the first selected T11O3 vehicle.
- the interaxle distance between the fifth axle and the sixth axle of the SEC vehicle is set equal to 4 m,
- the remaining interaxle distances (axles 6 to 10) of the SEC vehicle are set equal to those of the trailer of the selected R1223 vehicle,
- the five axle loads of the trailer of the SEC vehicle are determined by scaling the axles loads
  of the trailer of R1223 vehicle such that their sum is equal to the gross vehicle weight
  GVW<sub>second T1103</sub> of the second selected T1103 vehicle:

$$Q_{SEC\ trailer,i} = Q_{R1223\ trailer,i} \frac{GVW_{second\ T1103}}{GW_{R1223\ trailer}} \quad \text{with i} = 1, 2, ..., 5$$

• if the gross vehicle weight GVW<sub>SEC</sub> of the SEC vehicle exceeds 76 tonne, the axles loads of the trailer of the SEC vehicle are reduced as follows:

$$Q_{SEC\ trailer,i} = Q_{SEC\ trailer,i} \frac{760 - GVW_{first\ T1103}}{GVW_{second\ T1103}} \quad \text{with i} = 1, 2, ..., 5$$

During the generation of SEC vehicles, these vehicles are not restricted to travel only on the slow lane. However, the occurrence of SEC vehicles on the fast lane is very low, considered that 95% of the T11O3 vehicles registered in the WIM dataset travel on the slow lane.



#### Appendix 3C Generation of Truck Platoons from T1103 vehicles

The analysis of the traffic load effects is performed for truck platoons consisting of three T11O3 vehicles. The procedure described in Appendix 3A for the selection of T11O3 vehicles to form a SEC vehicle is used also for Truck Platooning. In the generation procedure is assumed that Truck Platoons travel only on the slow lane.

Two values of the intervehicle gap are considered, 0.3 s and 1.5 s as discussed in section 3.4.2 .The speed of the leading vehicle of the truck platoon is obtained from the WIM database and it is used to define the constant intervehicle distance, based on the assumed gaps of 0.3 s and 1.5 s, between the 5-axle vehicles forming the platoon.



## **APPENDIX 4 TRAFFIC LOAD EFFECTS IN BRIDGES**

#### Appendix 4A Traffic load effects induced by regular traffic

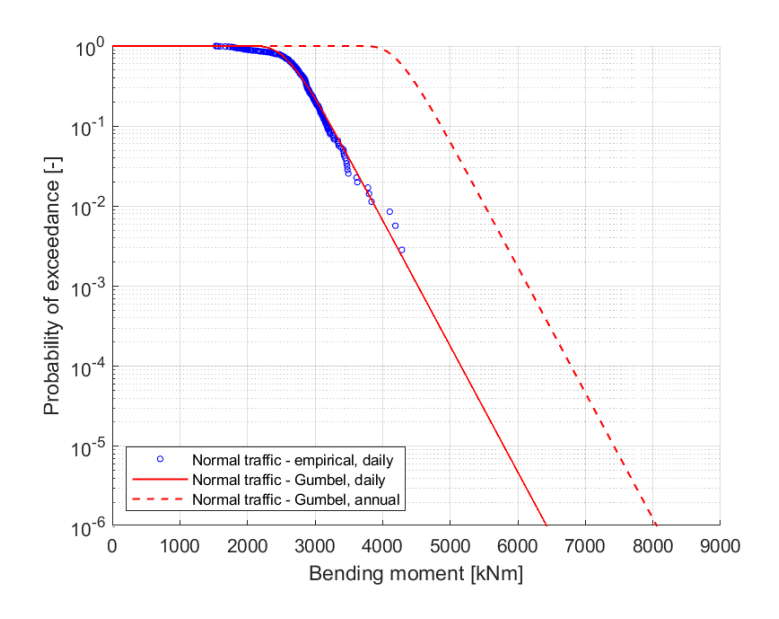


Figure 68: Probability of exceedance of the daily extreme bending moment in the midspan section of a simply supported bridge with length L equal to 20 m.

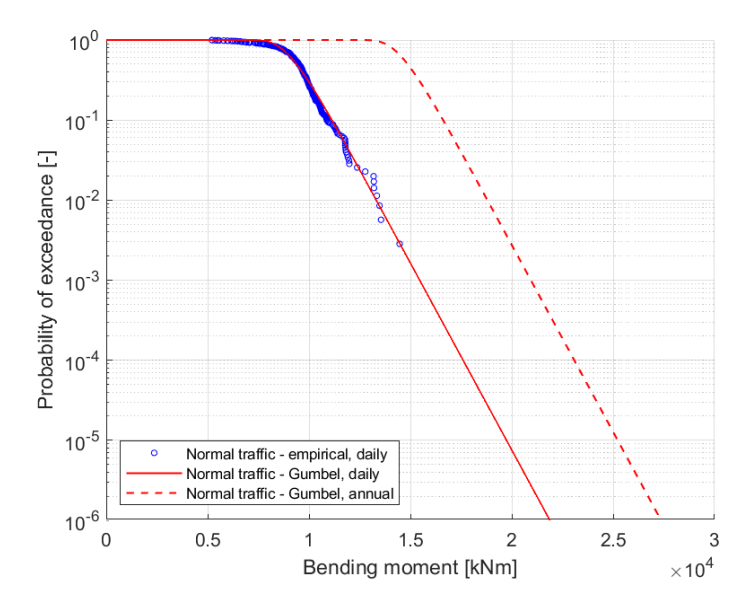


Figure 69: Probability of exceedance of the daily extreme bending moment in the midspan section of a simply supported bridge with length L equal to 50 m.



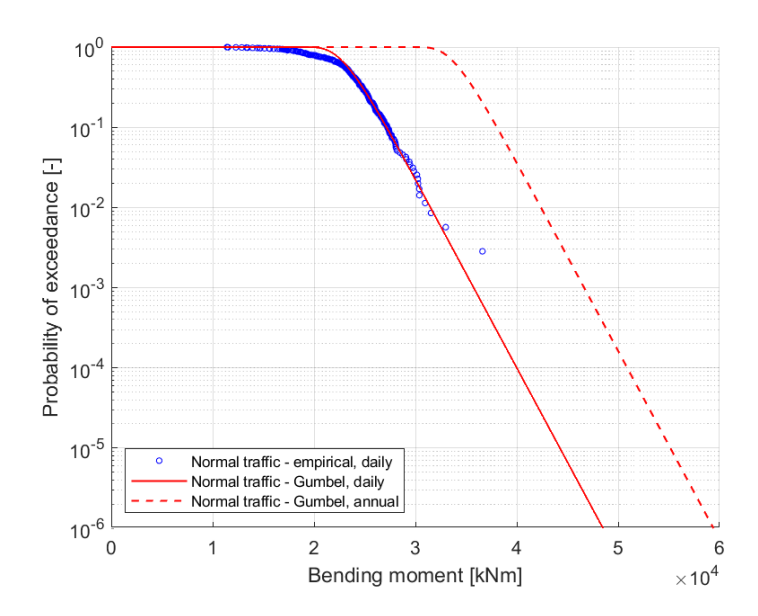


Figure 70: Probability of exceedance of the daily extreme bending moment in the midspan section of a simply supported bridge with length L equal to 100 m.

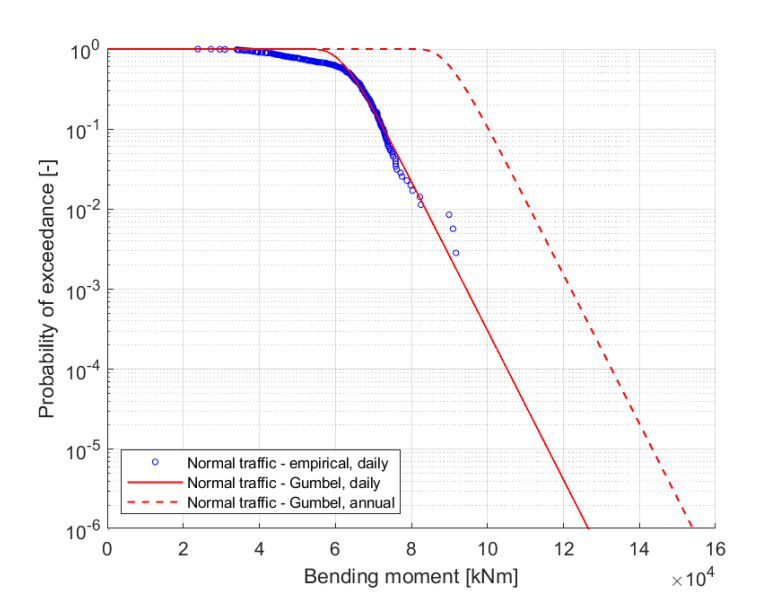


Figure 71: Probability of exceedance of the daily extreme bending moment in the midspan section of a simply supported bridge with length L equal to 100 m.



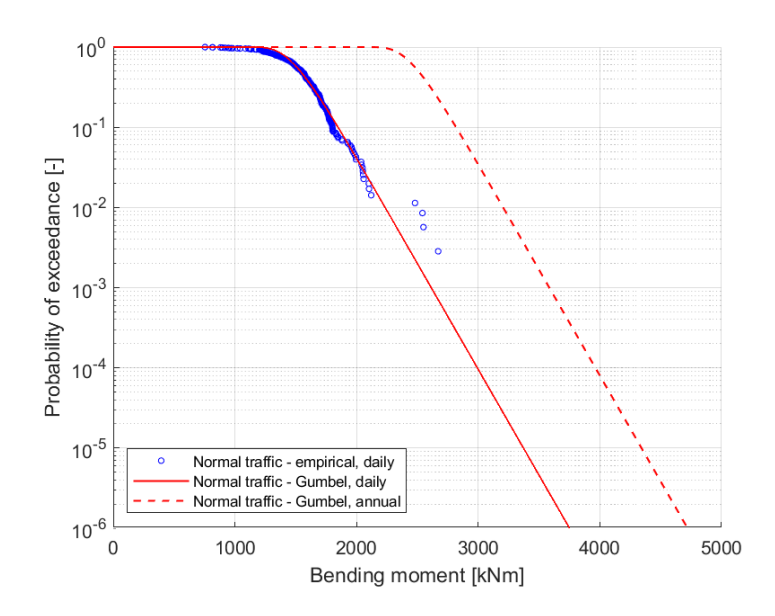


Figure 72: Probability of exceedance of the daily extreme bending moment at the inner support section of a two-span continuous bridge with span length L (each span) equal to 20 m.

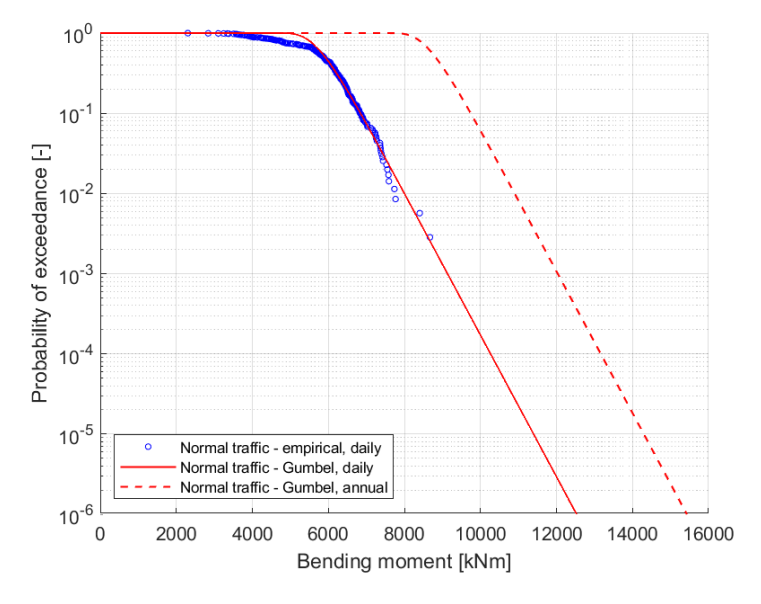


Figure 73: Probability of exceedance of the daily extreme bending moment at the inner support section of a two-span continuous bridge with span length L (each span) equal to 50 m.



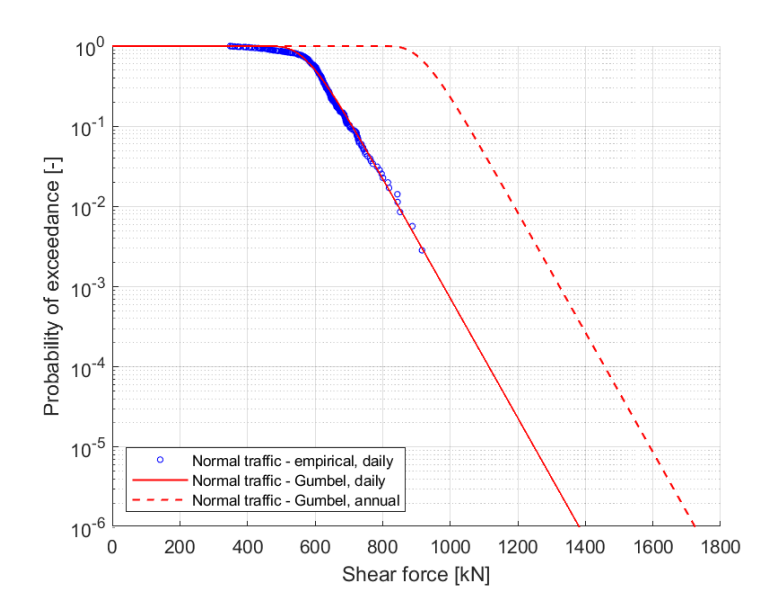


Figure 74: Probability of exceedance of the daily extreme shear force in the section to the left of the inner support of a two-span continuous bridge with span length L (each span) equal to 20 m.

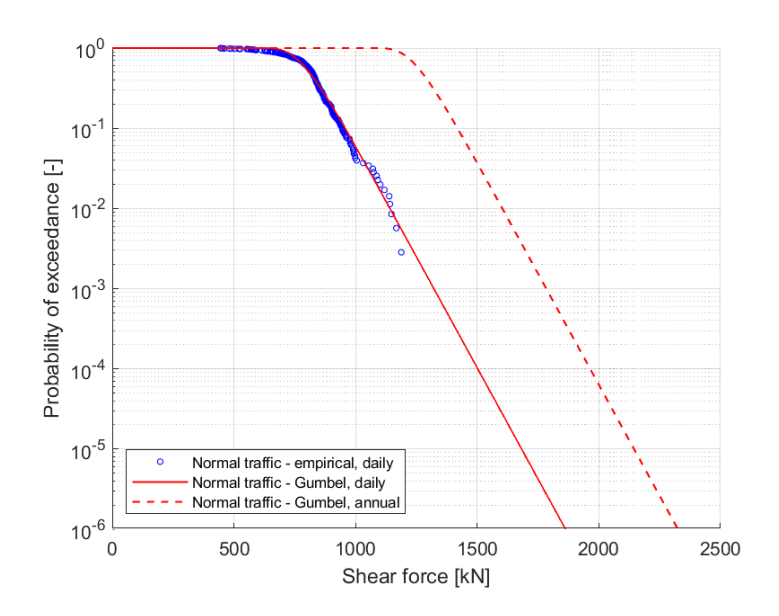


Figure 75: Probability of exceedance of the daily extreme shear force in the section to the left of the inner support section of a two-span continuous bridge with span length L (each span) equal to 50 m.



#### Appendix 4B Traffic load effects induced by SEC vehicles

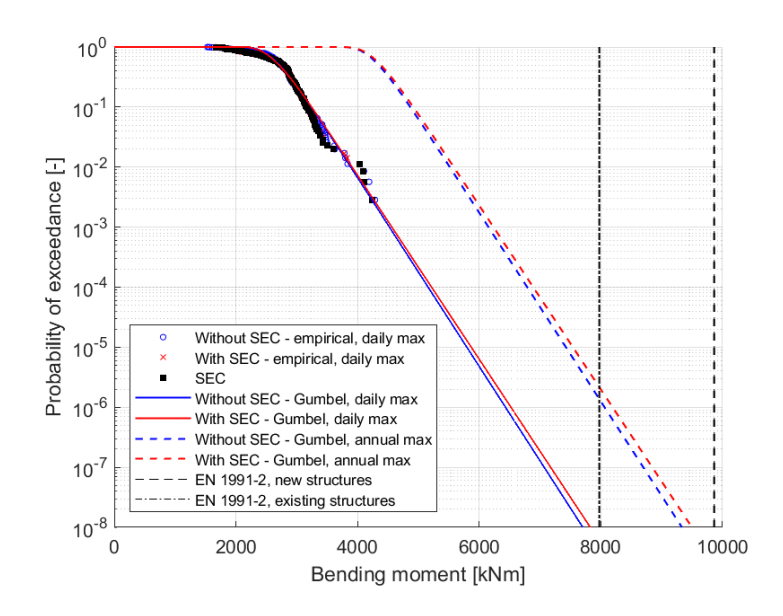


Figure 76: Probability of exceedance of the daily extreme bending moment in the midspan section of a simply supported bridge with length L equal to 20 m.

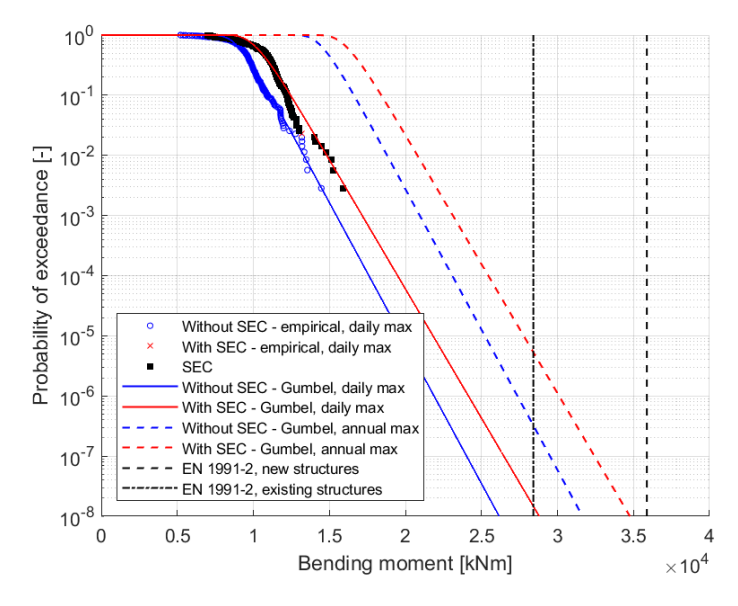


Figure 77: Probability of exceedance of the daily extreme bending moment in the midspan section of a simply supported bridge with length L equal to 50 m.



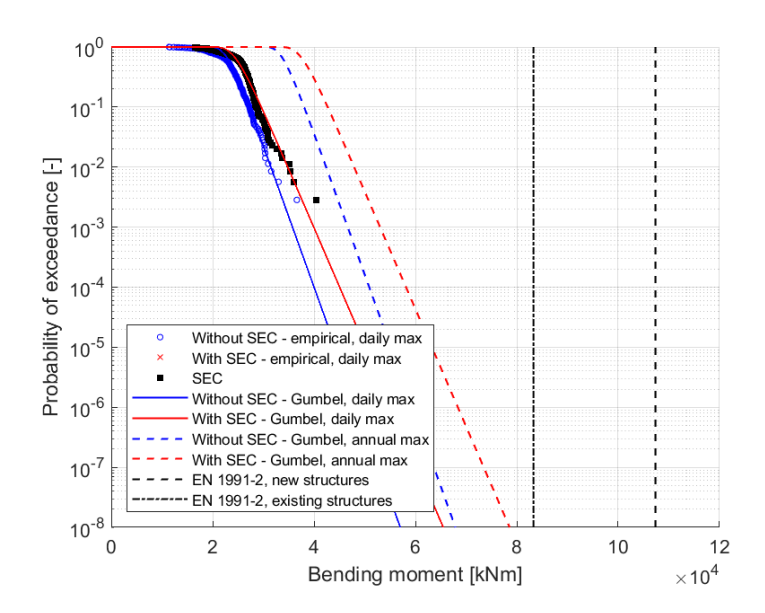


Figure 78: Probability of exceedance of the daily extreme bending moment in the midspan section of a simply supported bridge with length L equal to 100 m.

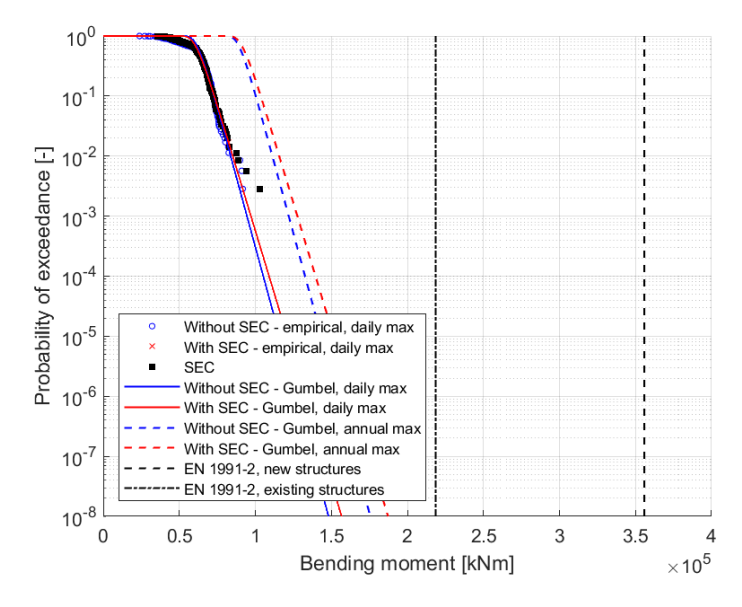


Figure 79: Probability of exceedance of the daily extreme bending moment in the midspan section of a simply supported bridge with length L equal to 200 m.



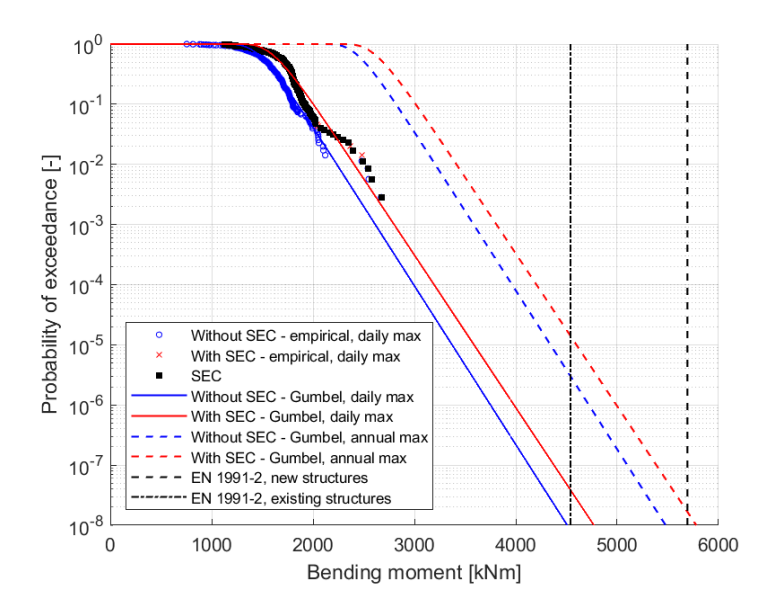


Figure 80: Probability of exceedance of the daily extreme bending moment at the inner support section of a two-span continuous bridge with span length L (each span) equal to 20 m.

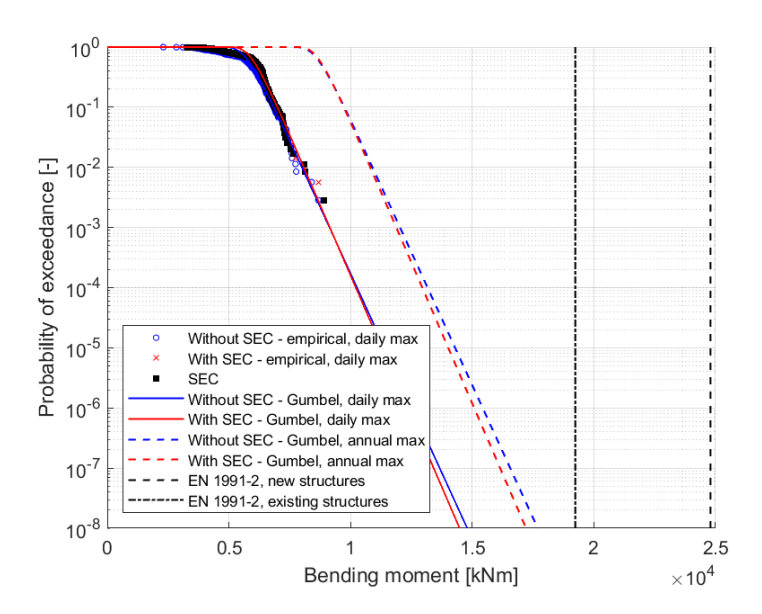


Figure 81: Probability of exceedance of the daily extreme bending moment at the inner support section of a two-span continuous bridge with span length L (each span) equal to 50 m.



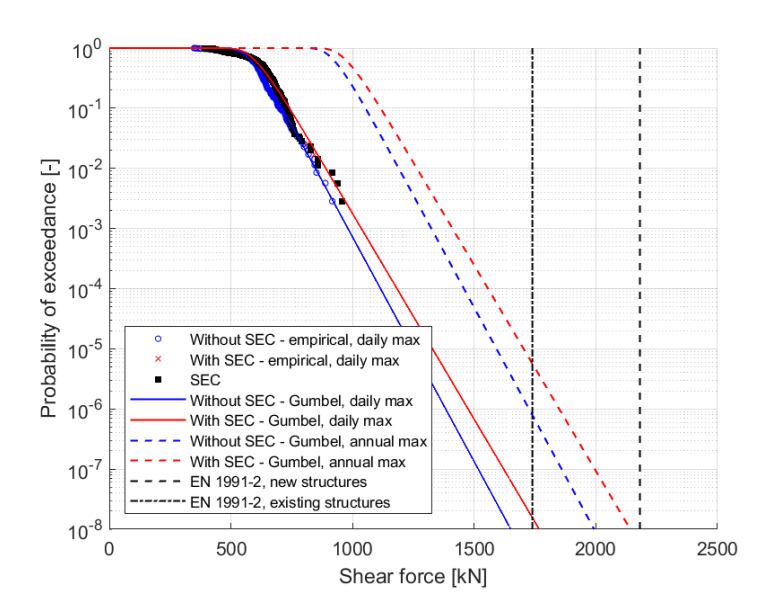


Figure 82: Probability of exceedance of the daily extreme shear force in the section to the left of the inner support of a two-span continuous bridge with span length L (each span) equal to 20 m.

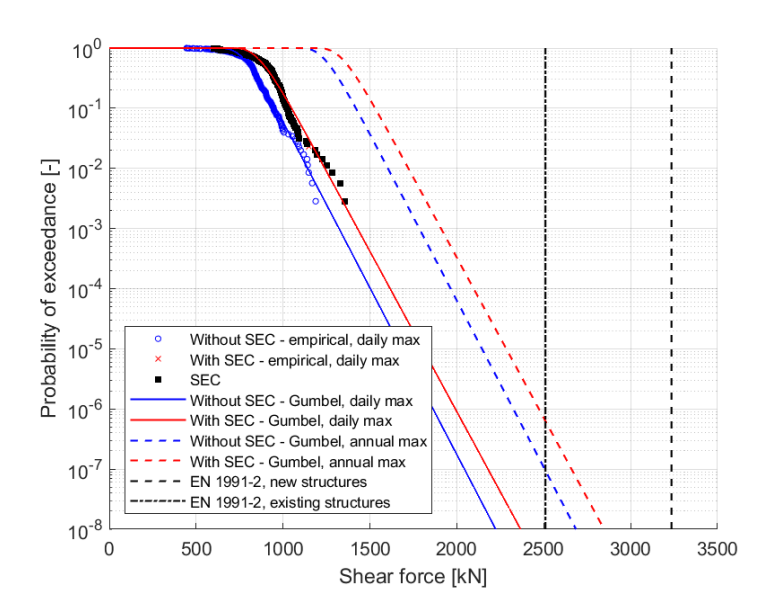


Figure 83: Probability of exceedance of the daily extreme shear force in the section to the left of the inner support section of a two-span continuous bridge with span length L (each span) equal to 50 m.



#### Appendix 4C Load effects induced by Truck Platoons

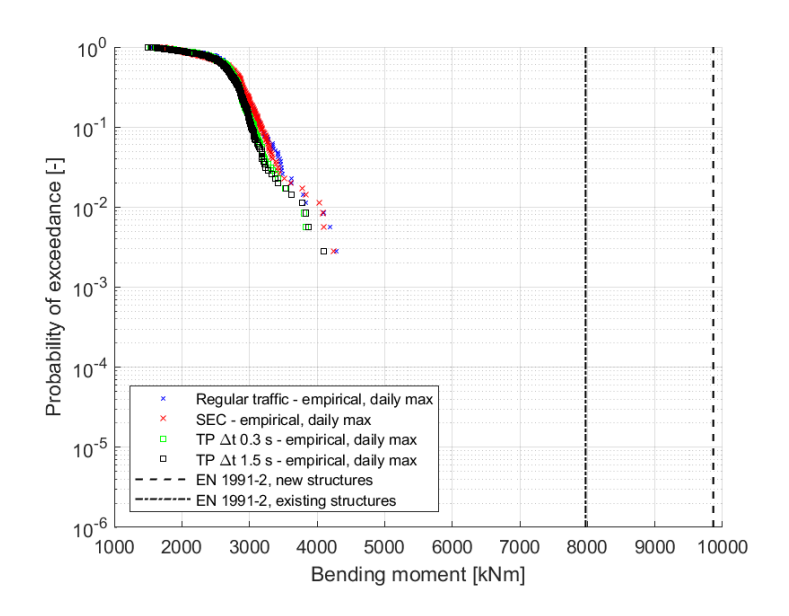


Figure 84: Probability of exceedance of the extreme bending moment in the midspan section of a simply supported bridge with length L equal to 20 m.

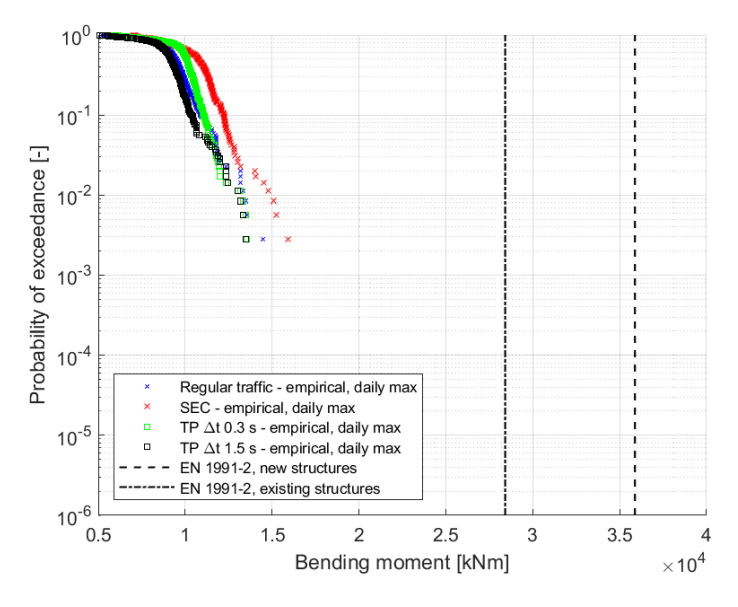


Figure 85: Probability of exceedance of the extreme bending moment in the midspan section of a simply supported bridge with length L equal to 50 m.



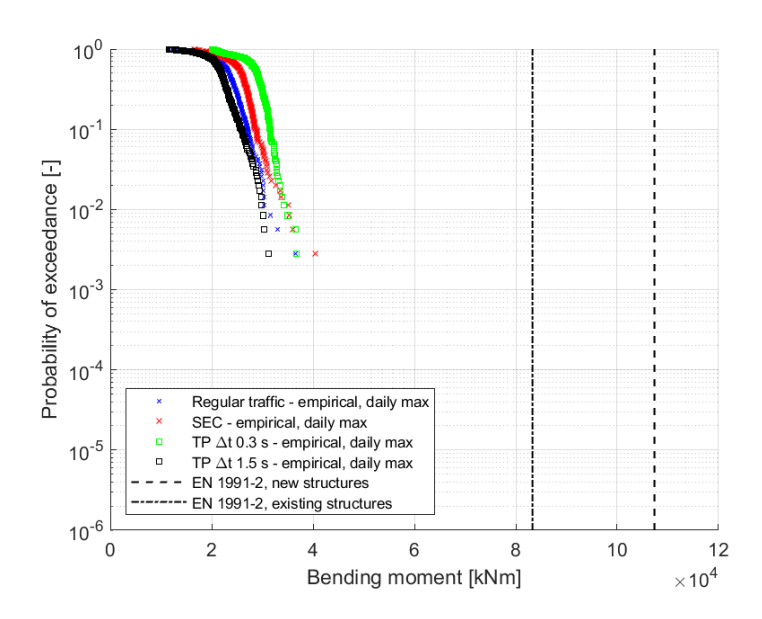


Figure 86: Probability of exceedance of the extreme bending moment in the midspan section of a simply supported bridge with length L equal to 100 m.

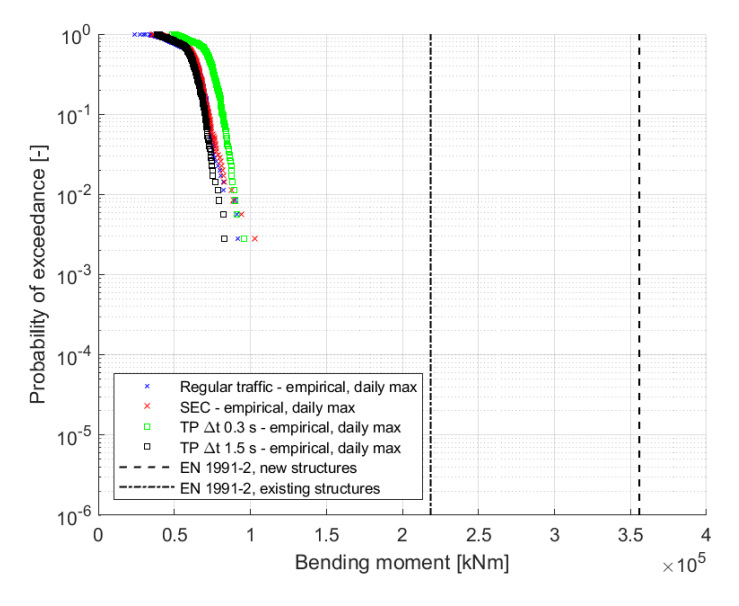


Figure 87: Probability of exceedance of the extreme bending moment in the midspan section of a simply supported bridge with length L equal to 200 m.



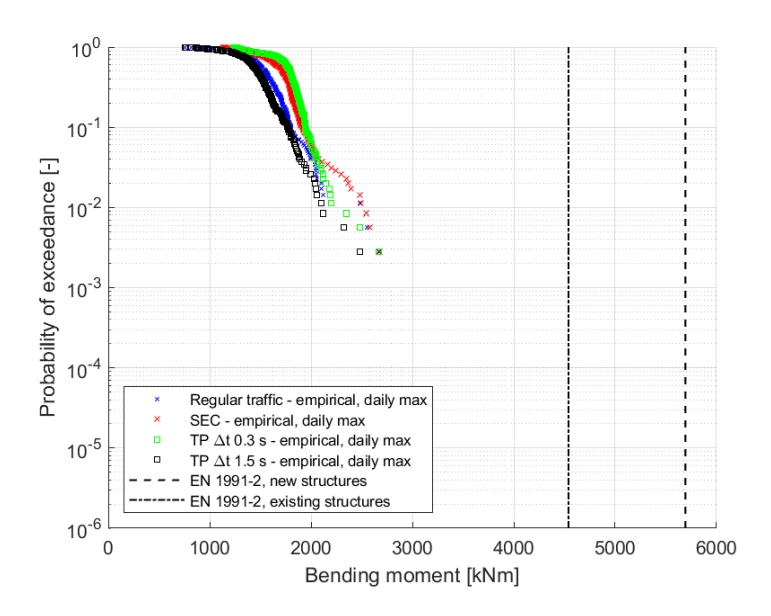


Figure 88: Probability of exceedance of the extreme bending moment at the inner support section of a two-span continuous bridge with span length L (each span) equal to 20 m.

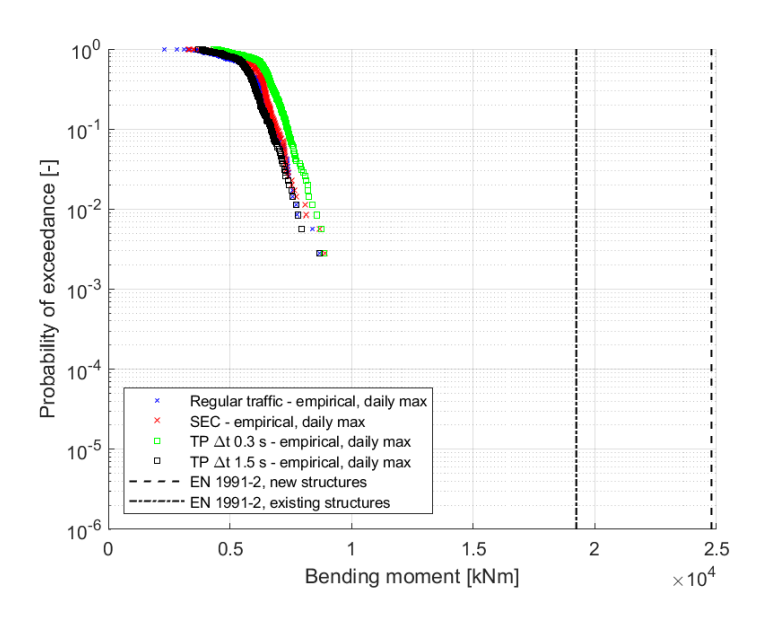


Figure 89: Probability of exceedance of the extreme bending moment at the inner support section of a two-span continuous bridge with span length L (each span) equal to 50 m.



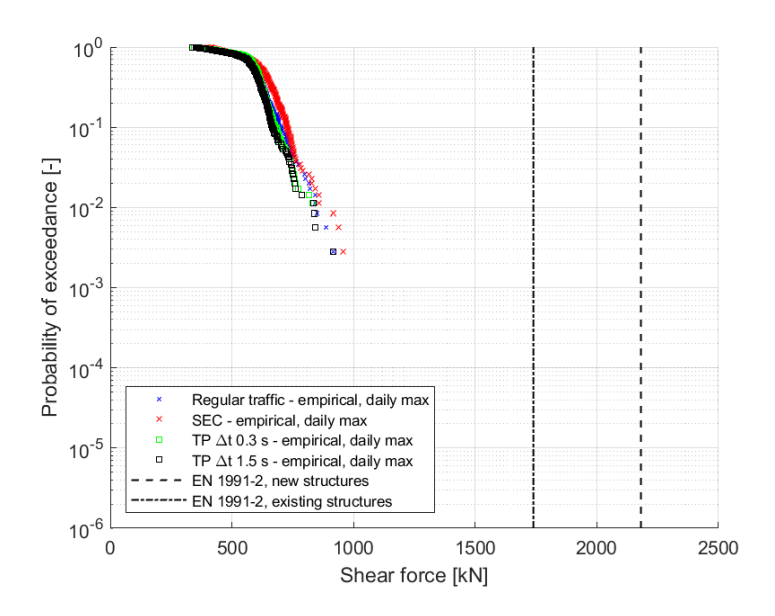


Figure 90: Probability of exceedance of the extreme shear force in the section to the left of the inner support of a two-span continuous bridge with span length L (each span) equal to 20 m.

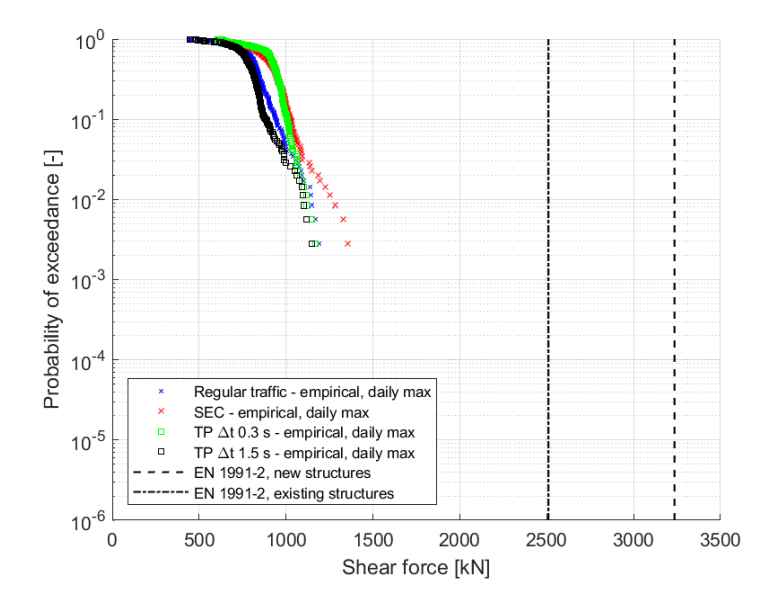


Figure 91: Probability of exceedance of the extreme shear force in the section to the left of the inner support section of a two-span continuous bridge with span length L (each span) equal to 50 m.



Appendix 4D Comparison between the load effects induced by individual SEC vehicles and the load effects due to regular vehicles

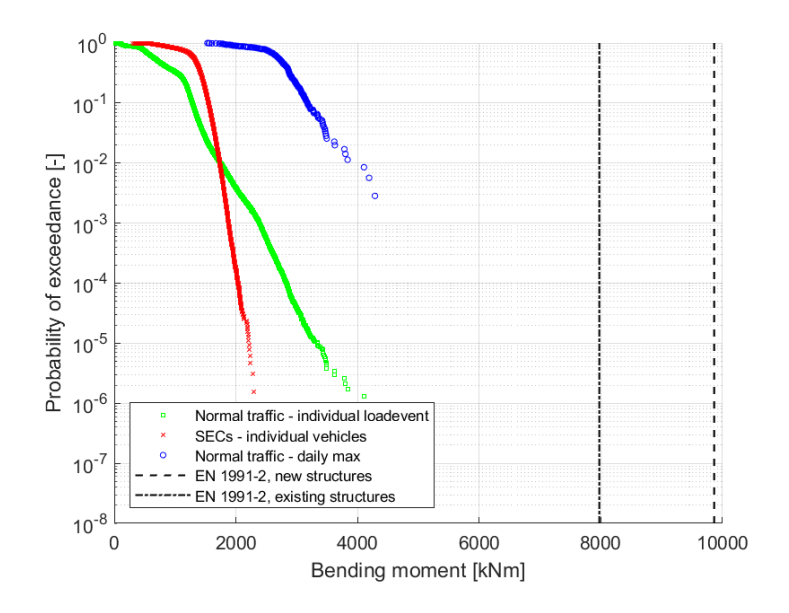


Figure 92: Probability of exceedance of the extreme bending moment in the midspan section of a simply supported bridge with length L equal to 20 m.

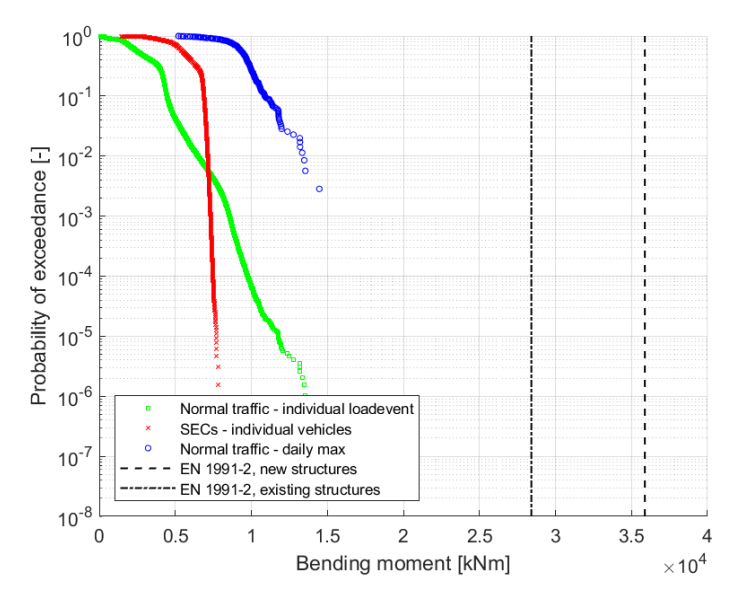


Figure 93: Probability of exceedance of the extreme bending moment in the midspan section of a simply supported bridge with length L equal to 50 m.



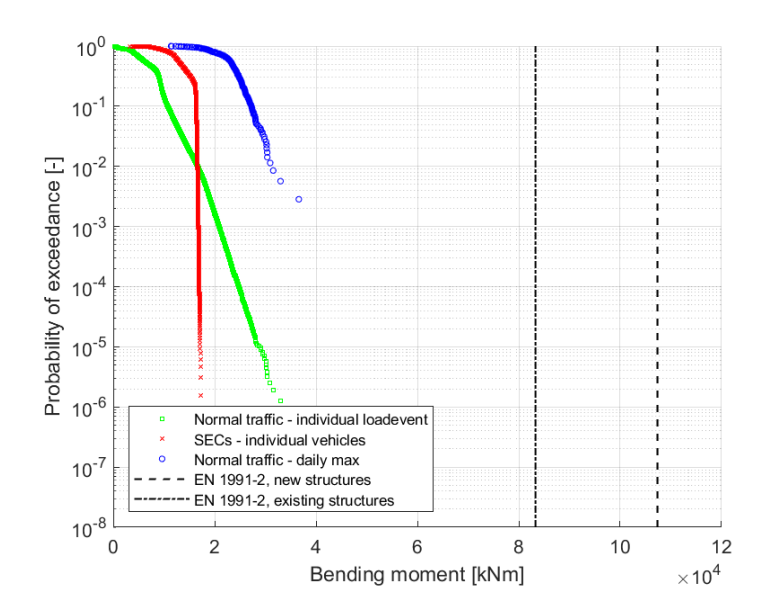


Figure 94: Probability of exceedance of the extreme bending moment in the midspan section of a simply supported bridge with length L equal to 100 m.

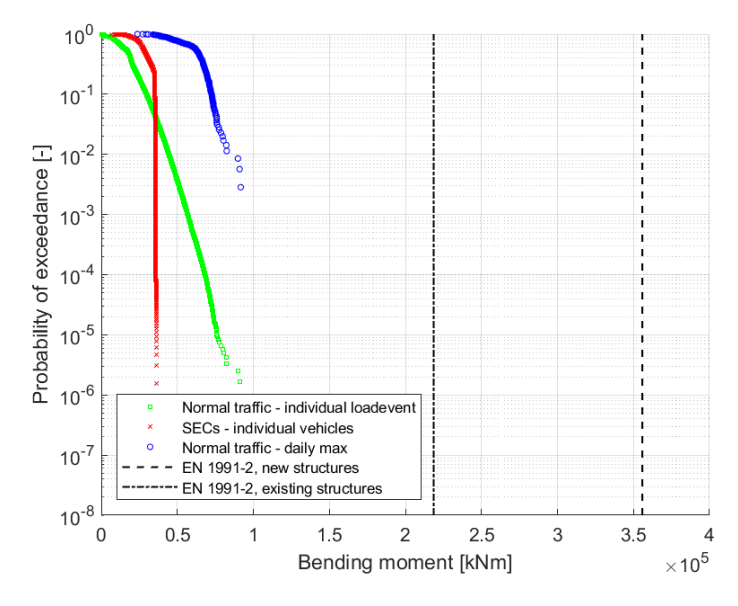


Figure 95: Probability of exceedance of the extreme bending moment in the midspan section of a simply supported bridge with length L equal to 200 m.



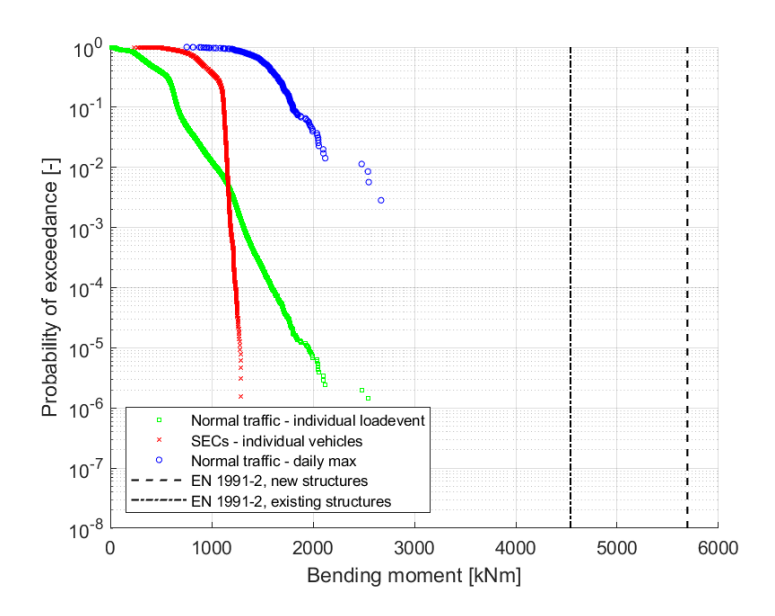


Figure 96: Probability of exceedance of the extreme bending moment at the inner support section of a two-span continuous bridge with span length L (each span) equal to 20 m.

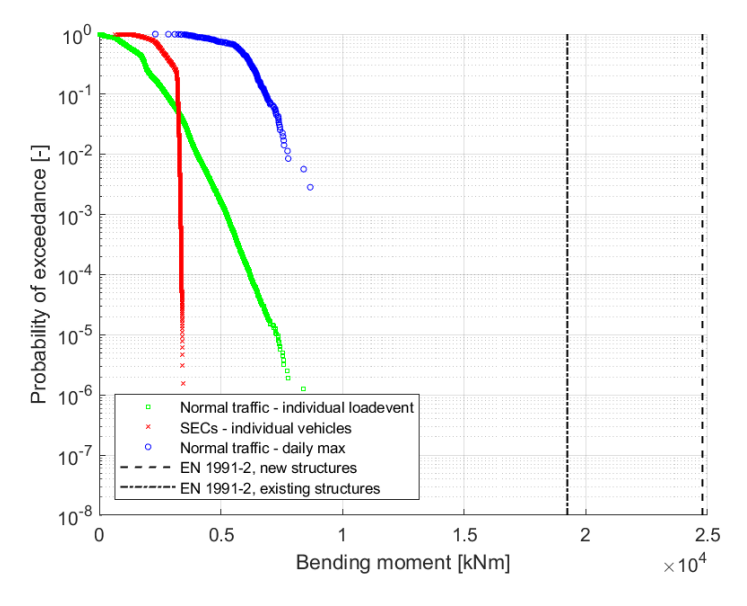


Figure 97: Probability of exceedance of the extreme bending moment at the inner support section of a two-span continuous bridge with span length L (each span) equal to 50 m.



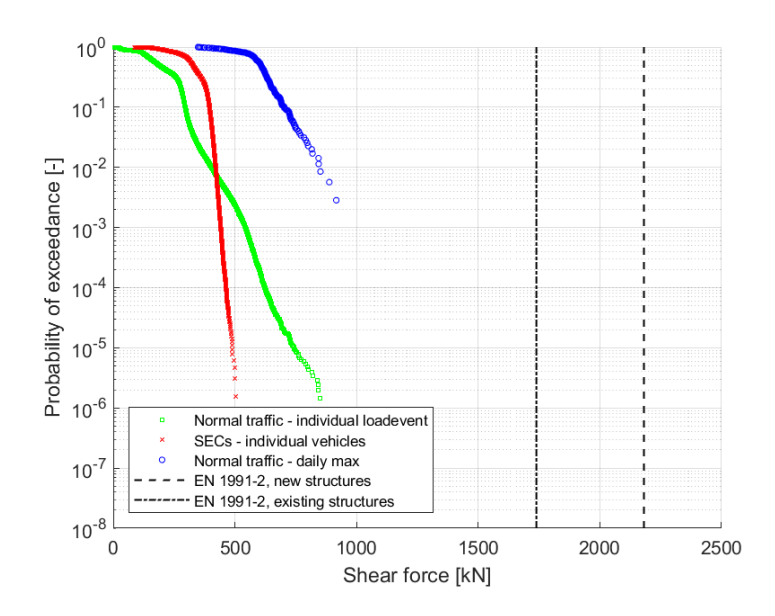


Figure 98: Probability of exceedance of the extreme shear force in the section to the left of the inner support of a twospan continuous bridge with span length L (each span) equal to 20 m.

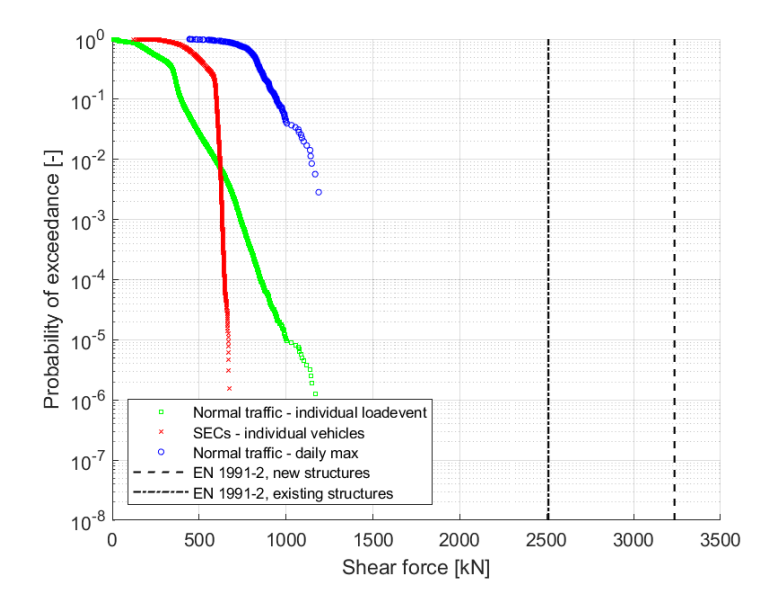


Figure 99: Probability of exceedance of the extreme shear force in the section to the left of the inner support section of a two-span continuous bridge with span length L (each span) equal to 50 m.



# APPENDIX 5 ASSESSMENT OF DESIGN LOAD EFFECTS BASED ON LOAD MODEL 1 OF NEN-EN 1991-2 FOR NEW AND EXISTING STRUCTURES AND OLD DUTCH STANDARDS

### Appendix 5A Design traffic load effects according to NEN-EN 1991-2 and NEN 8701

The design value of the bending moment  $M_{Ed}$  and shear force  $V_{Ed}$  are calculated according to EN 1990:2002 [3] as follows:

$$M_{Ed} = \gamma_O \cdot M_{E.k}$$

$$V_{\rm Ed} = \gamma_O \cdot V_{\rm Ek}$$

where

 $\gamma_Q$  is the partial safety factor for traffic load (=1.5 for new structures, 1.25 for existing

structures according to the RBK);

 $M_{Ek}$  and  $V_{Ek}$  are the characteristic values of traffic load effect, calculated using Load Model 1 (LM1) of NEN-EN 1991-2:2015 [9] and provision in NEN 8701:2011 [16].

The characteristic value of the traffic load effect  $(E_{Ek})$  is calculated according to NEN-EN 1991-2:2015 [9] and NEN 8701:2011 [16] as follows:

$$E_{Ek} = \psi \cdot \alpha_{trend} \cdot \alpha_{L} \cdot E_{LM1}$$

where

ψ is the correction factor for shortened reference period, defined in Table 1 in NEN 8701:2011 [16] for different span length *L* as

Table 19: Value of the correction factor ψ based on the reference period and structure span length.

	Ψ					
Ref. period [year]	Span length <i>L</i> [m]					
	20	40	50	100	≥ 200 m	
30	0.99	0.99	0.99	0.98	0.97	
100	1.00	1.00	1.00	1.00	1.00	

 $\alpha_{trend}$ 

is the reduction factor, defined in NEN 8701:2011 [16], accounting for the influence of trend in comparison to 2060. This factor was taken into account only for existing structure with the value for year 2050 taken (considering the year 2020 and the reference period of 30 years).

Table 20: Value of the reduction factor  $\alpha_{trend}$  based on the year and structure span length.

		lphatrend								
Year		Span length <i>L</i> [m]								
	20	40	50	100	≥ 200 m					
2050	0.98	0.97	0.96	0.95	0.95					



 $\alpha_L$  is the correction factor for existing bridges with span length L greater or equal to 100 m, defined in NEN 8701:2011[16] for as:

$$\begin{array}{lll} \alpha_L = & 1.2 - 0.002 \cdot L & 100 \text{ m} \leq L < 200 \text{ m} \\ \alpha_L = & 0.8 & L \geq 200 \text{ m} \\ \alpha_L = & 1.0 & \text{for new structures, regardless of L} \end{array}$$

The traffic load effect  $E_{LM1}$  is calculated according to LM1 in NEN-EN 1991-2:2015 [9]. This load model consists of two partial systems:

- 1) Double-axle concentrated loads (known as tandem system or TS), with each axle having the weight in kN:  $\alpha_O \cdot Q_k$
- 2) Uniformly distributed loads (UDL) having the following weight in kN/m<sup>2</sup>:  $\alpha_q \cdot q_k$

where:

 $\alpha_Q$  and  $\alpha_q$  are the adjustment factors for TS and UDL, respectively.

The bending moment and shear force caused by TS loads is calculated after finding the position of the two loads leading to the maximum value of the load effects. The bending moment caused by UDL is for both beam models calculated as:

$$M_{i,UDL} = q_k \cdot w_i \cdot L^2/8$$

while the shear force cause by UDL is calculated as:

$$V_{i,UDL} = 0.625 \cdot q_k \cdot w_i \cdot L$$

The parameters of the LM1 model, which were used in the calculation, are shown in Table 21.

Table 21: Parameters of the Load Model 1 used in the calculation of the design load effect.

	w [m]	Q <sub>k</sub> (TS) [kN]	q <sub>k</sub> (UDL) [kN/m²]	$\alpha_Q$	$\alpha_q$
Lane 1	3.0	300	9	1	1
Lane 2	3.0	200	2.5	1	1
Remaining area	1.2	0	2.5	1	1

The following assumptions were made for the calculation of characteristic value of the traffic load effect:

- Total carriegeway width w=7.2 m, in the scope of LM1 model split into two notional lanes with width  $w_1=3.0$  m and remaining area with width  $w_1=1.2$  m;
- The simply-supported and continuous beam models are used with the theoretical influence lines presented in section 3.6. For the simply-supported model, the design value of the bending moment is calculated at mid-span, while for the continuous beam model design values of the bending moment at the middle support and the shear force immediately left of the middle support are calculated;
- Both new and existing structures are considered; for new structures reference period T<sub>ref</sub> = 100 years is considered, for existing structures the reference period T<sub>ref</sub> = 30 years corresponding to assessment level "gebruiksniveau" in RBK [4] is chosen.



The calculated design values of the traffic load effect are shown in Table 22.

Table 22: Design traffic load effect for different structural system, span length and state of the structure.

		Span	Design traffi	c load effect
		length	New	Existing
Structural system / load effect	Unit	L [m]	structures	structures
Simply-supported beam / bending moment at mid span	kNm	20	9,863	7,974
	kNm	50	35,878	28,415
	kNm	100	107,363	83,295
	kNm	200	355,800	218,580
Continuous beam / bending moment at middle support	kNm	2.20	5,693	4,540
	kNm	2.50	24,793	19,235
Continuous beam / shear force at middle support	kN	2.20	2,181	1,739
	kN	2.50	3,235	2,510



# Appendix 5B Traffic load effects based on the old Dutch standards

For the definition of the input for the reliability assessment of existing concrete bridges, the traffic load effects in bridges are evaluated according to the following Dutch standards:

- VOSB 1938 GBV 1950
- VOSB 1963 GBV 1962
- VB 1974
- VBB 1995

The design load model, the impact factor and the load reduction factor for the design of road bridges given in the standards listed above are summarized in the following.

#### **VOSB 1938 - GBV 1950**

#### Design load model

The traffic load model of the standard VOSB 1938 consists of three concentrated forces, representing one vehicle with width of 2.5 m, and a uniformly distributed load per lane, as shown in Figure 100. The intensity of these loads depend on the class of the bridge. The standard VOSB 1938 differentiates between four classes of bridges. Highway bridges belong to "class A" which is characterized by a uniformly distributed load of 400 kg/m² and three axle loads of 20 tonne each.

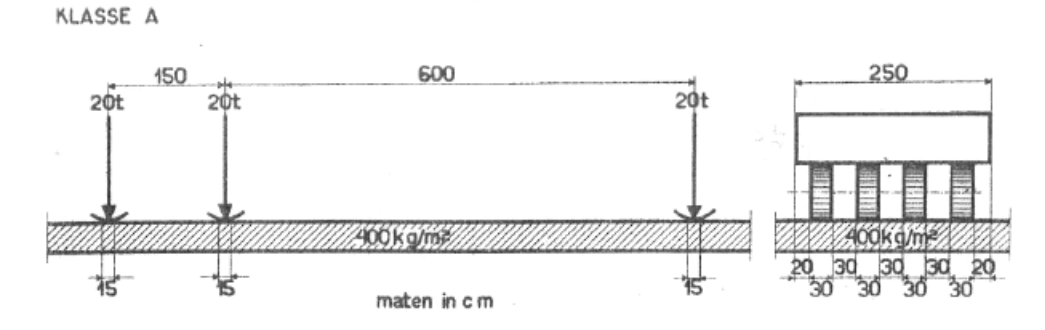


Figure 100: Traffic load model of VOSB 1938.

In case that the width of the carriageway is larger than 5 m, two or more vehicles are arranged in the transverse direction and the intensity of the concentrated forces and uniformly distributed load is reduced as follows:

2 vehicles: reduction of 10%3 vehicles: reduction of 30%4 vehicles: reduction of 40%

#### Impact factor

In the VOSB 1938, the impact factor S is defined as:

$$S = 1 + \frac{40}{100 + L}$$



where L is the theoretical length (in meters) of the considered element of the structure. For concrete structures, the standard GBV 1950 defines the impact factor as follows:

$$S = 1 + \frac{3}{10 + L}$$

Load reduction factor

No reduction factor is defined in the standards VOSB 1938 and GBV 1950.

#### VOSB 1963 - GBV 1962, VB 1974 and VBB 1995

The Dutch standards for the design of road bridges between 1963 and the introduction of the Eurocodes are based on the traffic load model showed in Figure 103. This load model differ from the one of VOSB 1938 in terms of the distance between the three axles. The intensity of the concentrated forces and the uniformly distributed load is differentiated in three classes (classes 30, 45 and 60). The values of the loads shown in Figure 103 are representative of highway bridges ("class 60")

#### Design load model

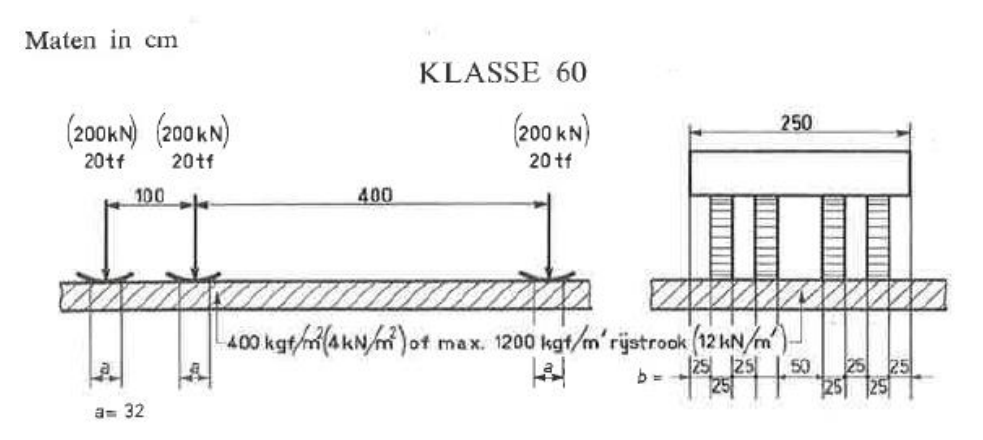


Figure 101: Traffic load model of VOSB 1963.

#### Impact factor

Different expressions of the impact factor are given in the standards:

VOSB 1963 - GBV 1962:

$$S = 1 + \frac{3}{10 + L}$$

where the length L is equal to the bridge length (in meters) for simply supported bridges, while in case of multiple spans it is equal to:

$$L = max \left(L_{max}, L_{min} + \frac{1}{2}L_{max}\right)$$



• VB 1974:

$$S = 1 + \frac{40}{100 + L}$$

where L is the theoretical length (in meters) of the considered element of the structure

• VBB 1995:

$$S = 1 + C_0 \frac{L}{h(100 + L)}$$

where:

- C<sub>0</sub> is a coefficient dependent on the type of element
- L/h is the slenderness ratio

## Load reduction factor

The load reduction factor is defined as follows:

• VOSB 1963 - GBV 1962:

$$B = 0.6 + \frac{40}{100 + L}$$

where the length L is equal to the bridge length (in meters) for simply supported bridges, while in case of multiple spans it is equal to:

$$L = max \left( L_{max}, L_{min} + \frac{1}{2} L_{max} \right)$$

- VB 1974: no reduction factor is mentioned
- VBB 1995:

$$B = 0.6 + \frac{40}{100 + L}$$

where the length L is equal to the bridge length (in meters) for simply supported bridges, while in case of multiple spans it is equal to:

$$L = max \left( L_{max}, L_{min} + \frac{1}{2} L_{max} \right)$$

Assessment of the characteristic value of the traffic load effects

The characteristic value of the traffic load effects have been evaluated according to the above listed standards by using the theoretical influence lines presented in section 3.6 of the simply-supported and continuous beam models.

The following assumptions were made for the calculation of characteristic value of the traffic load effect:

- the carriegeway consists of two 3 m wide lanes in one direction
- redistribution of the loads in the transverse direction is not considered



- the coefficient C<sub>0</sub> used to calculate the impact factor according to VBB 1995 is equal to 0.8 for the 20 m simply supported bridge (prestressed slab) and equal to 0.7 for the other spanlnegths and for the two-span bridges (predstressed box girder)
- the slenderness L/h used to calculate the impact factor according to VBB 1995 is equal to 20

The characteristic values of the traffic load effects are listed in Table 23.

Table 23: Characteristic value of the traffic load effect for different structural system and span length according to various Dutch standards.

			Characteristic value of the traffic load effect				
Structural system / load effect	Unit	Span L [m]	VOSB 1938 - GBV 1950	VOSB 1963 - GBV 1962	VB 1974	VBB 1995	
Simply-supported beam /	kNm	20	5,197	5,092	6,613	5,247	
bending moment at	kNm	50	18,569	15,652	21,787	16,298	
mid-span	kNm	100	51,451	38,790	56,640	40,403	
	kNm	200	157,605	111,200	169,433	114,750	
Continuous beam / bending	kNm	2.20	2,885	2,642	3,481	2,822	
moment at middle support	kNm	2.50	11,646	9,075	12,695	10,025	
Continuous beam / shear	kN	2.20	1,148	1,079	1,421	1,120	
force at middle support	kN	2.50	1,638	1,310	1,833	1,384	



# APPENDIX 6 RESULTS CONCRETE BRIDGE (ULS CONDITIONS)

# Appendix 6A Calibrated resistance and reliability indices

Table 24: Reference scenario: calibrated resistance depending on the elapsed service life, given a particular structural system and span length of the structure.

	Unit	Span	Calibrated resistance R [kN/kNm]			
		length	depending o	n the elapsed	service life t <sub>0</sub>	
Structural system		<i>L</i> [m]	0 years	30 years	50 years	70 years
Simply-supported beam, bending moment at	kNm	20	23,980	15,652	15,652	15,652
mid-span	kNm	50	92,791	63,991	63,991	63,991
	kNm	100	299,524	195,649	195,649	195,649
	kNm	200	1,840,182	1,474,115	1,474,115	1,474,115
Continuous beam, bending moment at middle support	kNm	2.20	16,995	9,815	9,815	9,815
	kNm	2.50	75,337	49,941	49,941	49,941
Continuous beam, shear force at middle support	kN	2.20	5,504	3,690	3,690	3,690
	kN	2.50	11,099	7,282	7,282	7,282

Table 25: Mean value of the resistance based on the old Dutch design standards, given a particular structural system and span length of the structure.

	Unit	Span length	Resistance R				
Structural system		<i>L</i> [m]	VOSB 1938 – GBV1950	VOSB 1963 - GBV 1962	VB 1974	VBB 1995	
Simply-supported beam,	kNm	20	20,051	19,645	24,096	20,241	
bending moment at	kNm	50	78,802	66,422	87,319	69,164	
mid-span	kNm	100	259,931	195,967	270,249	204,118	
	kNm	200	1,337,653	943,793	1,358,155	973,924	
Continuous beam, bending	kNm	2.20	11,848	10,851	13,503	11,590	
moment at middle support	kNm	2.50	58,834	45,848	60,574	50,645	
Continuous beam, shear force	kN	2.20	4,715	4,429	5,512	4,601	
at middle support	kN	2.50	8,276	6,619	8,745	6,990	



Table 26: Reference scenario reinforced concrete bridge (ULS conditions). Calculated cumulative and annual reliability for new and existing structures (depending on the elapsed service life), for different types of structures and span lengths.

	Span	Cumulative r	eliability β [-]	Annual rel	iability β [-]
Structural system	length	First year	Last year	First year	Last year
	<i>L</i> [m]	(t <sub>0</sub> )	(t <sub>0</sub> +T <sub>ref</sub> )	(t <sub>0</sub> )	(t <sub>0</sub> +T <sub>ref</sub> )
New structure: elapsed service life 0	year (t <sub>0</sub> =0 ye	$ear$ , $T_{ref} = 100$ year	ars)		
Simply-supported beam,	20	6.84	4.30	6.84	4.80
bending moment at mid-span	50	6.65	4.30	6.65	4.81
	100	7.32	4.30	7.32	4.76
	200	5.19	4.30	5.19	4.92
Continuous beam,	2-20	6.69	4.30	6.69	4.81
bending moment at middle support	2.50	7.32	4.30	7.32	4.76
Continuous beam,	2-20	6.76	4.30	6.76	4.81
shear force at middle support	2.50	7.40	4.30	7.40	4.76
Existing structure: elapsed service la	ife 30 years (	t <sub>0</sub> =30 years, T <sub>ref</sub> :	= 30 years)		
Simply-supported beam,	20	4,32	3,3	4,32	3,98
bending moment at mid-span	50	4,18	3,3	4,18	4,02
	100	4,15	3,3	4,15	3,97
	200	3,54	3,3	3,54	4,25
Continuous beam,	2.20	4,26	3,3	4,26	3,99
bending moment at middle support	2.50	4,15	3,3	4,15	3,97
Continuous beam,	2.20	4,26	3,3	4,26	3,99
shear force at middle support	2.50	4,21	3,3	4,21	3,96
Existing structure: elapsed service la	ife 50 years (1	t <sub>0</sub> =50 years, T <sub>ref</sub> :	= 30 years)		
Simply-supported beam,	20	4,32	3,3	4,32	3,98
bending moment at mid-span	50	4,18	3,3	4,18	4,02
	100	4,15	3,3	4,15	3,97
	200	3,54	3,3	3,54	4,25
Continuous beam,	2.20	4,26	3,3	4,26	3,99
bending moment at middle support	2.50	4,15	3,3	4,15	3,97
Continuous beam,	2-20	4,26	3,3	4,26	3,99
shear force at middle support	2.50	4,21	3,3	4,21	3,96
Existing structure: elapsed service la	ife 70 years (	t <sub>0</sub> =70 years, T <sub>ref</sub> :	= 30 years)		
Simply-supported beam,	20	4,32	3,3	4,32	3,98
bending moment at mid-span	50	4,18	3,3	4,18	4,02
	100	4,15	3,3	4,15	3,97
	200	3,54	3,3	3,54	4,25
Continuous beam,	2.20	4,26	3,3	4,26	3,99
bending moment at middle support	2.50	4,15	3,3	4,15	3,97
Continuous beam,	2.20	4,26	3,3	4,26	3,99
shear force at middle support	2.50	4,21	3,3	4,21	3,96



Table 27: Full replacement scenario for the reinforced concrete bridge (ULS conditions). Calculated cumulative, annual reliability and the end of normative service life for new and existing structures (depending on the elapsed service life) for different types of structures and span lengths.

	span	_	reliability β -]	Annual rel	iability β [-]	End of normative
Structural system	length L [m]	First year (t <sub>0</sub> )	Last year (t <sub>0</sub> +T <sub>ref</sub> )	First year (t₀)	Last year (t <sub>0</sub> +T <sub>ref</sub> )	service life [year]
New structure: elapsed service	e life 0 yea	r (t₀=0 year, T	r <sub>ef</sub> = 100 years	)		
Simply-supported beam,	20	6,81	4,27	6,81	4,78	98
bending moment at mid-span	50	6,31	3,94	6,31	4,51	81
	100	7,07	3,97	7,07	4,48	87
	200	5,12	4,21	5,12	4,84	92
Continuous beam, bending	2.20	6,56	4,09	6,56	4,63	89
moment at middle support	2.50	7,30	4,28	7,3	4,74	99
Continuous beam,	2.20	6,59	4,12	6,59	4,66	91
shear force at middle support	2.50	7,16	4,01	7,16	4,51	88
Existing structure: elapsed se	ervice life 3	0 years (t₀=30	years, $T_{ref} = 3$	0 years)		
Simply-supported beam,	20	4,29	3,27	4,29	3,95	28
bending moment at mid-span	50	3,86	2,95	3,86	3,75	_1
	100	3,93	3,03	3,93	3,75	16
	200	3,52	3,26	3,52	4,20	19
Continuous beam, bending	2.20	4,07	3,09	4,07	3,83	17
moment at middle support	2.50	4,14	3,28	4,14	3,96	29
Continuous beam,	2.20	4,10	3,12	4,09	3,86	19
shear force at middle support	2.50	4,02	3,06	4,02	3,76	18
Existing structure: elapsed se	ervice life 5	0 years (t₀=50	years, $T_{ref} = 3$	0 years)		
Simply-supported beam,	20	4,29	3,27	4,29	3,95	28
bending moment at mid-span	50	3,86	2,95	3,86	3,75	_1
	100	3,93	3,03	3,93	3,75	16
	200	3,52	3,26	3,52	4,20	19
Continuous beam, bending	2.20	4,07	3,09	4,07	3,83	17
moment at middle support	2.50	4,14	3,28	4,14	3,96	29
Continuous beam,	2.20	4,10	3,12	4,09	3,86	19
shear force at middle support	2.50	4,02	3,06	4,02	3,76	18
Existing structure: elapsed se	ervice life 7	0 years (t₀=70	years, T <sub>ref</sub> = 3	0 years)		
Simply-supported beam,	20	4,29	3,27	4,29	3,95	28
bending moment at mid-span	50	3,86	2,95	3,86	3,75	_1
	100	3,93	3,03	3,93	3,75	16
	200	3,52	3,26	3,52	4,20	19
Continuous beam, bending	2.20	4,07	3,09	4,07	3,83	17
moment at middle support	2.50	4,14	3,28	4,14	3,96	29
Continuous beam,	2.20	4,10	3,12	4,09	3,86	19
shear force at middle support	2.50	4,02	3,06	4,02	3,76	18

<sup>&</sup>lt;sup>1</sup>Theoretical end of service life reached before the first year of analysis.



Table 28: Gradual replacement scenario for the reinforced concrete bridge (ULS conditions). Calculated cumulative, annual reliability and the end of normative service life for new and existing structures (depending on the elapsed service life), for different types of structures and span lengths.

0111	span	_	e reliability β [-]	Annual rel	iability β [-]	End of normative
Structural system	length L [m]	First year (t <sub>0</sub> )	Last year (t <sub>0</sub> + T <sub>ref</sub> )	First year (t <sub>0</sub> )	Last year (t <sub>0</sub> + T <sub>ref</sub> )	service life [years]
New structure: elapsed service	e life 0 yea	r (t <sub>0</sub> =0 years,	$T_{ref} = 100 \ year$	s)		
Simply-supported beam,	20	6,84	4,29	6,84	4,79	99
bending moment at mid-span	50	6,65	4,17	6,65	4,69	92
	100	7,32	4,18	7,31	4,65	95
	200	5,14	4,27	5,14	4,89	97
Continuous beam, bending	2.20	6,76	4,23	6,76	4,74	96
moment at middle support	2.50	7,32	4,29	7,31	4,75	99
Continuous beam,	2.20	6,76	4,24	6,76	4,75	97
shear force at middle support	2.50	7,39	4,2	7,39	4,66	95
Existing structure: elapsed se	ervice life 3	0 years (t <sub>0</sub> =30	year, $T_{ref} = 30$	years)		
Simply-supported beam,	20	4,32	3,30	4,32	3,97	29
bending moment at mid-span	50	4,18	3,29	4,18	4,00	28
	100	4,15	3,29	4,15	3,96	29
	200	3,54	3,30	3,54	4,25	29
Continuous beam, bending	2.20	4,26	3,29	4,26	3,98	29
moment at middle support	2.50	4,15	3,30	4,15	3,97	29
Continuous beam,	2.20	4,26	3,29	4,26	3,99	29
shear force at middle support	2.50	4,21	3,29	4,21	3,95	29
Existing structure: elapsed se	ervice life 5	0 years (t <sub>0</sub> =50	$year, T_{ref} = 30$	years)		
Simply-supported beam,	20	4,32	3,30	4,32	3,97	29
bending moment at mid-span	50	4,18	3,29	4,18	4,00	28
	100	4,15	3,29	4,15	3,96	29
	200	3,54	3,30	3,54	4,25	29
Continuous beam, bending	2.20	4,26	3,29	4,26	3,98	29
moment at middle support	2.50	4,15	3,30	4,15	3,97	29
Continuous beam,	2.20	4,26	3,29	4,26	3,99	29
shear force at middle support	2.50	4,21	3,29	4,21	3,95	29
Existing structure: elapsed se	ervice life 7	L	· · · · · · · · · · · · · · · · · · ·	·	, , , , , , , , , , , , , , , , , , , ,	
Simply-supported beam,	20	4,32	3,30	4,32	3,97	29
bending moment at mid-span	50	4,18	3,29	4,18	4,00	28
	100	4,15	3,29	4,15	3,96	29
	200	3,54	3,30	3,54	4,25	29
Continuous beam, bending	2.20	4,26	3,29	4,26	3,98	29
moment at middle support	2.50	4,15	3,30	4,15	3,97	29
Continuous beam,	2.20	4,26	3,29	4,26	3,99	29
shear force at middle support	2.50	4,21	3,29	4,21	3,95	29



Table 29: Reference scenario for the reinforced concrete bridge (ULS conditions) with the resistance and permanent load effect calculated based on various old Dutch standards. Calculated cumulative, annual reliability and the end of normative service life for new and existing structures (depending on the elapsed service life), for different types of structures and span lengths

	Span	Cumulative r	eliability β [-]	Annual rel	iability β [-]
Structural system	length	First year	Last year	First year	Last year
	<i>L</i> [m]	(t <sub>0</sub> )	(t <sub>0</sub> +T <sub>ref</sub> )	(t <sub>0</sub> )	(t <sub>0</sub> +T <sub>ref</sub> )
According to VOSB 1938 - GBV 195	i0 (t₀=70 year,	$T_{ref} = 30 \text{ years}$			
Simply-supported beam,	20	5,94	5,02	5,94	5,42
bending moment at mid-span	50	6,24	5,36	6,24	5,74
	100	7,09	6,06	7,09	6,33
	200	6,76	6,34	6,76	6,71
Continuous beam,	2.20	5,88	4,96	5,88	5,37
bending moment at middle support	2.50	6,71	5,62	6,71	5,92
Continuous beam,	2.20	6,10	5,20	6,10	5,59
shear force at middle support	2.50	6,51	5,39	6,51	5,70
According to VOSB 1963 - GBV 196	2 (t <sub>0</sub> =60 year,	$T_{ref} = 30 \ years)$			
Simply-supported beam,	20	5,86	4,93	5,86	5,34
bending moment at mid-span	50	5,60	4,66	5,60	5,11
	100	6,17	5,01	6,17	5,36
	200	6,31	5,69	6,31	6,06
Continuous beam,	2.20	5,54	4,59	5,54	5,05
bending moment at middle support	2.50	5,87	4,67	5,87	5,04
Continuous beam,	2.20	5,86	4,94	5,86	5,35
shear force at middle support	2.50	5,75	4,53	5,75	4,92
According to VB 1974 (t <sub>0</sub> =50 year, T <sub>t</sub>	ref = 30 years)				
Simply-supported beam,	20	6,52	5,65	6,52	6,00
bending moment at mid-span	50	6,46	5,62	6,46	5,98
	100	6,92	5,96	6,92	6,26
	200	6,38	5,99	6,38	6,41
Continuous beam,	2.20	6,24	5,36	6,23	5,74
bending moment at middle support	2.50	6,55	5,52	6,55	5,84
Continuous beam,	2.20	6,54	5,69	6,54	6,04
shear force at middle support	2.50	6,47	5,40	6,47	5,72
According to VBB 1995 (t₀=30 year,	$T_{ref} = 30 \text{ years}$	s)			
Simply-supported beam,	20	5,98	5,06	5,98	5,45
bending moment at mid-span	50	5,75	4,83	5,75	5,26
	100	6,31	5,17	6,31	5,50
	200	6,36	5,76	6,36	6,12
Continuous beam,	2.20	5,08	4,87	5,80	5,29
bending moment at middle support	2.50	6,22	5,06	6,22	5,40
Continuous beam,	2.20	6,00	5,10	6,00	5,50
shear force at middle support	2.50	5,94	4,75	5,94	5,12



Table 30: Full replacement scenario for the reinforced concrete bridge (ULS conditions) with the resistance and permanent load effect calculated based on various old Dutch standards. Calculated cumulative, annual reliability and the time to reach the annual reliability index corresponding to the reference scenario at the end of 30-year reference period for new and existing structures (depending on the elapsed service life), given different types of structures and span lengths

	span	_	reliability β -]	Annual rel	iability β [-]	Time to reach annual reliability β
Structural system	length L [m]	First year (t <sub>0</sub> )	Last year (t <sub>0</sub> + T <sub>ref</sub> )	First year (t <sub>0</sub> )	Last year (t <sub>0</sub> + T <sub>ref</sub> )	corresponding to (t <sub>0</sub> + T <sub>ref</sub> ) in reference scenario [years]
According to VOSB 1938 - GI	BV 1950 (t <sub>0</sub> =	=70 year, T <sub>ref</sub> =	= 30 years)			
Simply-supported beam,	20	5,91	4,98	5,91	5,39	27
bending moment at mid-span	50	5,89	4,98	5,89	5,39	10
	100	6,81	5,73	6,81	6,03	18
	200	6,73	6,27	6,73	6,63	23
Continuous beam, bending	2.20	5,68	4,74	5,68	5,18	19
moment at middle support	2.50	6,70	5,60	6,70	5,90	28
Continuous beam,	2.20	5,93	5,01	5,93	5,42	20
shear force at middle support	2.50	6,25	5,09	6,24	5,43	19
According to VOSB 1963 - Gi	BV 1962 (t <sub>0</sub> =	=60 year, T <sub>ref</sub> =	30 years)			
Simply-supported beam,	20	5,83	4,9	5,83	5,31	27
bending moment at mid-span	50	5,23	4,26	5,23	4,76	10
	100	5,86	4,66	5,86	5,03	18
	200	6,27	5,58	6,27	5,94	23
Continuous beam, bending	2.20	5,34	4,37	5,34	4,85	18
moment at middle support	2.50	5,85	4,65	5,85	5,02	28
Continuous beam,	2.20	5,69	4,75	5,69	5,19	20
shear force at middle support	2.50	5,46	4,21	5,46	4,64	19
According to VB 1974 (t <sub>0</sub> =50)	/ear, T <sub>ref</sub> = 3	30 years)				
Simply-supported beam,	20	6,49	5,62	6,49	5,97	27
bending moment at mid-span	50	6,12	5,25	6,12	5,64	10
	100	6,67	5,66	6,67	5,97	18
	200	6,35	5,92	6,35	6,33	23
Continuous beam, bending	2.20	6,04	5,15	6,04	5,55	18
moment at middle support	2.50	6,54	5,50	6,54	5,82	28
Continuous beam,	2.20	6,37	5,51	6,37	5,88	20
shear force at middle support	2.50	6,22	5,11	6,22	5,45	19
According to VBB 1995 (t <sub>0</sub> =30		: 30 years)				
Simply-supported beam,	20	5,95	5,02	5,95	5,43	27
bending moment at mid-span	50	5,39	4,43	5,39	4,91	10
	100	6,00	4,82	6,00	5,18	18
	200	6,32	5,65	6,32	6,01	23
Continuous beam, bending	2.20	5,59	4,65	5,59	5,10	18
moment at middle support	2.50	6,20	5,04	6,20	5,38	28
Continuous beam,	2.20	5,83	4,91	5,83	5,33	20
shear force at middle support	2.50	5,66	4,43	5,66	4,83	19



Table 31: Gradual replacement scenario for the reinforced concrete bridge (ULS conditions) with the resistance and permanent load effect calculated based on various old Dutch standards. Calculated cumulative, annual reliability and the time to reach the annual reliability index corresponding to the reference scenario at the end of 30-year reference period for new and existing structures (depending on the elapsed service life), given different types of structures and span lengths

Structural system	span length L [m]	Cumulative reliability β [-]		Annual reliability β [-]		Time to reach annual reliability β
		First year (t <sub>0</sub> )	Last year (t <sub>0</sub> + T <sub>ref</sub> )	First year (t <sub>0</sub> )	Last year (t <sub>0</sub> + T <sub>ref</sub> )	corresponding to (t <sub>0</sub> + T <sub>ref</sub> ) in reference scenario [years]
According to VOSB 1938 - GI	BV 1950 (t <sub>0</sub> =	=70 year, T <sub>ref</sub> =	= 30 years)			
Simply-supported beam, bending moment at mid-span	20	5,94	5,01	5,94	5,42	29
	50	6,24	5,35	6,24	5,72	28
	100	7,09	6,05	7,09	6,32	28
	200	6,76	6,34	6,76	6,71	28
Continuous beam, bending moment at middle support	2.20	5,88	4,96	5,88	5,37	28
	2.50	6,71	5,63	6,71	5,92	28
Continuous beam, shear force at middle support	2.20	6,10	5,19	6,10	5,58	28
	2.50	6,51	5,38	6,51	5,69	28
According to VOSB 1963 - GI	BV 1962 (t <sub>0</sub> =	=60 year, T <sub>ref</sub> =	30 years)			
Simply-supported beam, bending moment at mid-span	20	5,86	4,93	5,86	5,34	29
	50	5,60	4,65	5,60	5,09	28
	100	6,17	5,00	6,17	5,34	28
	200	6,31	5,69	6,31	6,05	28
Continuous beam, bending moment at middle support	2.20	5,54	4,59	5,54	5,04	28
	2.50	5,87	4,67	5,87	5,04	28
Continuous beam, shear force at middle support	2.20	5,86	4,93	5,86	5,35	28
	2.50	5,75	4,52	5,75	4,91	28
According to VB 1974 (t <sub>0</sub> =50)	/ear, T <sub>ref</sub> = 3	30 years)				
Simply-supported beam, bending moment at mid-span	20	6,52	5,65	6,52	6,00	29
	50	6,46	5,61	6,46	5,96	28
	100	6,92	5,95	6,92	6,25	28
	200	6,38	5,99	6,38	6,40	28
Continuous beam, bending moment at middle support	2.20	6,24	5,36	6,23	5,73	28
	2.50	6,55	5,52	6,55	5,84	28
Continuous beam,	2.20	6,54	5,68	6,54	6,04	28
shear force at middle support	2.50	6,47	5,38	6,47	5,71	28
According to VBB 1995 (t <sub>0</sub> =30		: 30 years)				
Simply-supported beam, bending moment at mid-span	20	5,98	5,05	5,98	5,45	29
	50	5,75	4,82	5,75	5,24	28
	100	6,31	5,16	6,31	5,49	28
	200	6,36	5,76	6,36	6,12	28
Continuous beam, bending moment at middle support	2.20	5,80	4,87	5,80	5,29	28
	2.50	6,22	5,06	6,22	5,40	28
Continuous beam,	2.20	6,00	5,09	6,00	5,49	28
shear force at middle support	2.50	5,94	4,74	5,94	5,10	28



Appendix 6B Comparison between the reference, full replacement and gradual replacement scenarios

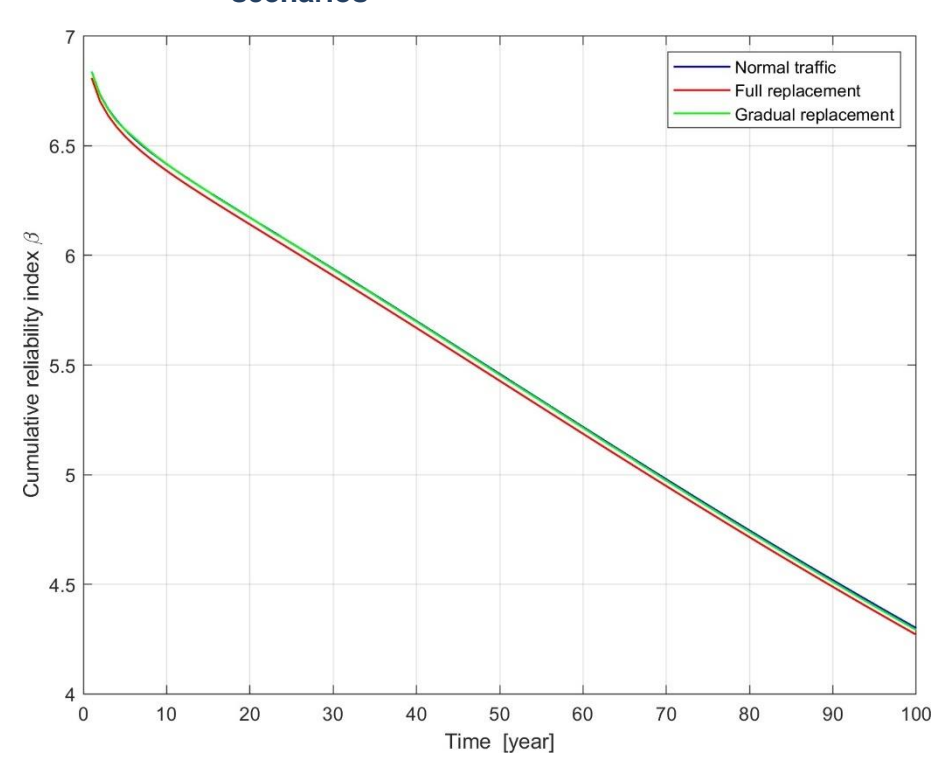


Figure 102: Comparison of cumulative reliability given different traffic scenarios for the new structure (L = 20 m, simply-supported beam).

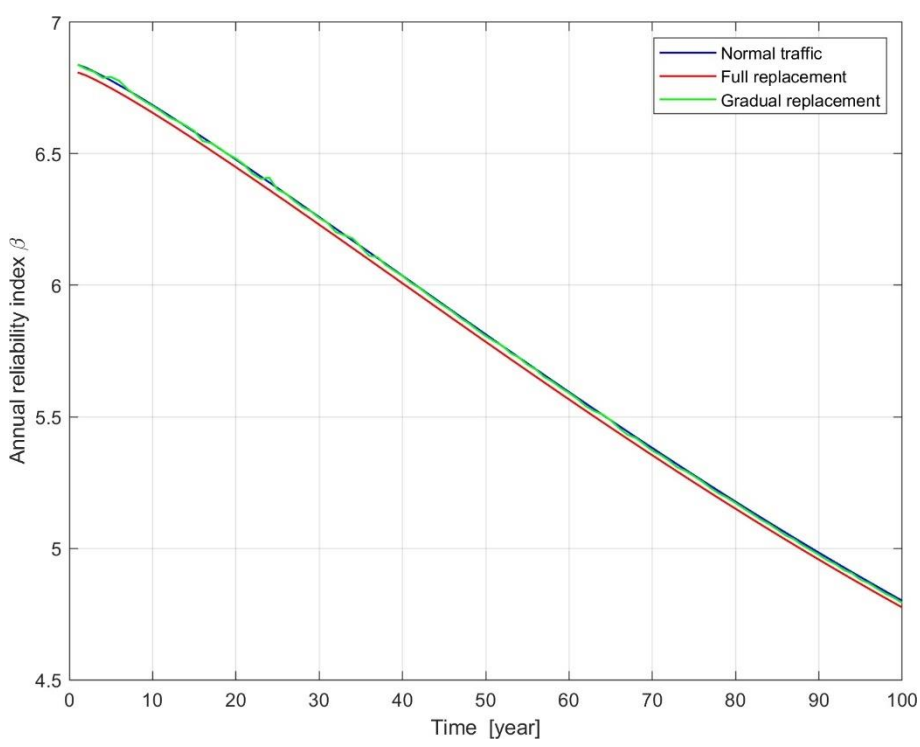


Figure 103: Comparison of annual reliability given different traffic scenarios for the new structure (L = 20 m, simply-supported beam).



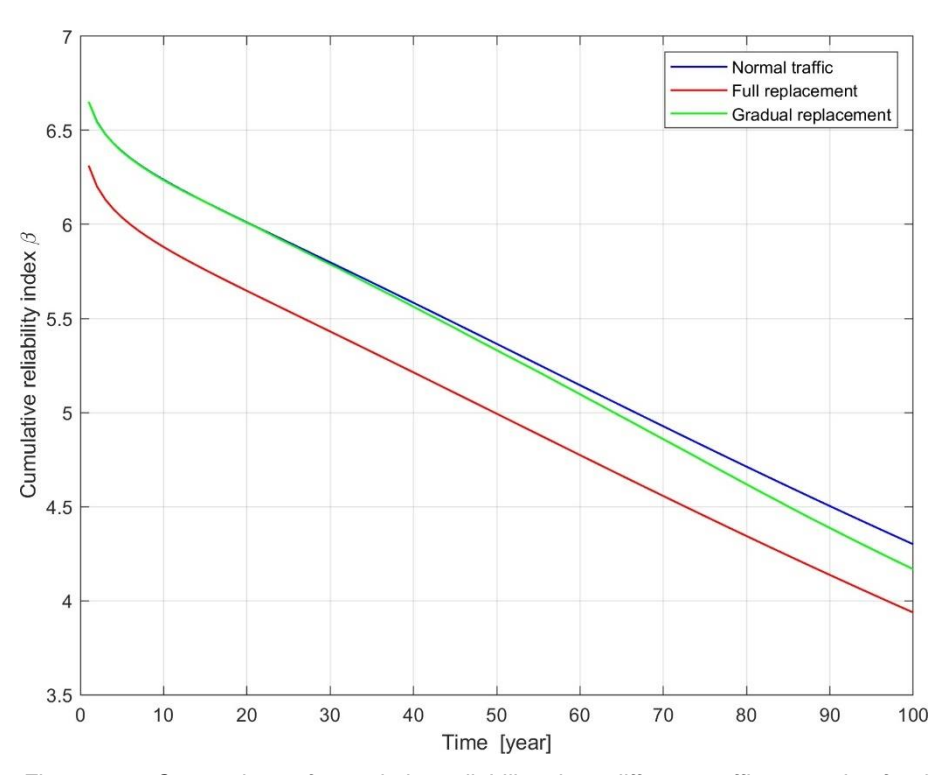


Figure 104: Comparison of cumulative reliability given different traffic scenarios for the new structure (L = 50 m, simply-supported beam).

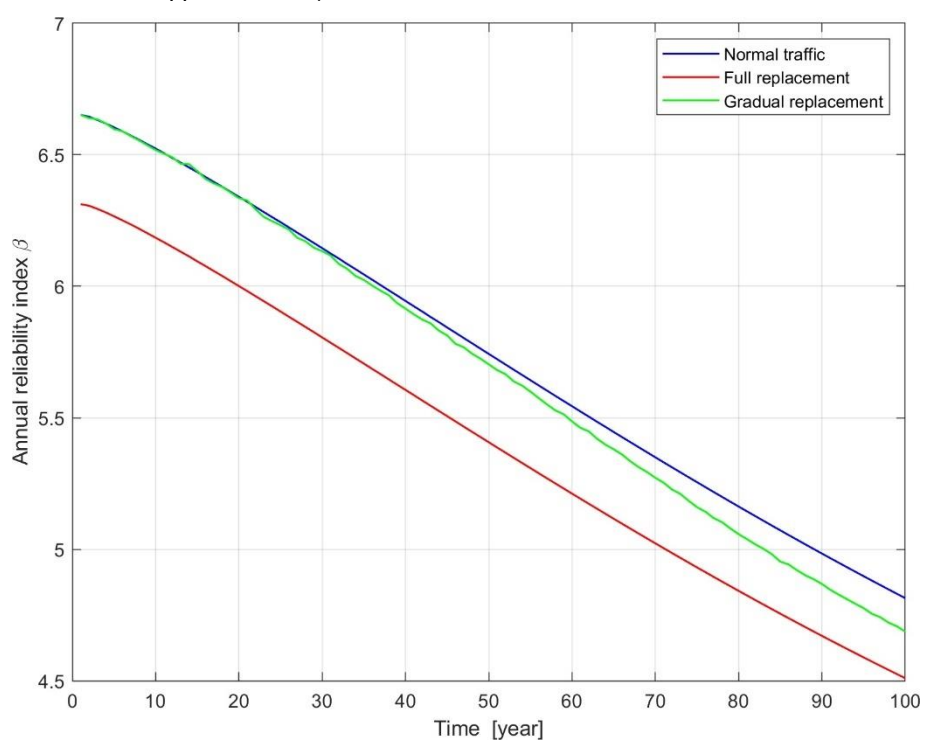


Figure 105: Comparison of annual reliability given different traffic scenarios for the new structure (L = 50 m, simply-supported beam).



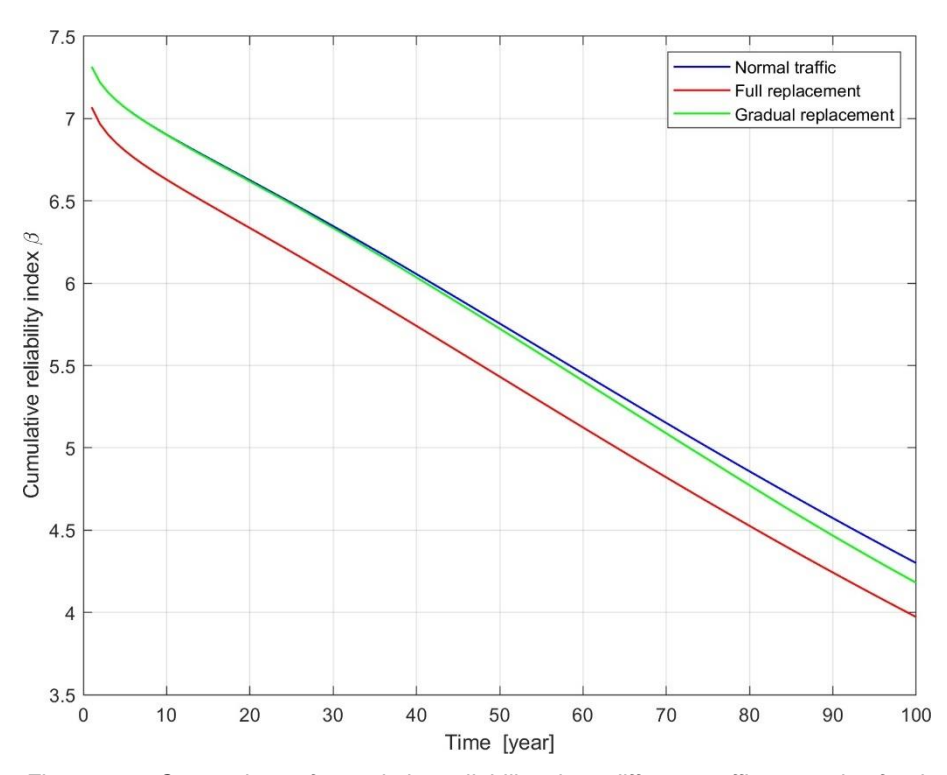


Figure 106: Comparison of cumulative reliability given different traffic scenarios for the new structure (L = 100 m, simply-supported beam).

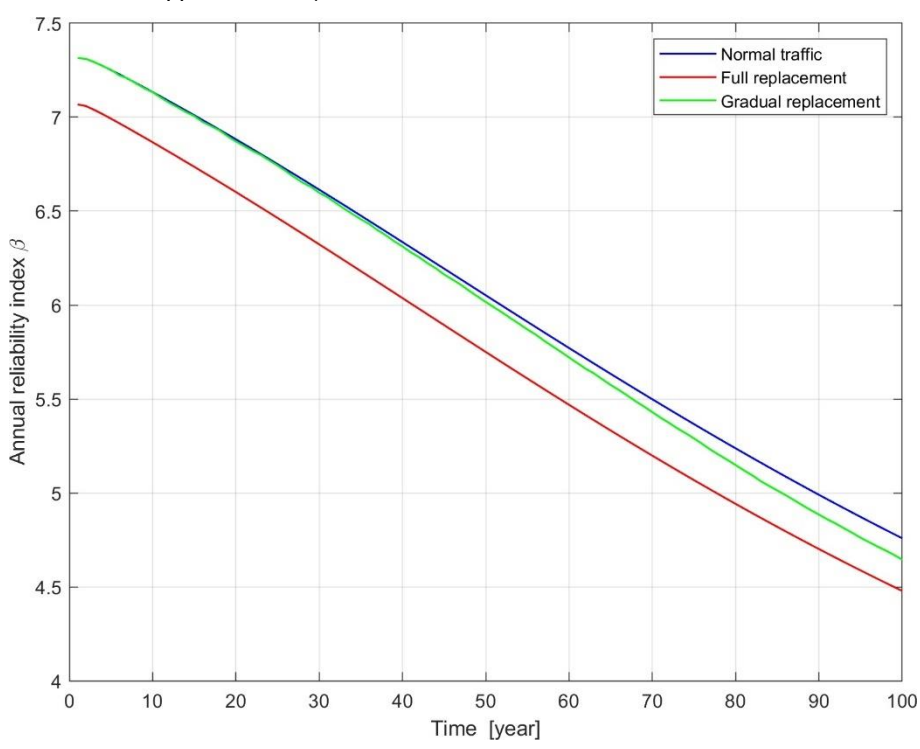


Figure 107: Comparison of annual reliability given different traffic scenarios for the new structure (L = 100 m, simply-supported beam).



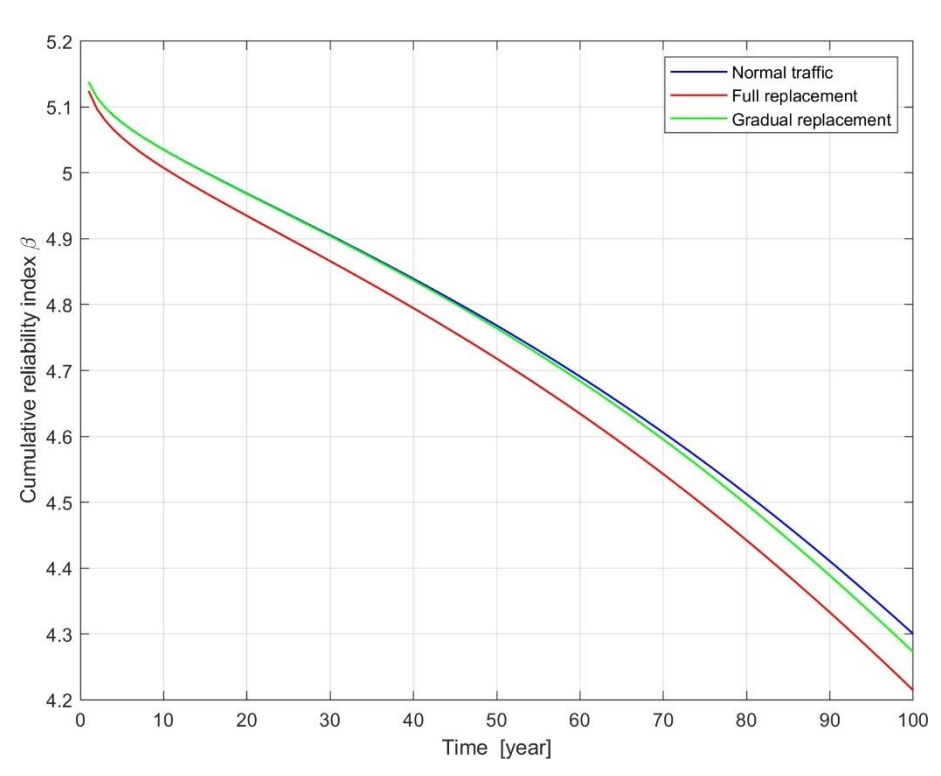


Figure 108: Comparison of cumulative reliability given different traffic scenarios for the new structure (L = 200 m, simply-supported beam).

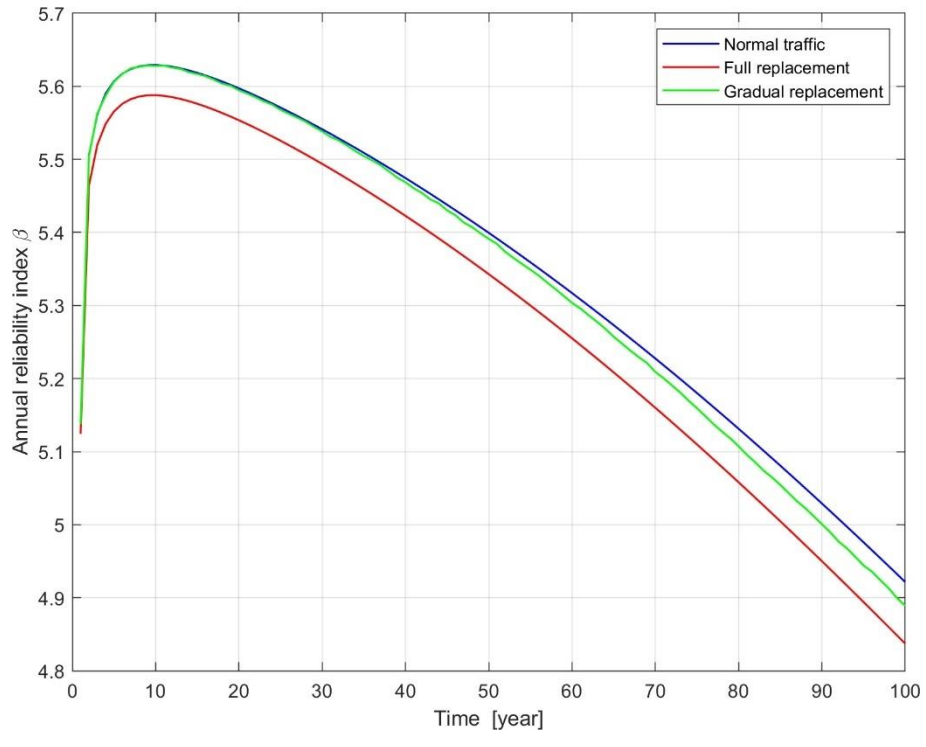


Figure 109: Comparison of annual reliability given different traffic scenarios for the new structure (L = 200 m, simply-supported beam).



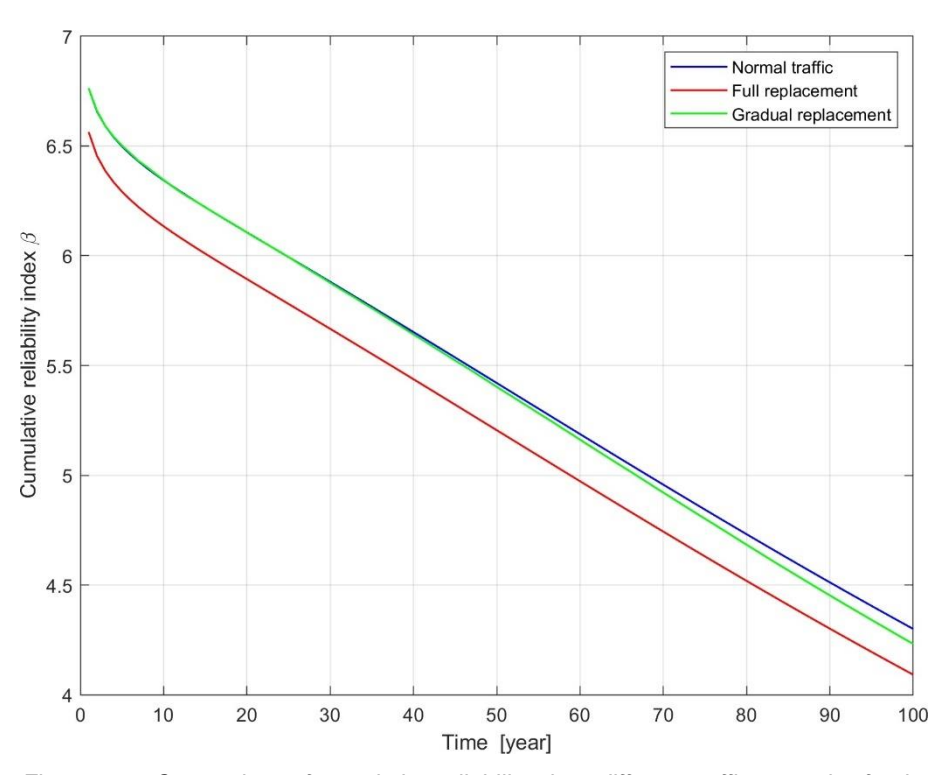


Figure 110: Comparison of cumulative reliability given different traffic scenarios for the new structure (L = 2.20 m, bending moment, continuous beam).

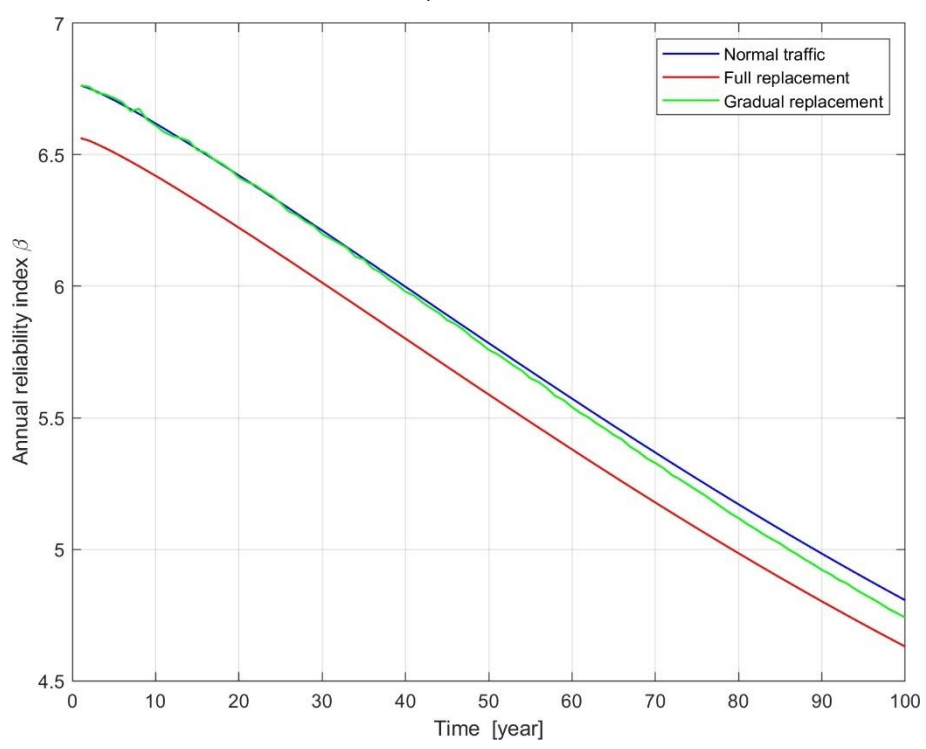


Figure 111: Comparison of annual reliability given different traffic scenarios for the new structure (L = 2.20 m, bending moment, continuous beam).



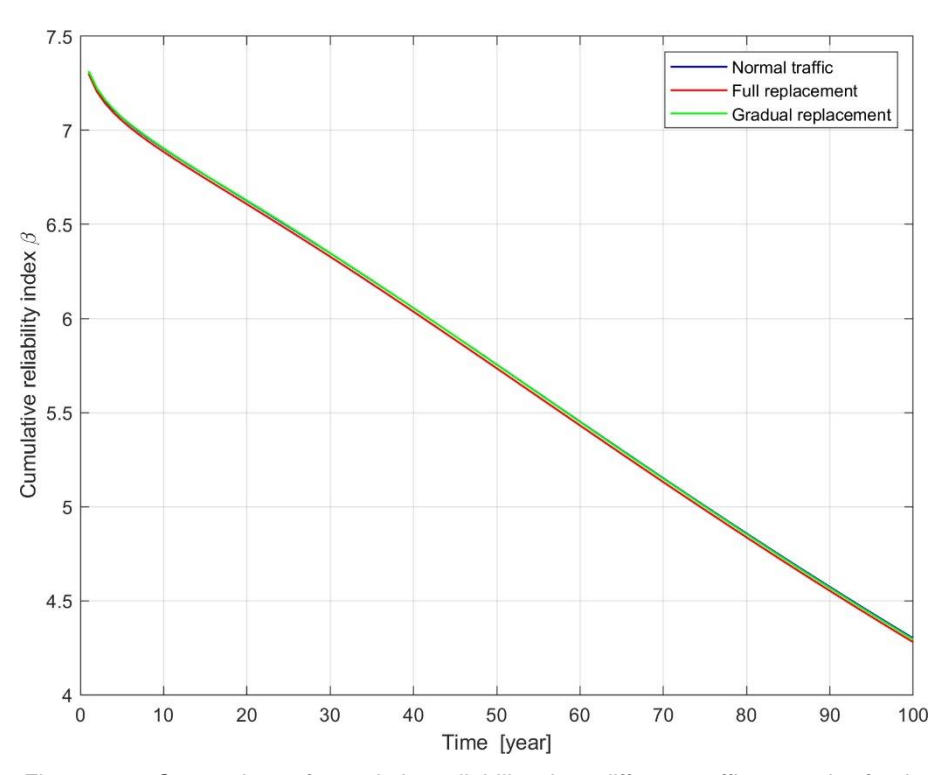


Figure 112: Comparison of cumulative reliability given different traffic scenarios for the new structure (L = 2.50 m, bending moment, continuous beam).

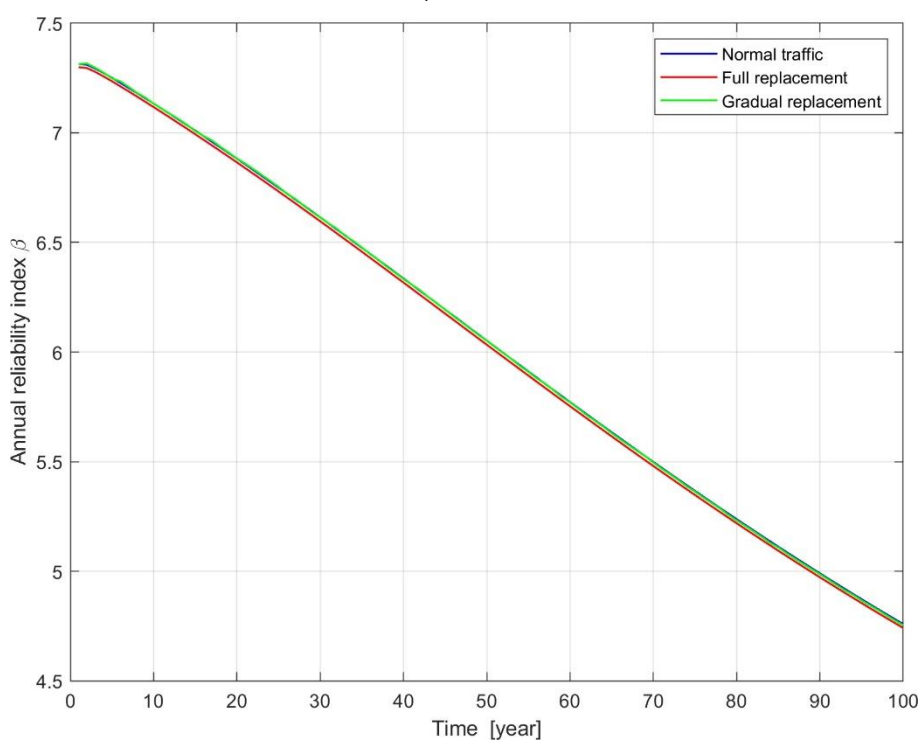


Figure 113: Comparison of annual reliability given different traffic scenarios for the new structure (L = 2.50 m, bending moment, continuous beam).



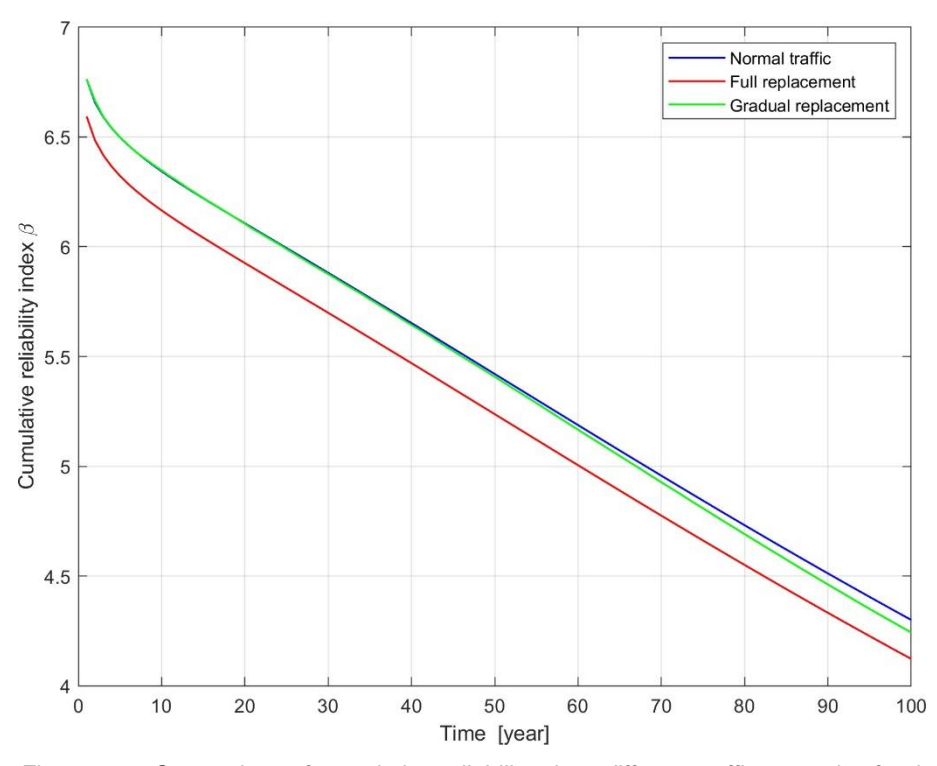


Figure 114: Comparison of cumulative reliability given different traffic scenarios for the new structure (L = 2.20 m, shear force, continuous beam).

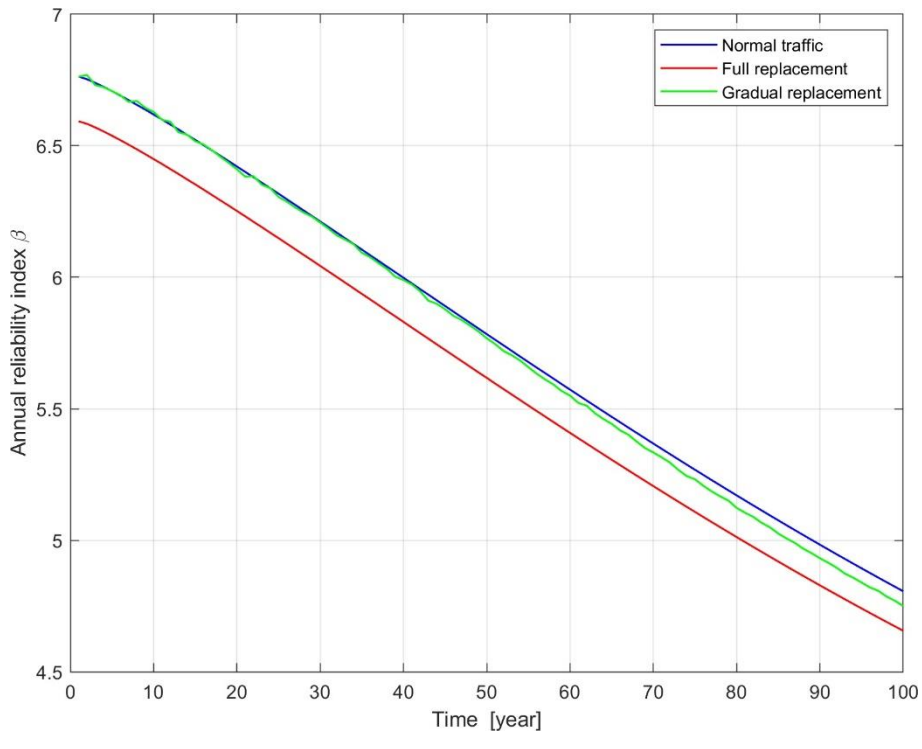


Figure 115: Comparison of annual reliability given different traffic scenarios for the new structure (L = 2.20 m, shear force, continuous beam).



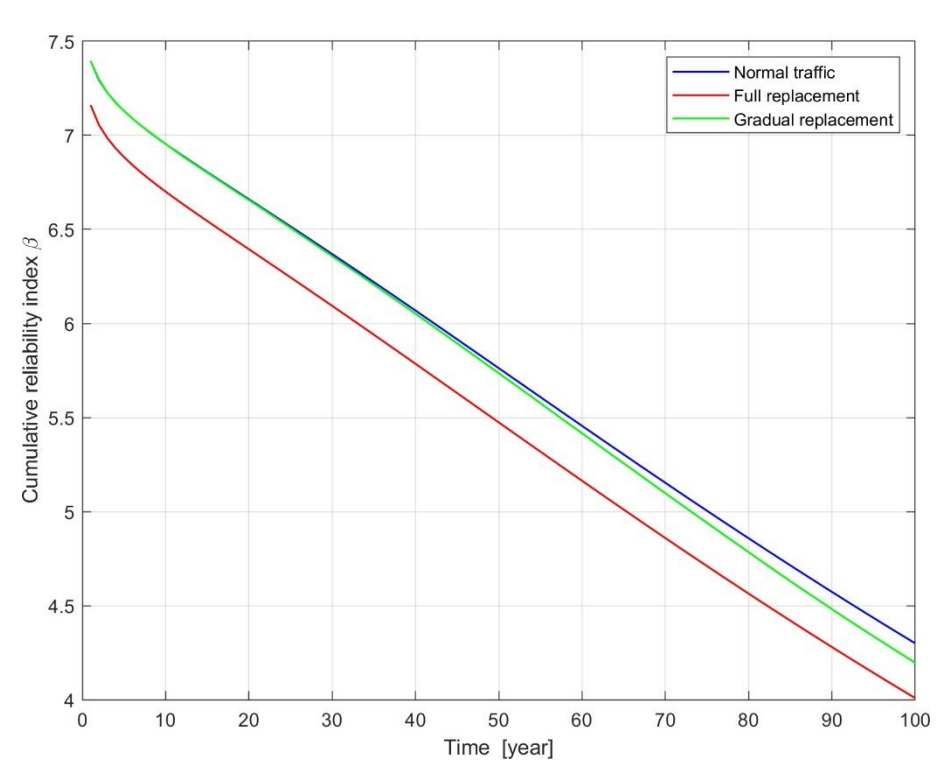


Figure 116: Comparison of cumulative reliability given different traffic scenarios for the new structure (L = 2.50 m, shear force, continuous beam).

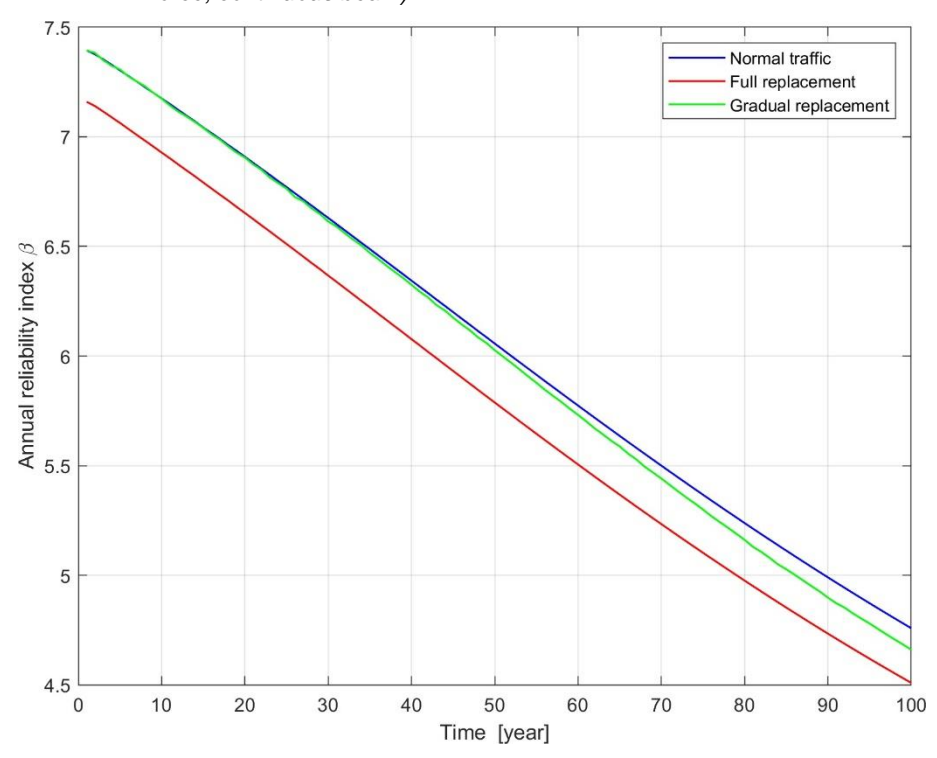


Figure 117: Comparison of annual reliability given different traffic scenarios for the new structure (L = 2.50 m, shear force, continuous beam).



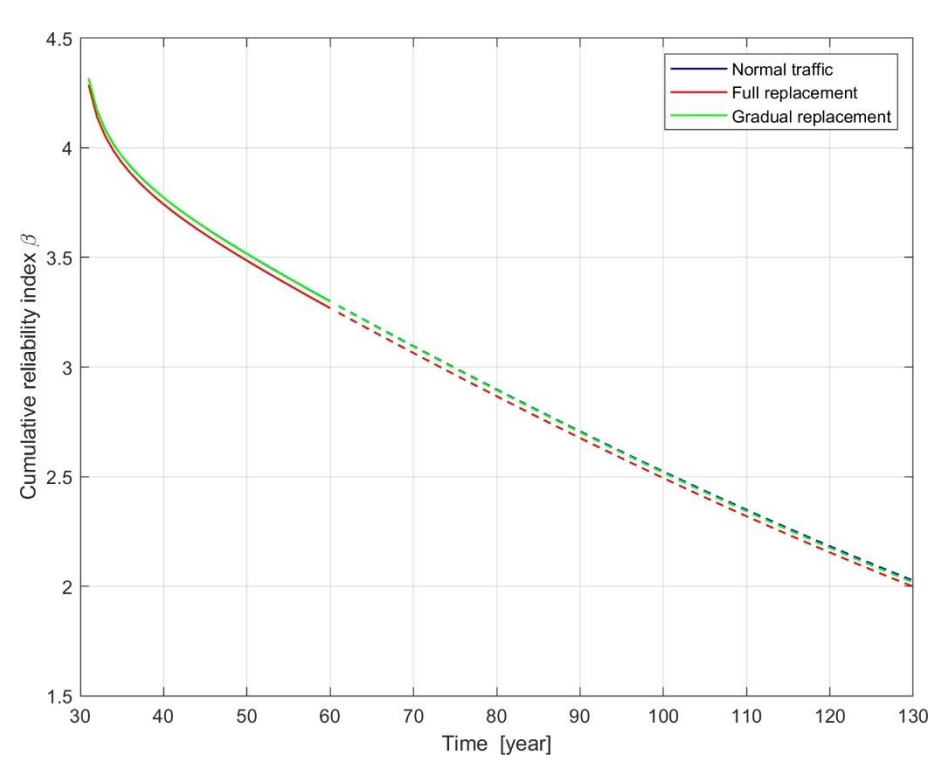


Figure 118: Comparison of cumulative reliability given different traffic scenarios for the existing structure (elapsed 30 years, L = 20 m, simply-supported beam).

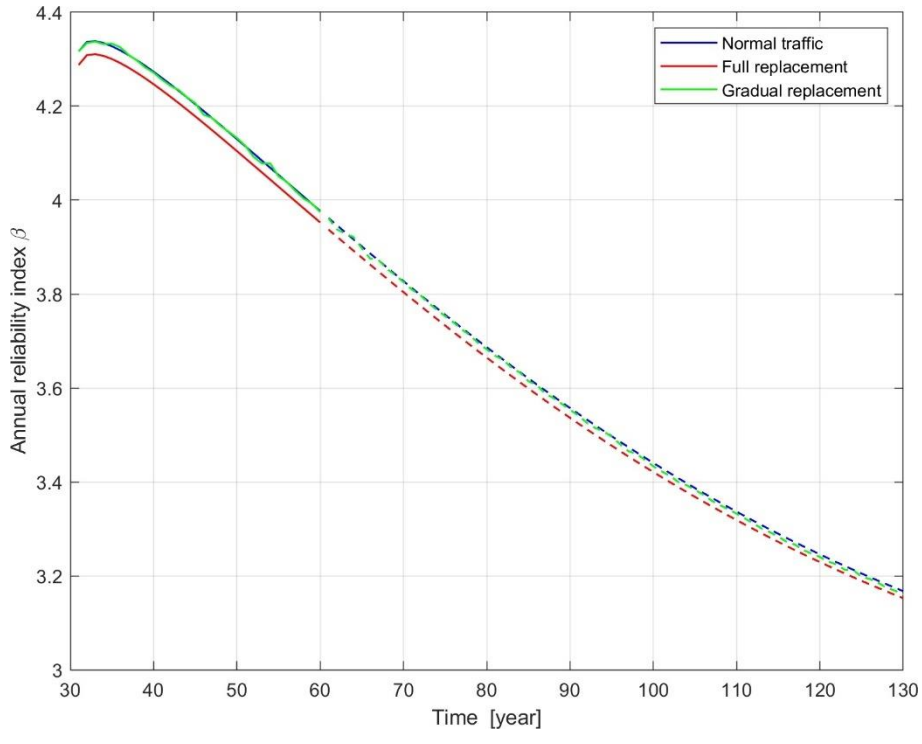


Figure 119: Comparison of annual reliability given different traffic scenarios for the existing structure (elapsed 30 years, L = 20 m, simply-supported beam).



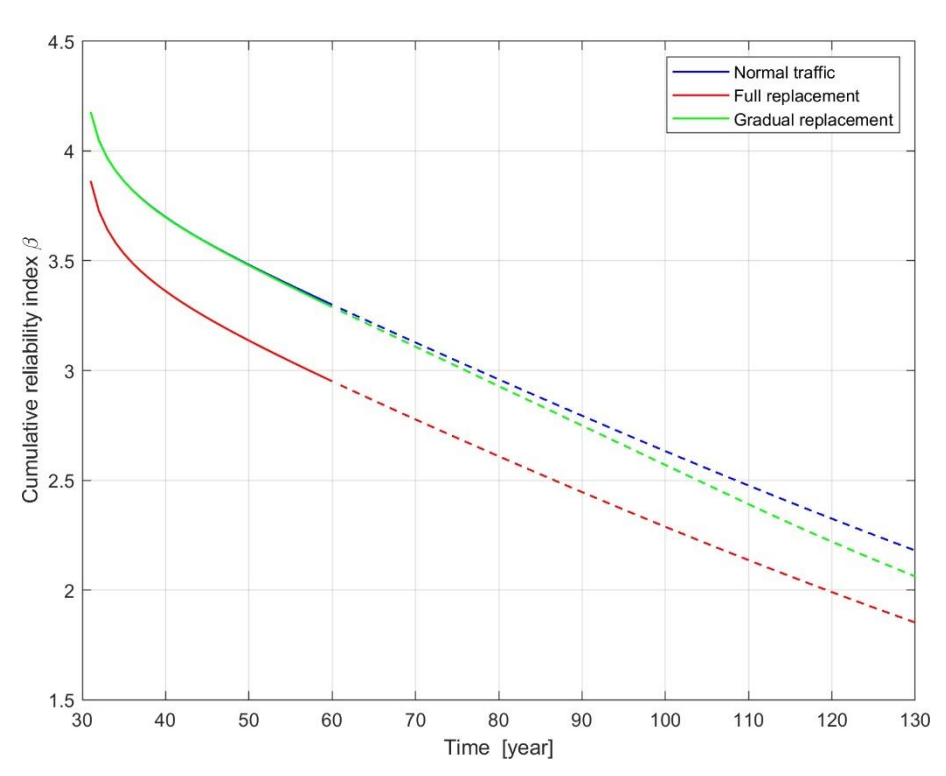


Figure 120: Comparison of cumulative reliability given different traffic scenarios for the existing structure (elapsed 30 years, L = 50 m, simply-supported beam).

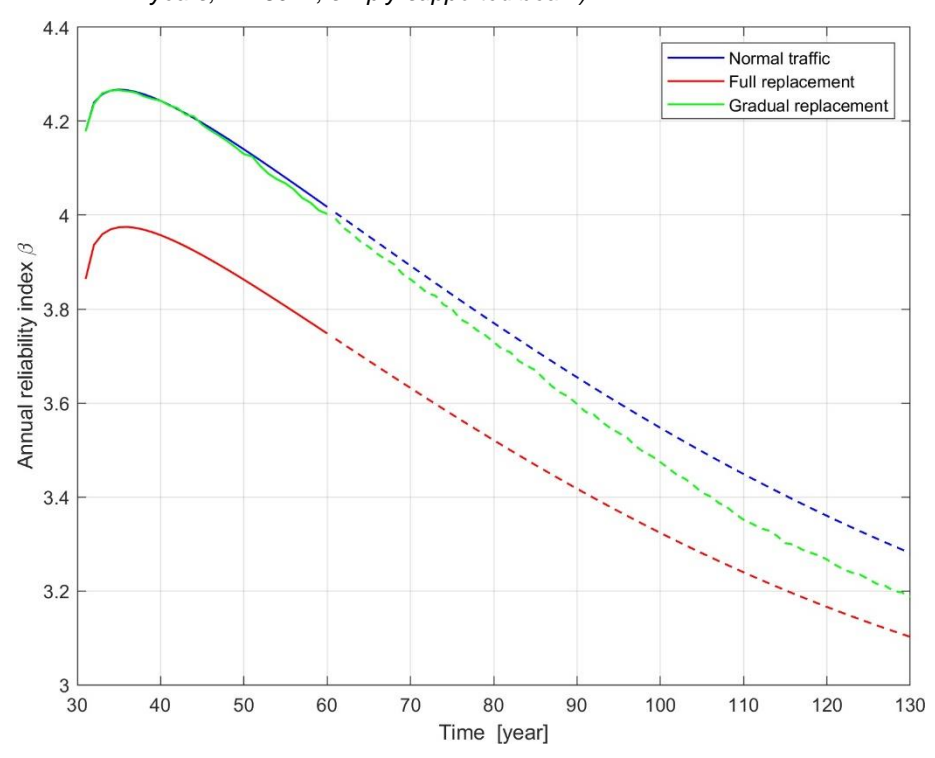


Figure 121: Comparison of annual reliability given different traffic scenarios for the existing structure (elapsed 30 years, L = 50 m, simply-supported beam).



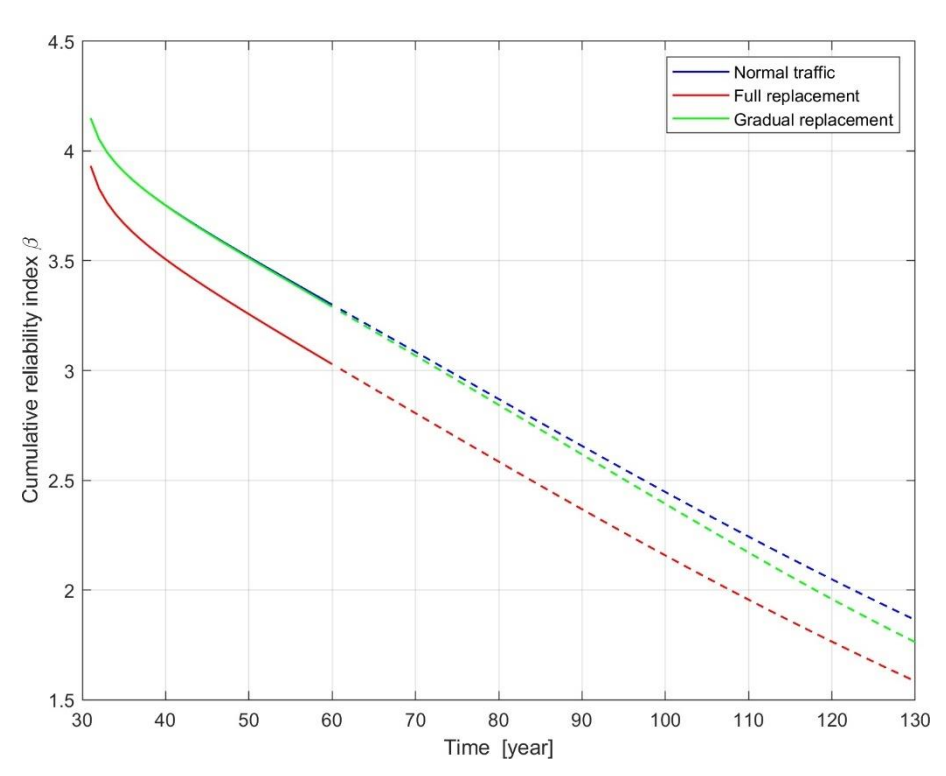


Figure 122: Comparison of cumulative reliability given different traffic scenarios for the existing structure (elapsed 30 years, L = 100 m, simply-supported beam).

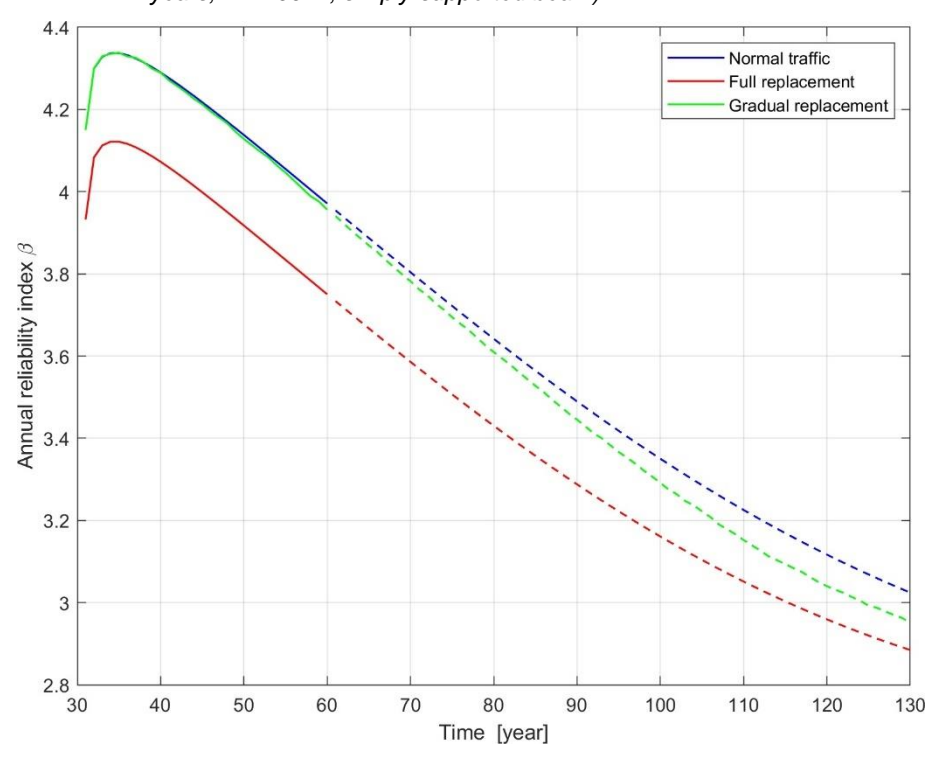


Figure 123: Comparison of annual reliability given different traffic scenarios for the existing structure (elapsed 30 years, L = 100 m, simply-supported beam).



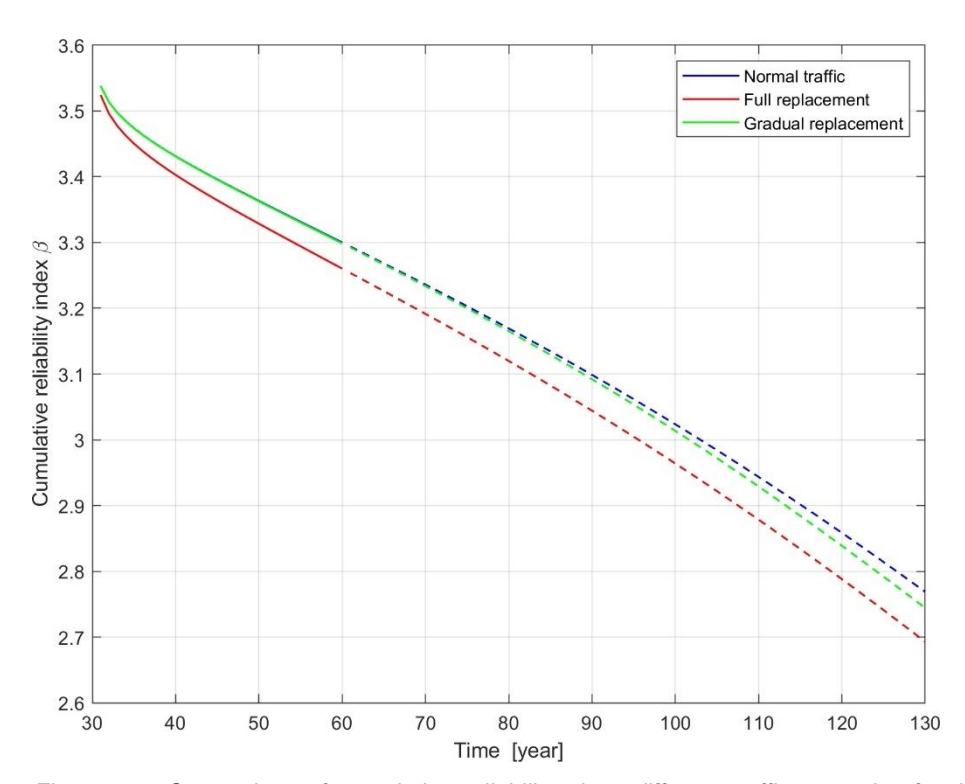


Figure 124: Comparison of cumulative reliability given different traffic scenarios for the existing structure (elapsed 30 years, L = 200 m, simply-supported beam).

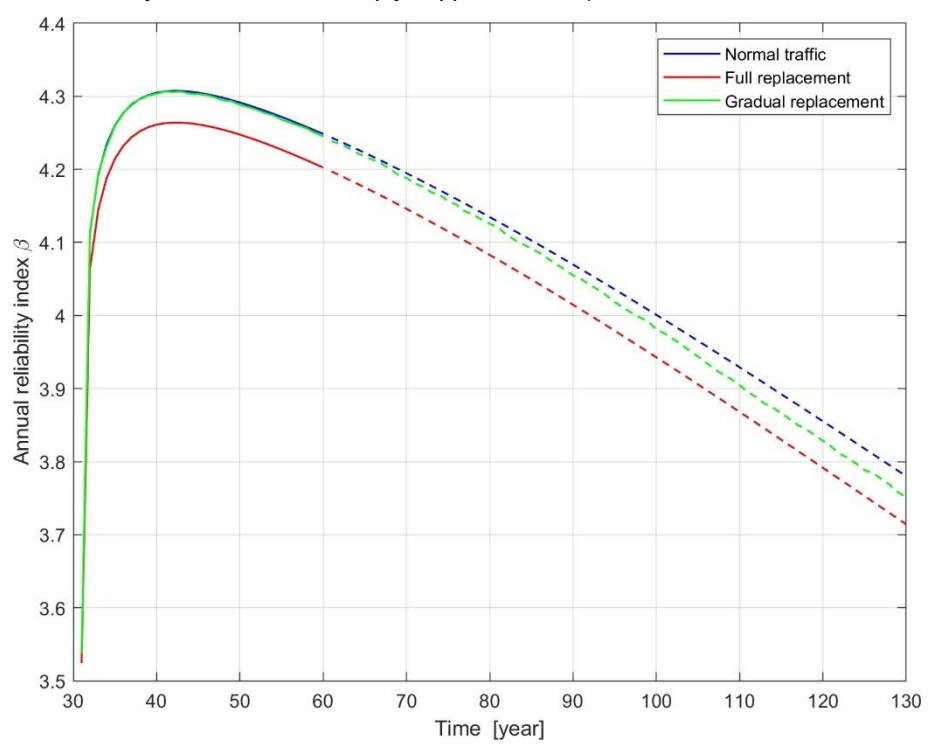


Figure 125: Comparison of annual reliability given different traffic scenarios for the existing structure (elapsed 30 years, L = 200 m, simply-supported beam).



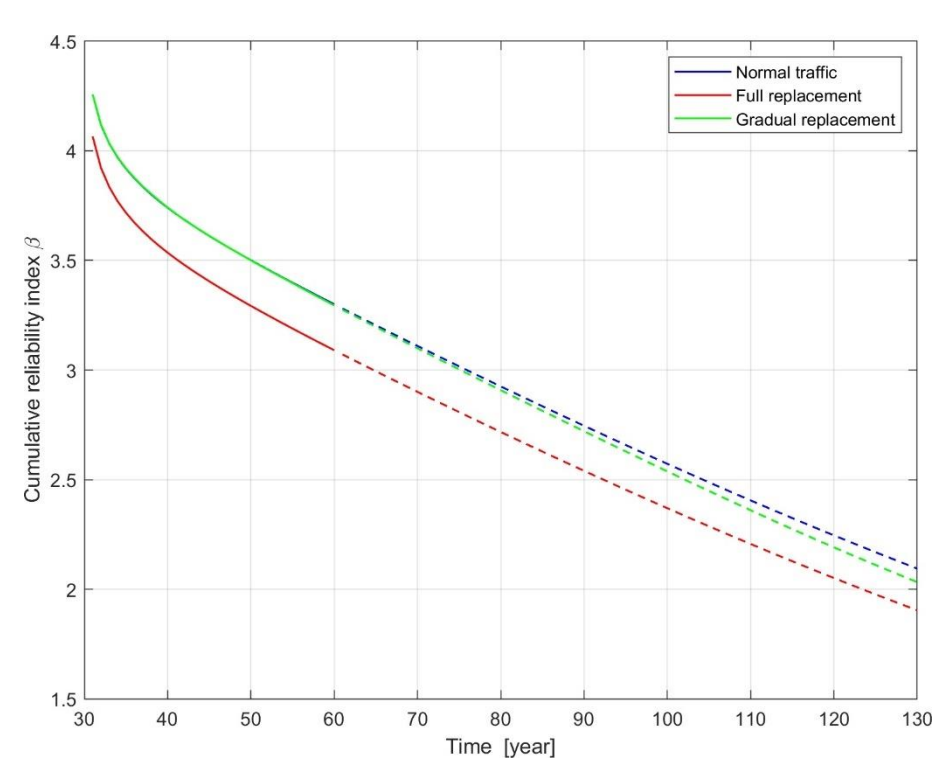


Figure 126: Comparison of cumulative reliability given different traffic scenarios for the existing structure (elapsed 30 years, L = 2.20 m, bending moment, continuous beam).

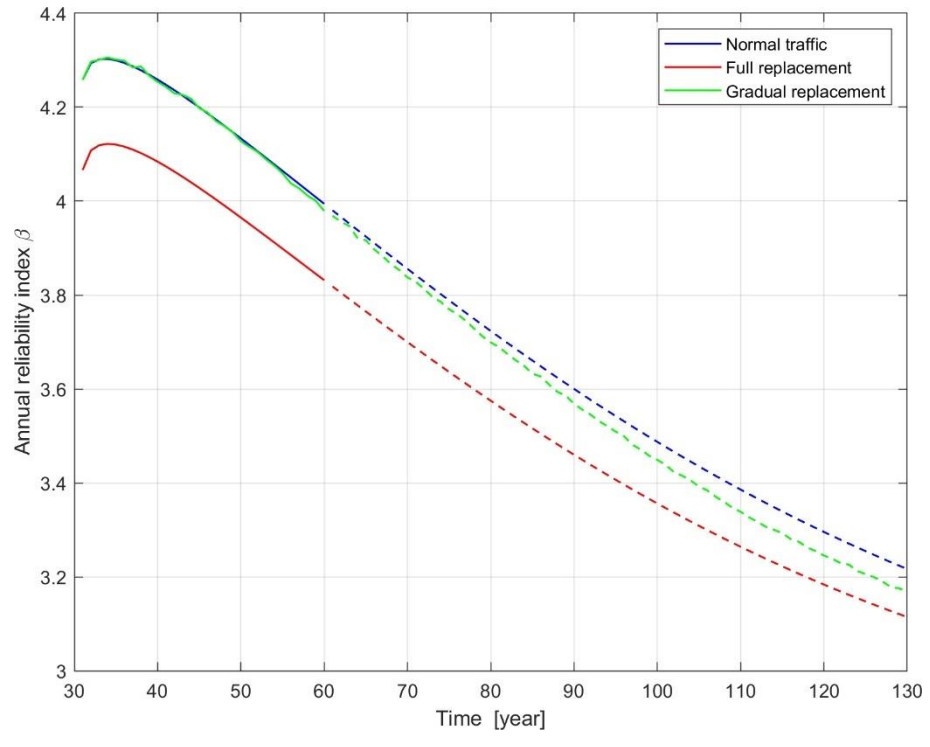


Figure 127: Comparison of annual reliability given different traffic scenarios for the existing structure (elapsed 30 years, L = 2 · 20 m, bending moment, continuous beam).



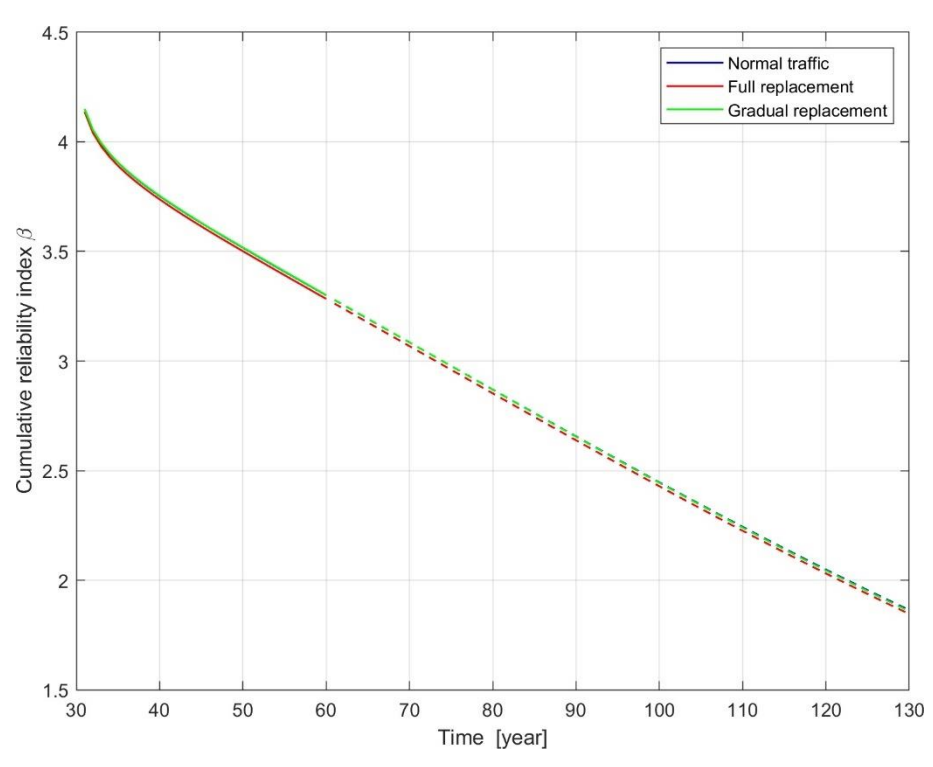


Figure 128: Comparison of cumulative reliability given different traffic scenarios for the existing structure (elapsed 30 years, L = 2.50 m, bending moment, continuous beam).

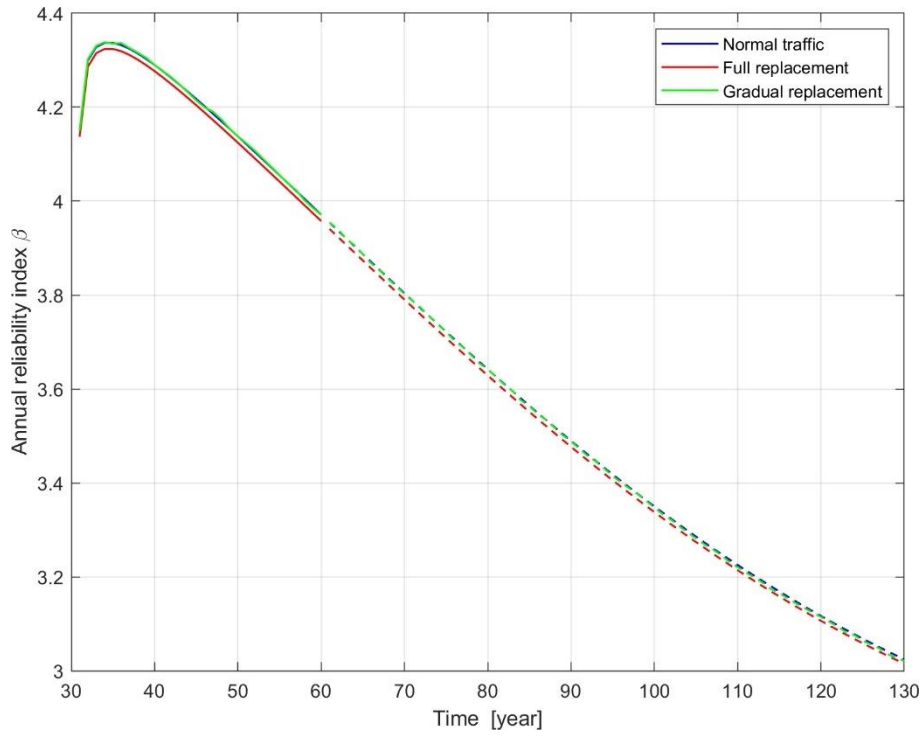


Figure 129: Comparison of annual reliability given different traffic scenarios for the existing structure (elapsed 30 years, L = 2.50 m, bending moment, continuous beam).



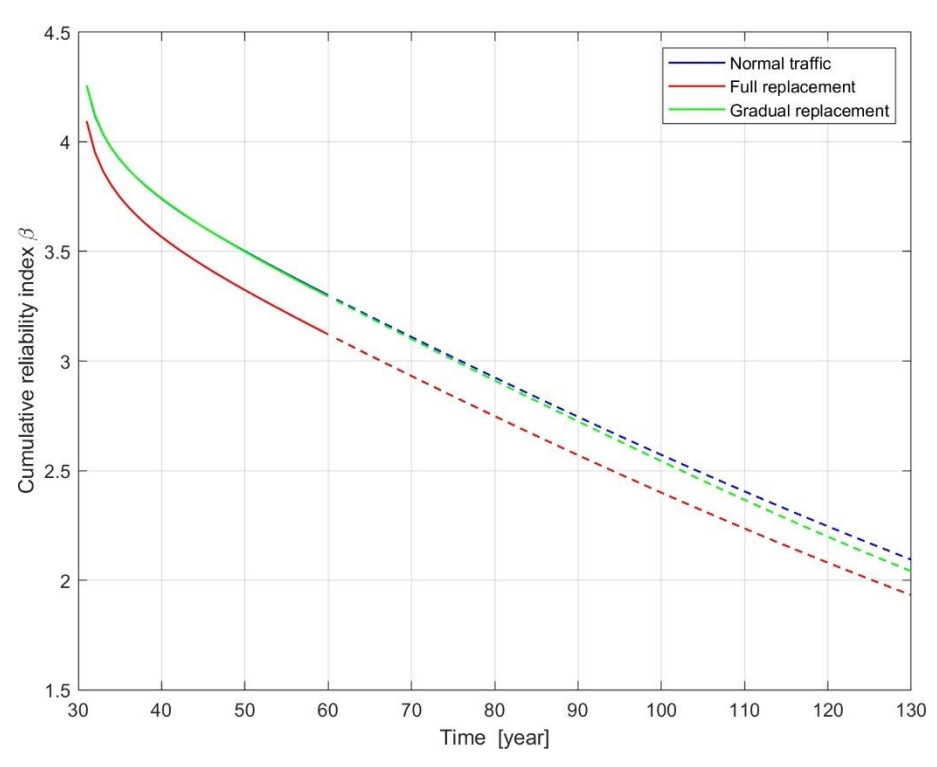


Figure 130: Comparison of cumulative reliability given different traffic scenarios for the existing structure (elapsed 30 years, L = 2.20 m, shear force, continuous beam).

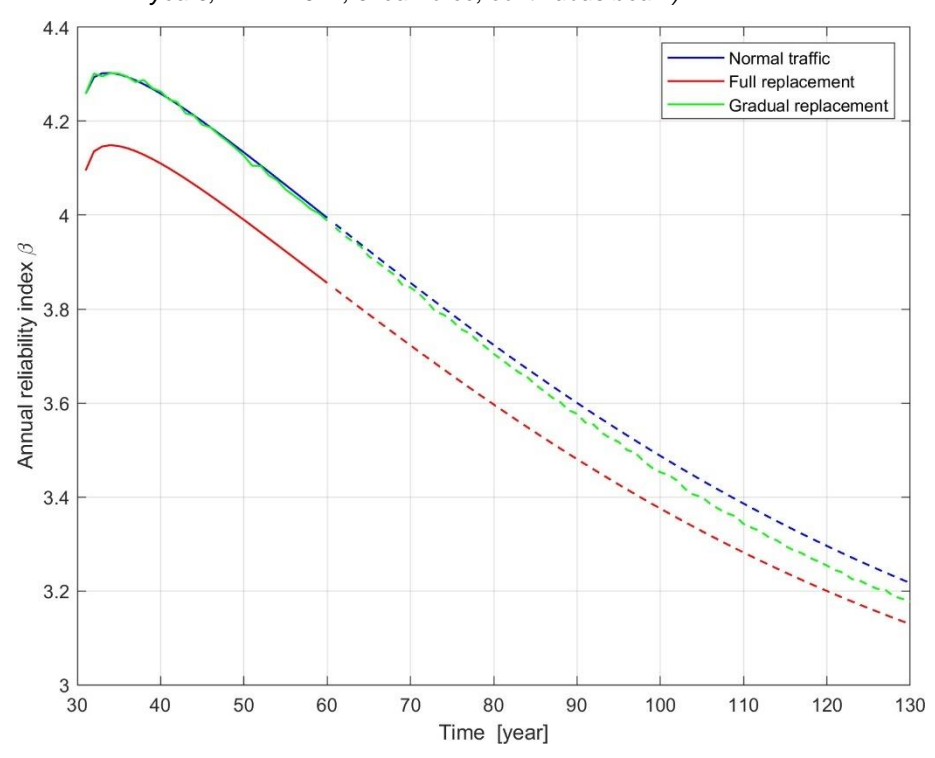


Figure 131: Comparison of annual reliability given different traffic scenarios for the existing structure (elapsed 30 years, L = 2.20 m, shear force, continuous beam).



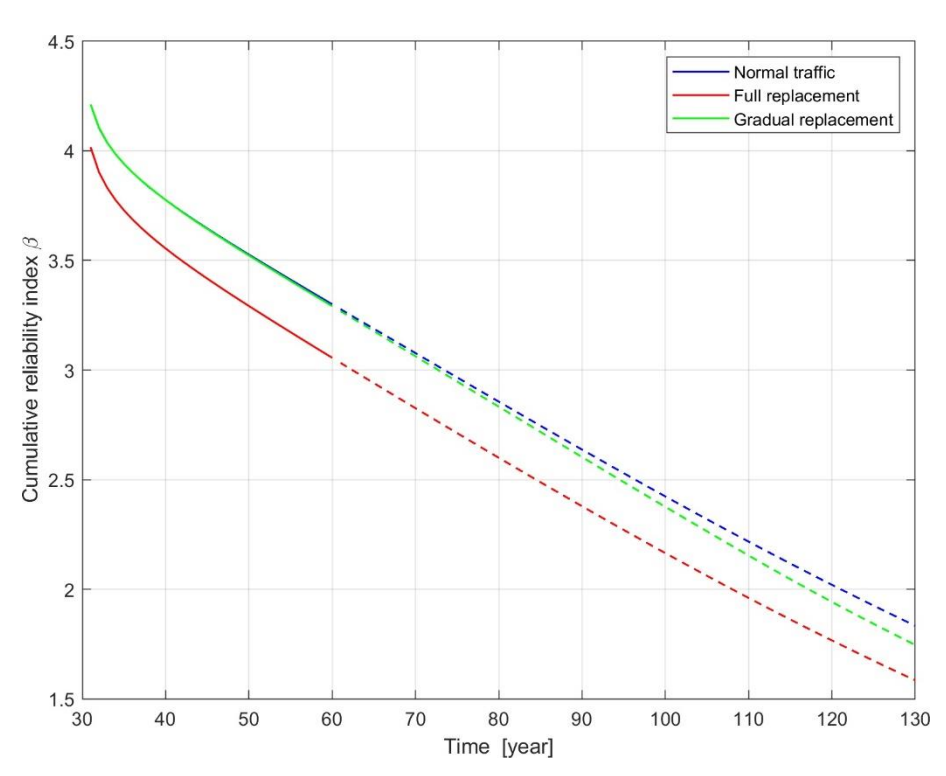


Figure 132: Comparison of cumulative reliability given different traffic scenarios for the existing structure (elapsed 30 years, L = 2.50 m, shear force, continuous beam).

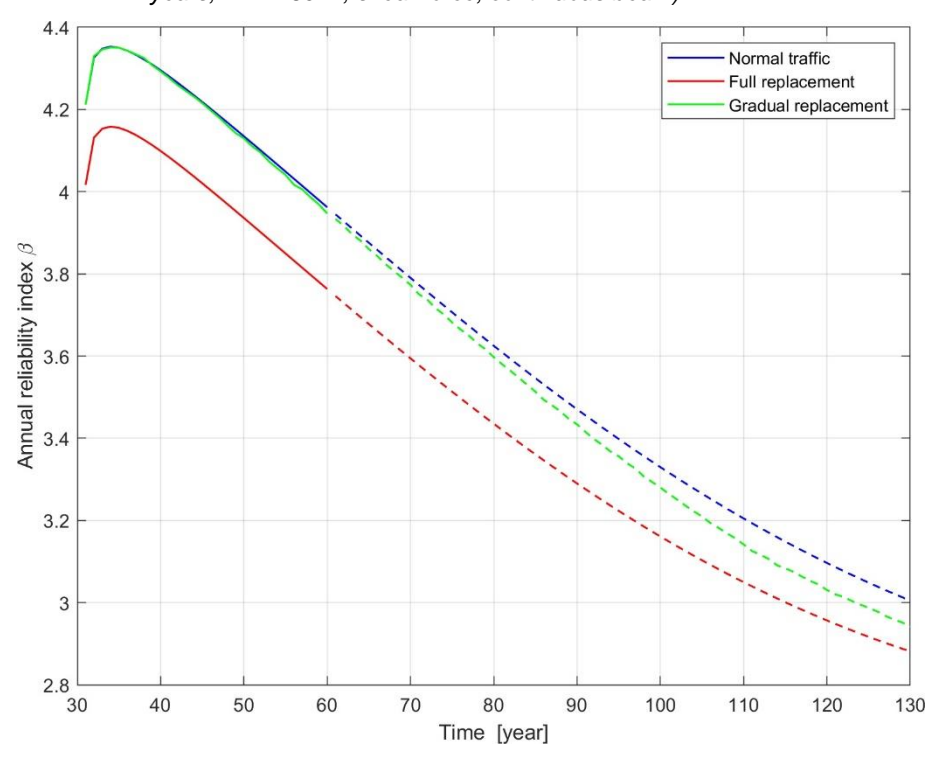


Figure 133: Comparison of annual reliability given different traffic scenarios for the existing structure (elapsed 30 years, L = 2.50 m, shear force, continuous beam).



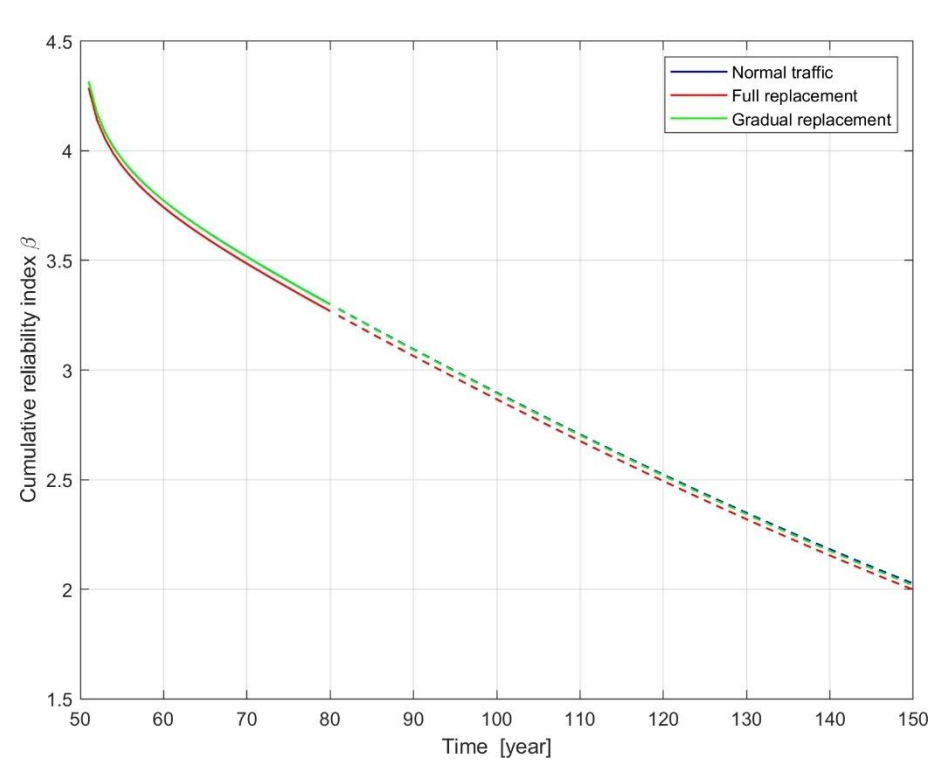


Figure 134: Comparison of cumulative reliability given different traffic scenarios for the existing structure (elapsed 50 years, L = 20 m, simply-supported beam).

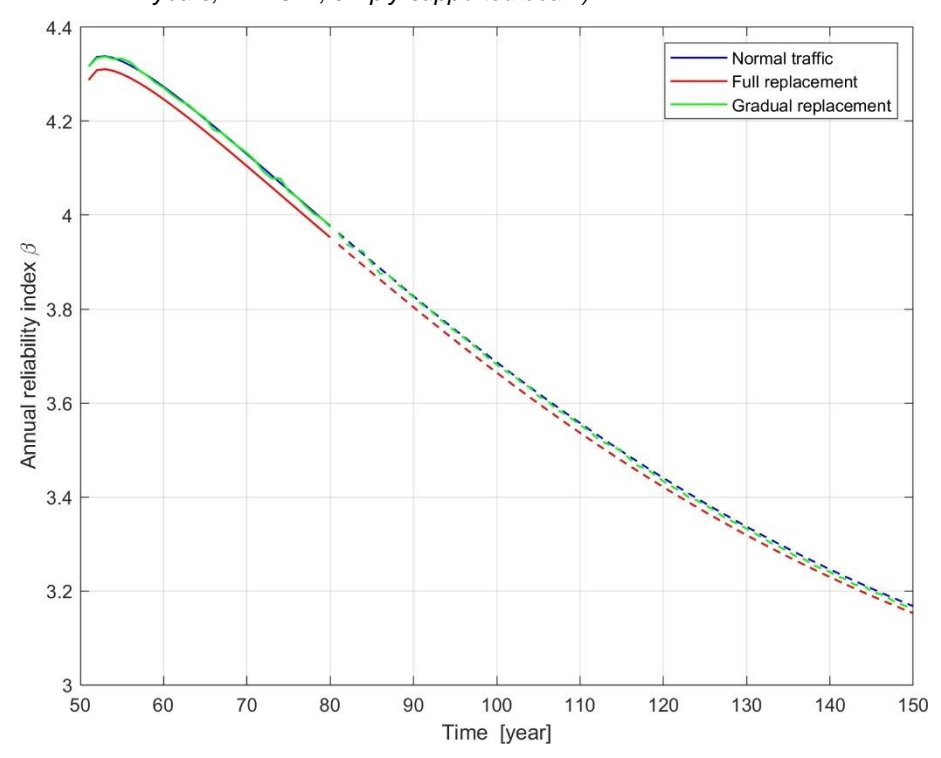


Figure 135: Comparison of annual reliability given different traffic scenarios for the existing structure (elapsed 50 years, L = 20 m, simply-supported beam).



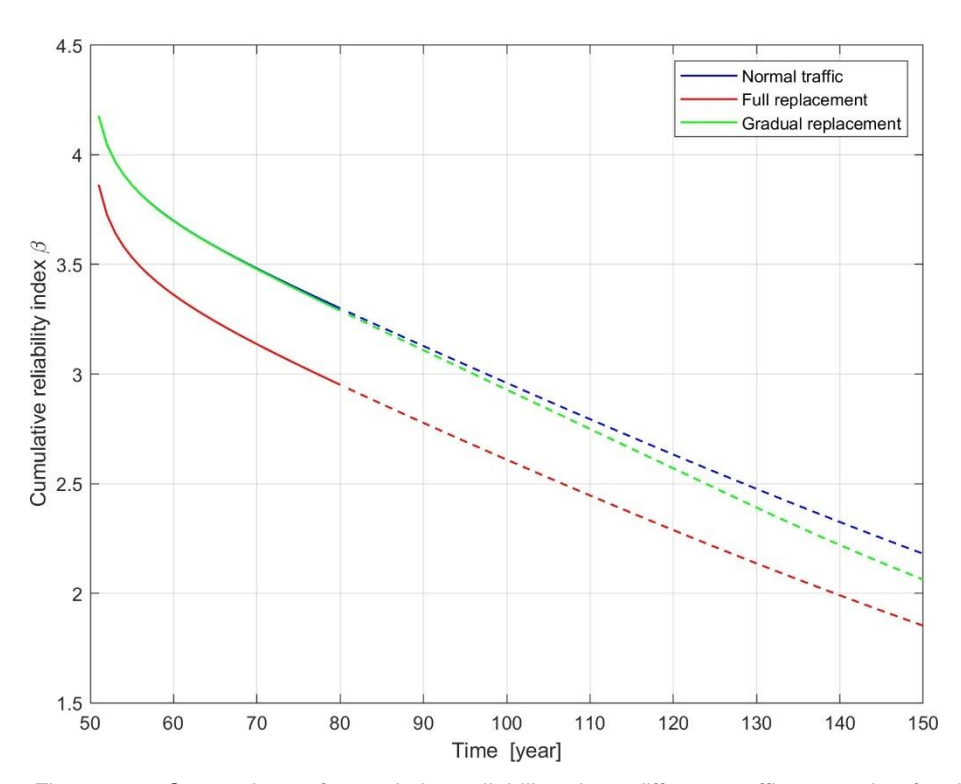


Figure 136: Comparison of cumulative reliability given different traffic scenarios for the existing structure (elapsed 50 years, L = 50 m, simply-supported beam).

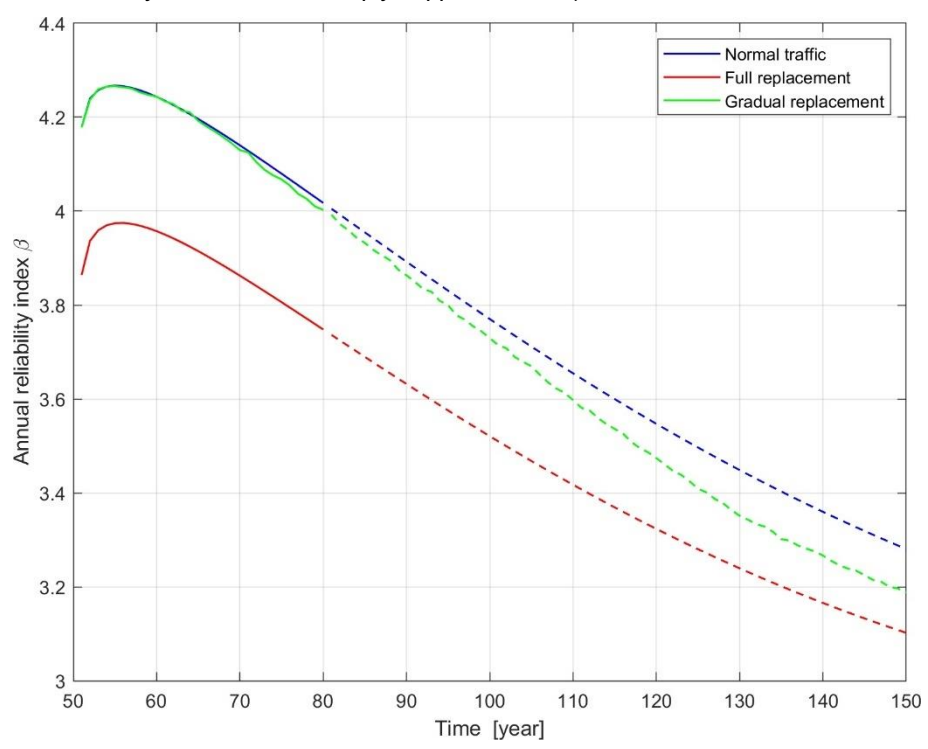


Figure 137: Comparison of annual reliability given different traffic scenarios for the existing structure (elapsed 50 years, L = 50 m, simply-supported beam).



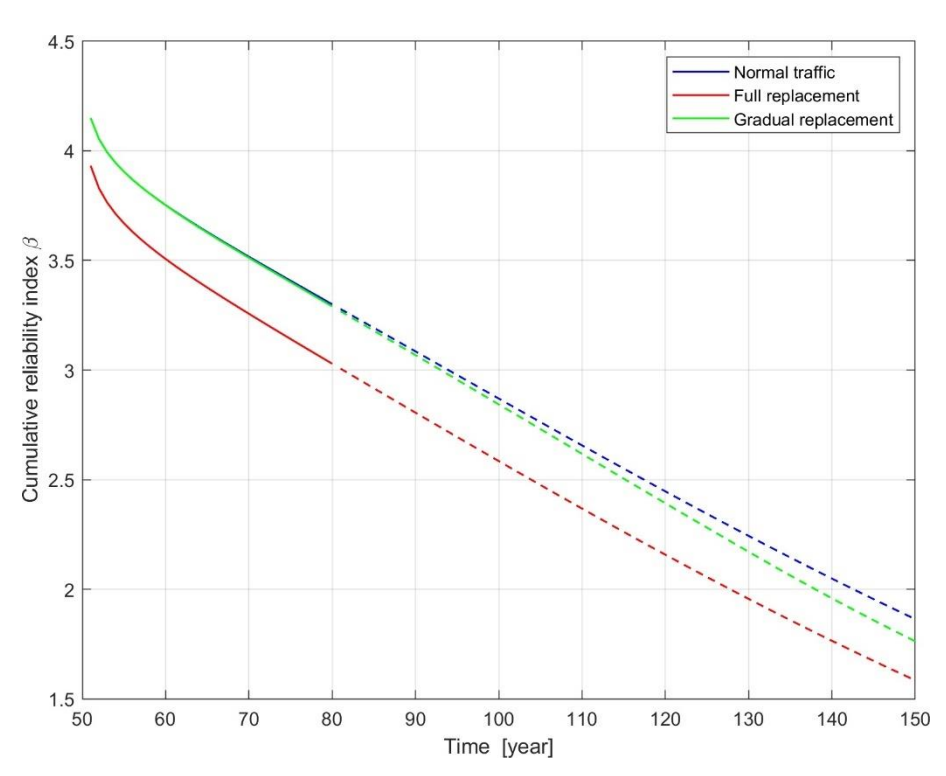


Figure 138: Comparison of cumulative reliability given different traffic scenarios for the existing structure (elapsed 50 years, L = 100 m, simply-supported beam).

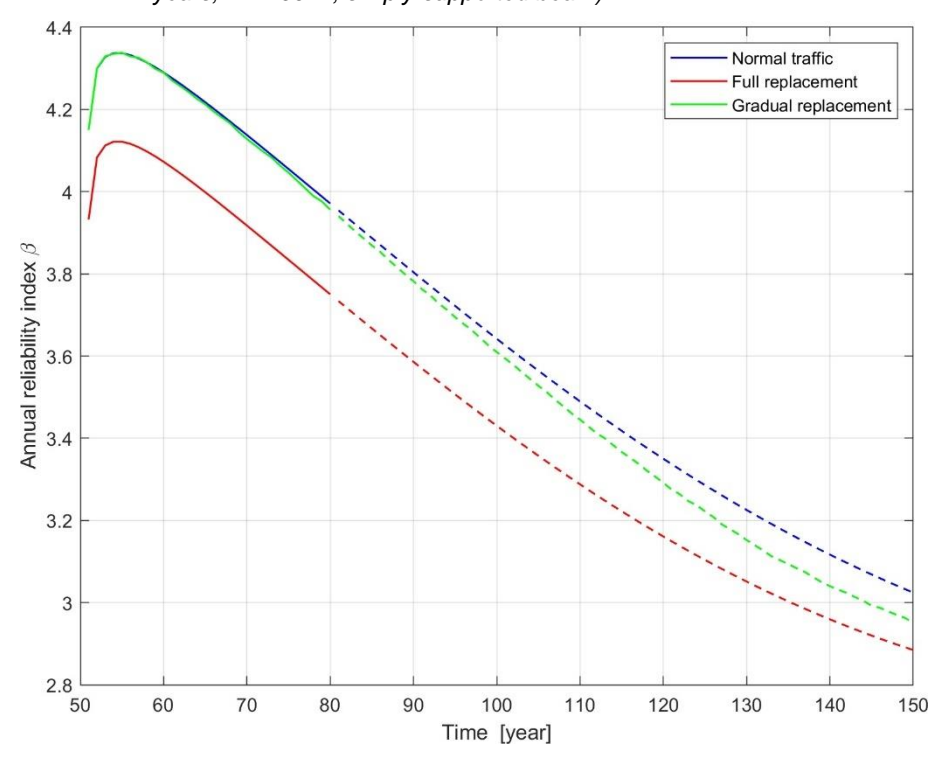


Figure 139: Comparison of annual reliability given different traffic scenarios for the existing structure (elapsed 50 years, L = 100 m, simply-supported beam).



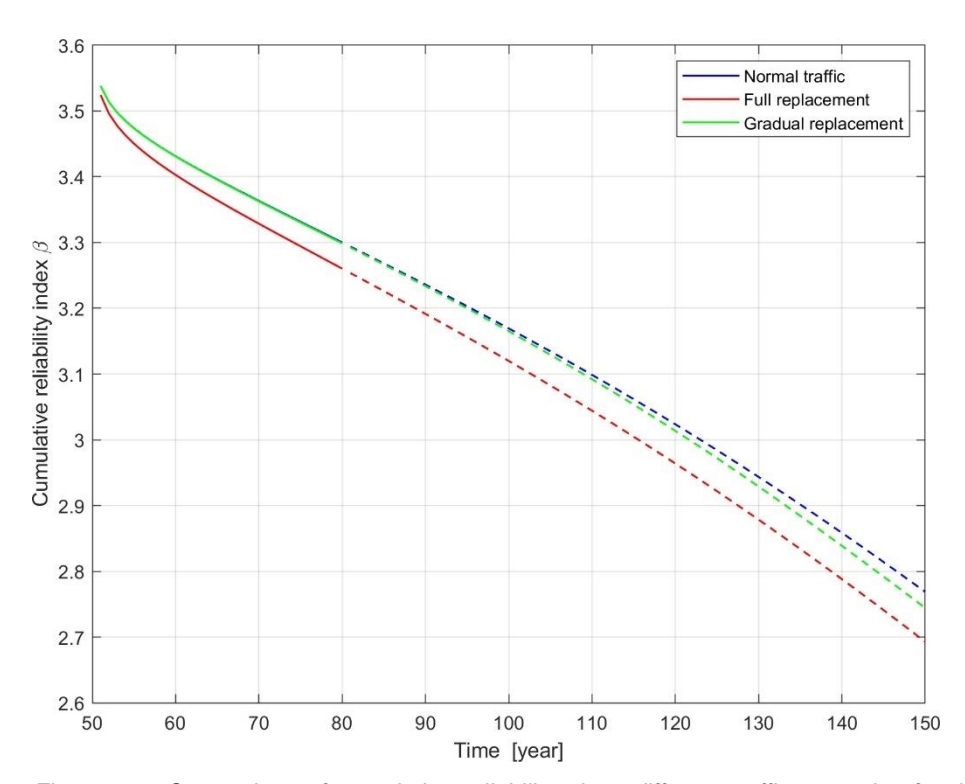


Figure 140: Comparison of cumulative reliability given different traffic scenarios for the existing structure (elapsed 50 years, L = 200 m, simply-supported beam).

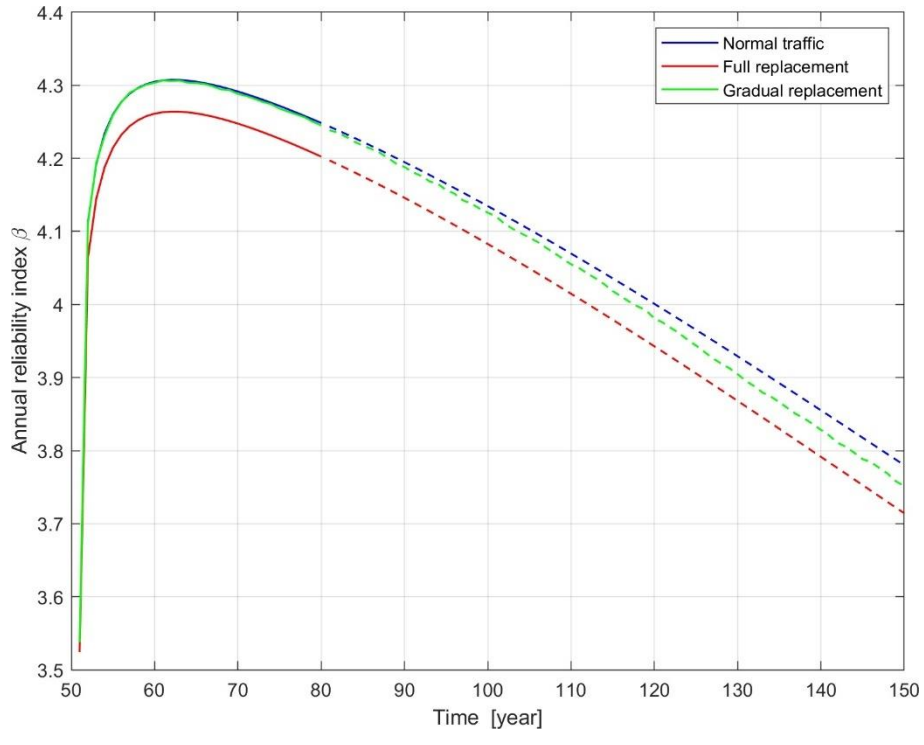


Figure 141: Comparison of annual reliability given different traffic scenarios for the existing structure (elapsed 50 years, L = 200 m, simply-supported beam).



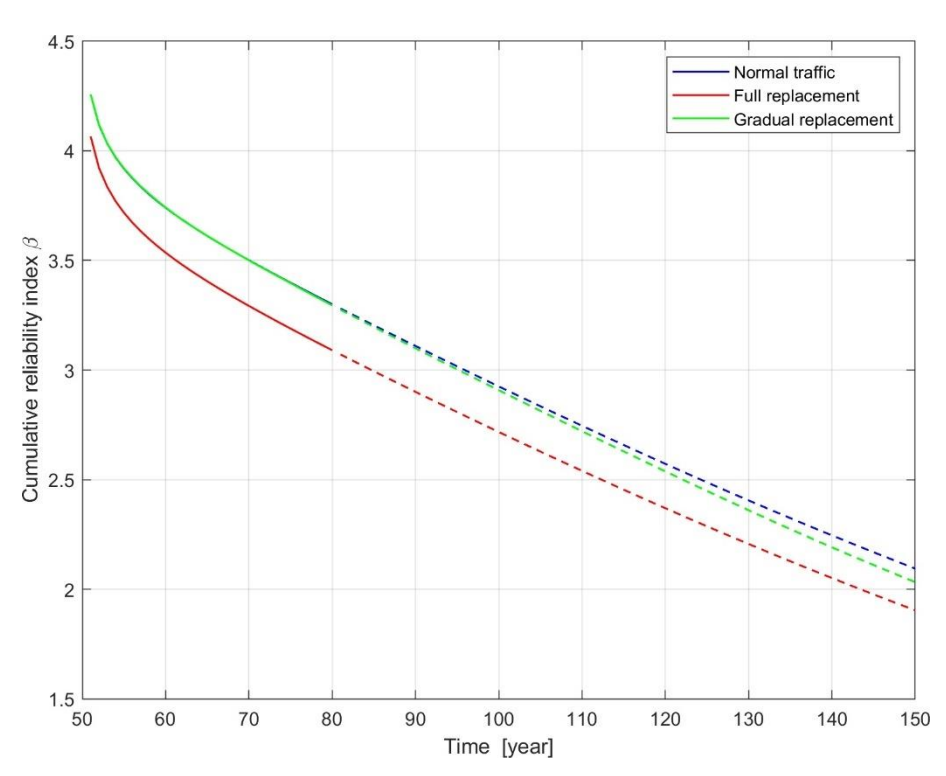


Figure 142: Comparison of cumulative reliability given different traffic scenarios for the existing structure (elapsed 50 years, L = 2.20 m, bending moment, continuous beam).

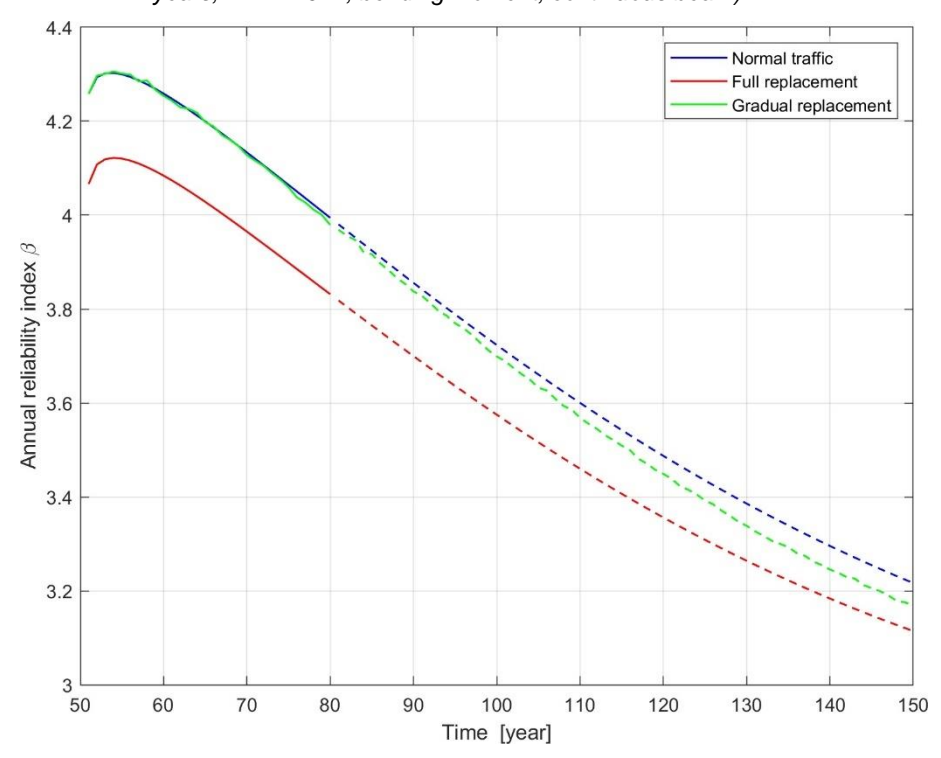


Figure 143: Comparison of annual reliability given different traffic scenarios for the existing structure (elapsed 50 years, L = 2 · 20 m, bending moment, continuous beam).



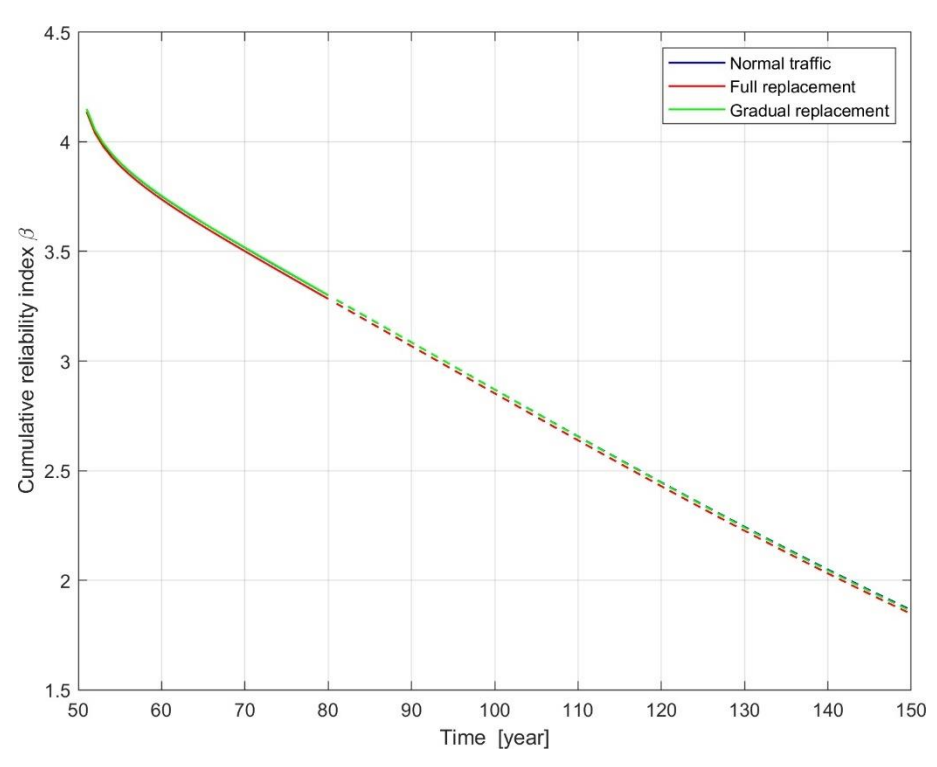


Figure 144: Comparison of cumulative reliability given different traffic scenarios for the existing structure (elapsed 50 years, L = 2.50 m, bending moment, continuous beam).

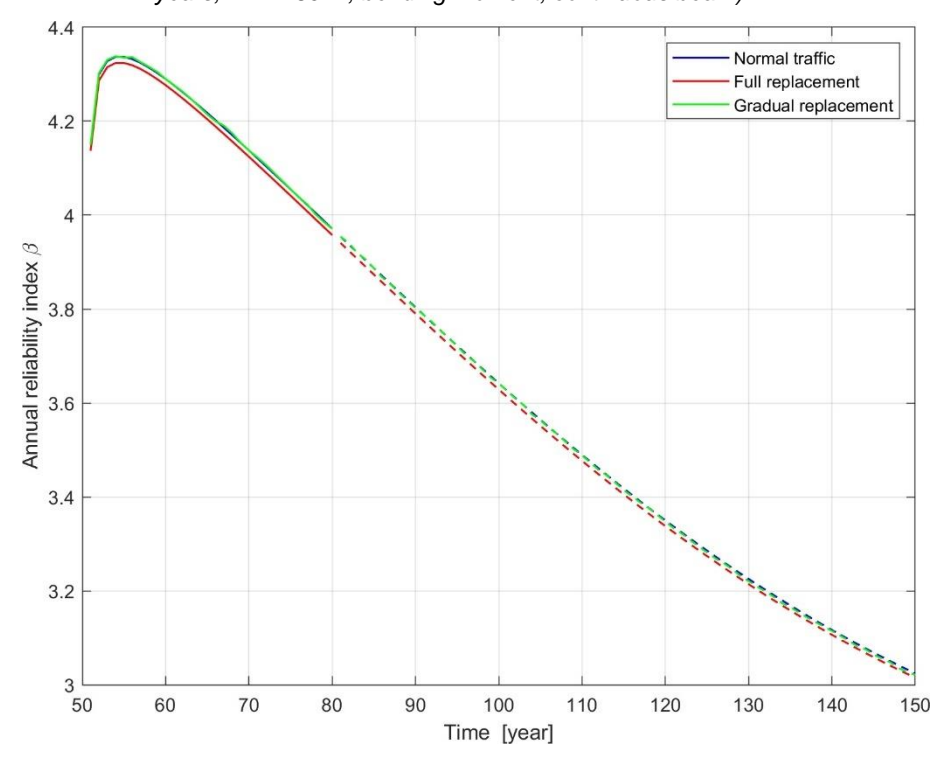


Figure 145: Comparison of annual reliability given different traffic scenarios for the existing structure (elapsed 50 years, L = 2.50 m, bending moment, continuous beam).



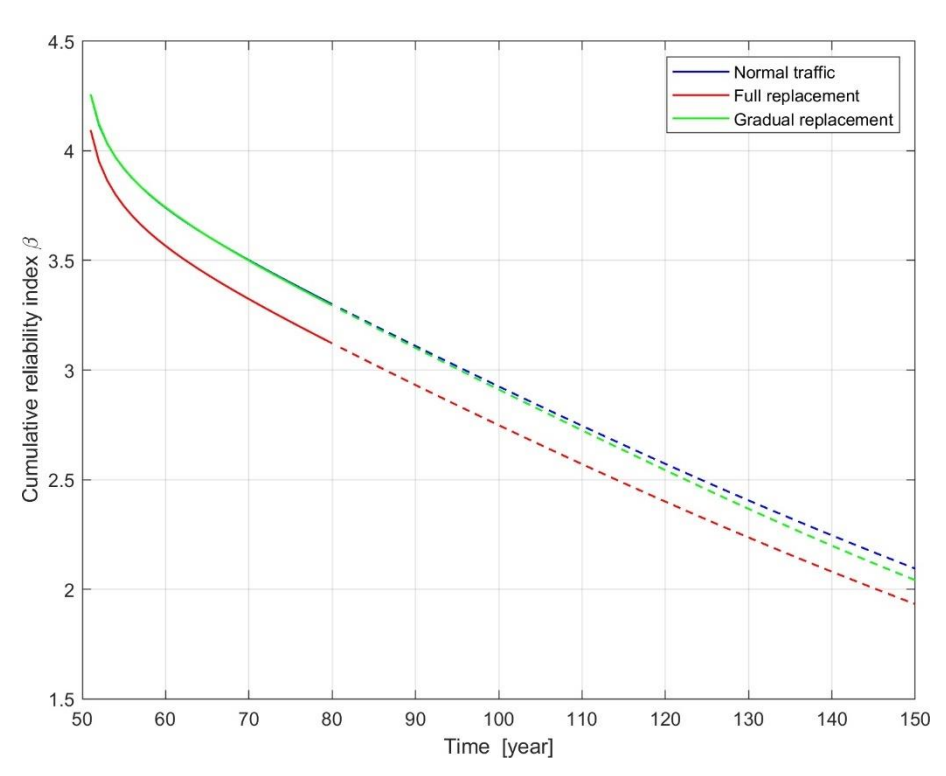


Figure 146: Comparison of cumulative reliability given different traffic scenarios for the existing structure (elapsed 50 years, L = 2.20 m, shear force, continuous beam).

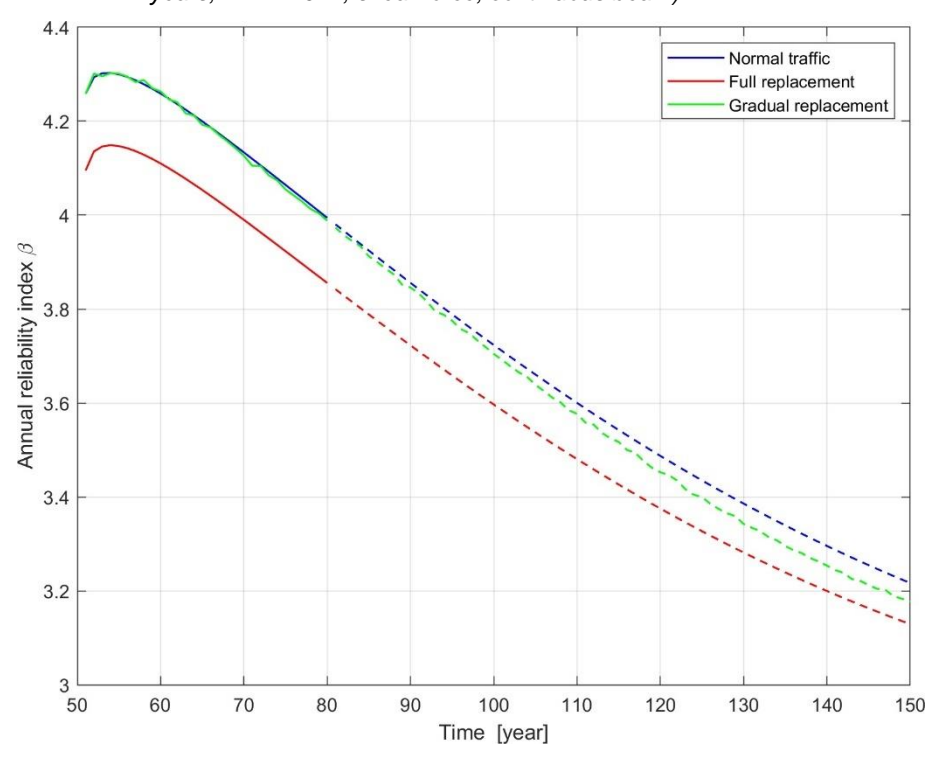


Figure 147: Comparison of annual reliability given different traffic scenarios for the existing structure (elapsed 50 years, L = 2.20 m, shear force, continuous beam).



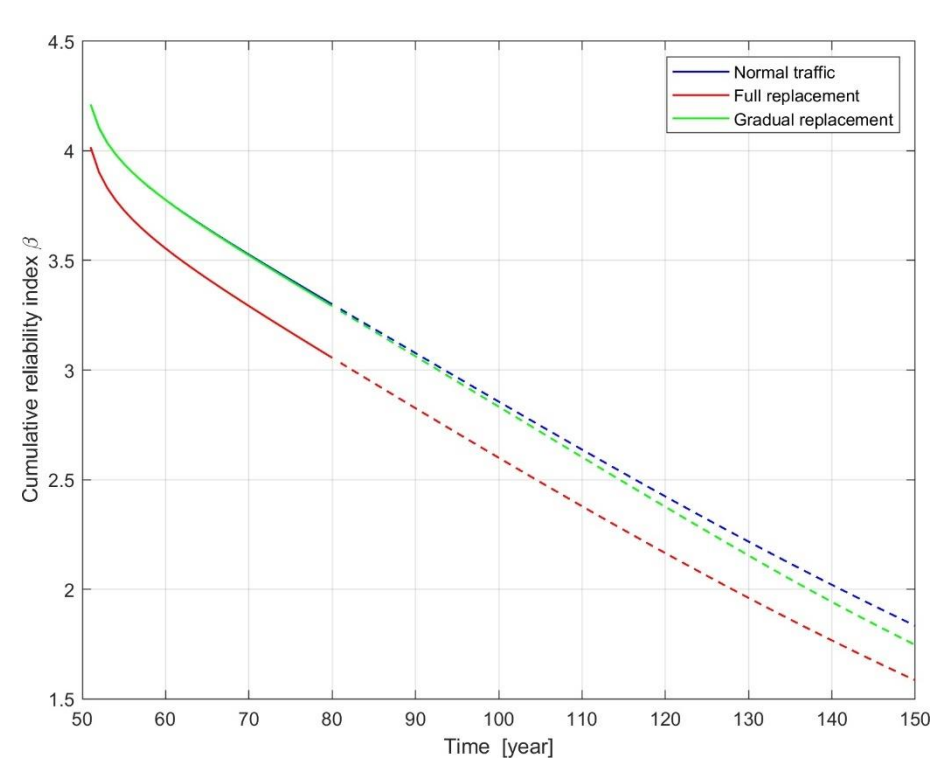


Figure 148: Comparison of cumulative reliability given different traffic scenarios for the existing structure (elapsed 50 years, L = 2.50 m, shear force, continuous beam).

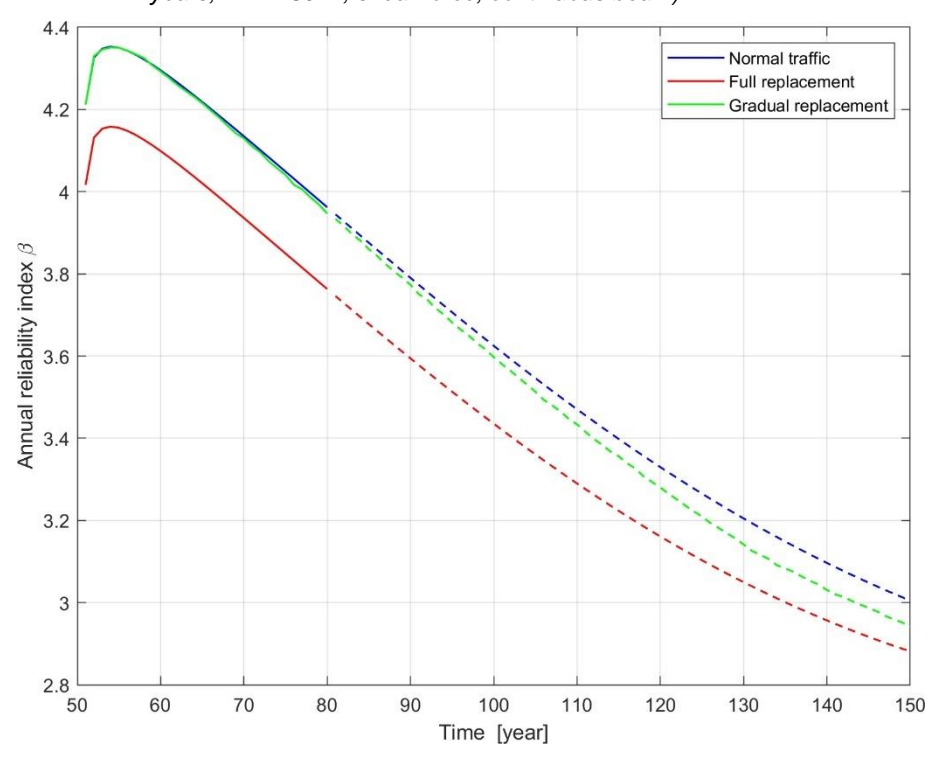


Figure 149: Comparison of annual reliability given different traffic scenarios for the existing structure (elapsed 50 years, L = 2.50 m, shear force, continuous beam).



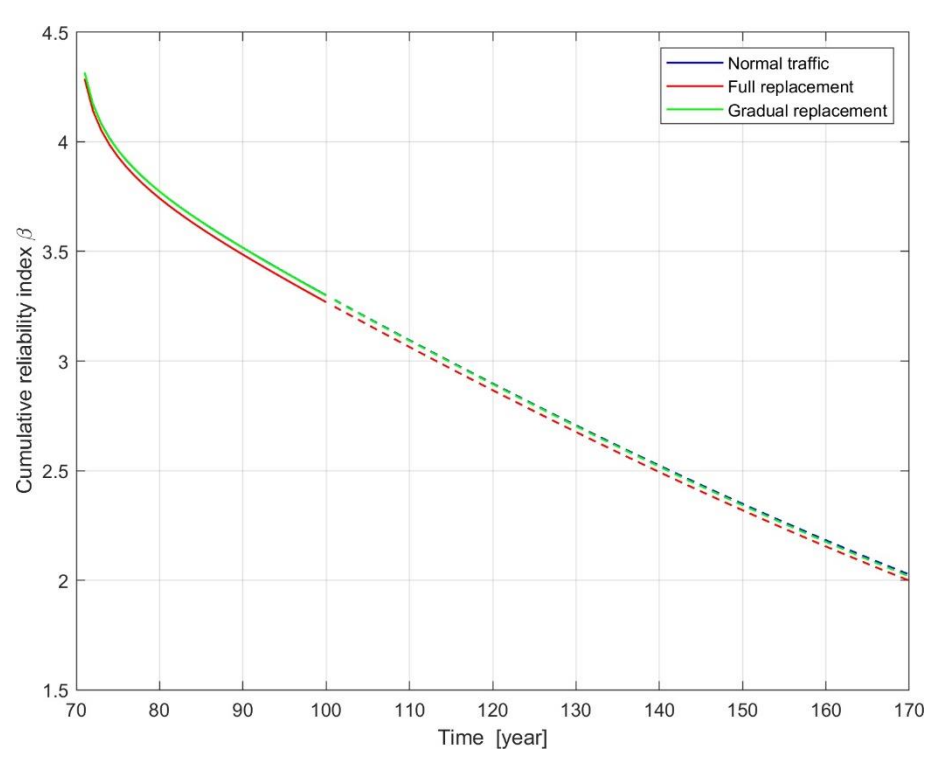


Figure 150: Comparison of cumulative reliability given different traffic scenarios for the existing structure (elapsed 70 years, L = 20 m, simply-supported beam).

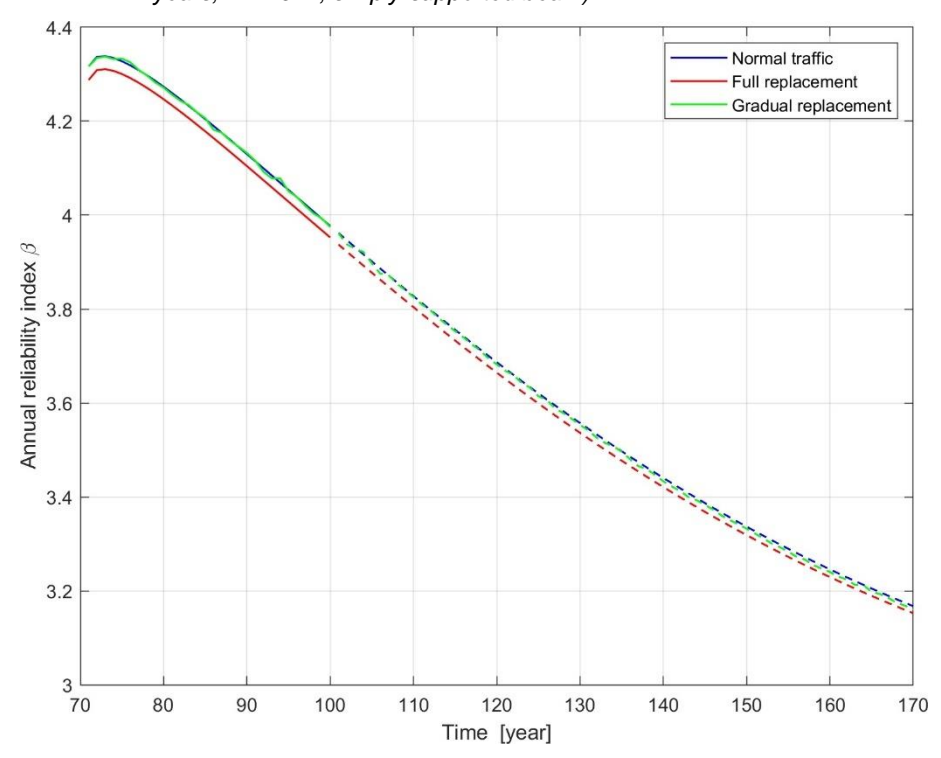


Figure 151: Comparison of annual reliability given different traffic scenarios for the existing structure (elapsed 70 years, L = 20 m, simply-supported beam).



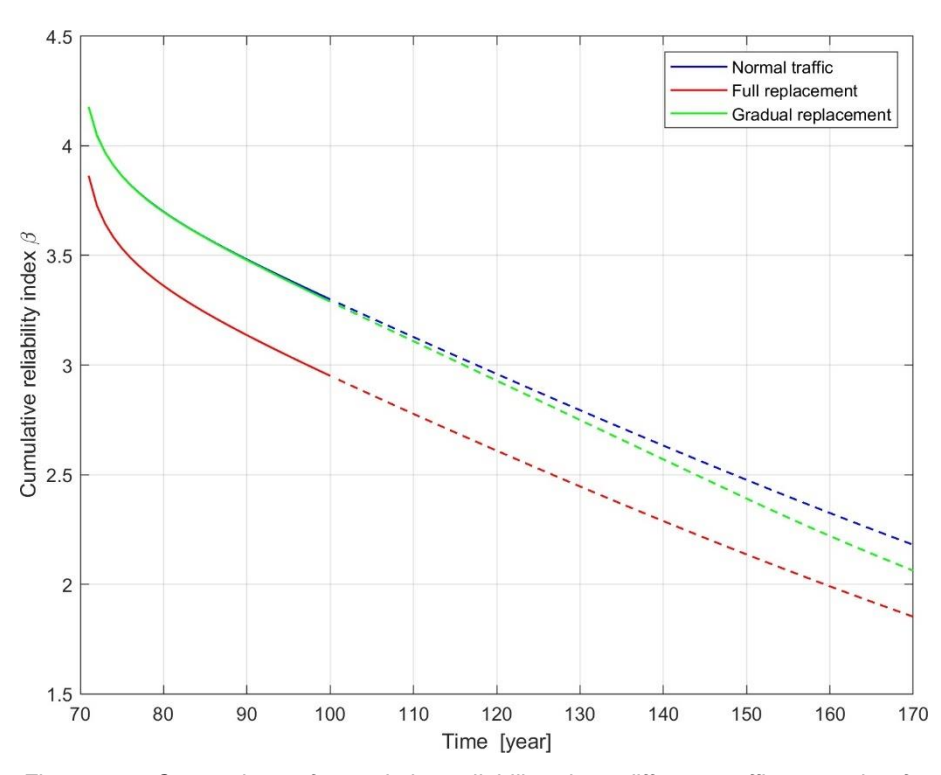


Figure 152: Comparison of cumulative reliability given different traffic scenarios for the existing structure (elapsed 70 years, L = 50 m, simply-supported beam).

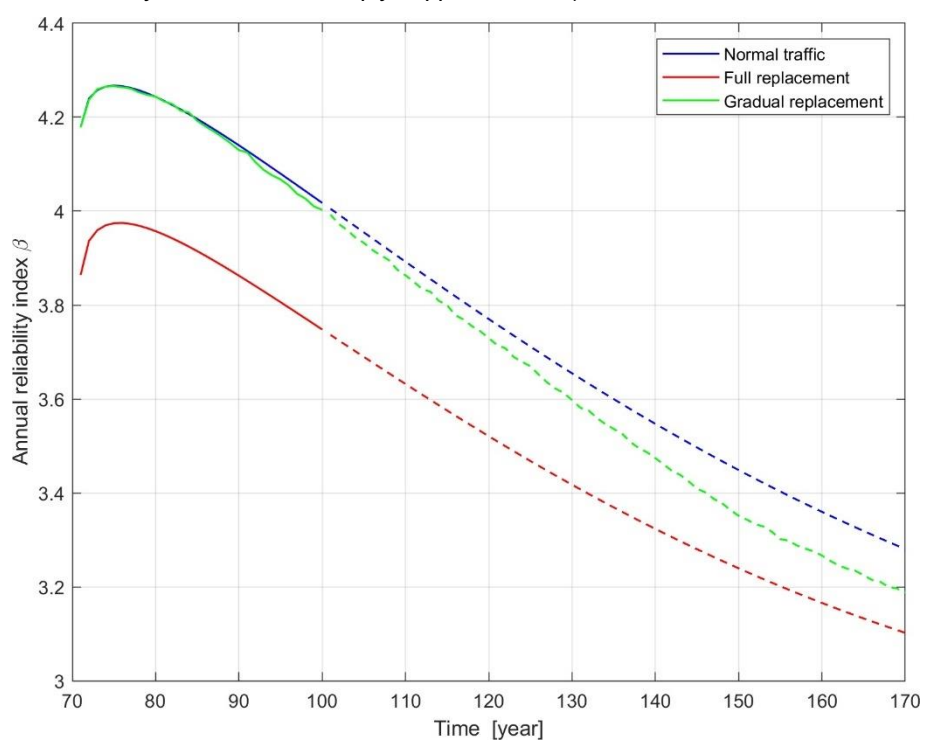


Figure 153: Comparison of annual reliability given different traffic scenarios for the existing structure (elapsed 70 years, L = 50 m, simply-supported beam).



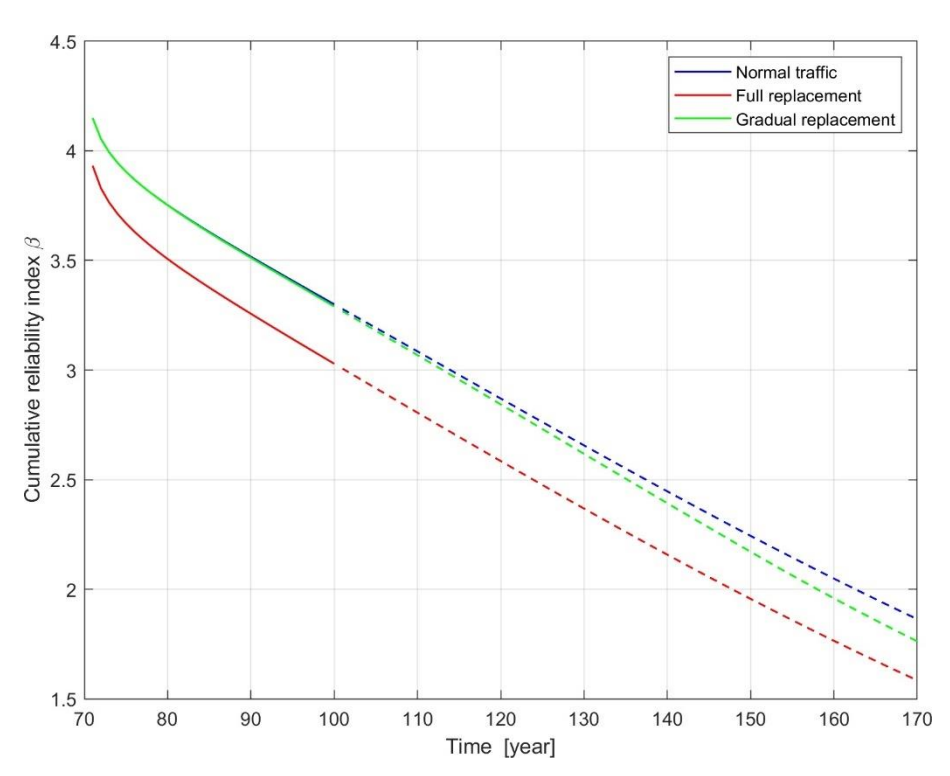


Figure 154: Comparison of cumulative reliability given different traffic scenarios for the existing structure (elapsed 70 years, L = 100 m, simply-supported beam).

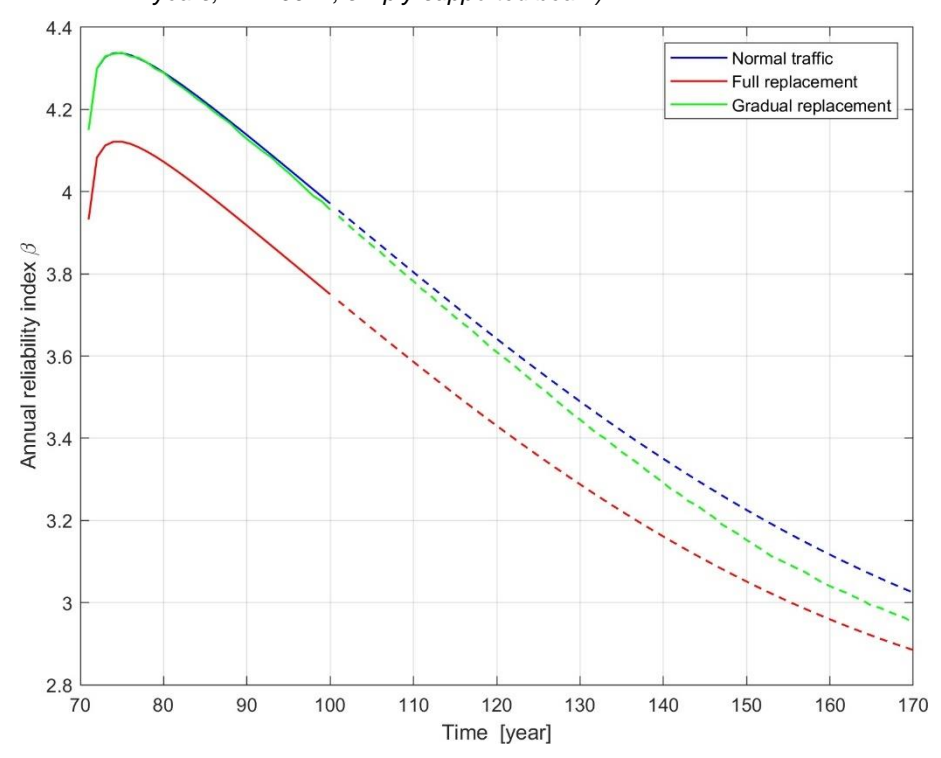


Figure 155: Comparison of annual reliability given different traffic scenarios for the existing structure (elapsed 70 years, L = 100 m, simply-supported beam).



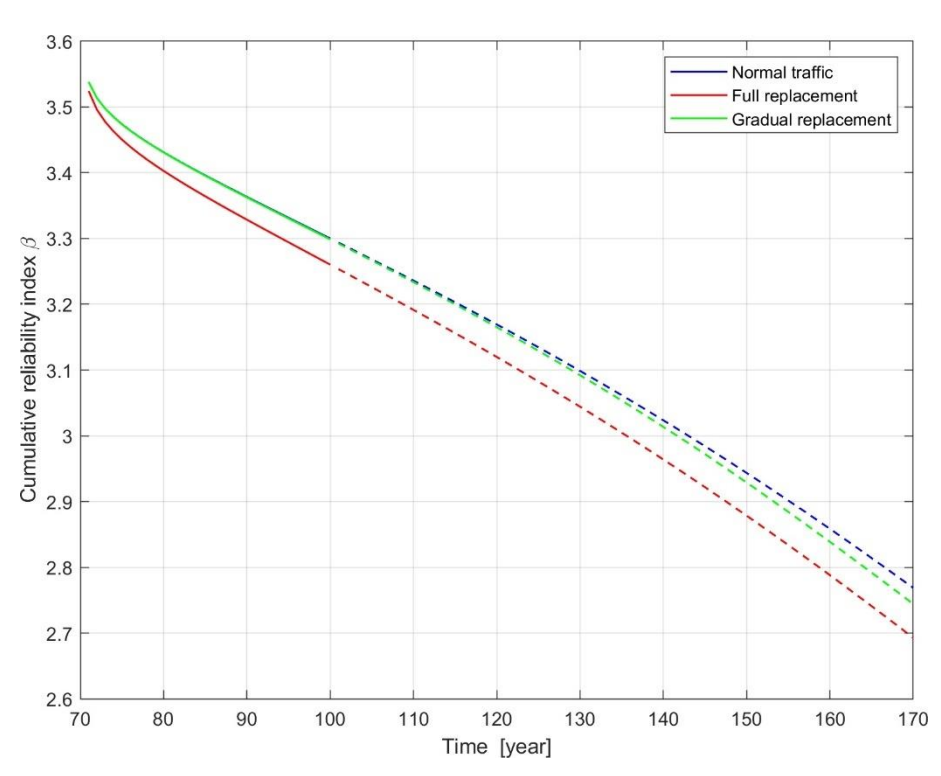


Figure 156: Comparison of cumulative reliability given different traffic scenarios for the existing structure (elapsed 70 years, L = 200 m, simply-supported beam).

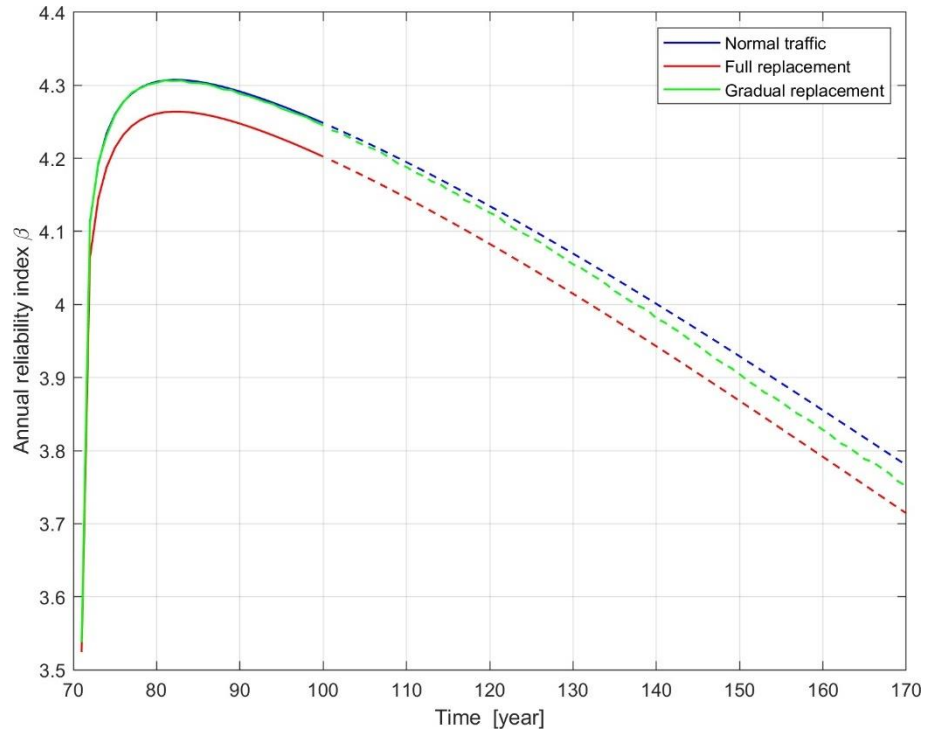


Figure 157: Comparison of annual reliability given different traffic scenarios for the existing structure (elapsed 70 years, L = 200 m, simply-supported beam).



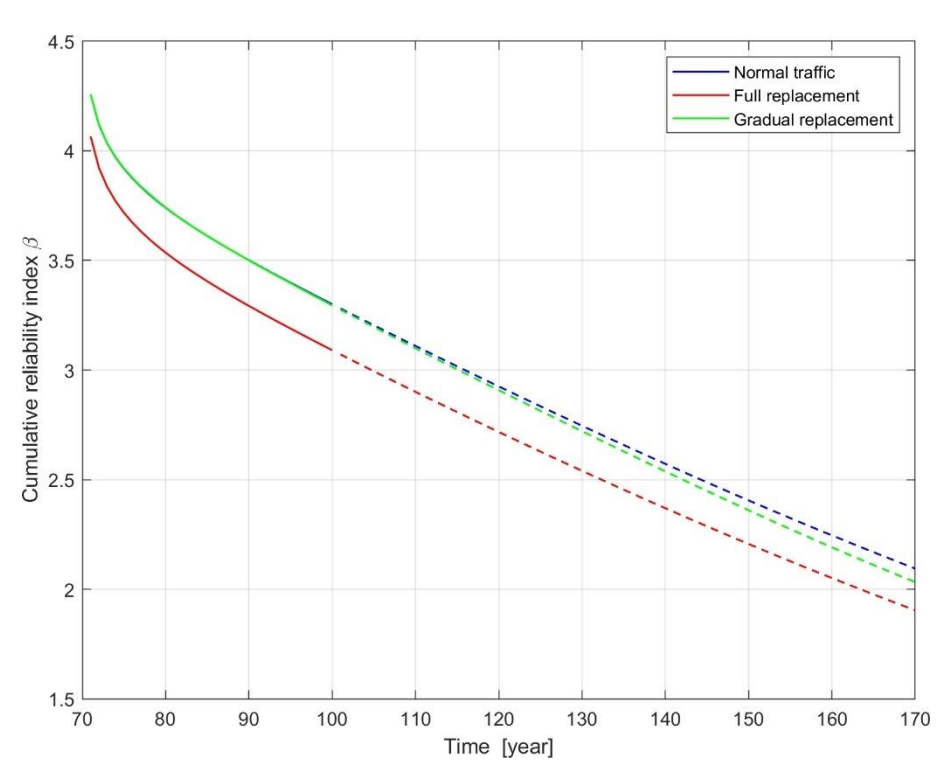


Figure 158: Comparison of cumulative reliability given different traffic scenarios for the existing structure (elapsed 70 years, L = 2.20 m, bending moment, continuous beam).

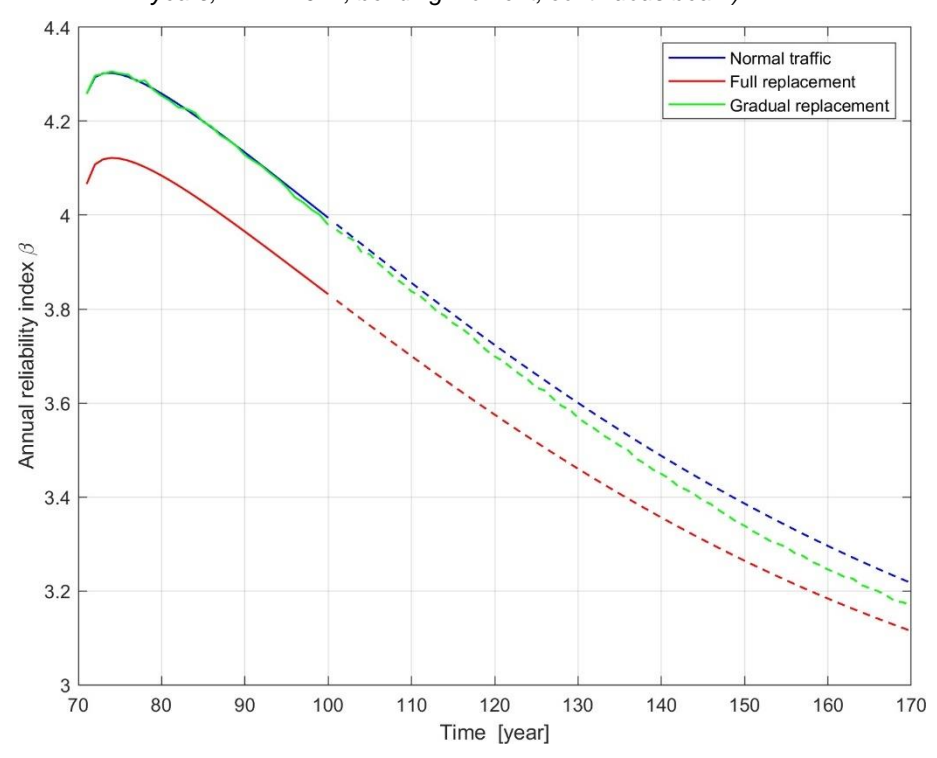


Figure 159: Comparison of annual reliability given different traffic scenarios for the existing structure (elapsed 70 years, L = 2 · 20 m, bending moment, continuous beam).



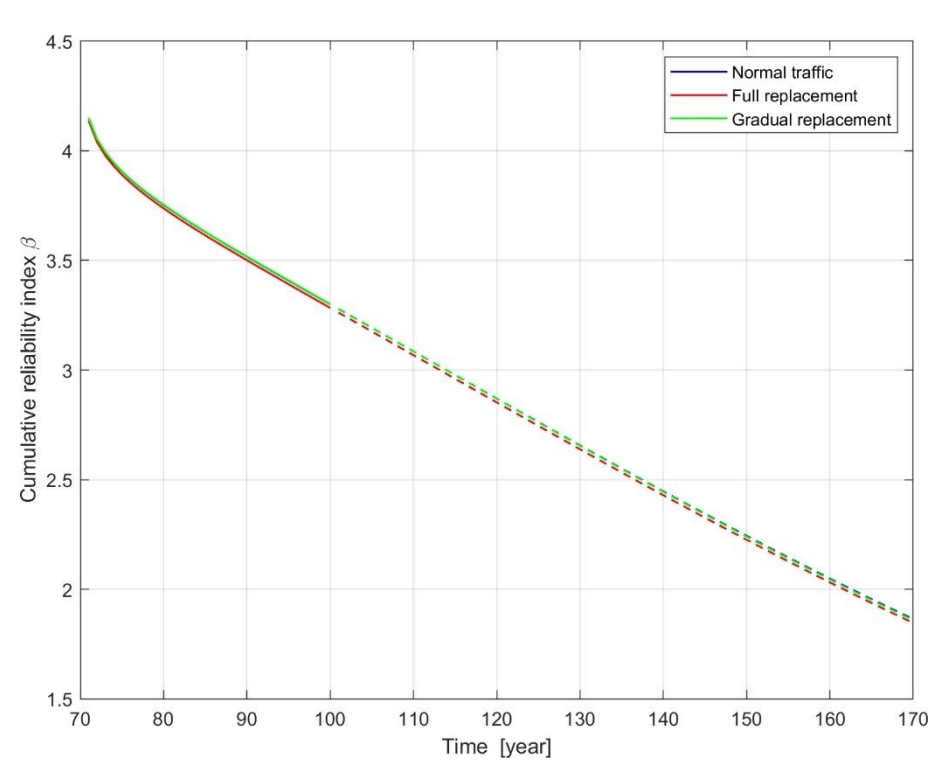


Figure 160: Comparison of cumulative reliability given different traffic scenarios for the existing structure (elapsed 70 years, L = 2.50 m, bending moment, continuous beam).

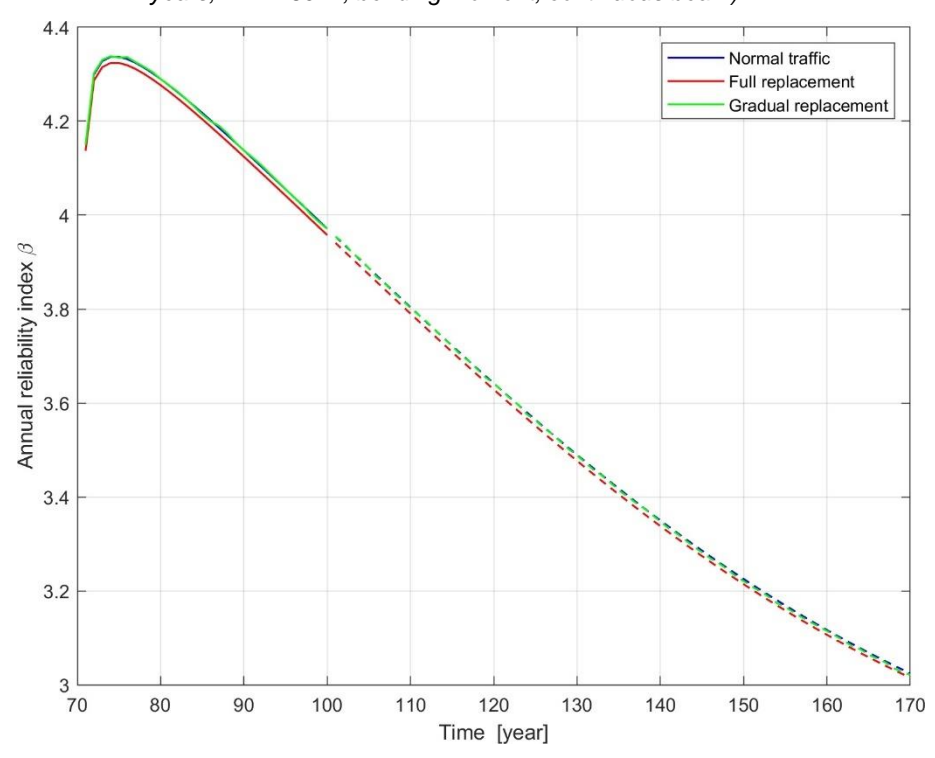


Figure 161: Comparison of annual reliability given different traffic scenarios for the existing structure (elapsed 70 years, L = 2.50 m, bending moment, continuous beam).



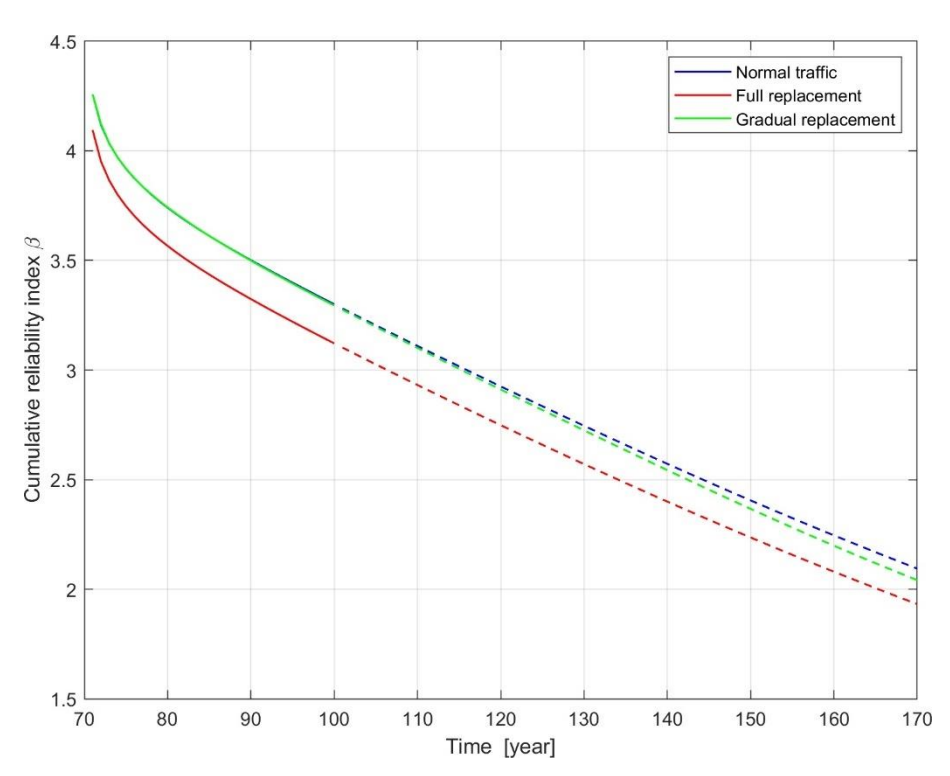


Figure 162: Comparison of cumulative reliability given different traffic scenarios for the existing structure (elapsed 70 years, L = 2.20 m, shear force, continuous beam).

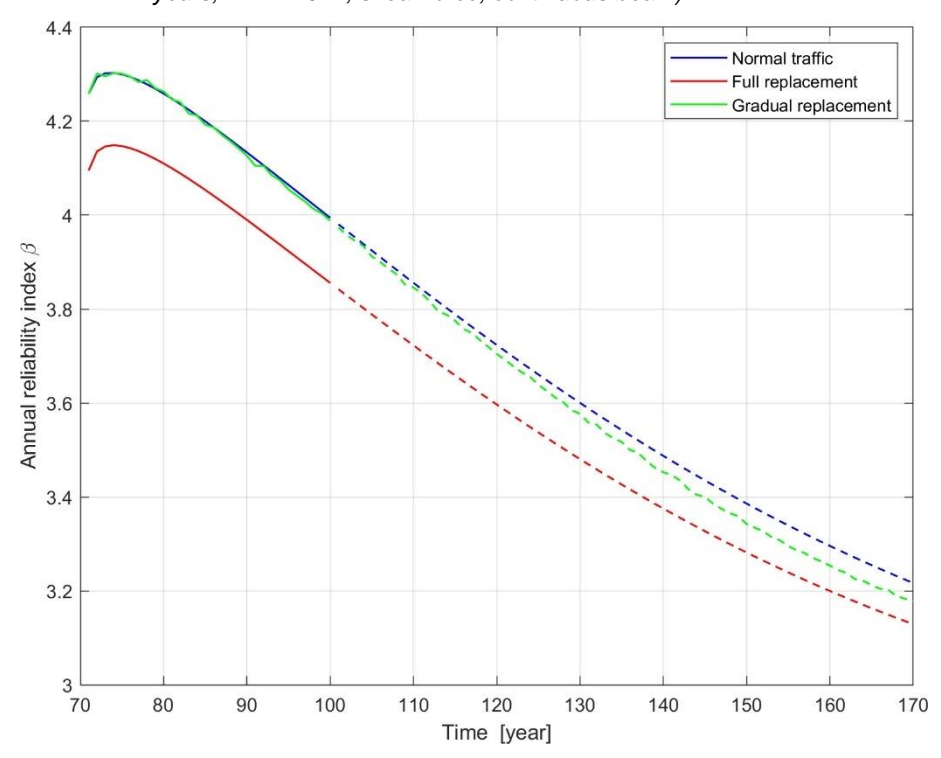


Figure 163: Comparison of annual reliability given different traffic scenarios for the existing structure (elapsed 70 years, L = 2.20 m, shear force, continuous beam).



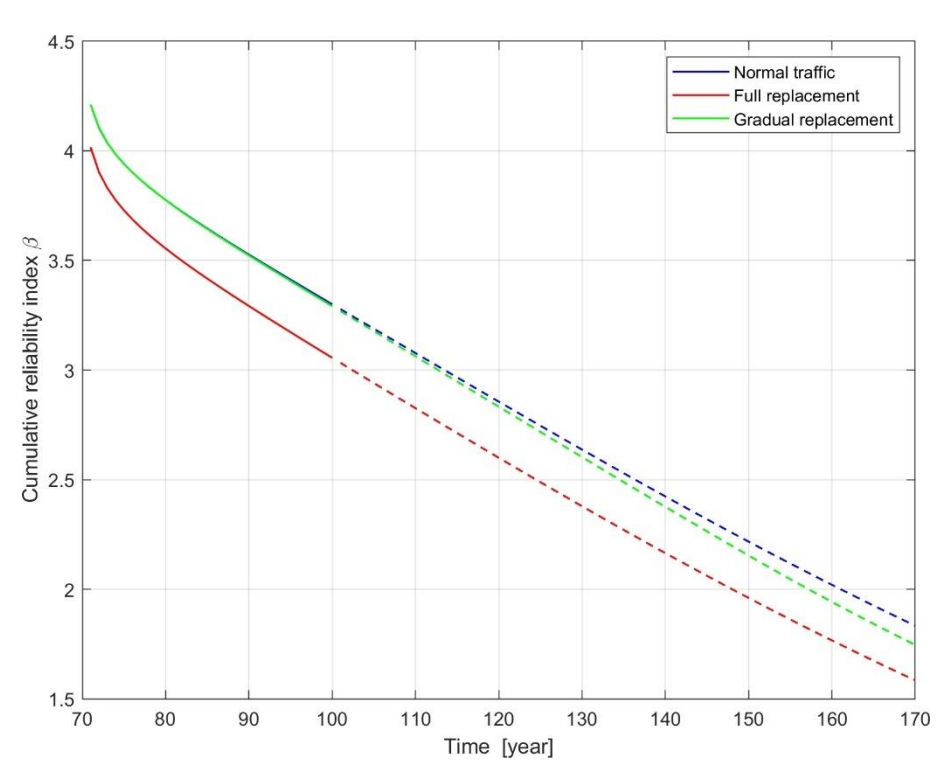


Figure 164: Comparison of cumulative reliability given different traffic scenarios for the existing structure (elapsed 70 years, L = 2.50 m, shear force, continuous beam).

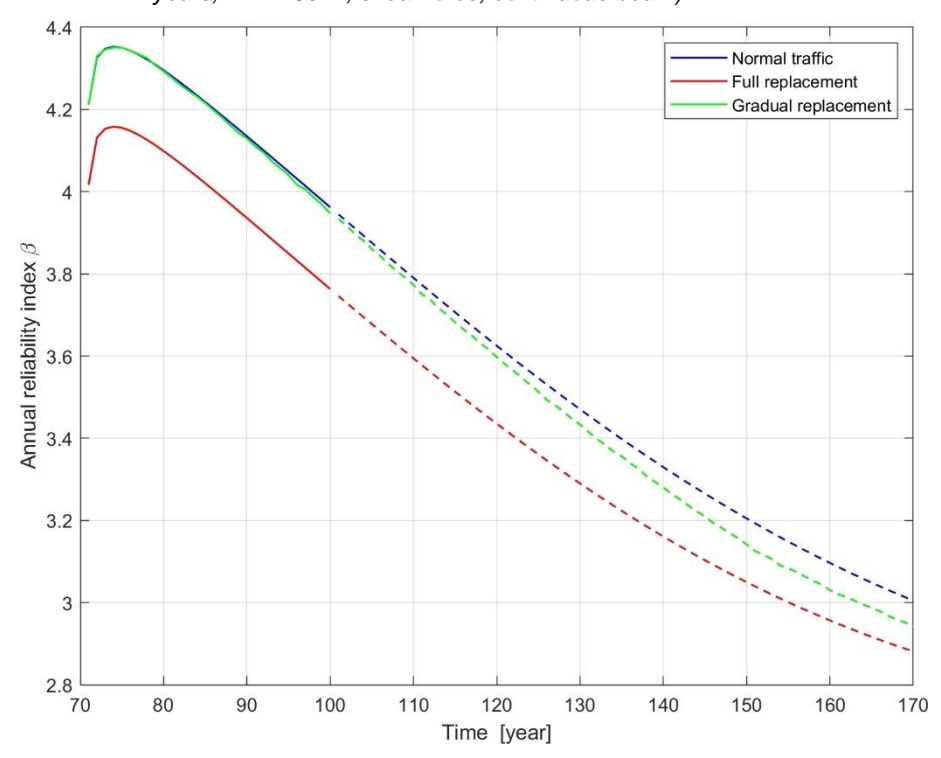


Figure 165: Comparison of annual reliability given different traffic scenarios for the existing structure (elapsed 70 years, L = 2.50 m, shear force, continuous beam).



Appendix 6C Comparison between the reference, full replacement and gradual replacement scenarios based on old Dutch standards

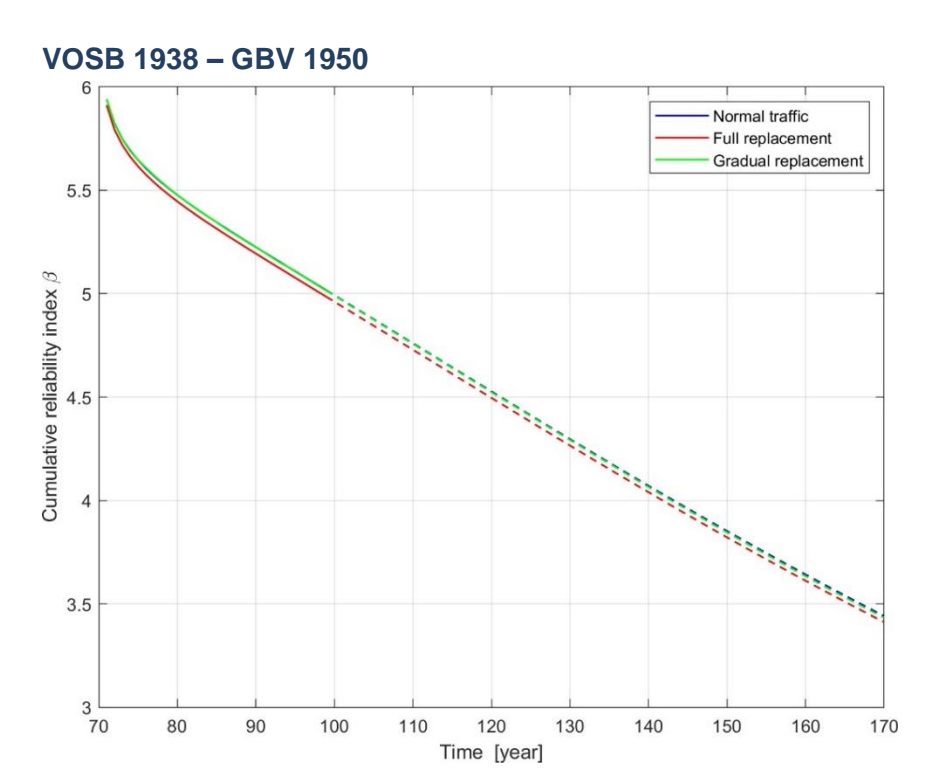


Figure 166: Comparison of cumulative reliability given different traffic scenarios based on the VOSB 1938 – GBV1950 standard(elapsed 70 years, L = 20 m, simply-supported beam).

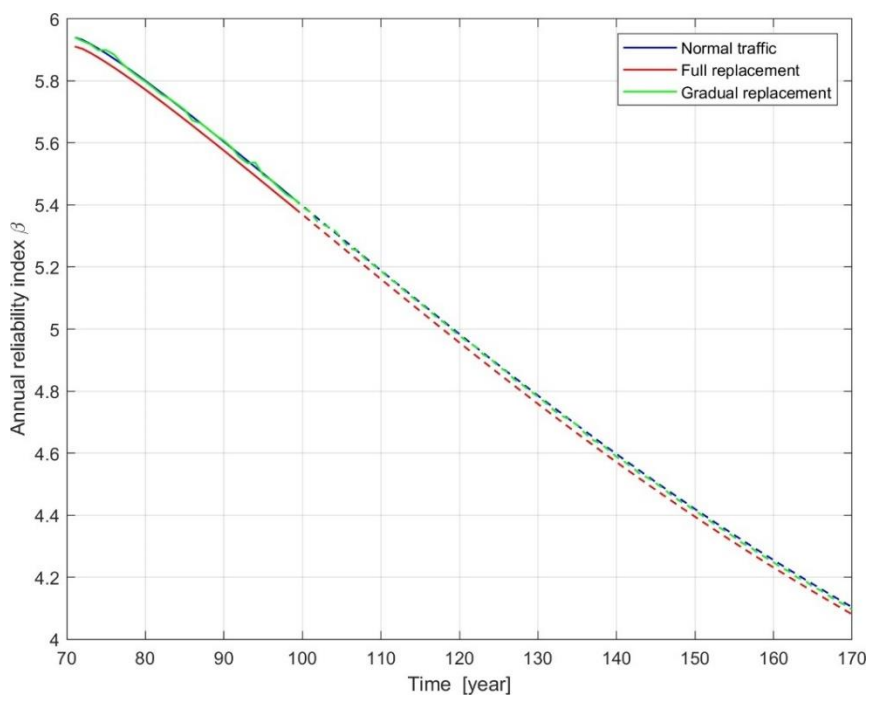


Figure 167: Comparison of annual reliability given different traffic scenarios based on the VOSB 1938 – GBV1950 standard(elapsed 70 years, L = 20 m, simply-supported beam).



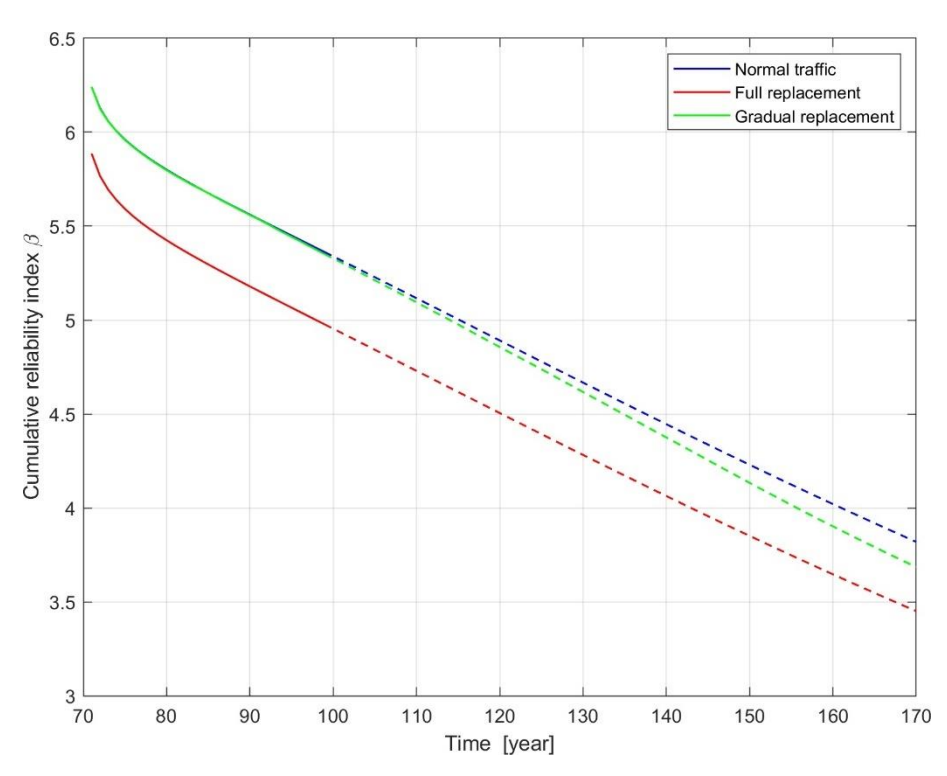


Figure 168: Comparison of cumulative reliability given different traffic scenarios based on the VOSB 1938 – GBV1950 standard(elapsed 70 years, L = 50 m, simply-supported beam).

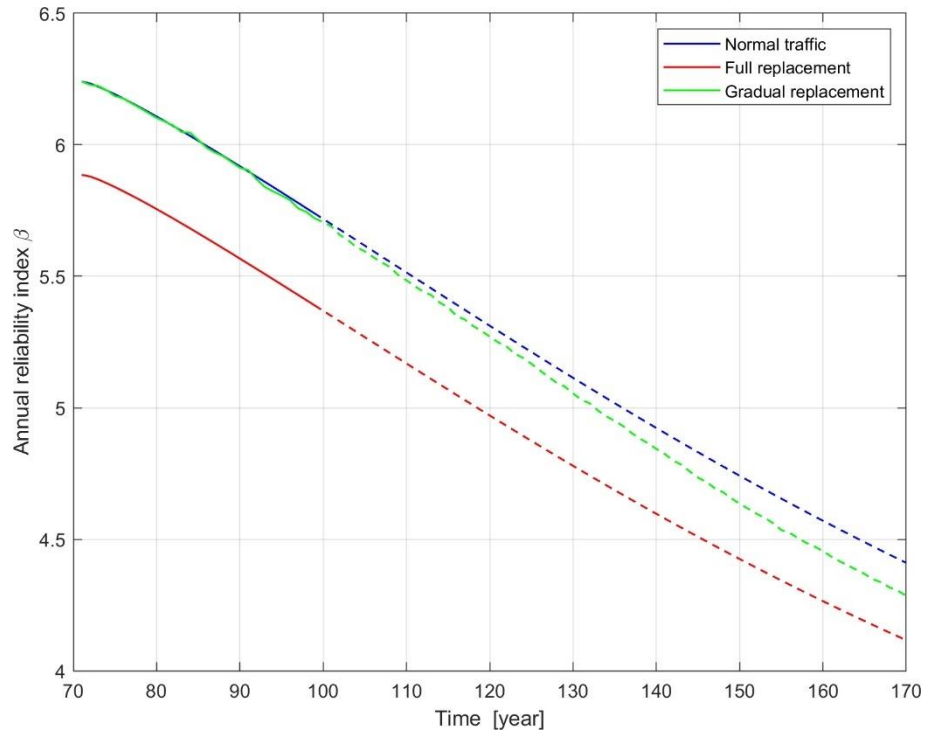


Figure 169: Comparison of annual reliability given different traffic scenarios based on the VOSB 1938 – GBV1950 standard (elapsed 70 years, L = 50 m, simply-supported beam).



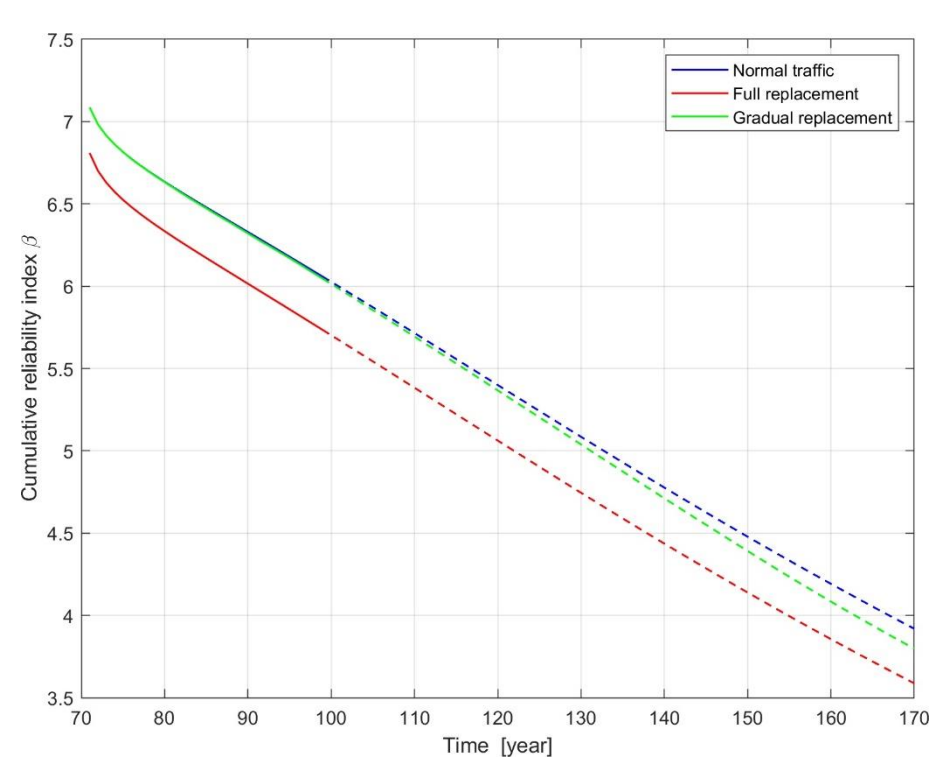


Figure 170: Comparison of cumulative reliability given different traffic scenarios based on the VOSB 1938 – GBV1950 standard (elapsed 70 years, L = 100 m, simply-supported beam).

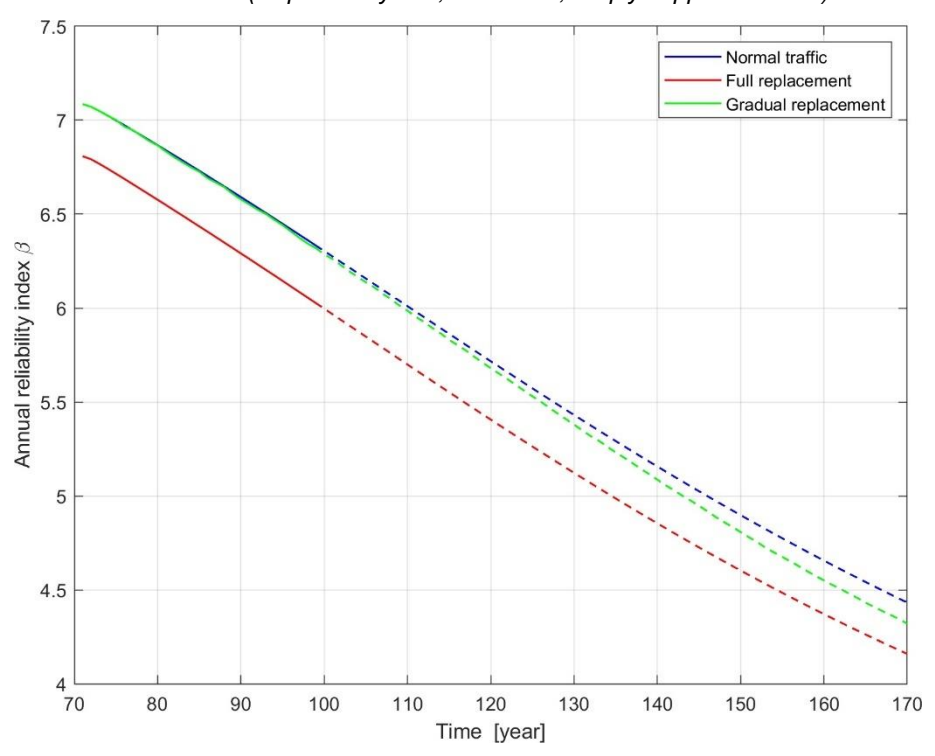


Figure 171: Comparison of annual reliability given different traffic scenarios based on the VOSB 1938 – GBV1950 standard (elapsed 70 years, L = 100 m, simply-supported beam).



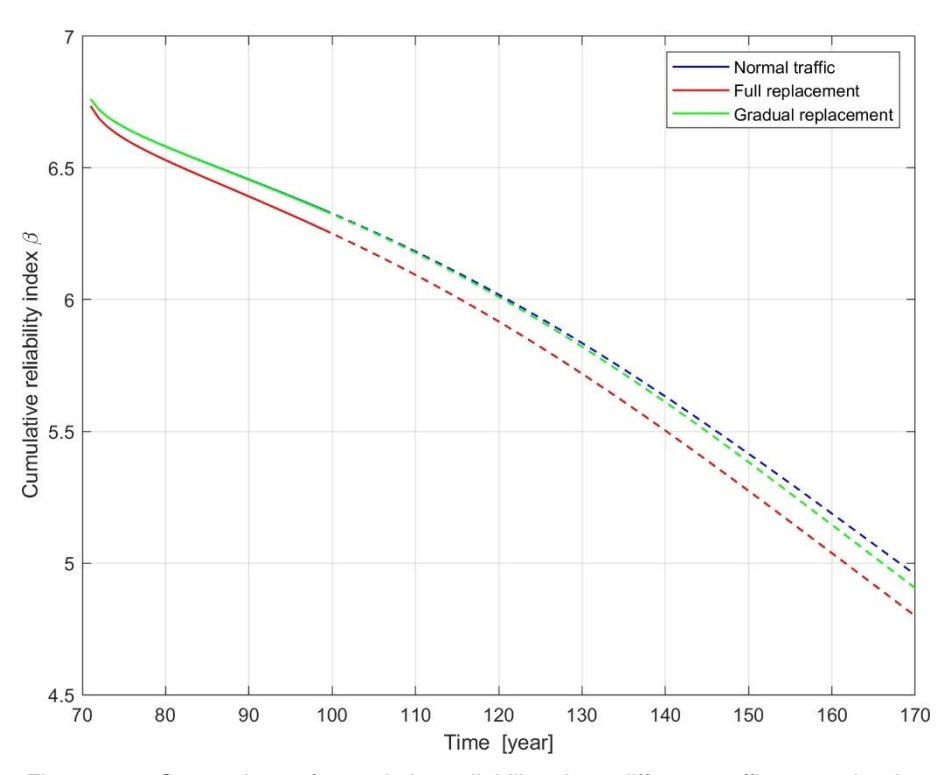


Figure 172: Comparison of cumulative reliability given different traffic scenarios based on the VOSB 1938 – GBV1950 standard (elapsed 70 years, L = 200 m, simply-supported beam).

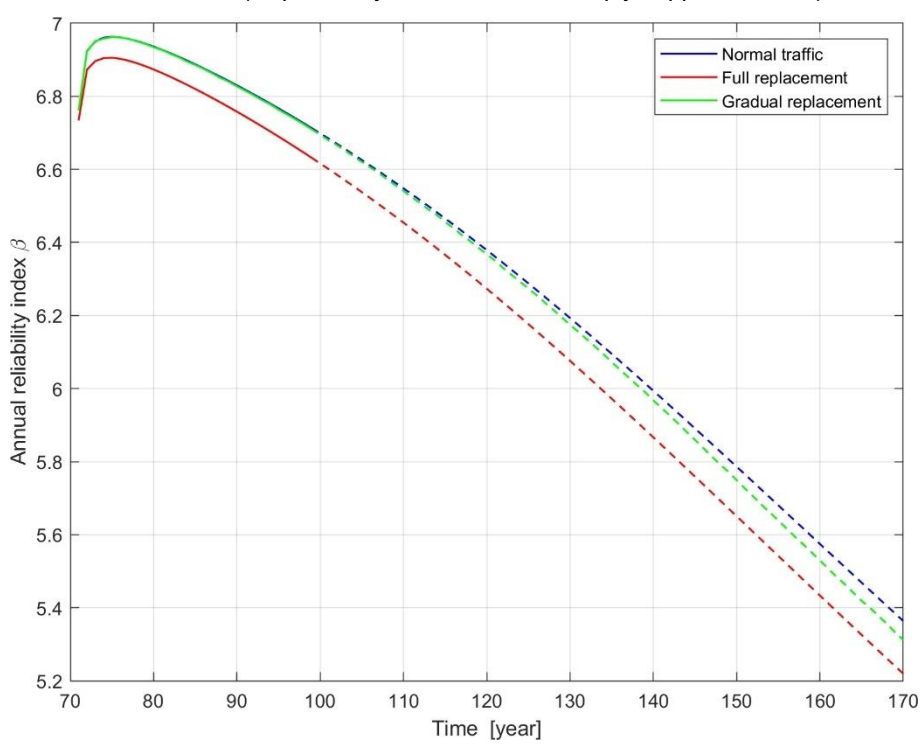


Figure 173: Comparison of annual reliability given different traffic scenarios based on the VOSB 1938 – GBV1950 standard (elapsed 70 years, L = 200 m, simply-supported beam).



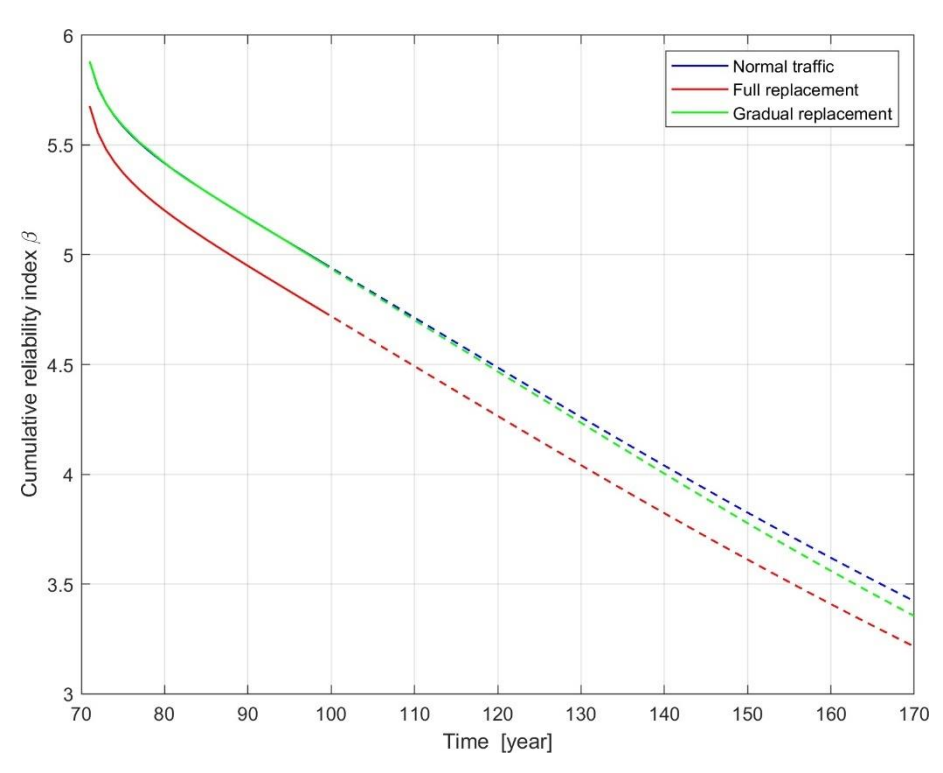


Figure 174: Comparison of cumulative reliability given different traffic scenarios based on the VOSB 1938 – GBV1950 standard (elapsed 70 years, L = 2 · 20 m, bending moment, continuous beam).

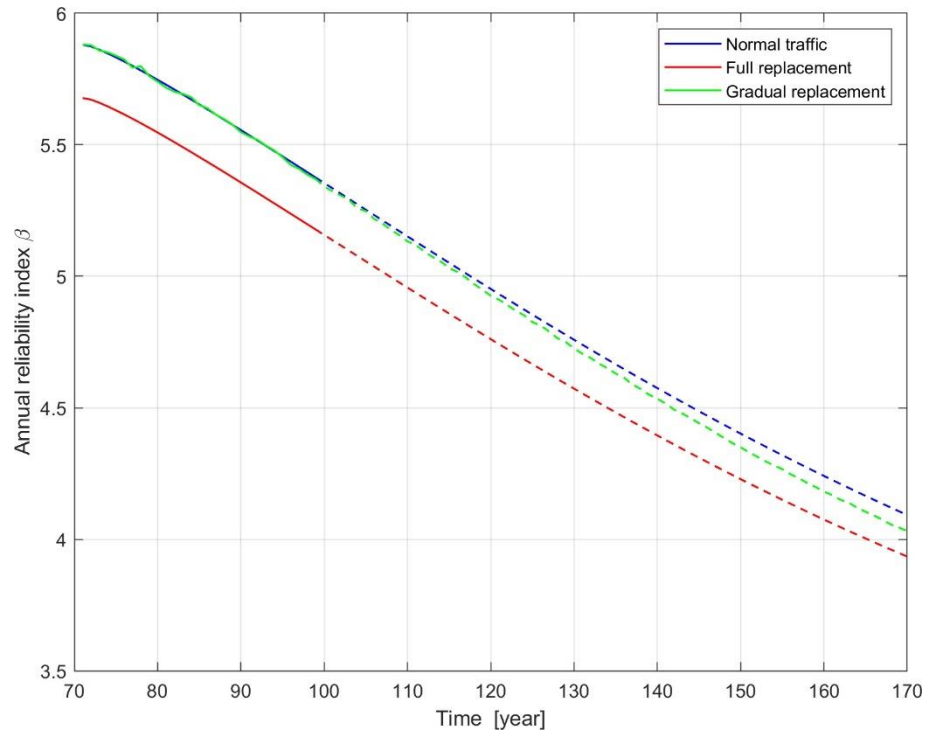


Figure 175: Comparison of annual reliability given different traffic scenarios based on the VOSB 1938 – GBV1950 standard (elapsed 70 years, L = 2.20 m, bending moment, continuous beam).



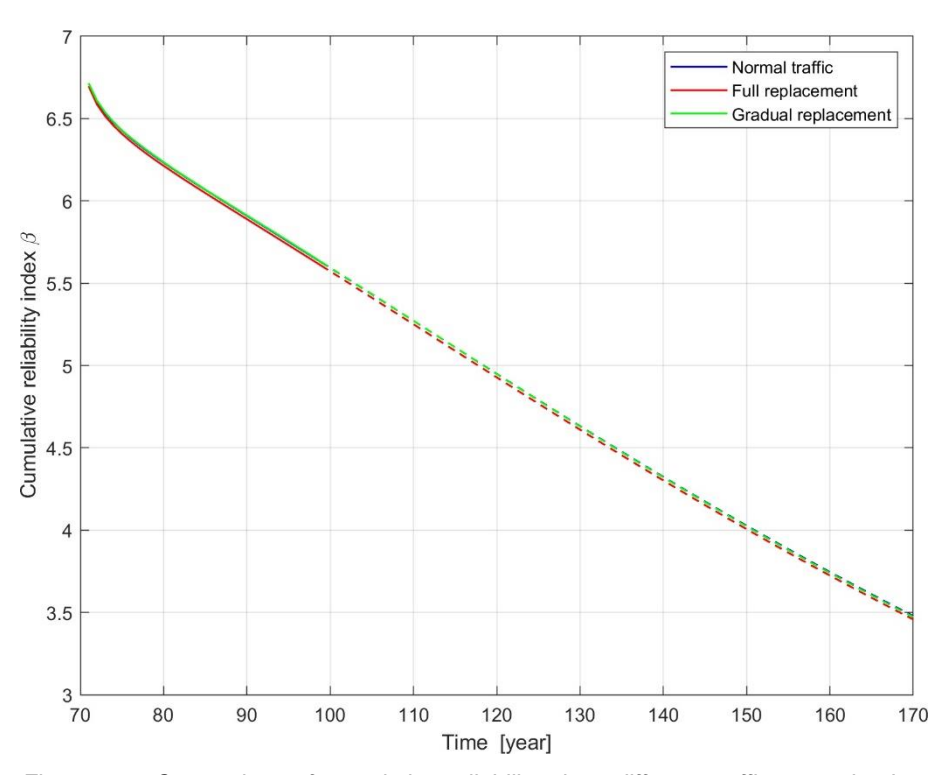


Figure 176: Comparison of cumulative reliability given different traffic scenarios based on the VOSB 1938 – GBV1950 standard (elapsed 70 years, L = 2 · 50 m, bending moment, continuous beam).

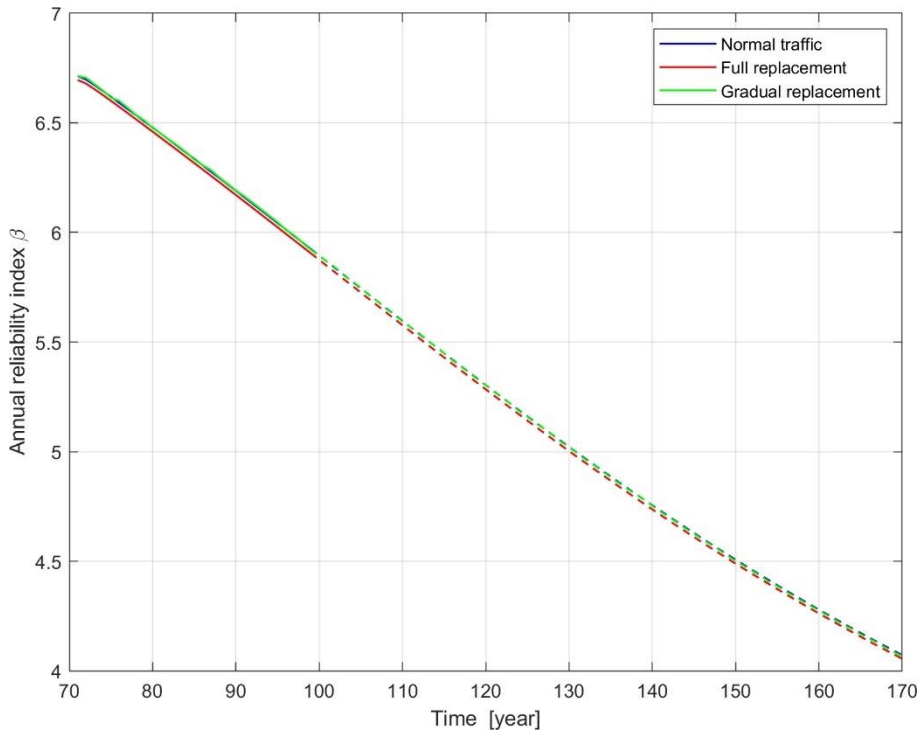


Figure 177: Comparison of annual reliability given different traffic scenarios based on the VOSB 1938 – GBV1950 standard (elapsed 70 years, L = 2.50 m, bending moment, continuous beam).



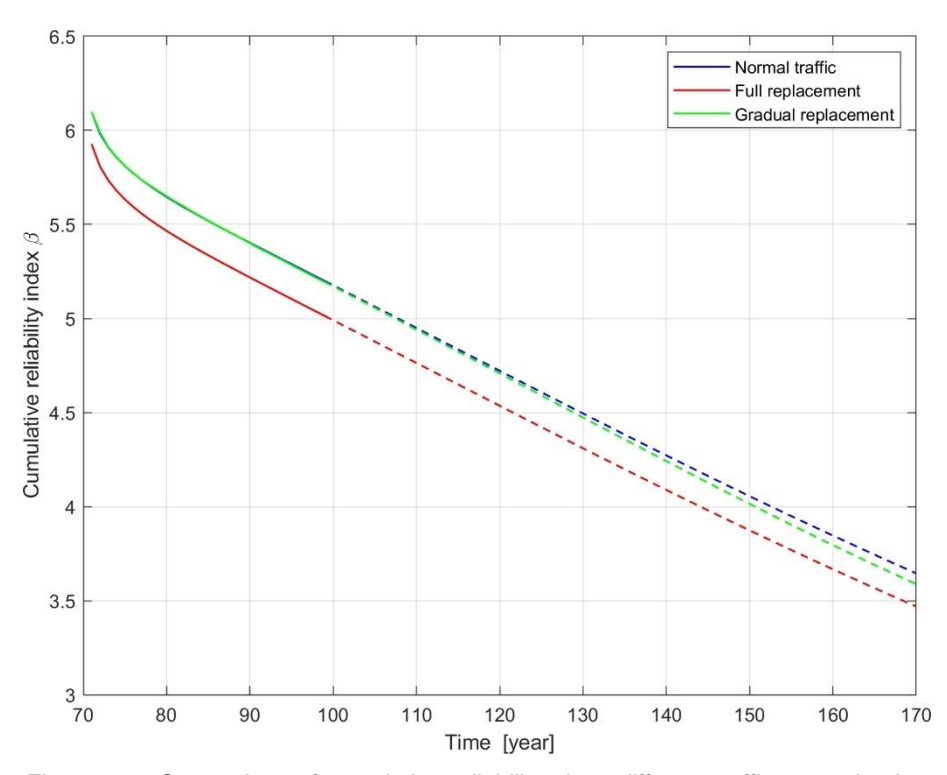


Figure 178: Comparison of cumulative reliability given different traffic scenarios based on the VOSB 1938 – GBV1950 standard (elapsed 70 years, L = 2 · 20 m, shear force, continuous beam).

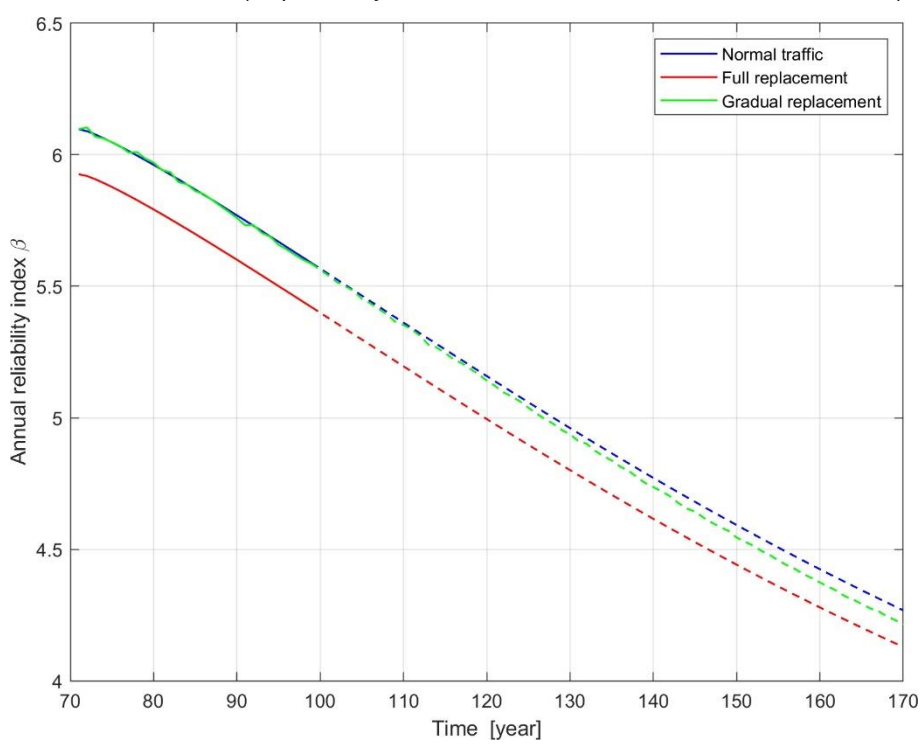


Figure 179: Comparison of annual reliability given different traffic scenarios based on the VOSB 1938 – GBV1950 standard (elapsed 70 years, L = 2.20 m, shear force, continuous beam).



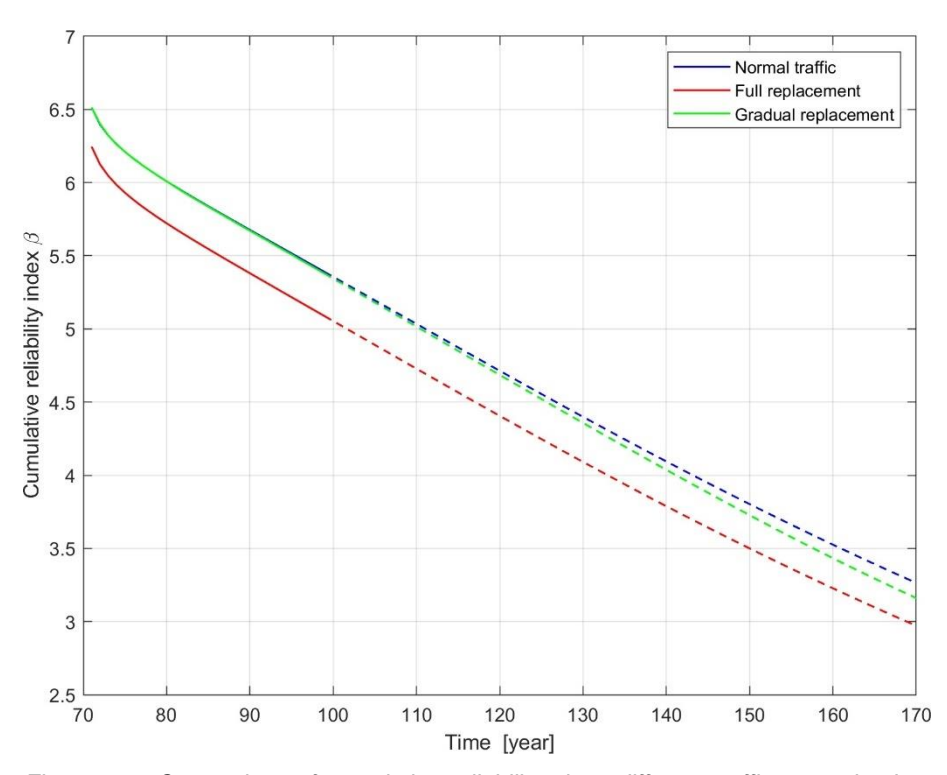


Figure 180: Comparison of cumulative reliability given different traffic scenarios based on the VOSB 1938 – GBV1950 standard (elapsed 70 years, L = 2.50 m, shear force, continuous beam).

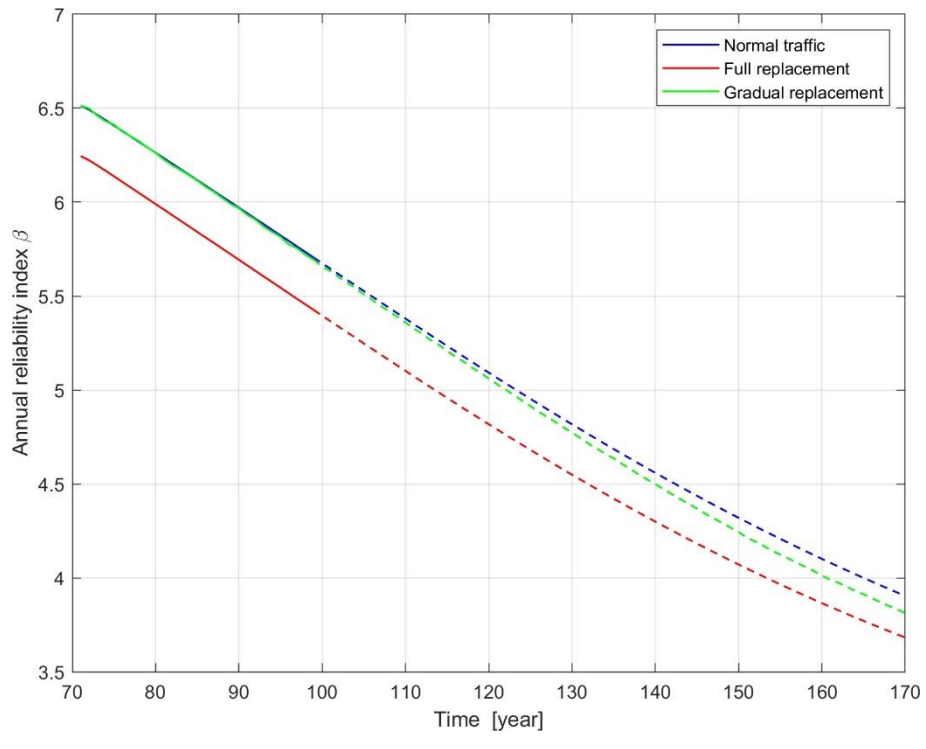


Figure 181: Comparison of annual reliability given different traffic scenarios based on the VOSB 1938 – GBV 1950 standard (elapsed 70 years, L = 2.50 m, shear force, continuous beam).



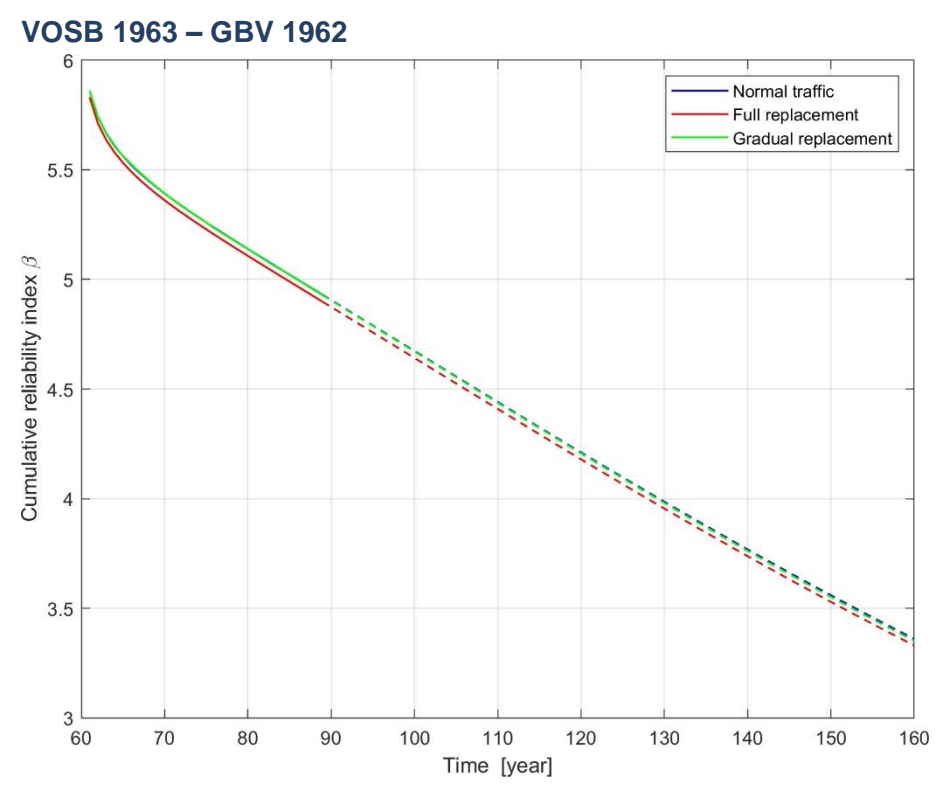


Figure 182: Comparison of cumulative reliability given different traffic scenarios based on the VOSB 1963 – GBV 1961 standard (elapsed 60 years, L = 20 m, simply-supported beam).

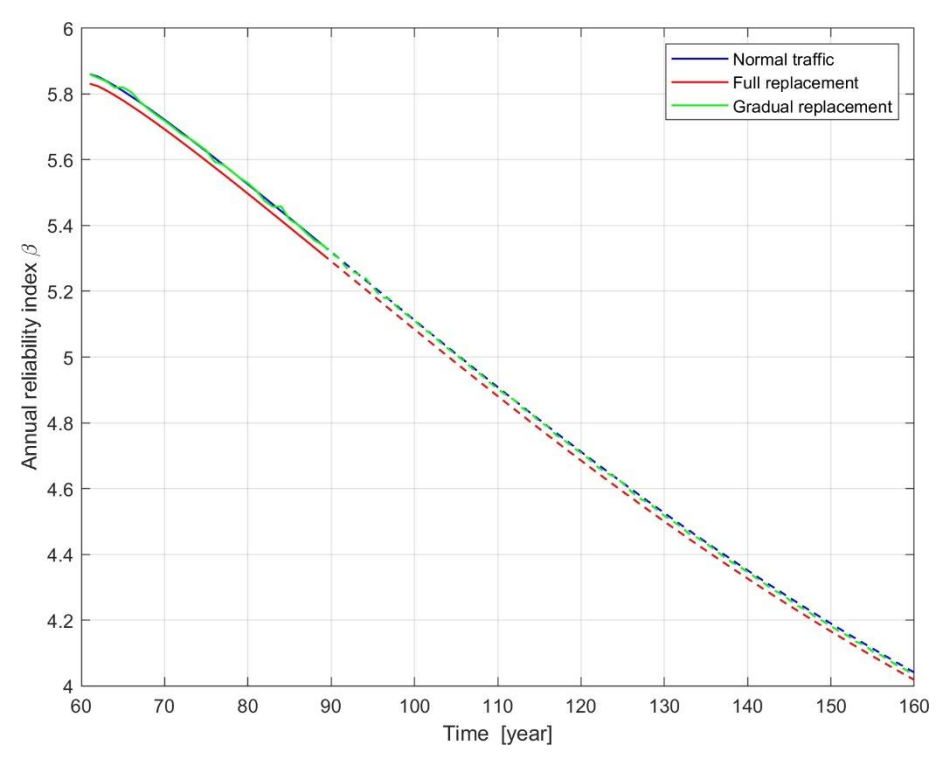


Figure 183: Comparison of annual reliability given different traffic scenarios based on the VOSB 1963 – GBV 1961 standard (elapsed 60 years, L = 20 m, simply-supported beam).



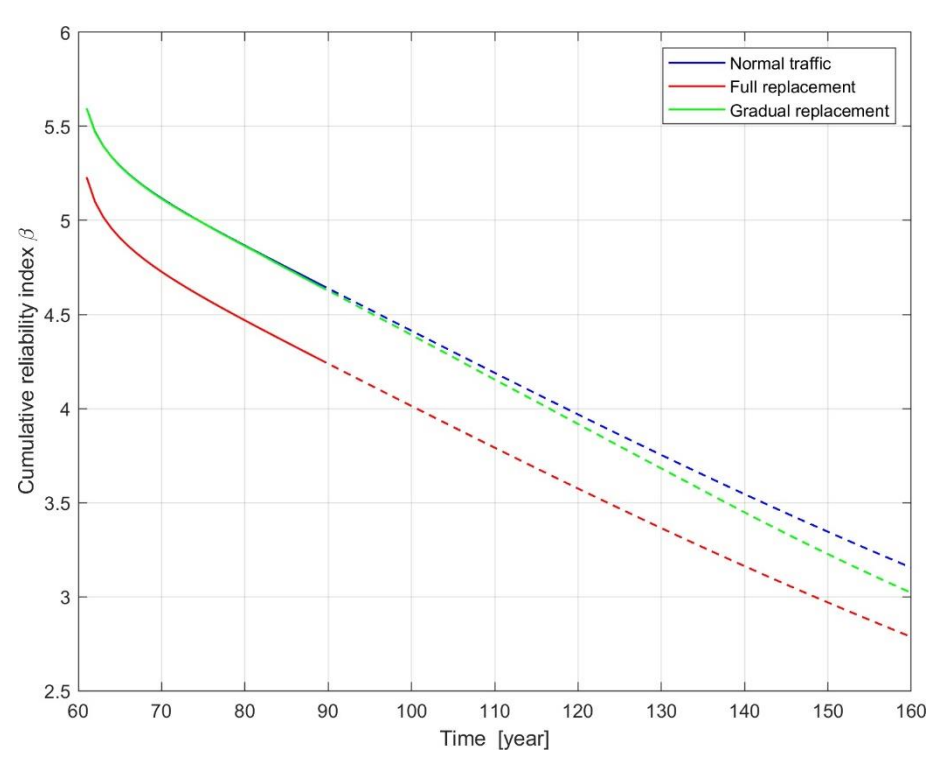


Figure 184: Comparison of cumulative reliability given different traffic scenarios based on the VOSB 1963 – GBV 1961 standard (elapsed 60 years, L = 50 m, simply-supported beam).

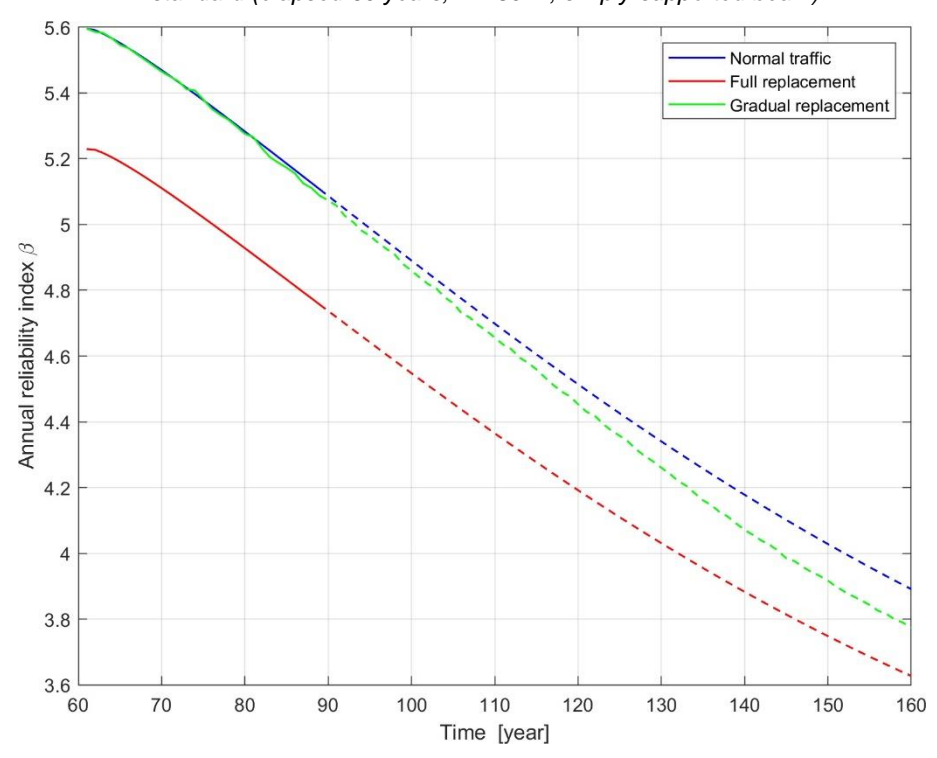


Figure 185: Comparison of annual reliability given different traffic scenarios based on the VOSB 1963 – GBV 1961 standard (elapsed 60 years, L = 50 m, simply-supported beam).



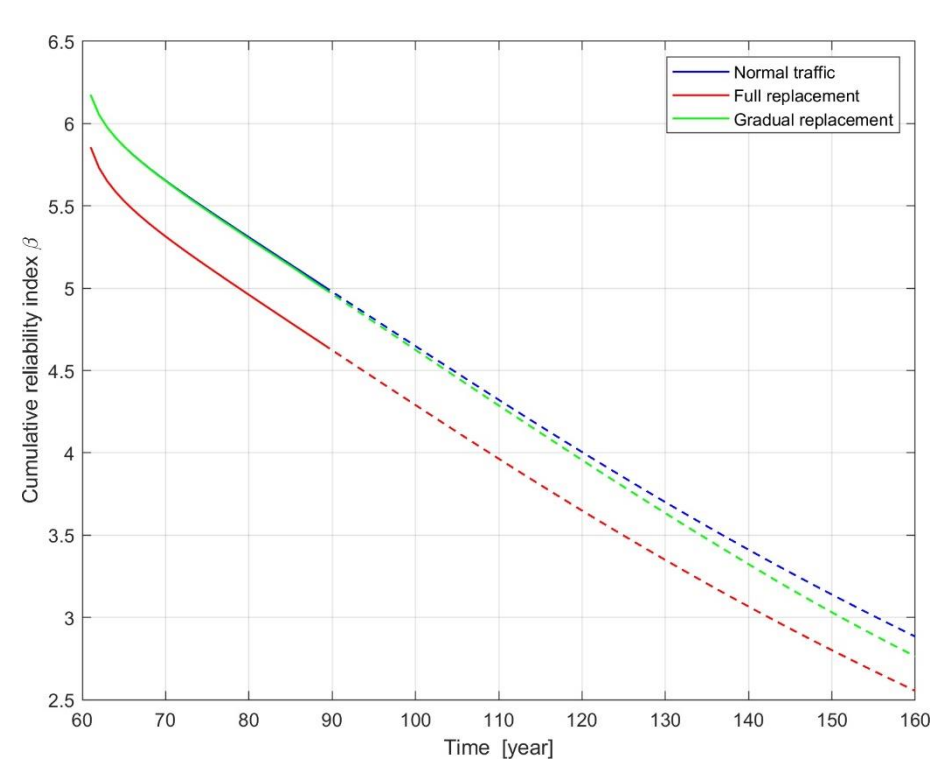


Figure 186: Comparison of cumulative reliability given different traffic scenarios based on the VOSB 1963 – GBV 1961 standard (elapsed 60 years, L = 100 m, simply-supported beam).

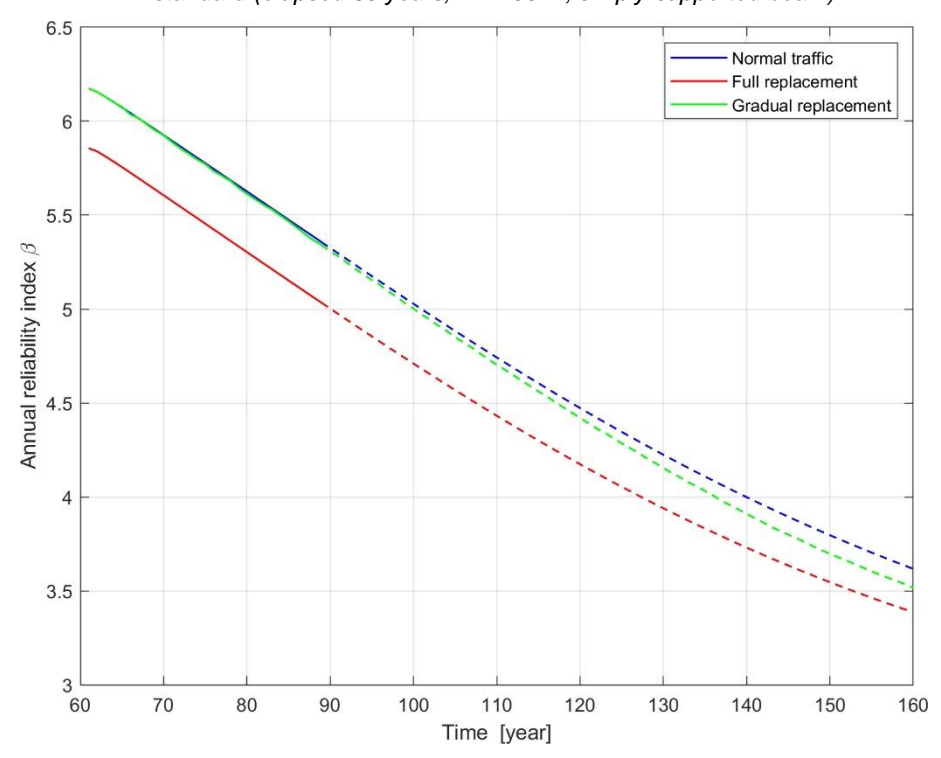


Figure 187: Comparison of annual reliability given different traffic scenarios based on the VOSB 1963 – GBV 1961 standard (elapsed 60 years, L = 100 m, simply-supported beam).



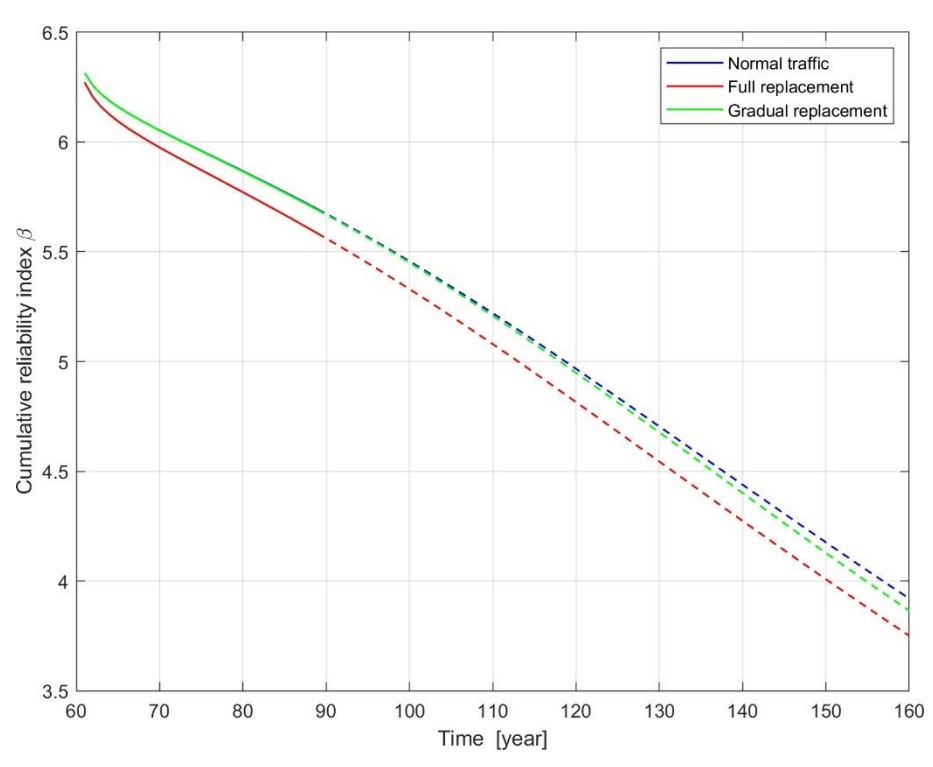


Figure 188: Comparison of cumulative reliability given different traffic scenarios based on the VOSB 1963 – GBV 1961 standard (elapsed 60 years, L = 200 m, simply-supported beam).

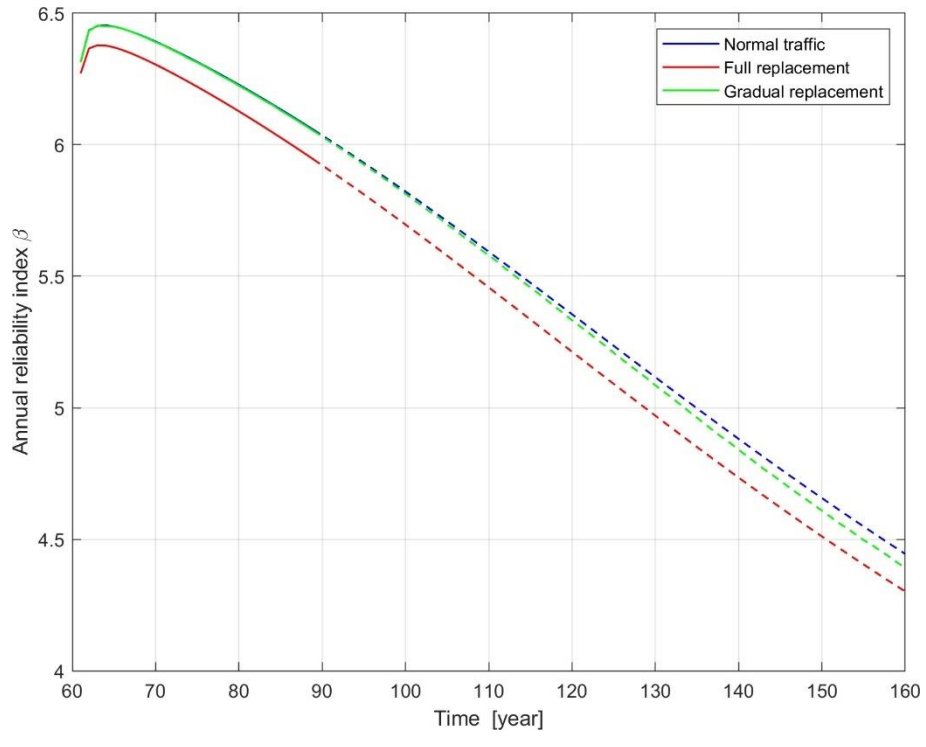


Figure 189: Comparison of annual reliability given different traffic scenarios based on the VOSB 1963 – GBV 1961 standard (elapsed 60 years, L = 200 m, simply-supported beam).



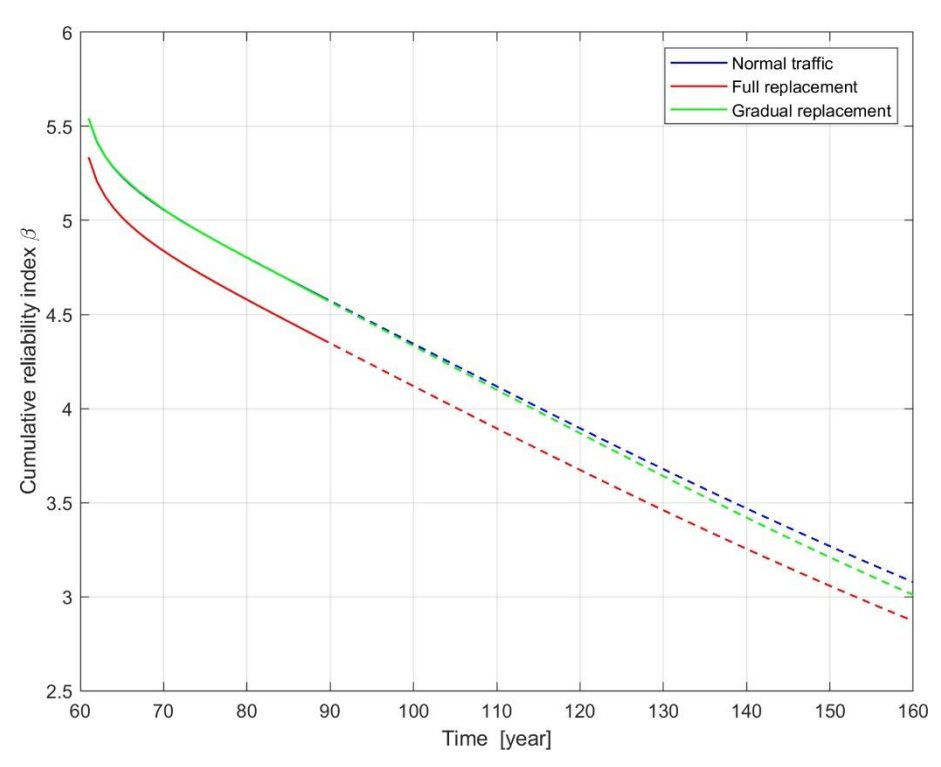


Figure 190: Comparison of cumulative reliability given different traffic scenarios based on the VOSB 1963 – GBV 1961 standard (elapsed 60 years, L = 2 · 20 m, bending moment, continuous beam).

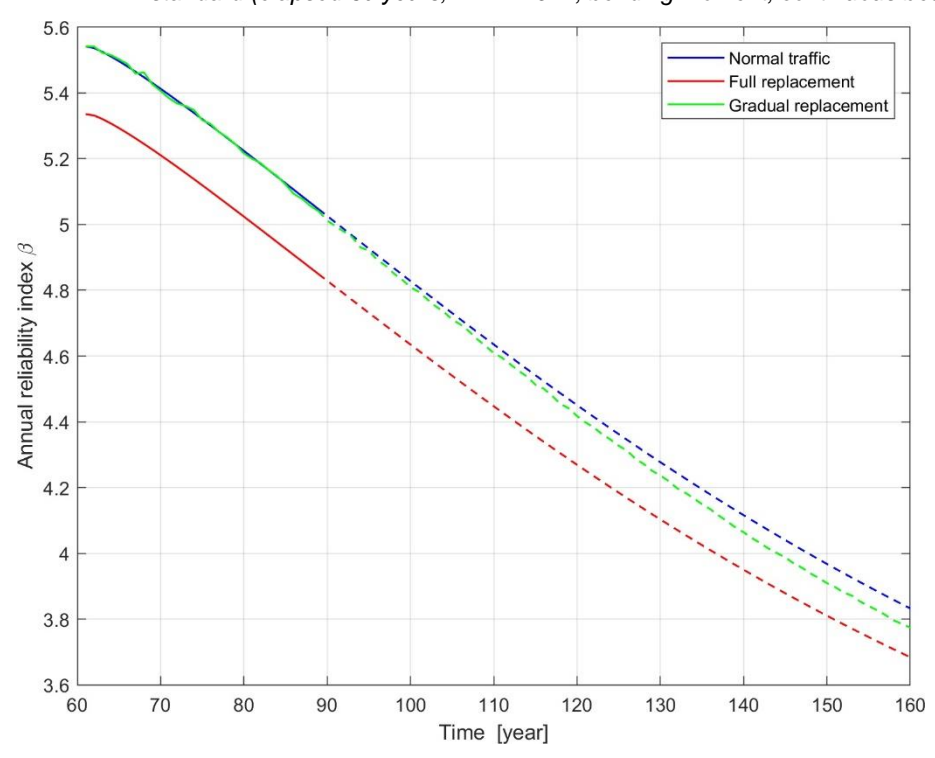


Figure 191: Comparison of annual reliability given different traffic scenarios based on the VOSB 1963 – GBV 1961 standard (elapsed 60 years, L = 2 · 20 m, bending moment, continuous beam).



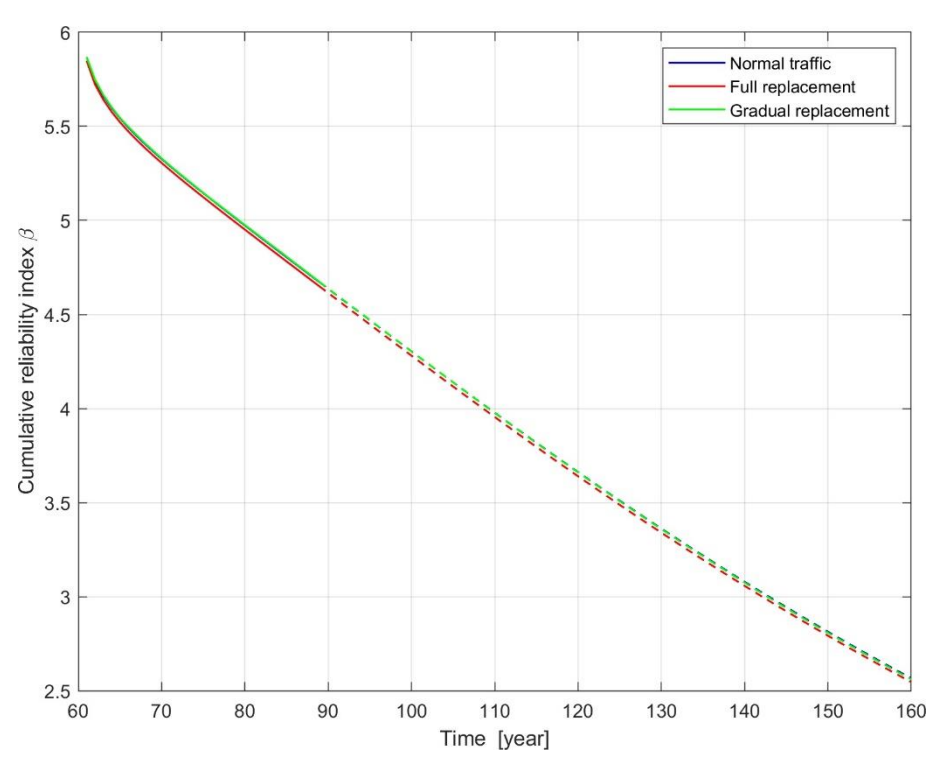


Figure 192: Comparison of cumulative reliability given different traffic scenarios based on the VOSB 1963 – GBV 1961 standard (elapsed 60 years, L = 2 · 50 m, bending moment, continuous beam).

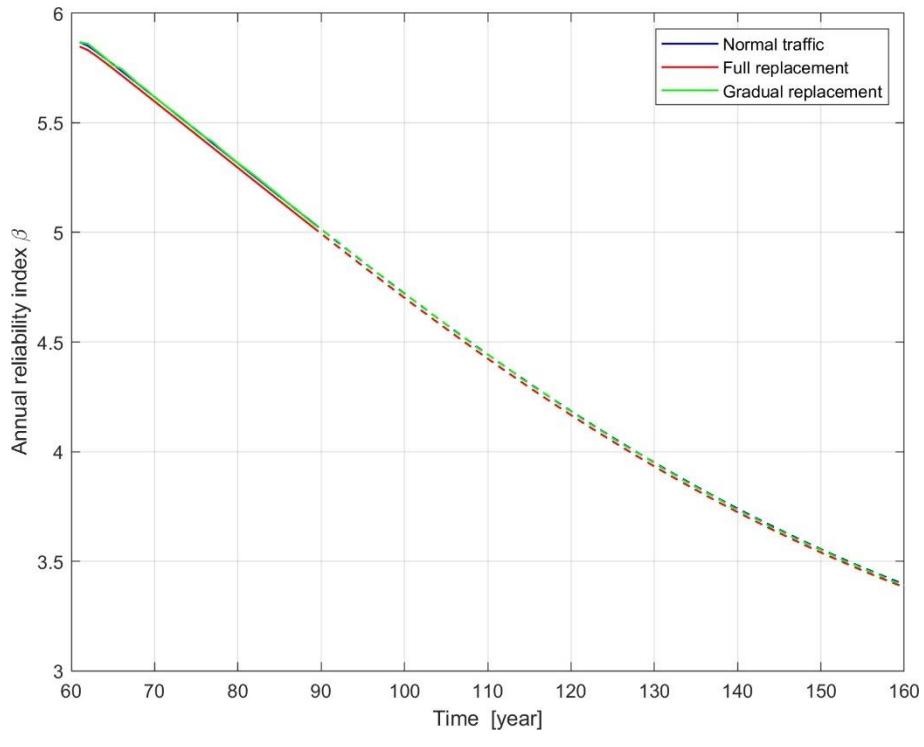


Figure 193: Comparison of annual reliability given different traffic scenarios based on the VOSB 1963 – GBV 1961 standard (elapsed 60 years, L = 2 · 50 m, bending moment, continuous beam).



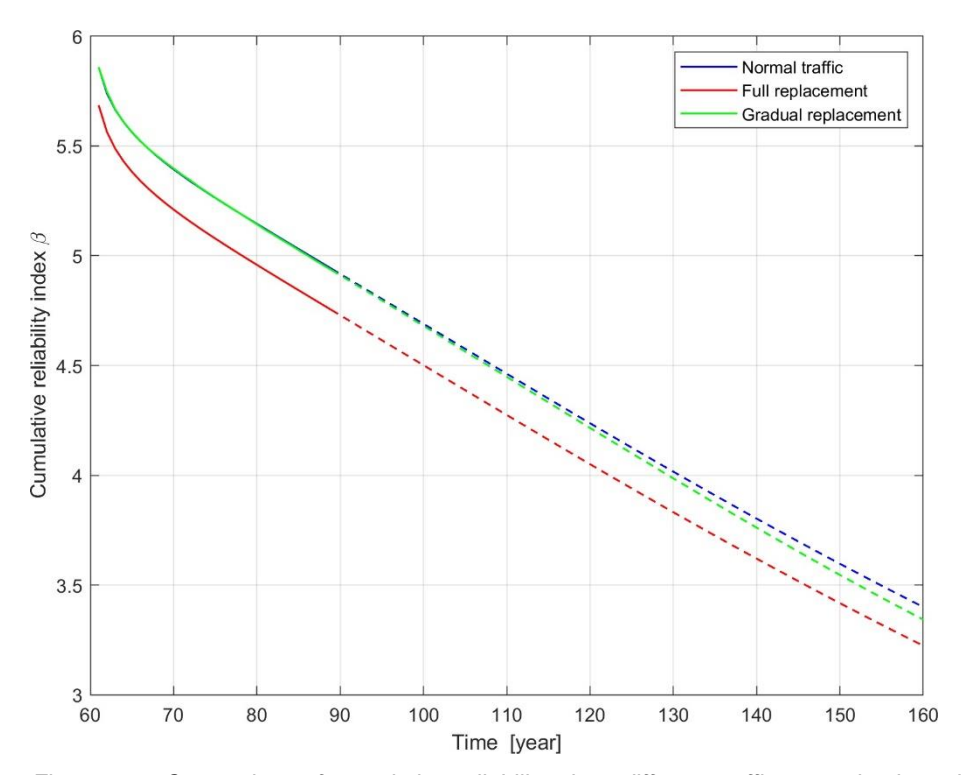


Figure 194: Comparison of cumulative reliability given different traffic scenarios based on the VOSB 1963 – GBV 1961 standard (elapsed 60 years, L = 2 · 20 m, shear force, continuous beam).

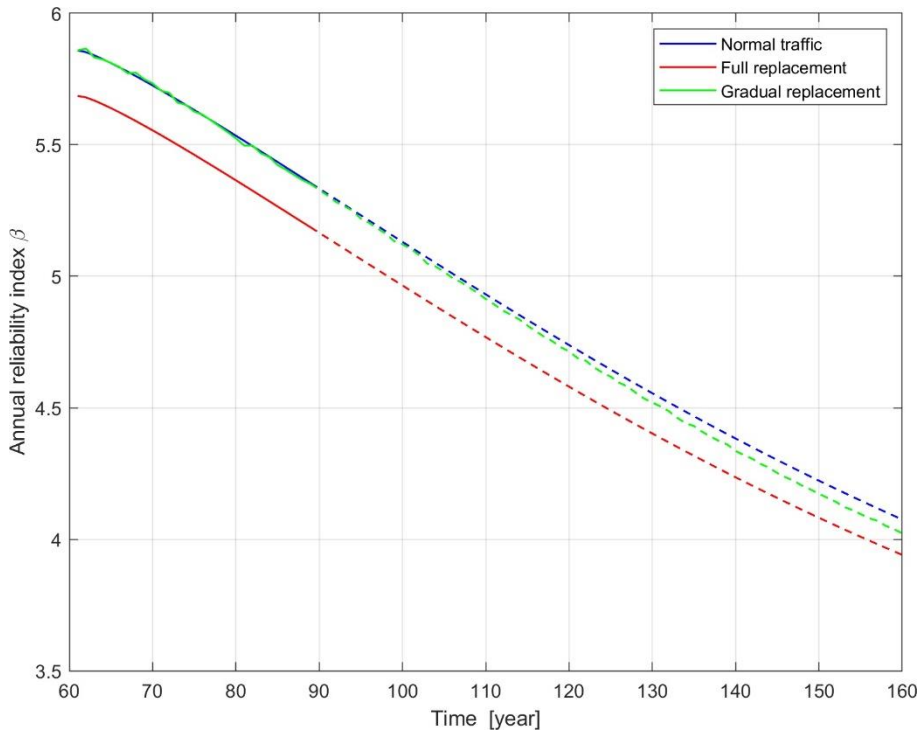


Figure 195: Comparison of annual reliability given different traffic scenarios based on the VOSB 1963 – GBV 1961 standard (elapsed 60 years, L = 2 · 20 m, shear force, continuous beam).



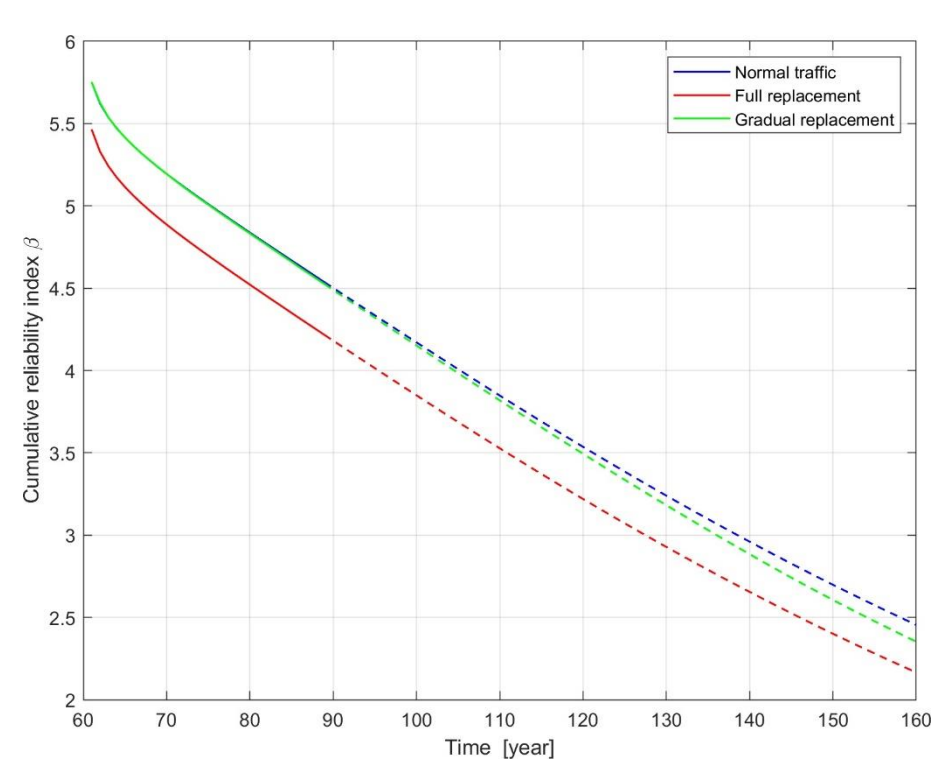


Figure 196: Comparison of cumulative reliability given different traffic scenarios based on the VOSB 1963 – GBV 1961 standard (elapsed 60 years, L = 2 ·50 m, shear force, continuous beam).

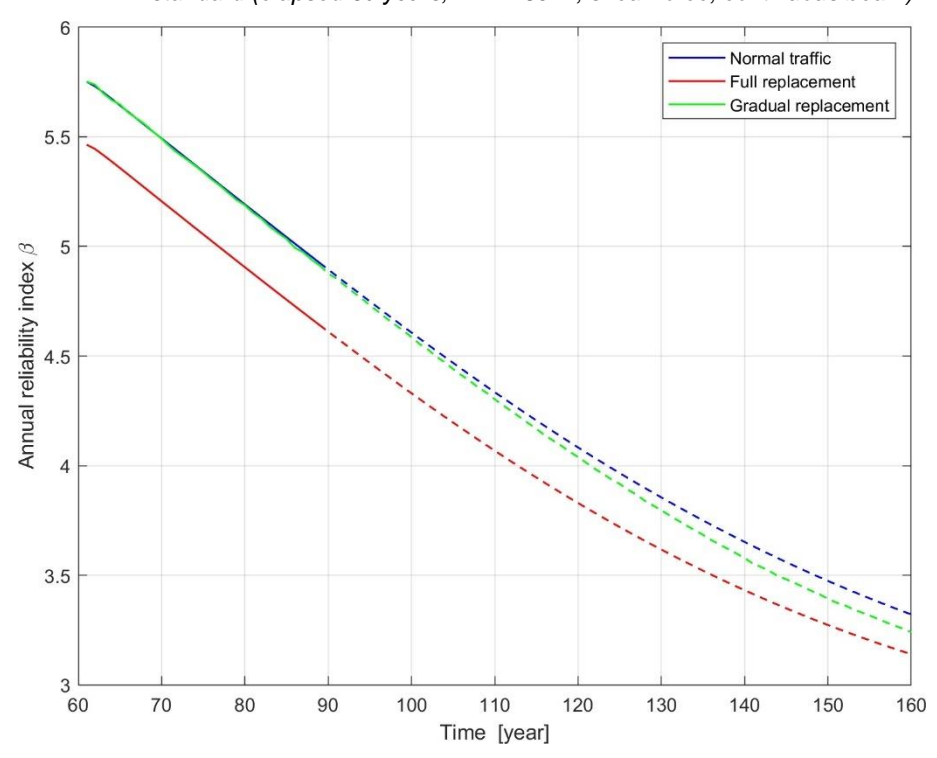


Figure 197: Comparison of annual reliability given different traffic scenarios based on the VOSB 1963 – GBV 1961 standard (elapsed 60 years, L = 2.50 m, shear force, continuous beam).



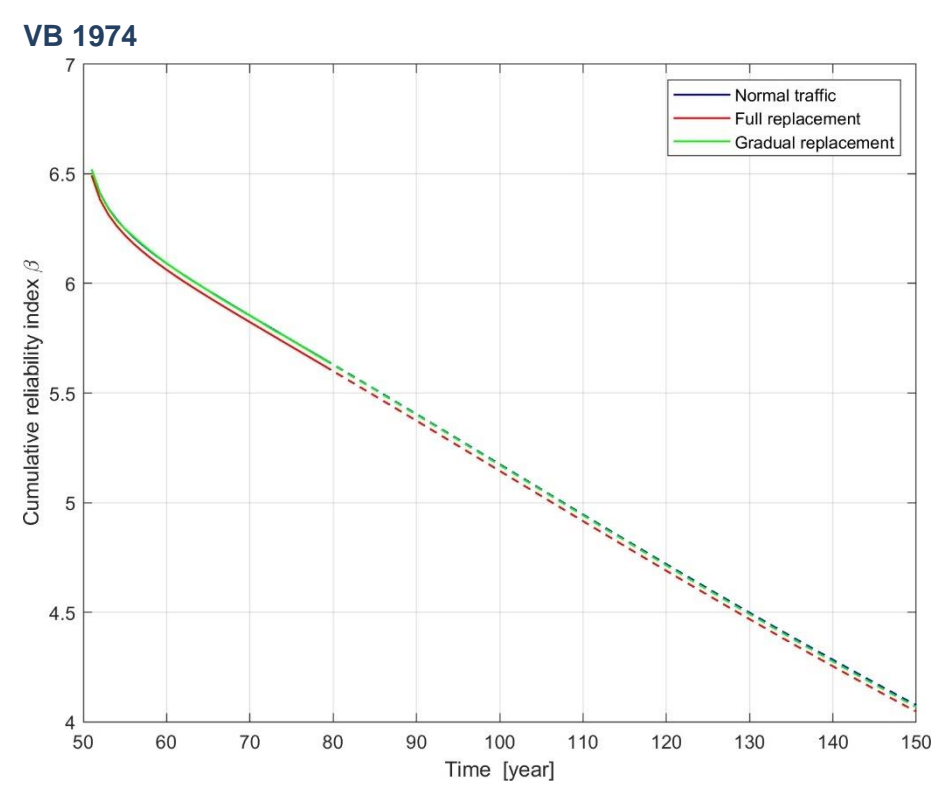


Figure 198: Comparison of cumulative reliability given different traffic scenarios based on the VB 1974 standard (elapsed 50 years, L = 20 m, simply-supported beam).

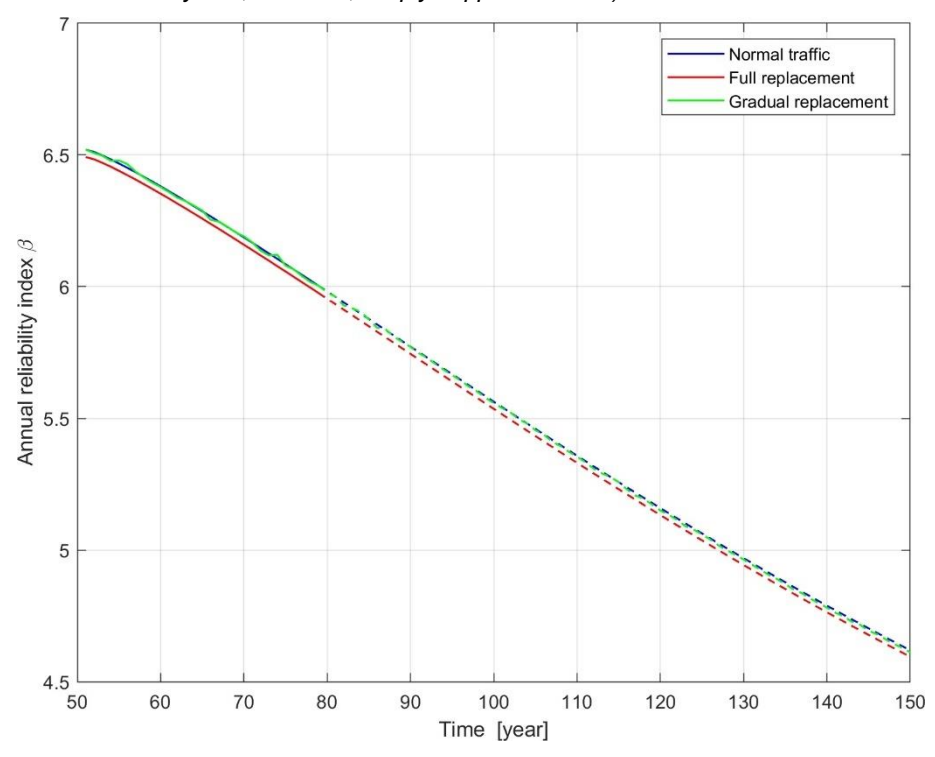


Figure 199: Comparison of annual reliability given different traffic scenarios based on the VB 1974 standard (elapsed 50 years, L = 20 m, simply-supported beam).



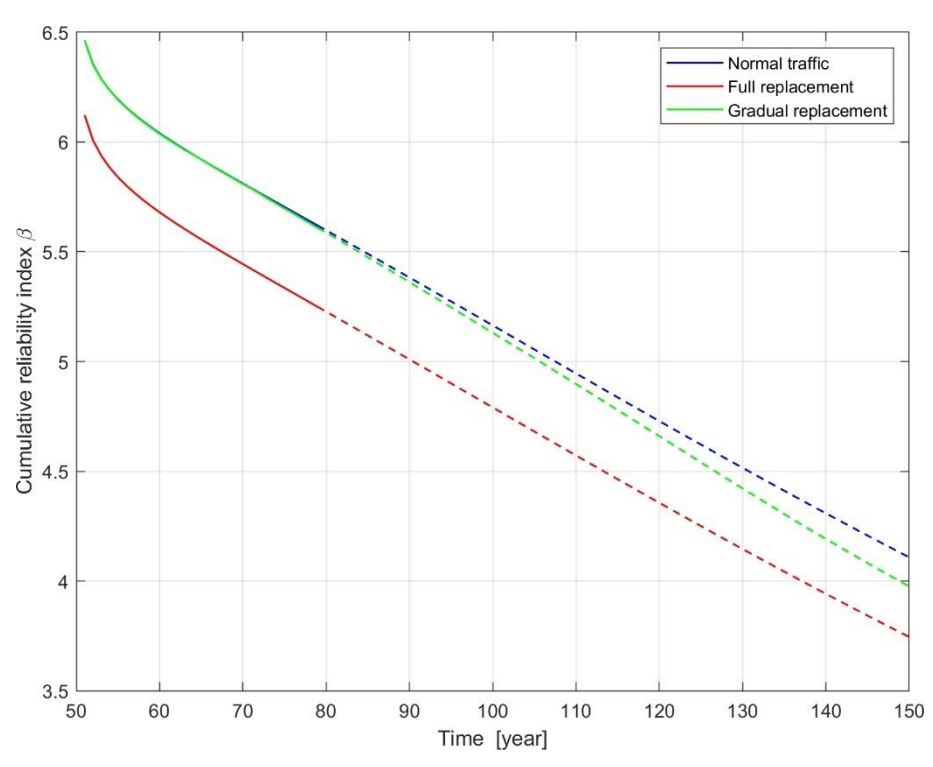


Figure 200: Comparison of cumulative reliability given different traffic scenarios based on the VB 1974 standard (elapsed 50 years, L = 50 m, simply-supported beam).

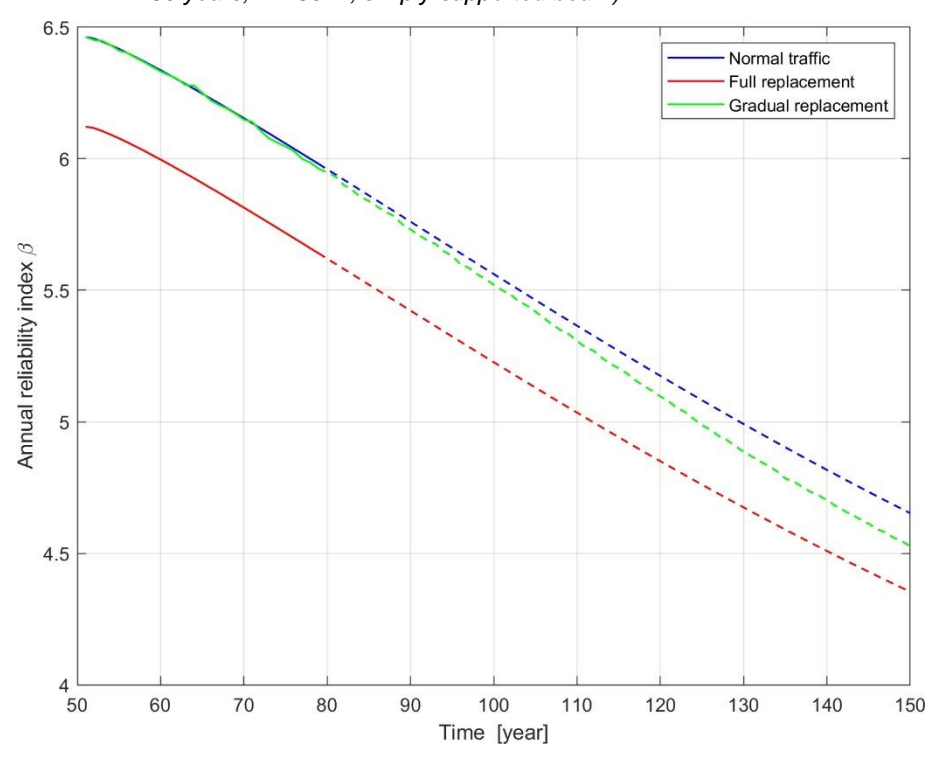


Figure 201: Comparison of annual reliability given different traffic scenarios based on the VB 1974 standard (elapsed 50 years, L = 50 m, simply-supported beam).



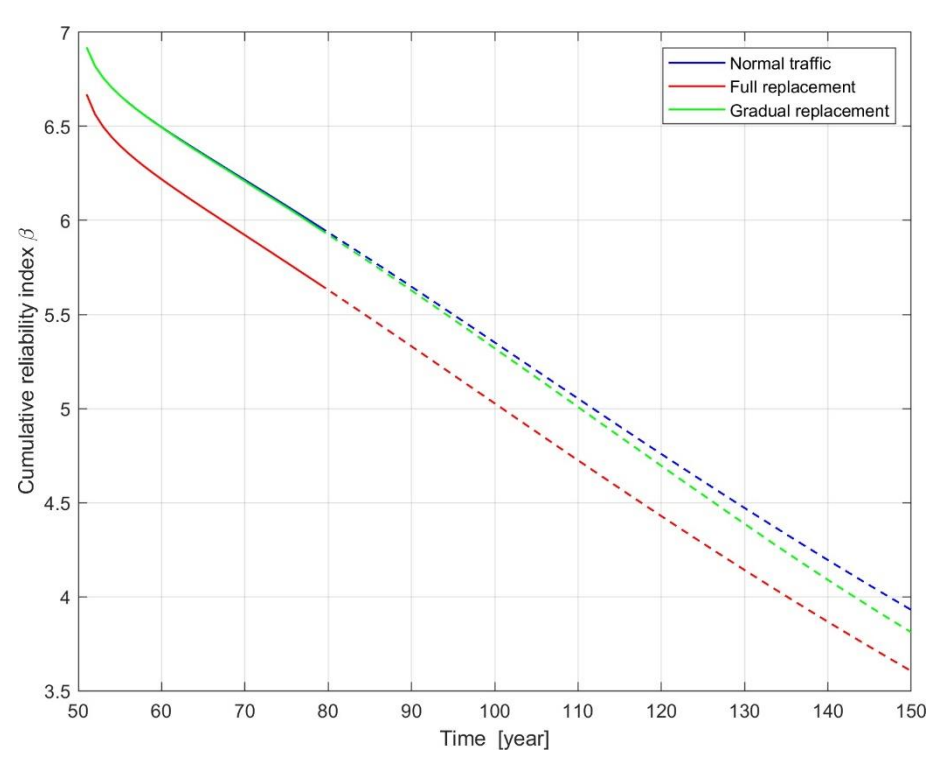


Figure 202: Comparison of cumulative reliability given different traffic scenarios based on the VB 1974 standard (elapsed 50 years, L = 100 m, simply-supported beam).

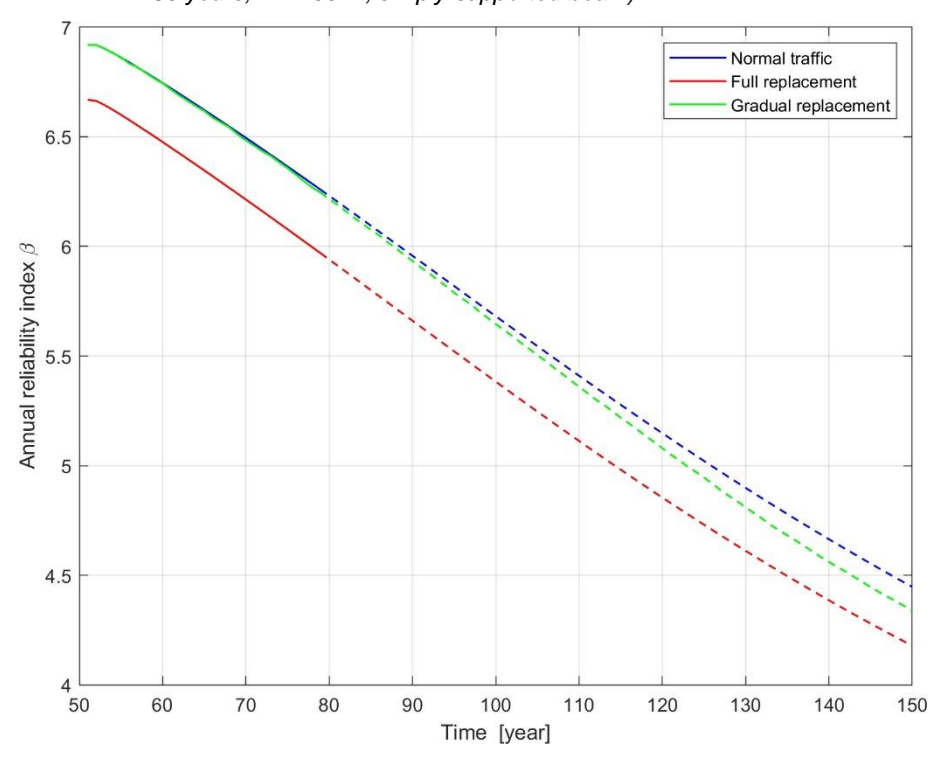


Figure 203: Comparison of annual reliability given different traffic scenarios based on the VB 1974 standard (elapsed 50 years, L = 100 m, simply-supported beam).



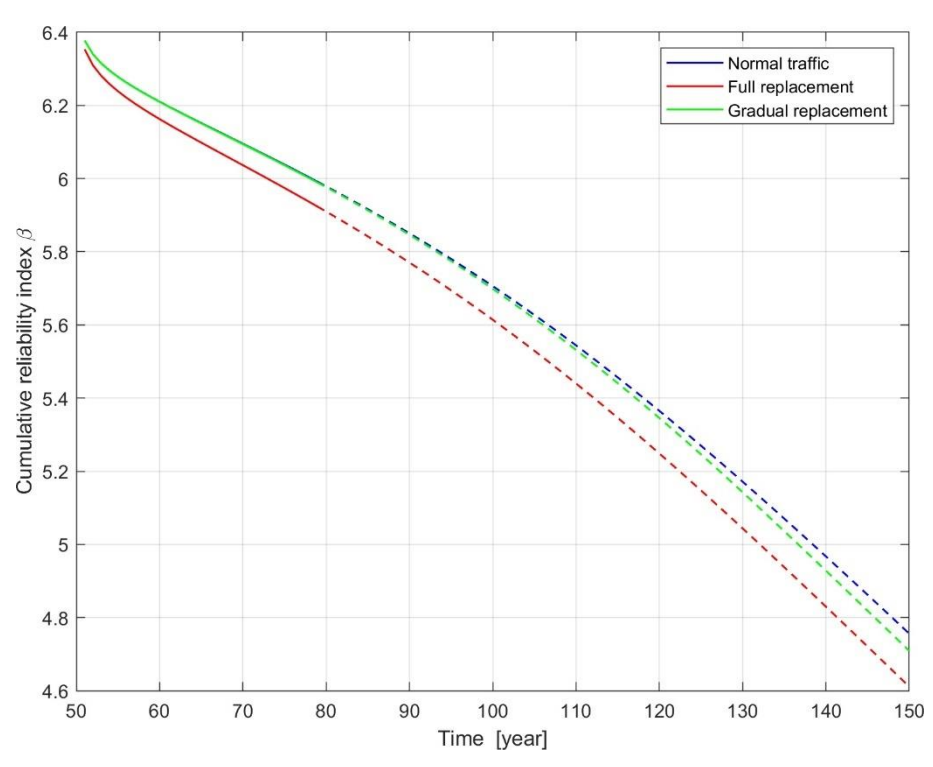


Figure 204: Comparison of cumulative reliability given different traffic scenarios based on the VB 1974 standard (elapsed 50 years, L = 200 m, simply-supported beam).

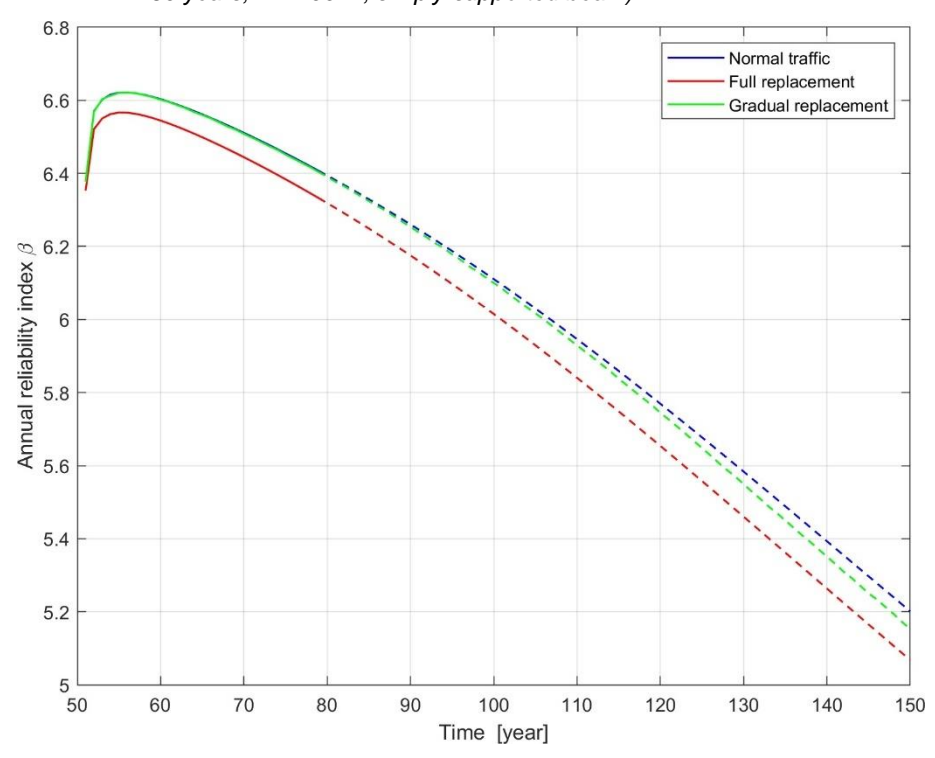


Figure 205: Comparison of annual reliability given different traffic scenarios based on the VB 1974 standard (elapsed 50 years, L = 200 m, simply-supported beam).



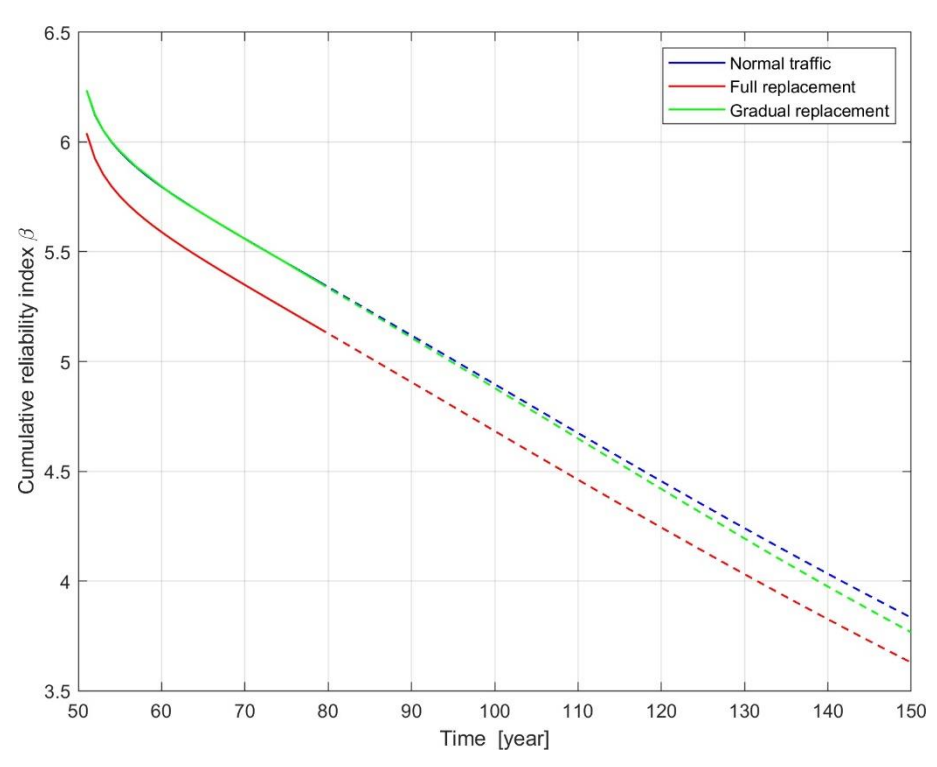


Figure 206: Comparison of cumulative reliability given different traffic scenarios based on the VB 1974 standard (elapsed 50 years, L = 2·20 m, bending moment, continuous beam).

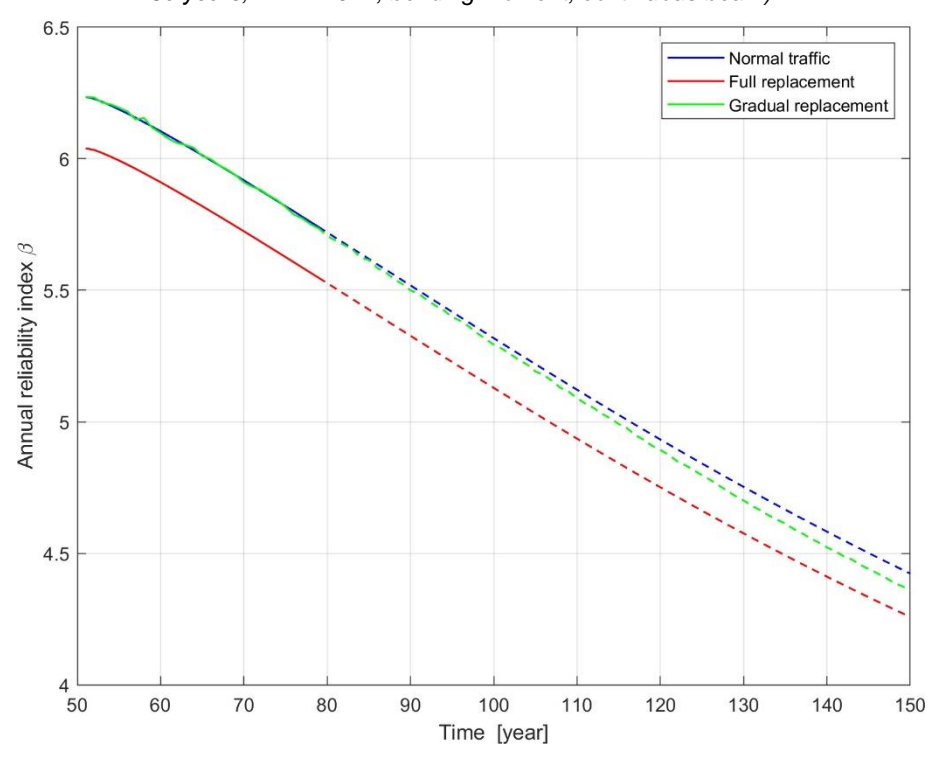


Figure 207: Comparison of annual reliability given different traffic scenarios based on the VB 1974 standard (elapsed 50 years, L = 2.20 m, bending moment, continuous beam).



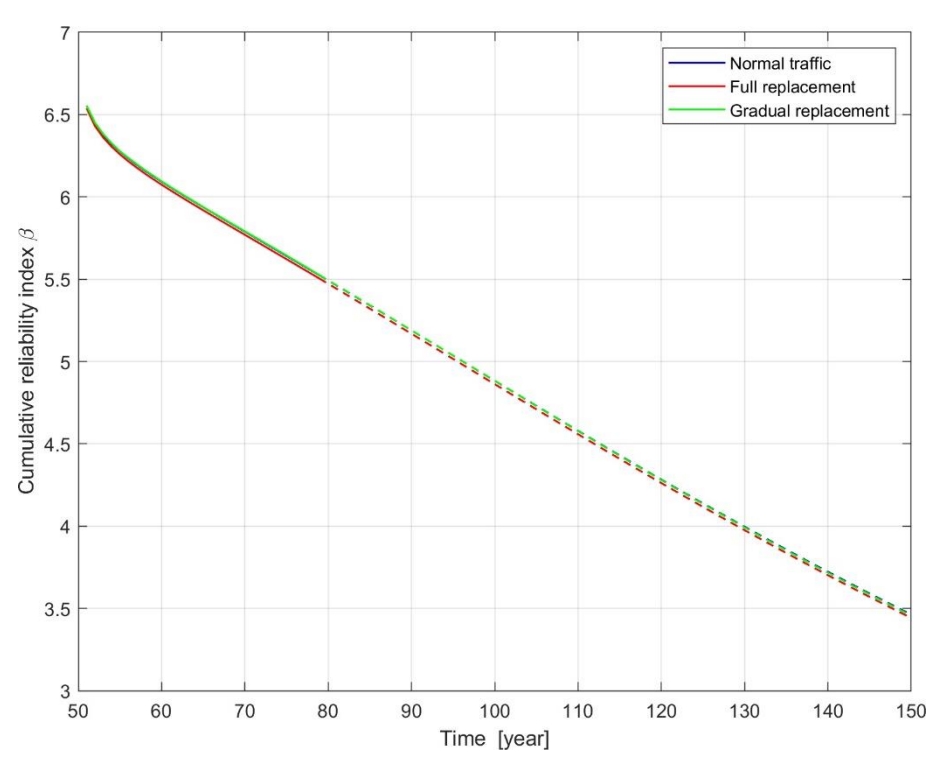


Figure 208: Comparison of cumulative reliability given different traffic scenarios based on the VB 1974 standard (elapsed 50 years, L = 2 · 50 m, bending moment, continuous beam).

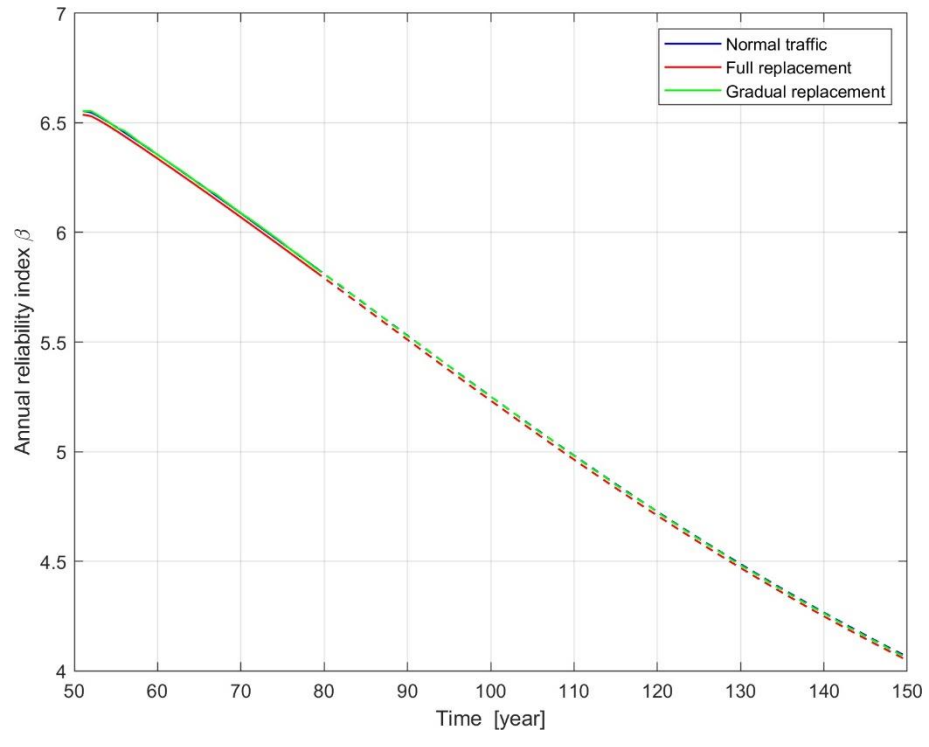


Figure 209: Comparison of annual reliability given different traffic scenarios based on the VB 1974 standard (elapsed 50 years, L = 2.50 m, bending moment, continuous beam).



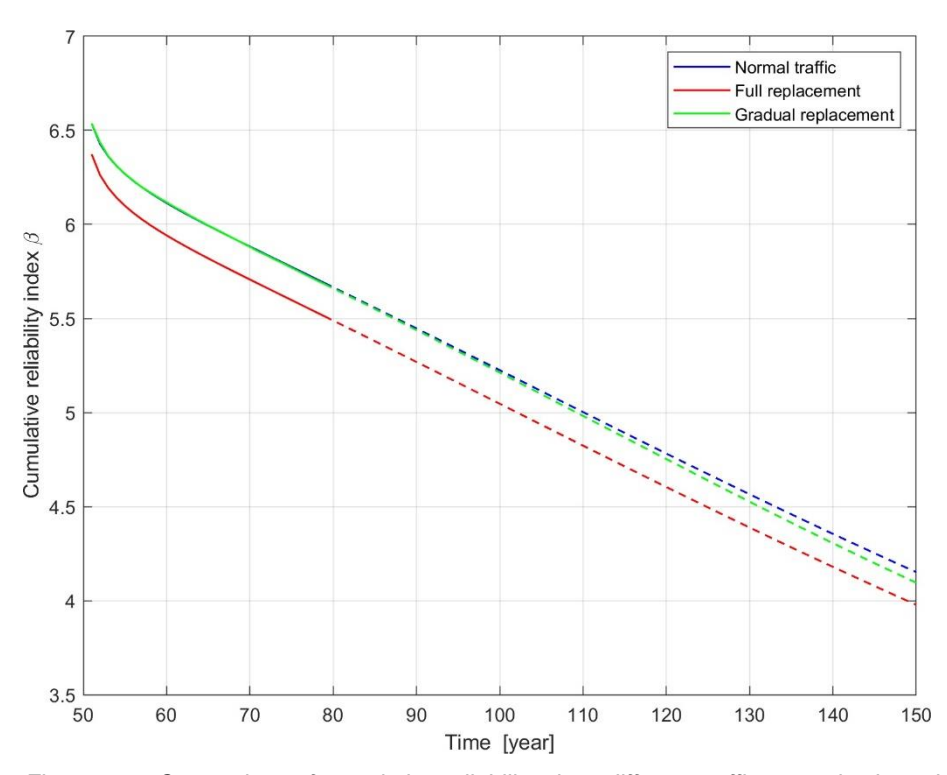


Figure 210: Comparison of cumulative reliability given different traffic scenarios based on the VB 1974 standard (elapsed 50 years, L = 2 · 20 m, shear force, continuous beam).

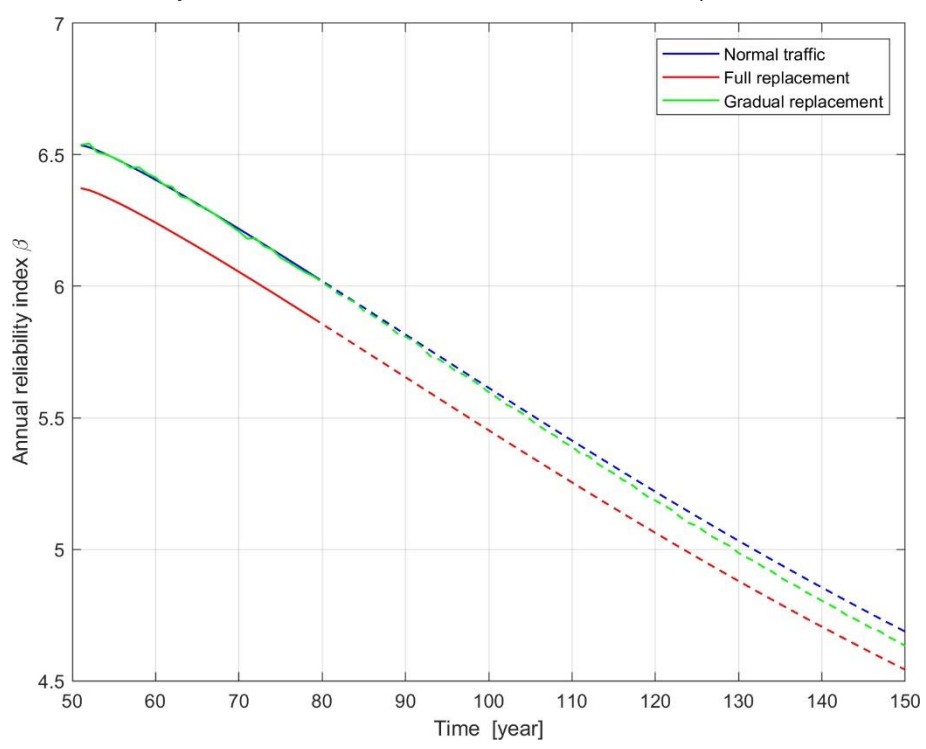


Figure 211: Comparison of annual reliability given different traffic scenarios based on the VB 1974 standard (elapsed 50 years, L = 2.20 m, shear force, continuous beam).



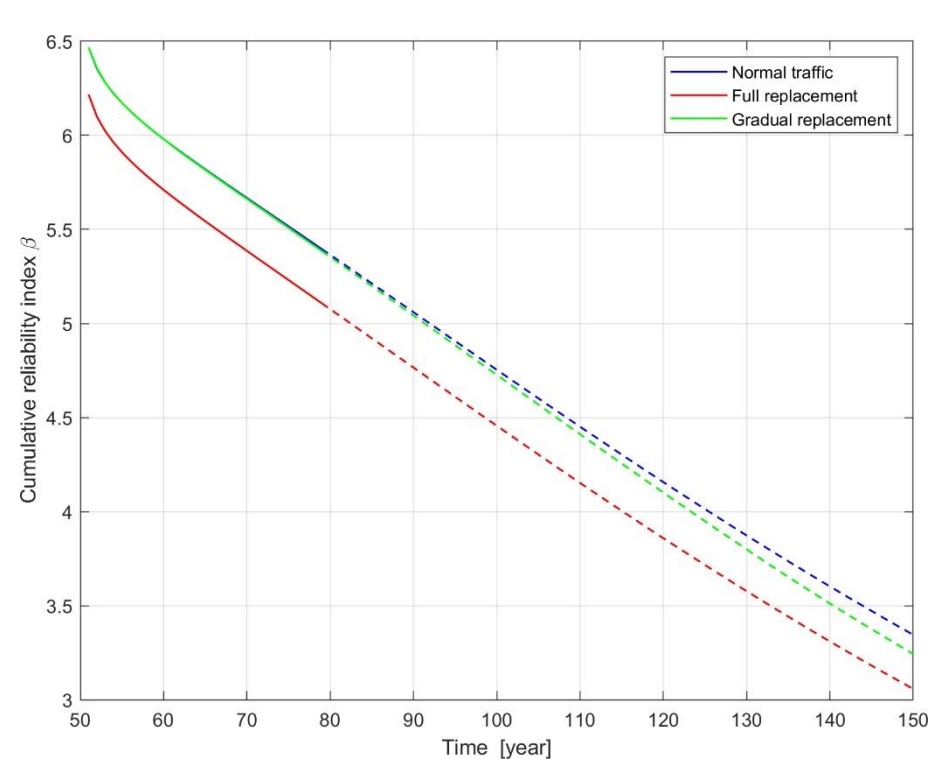


Figure 212: Comparison of cumulative reliability given different traffic scenarios based on the VB 1974 standard (elapsed 50 years, L = 2 · 50 m, shear force, continuous beam).

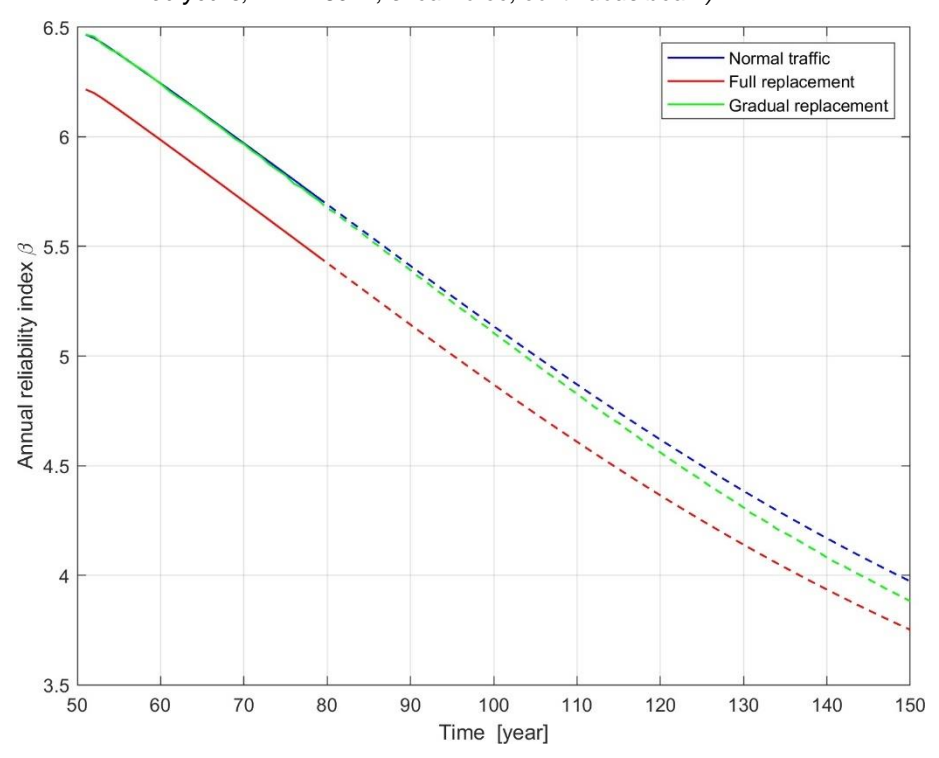


Figure 213: Comparison of annual reliability given different traffic scenarios based on the VB 1974 standard (elapsed 50 years, L = 2.50 m, shear force, continuous beam).



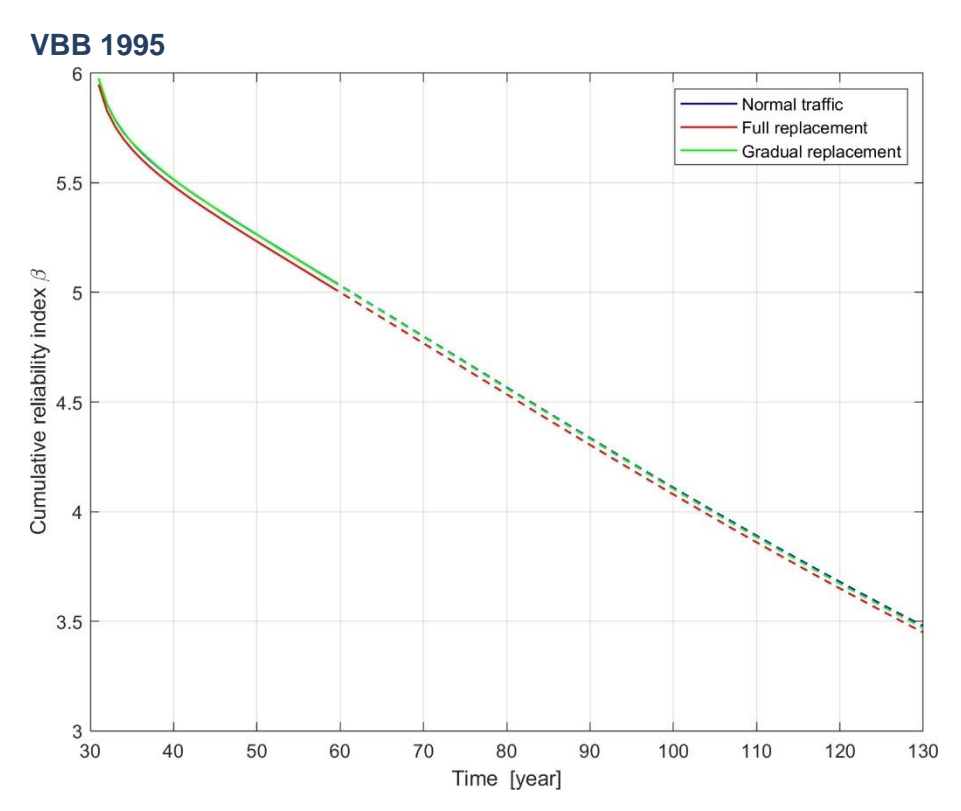


Figure 214: Comparison of cumulative reliability given different traffic scenarios based on the VBB 1995 standard (elapsed 30 years, L = 20 m, simply-supported beam).

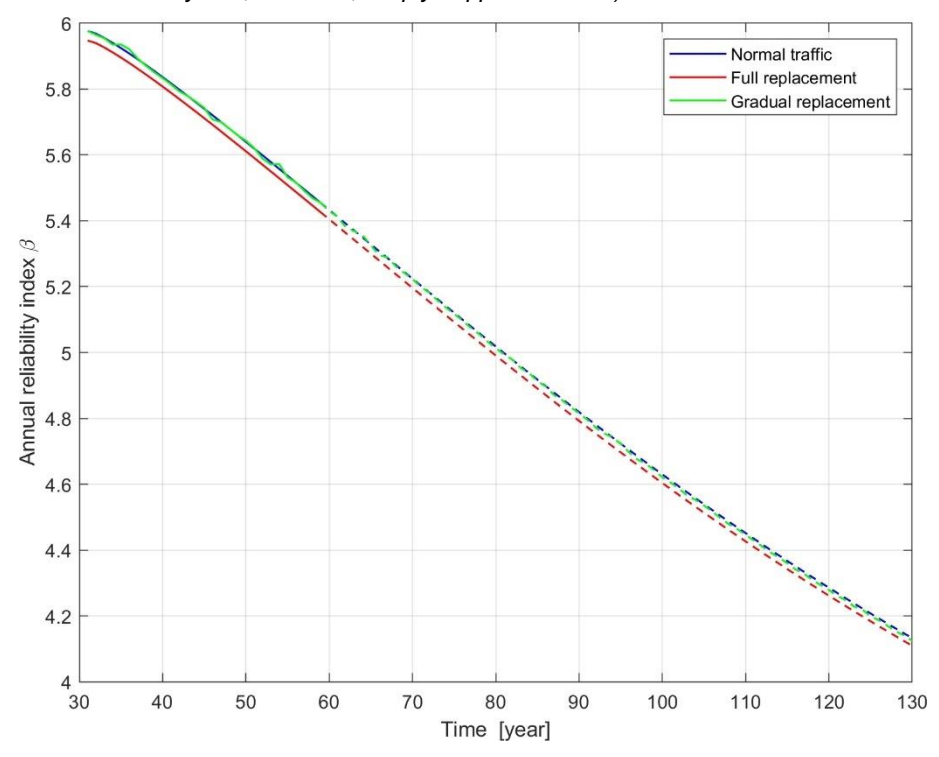


Figure 215: Comparison of annual reliability given different traffic scenarios based on the VBB 1995 standard (elapsed 30 years, L = 20 m, simply-supported beam).



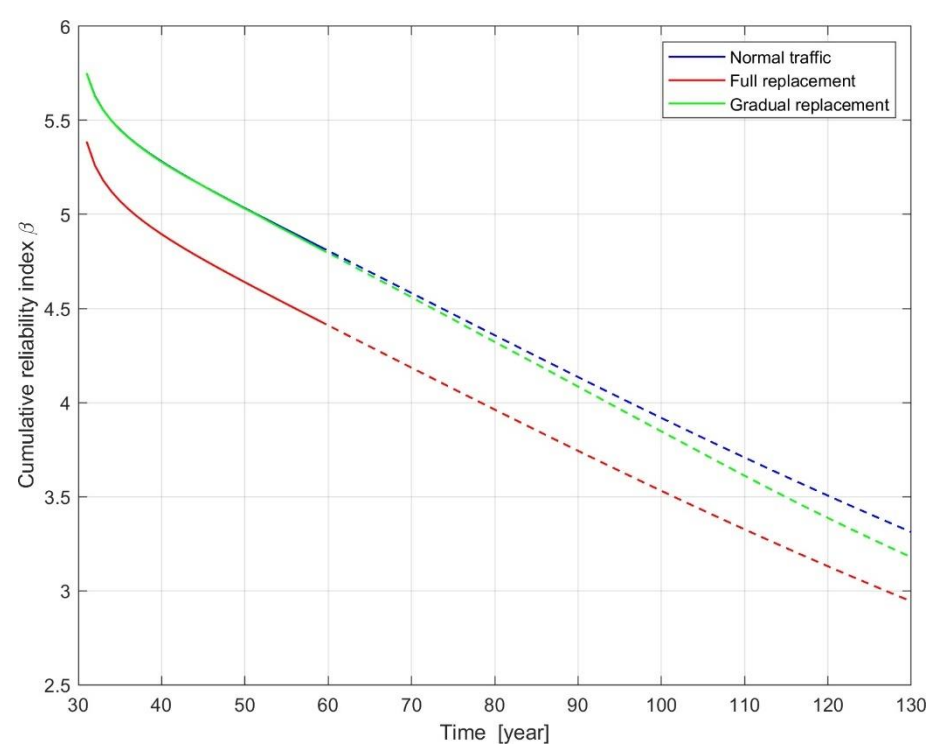


Figure 216: Comparison of cumulative reliability given different traffic scenarios based on the VBB 1995 standard (elapsed 30 years, L = 50 m, simply-supported beam).

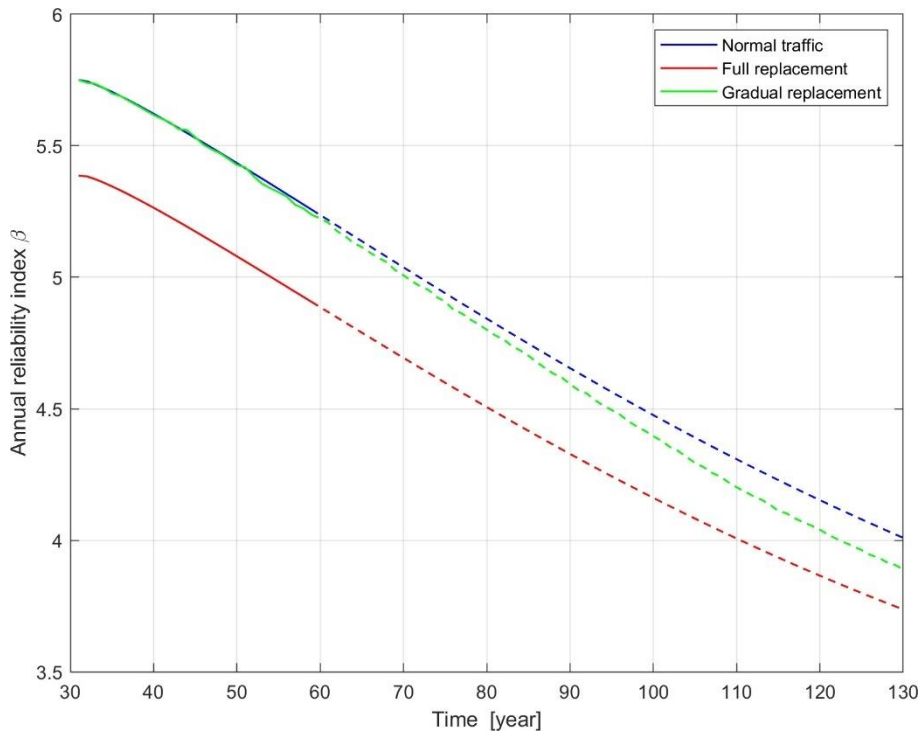


Figure 217: Comparison of annual reliability given different traffic scenarios based on the VBB 1995 standard (elapsed 30 years, L = 50 m, simply-supported beam).



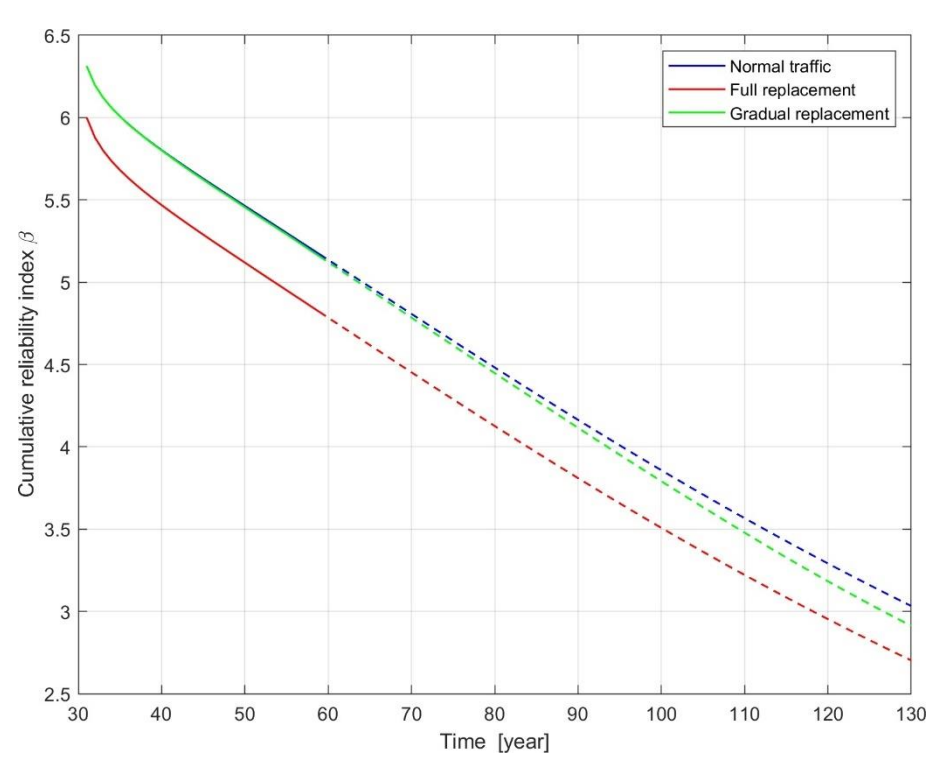


Figure 218: Comparison of cumulative reliability given different traffic scenarios based on the VBB 1995 standard (elapsed 30 years, L = 100 m, simply-supported beam).

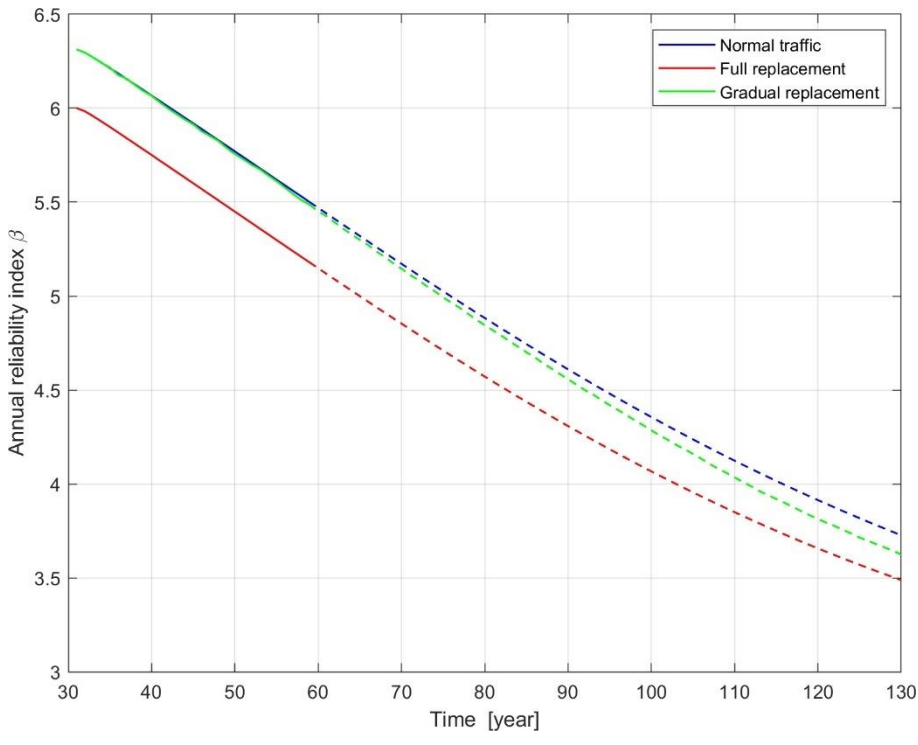


Figure 219: Comparison of annual reliability given different traffic scenarios based on the VBB 1995 standard (elapsed 30 years, L = 100 m, simply-supported beam).



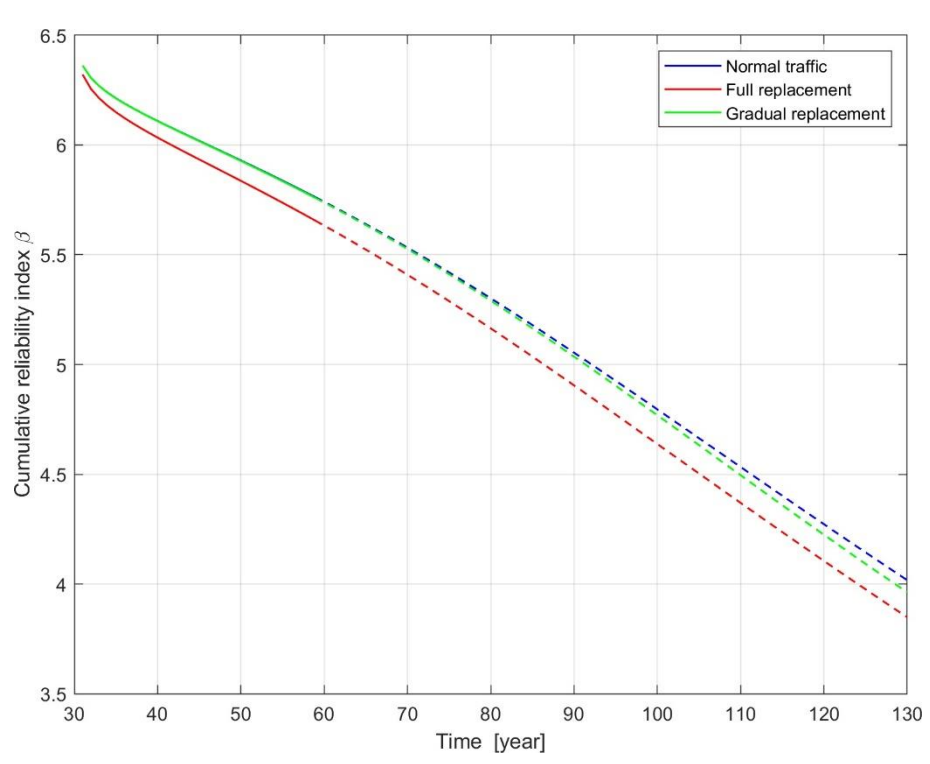


Figure 220: Comparison of cumulative reliability given different traffic scenarios based on the VBB 1995 standard (elapsed 30 years, L = 200 m, simply-supported beam).

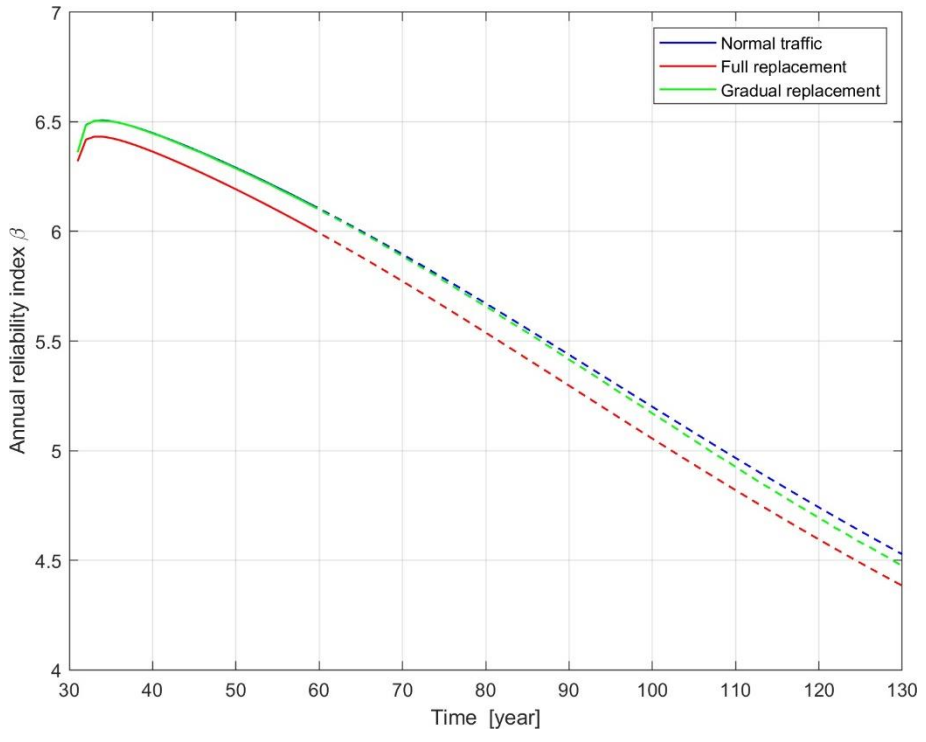


Figure 221: Comparison of annual reliability given different traffic scenarios based on the VBB 1995 standard (elapsed 30 years, L = 200 m, simply-supported beam).



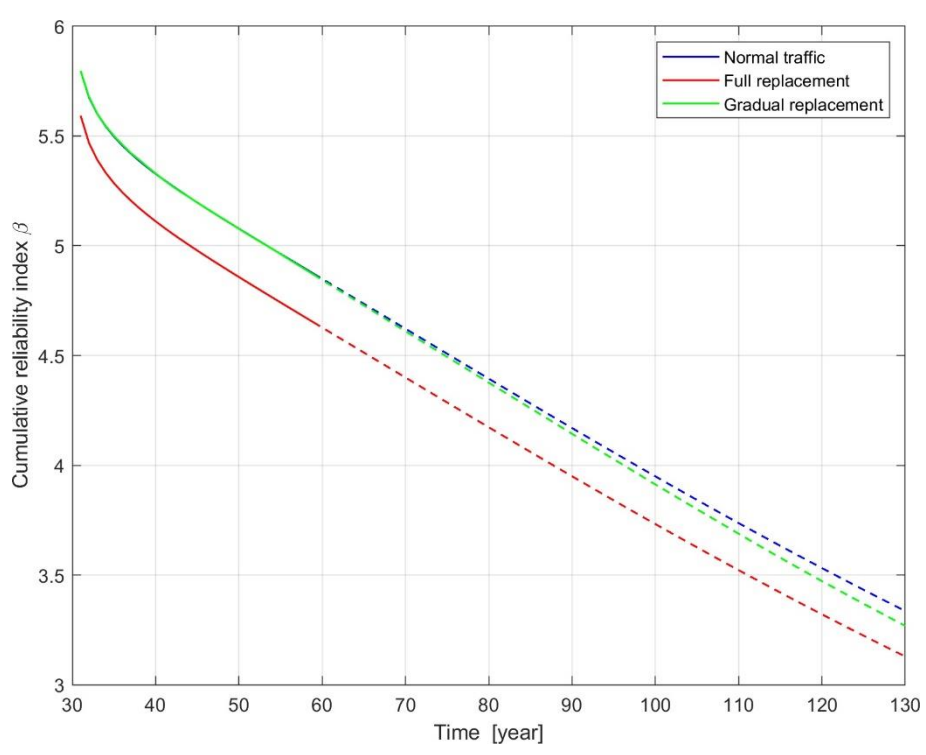


Figure 222: Comparison of cumulative reliability given different traffic scenarios based on the VBB 1995 standard (elapsed 30 years, L = 2 · 20 m, bending moment, continuous beam).

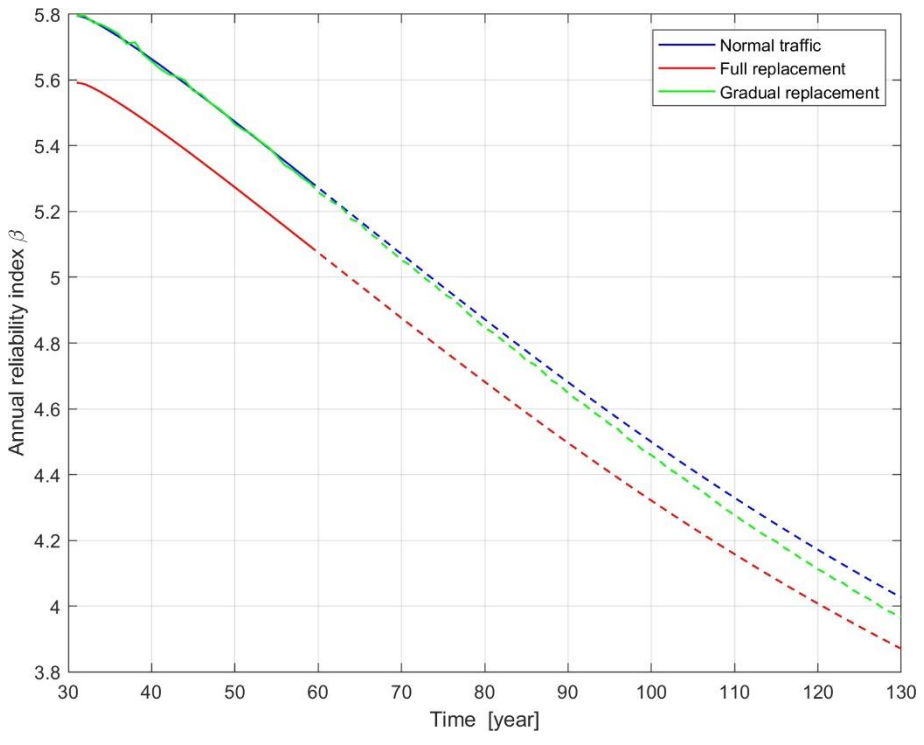


Figure 223: Comparison of annual reliability given different traffic scenarios based on the VBB 1995 standard (elapsed 30 years, L = 2.20 m, bending moment, continuous beam).



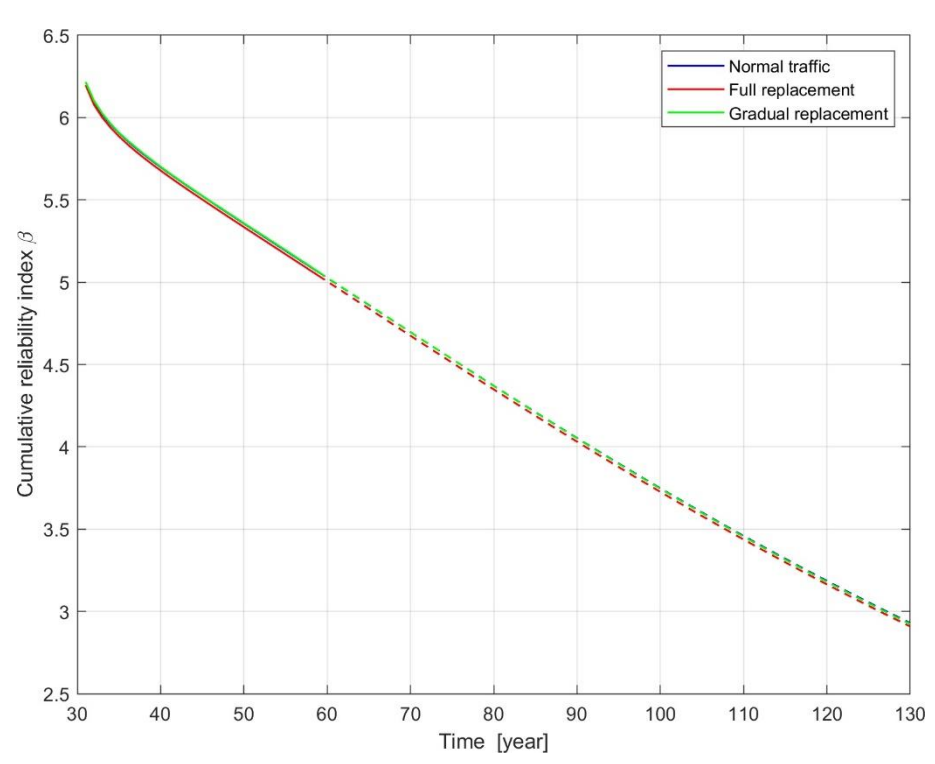


Figure 224: Comparison of cumulative reliability given different traffic scenarios based on the VBB 1995 standard (elapsed 30 years, L = 2 ·50 m, bending moment, continuous beam).

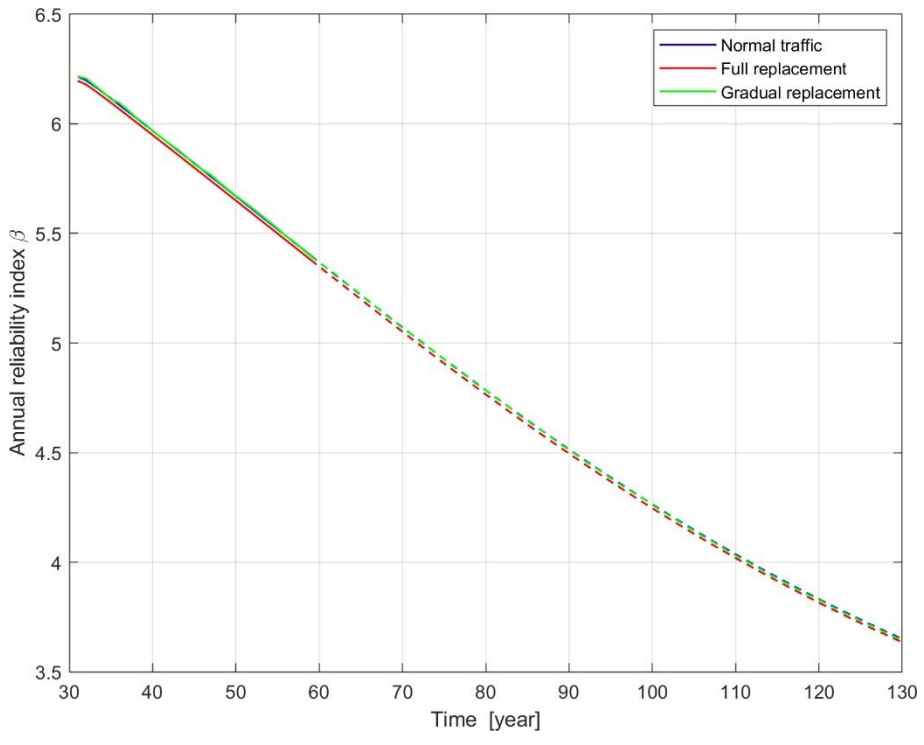


Figure 225: Comparison of annual reliability given different traffic scenarios based on the VBB 1995 standard (elapsed 30 years, L = 2.50 m, bending moment, continuous beam).



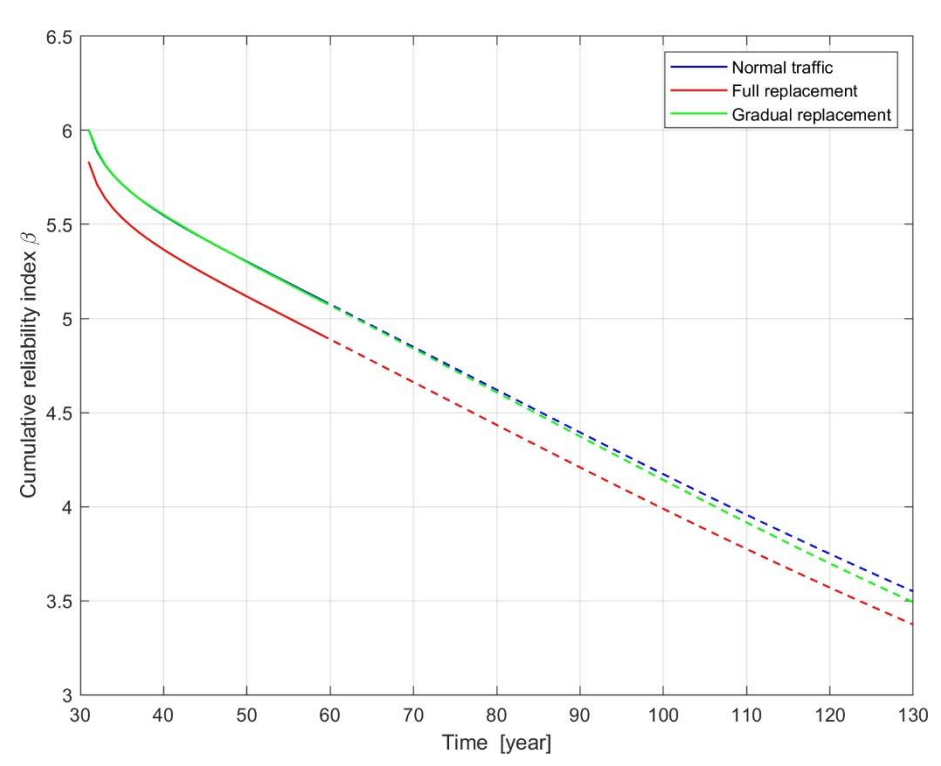


Figure 226: Comparison of cumulative reliability given different traffic scenarios based on the VBB 1995 standard (elapsed 30 years, L = 2 · 20 m, shear force, continuous beam).

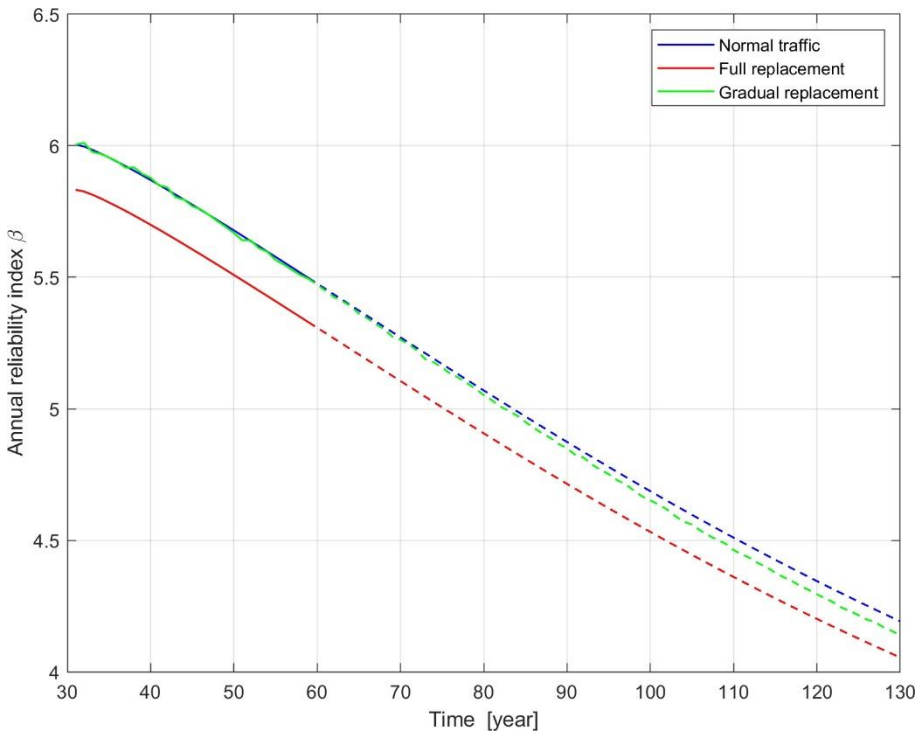


Figure 227: Comparison of annual reliability given different traffic scenarios based on the VBB 1995 standard (elapsed 30 years, L = 2.20 m, shear force, continuous beam).



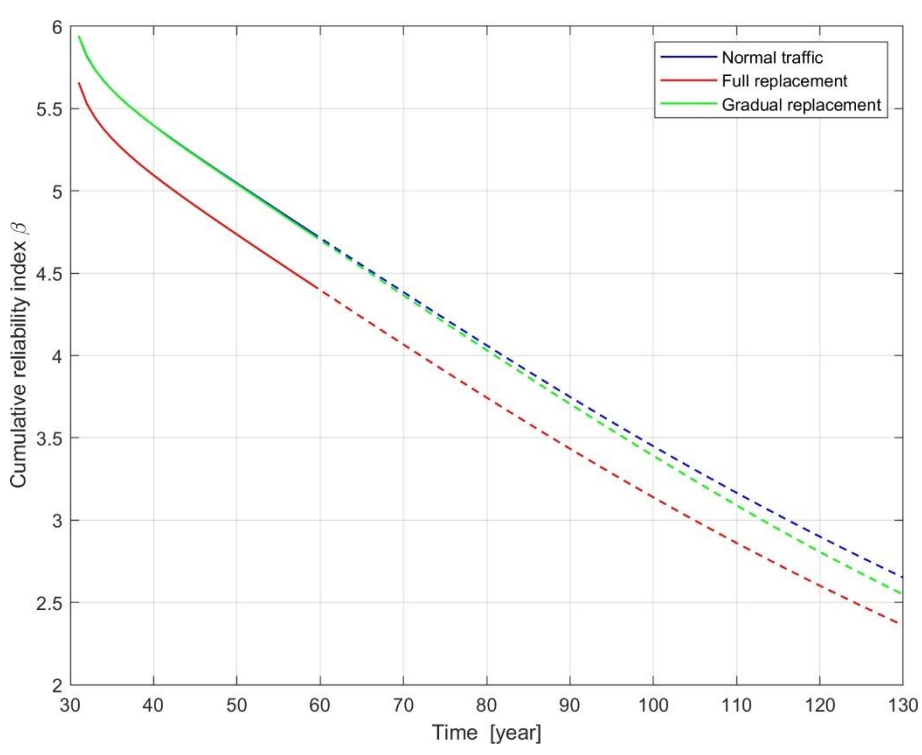


Figure 228: Comparison of cumulative reliability given different traffic scenarios based on the VBB 1995 standard (elapsed 30 years, L = 2 ·50 m, shear force, continuous beam).

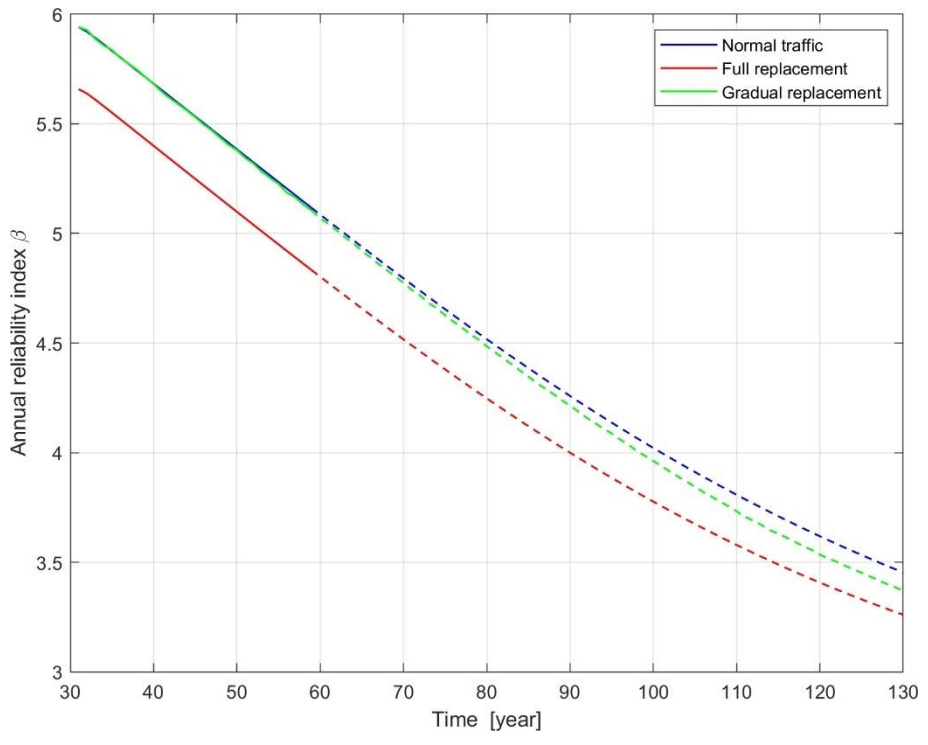


Figure 229: Comparison of annual reliability given different traffic scenarios based on the VBB 1995 standard (elapsed 30 years, L = 2.50 m, bending moment, continuous beam).



## APPENDIX 7 RESULTS STEEL BRIDGE (ULS CONDITIONS)

Table 32: Reference scenario: calibrated resistance depending for a steel bridge in ultimate limit state conditions.

	Span	Calibrated resistance R [kNm] depending on the elapsed service life to		
	length			
	L [m]	0 year	30 years	
Simply-supported beam,	50	69,927	42,210	
bending moment at mid-span				

Table 33: Results steel bridge under ULS conditions. Calculated cumulative, annual reliability and the end of normative service life for the three scenarios. The results relate to the bending moment at the midspan of a simply supported beam (L=50 m).

Circumstance and a second		Cumulative reliability β [-]		Annual reliability β [-]		End of normative		
Structural system			First year (t₀)	Last year (t <sub>0</sub> + T <sub>ref</sub> )	First year (t <sub>0</sub> )	Last year (t <sub>0</sub> + T <sub>ref</sub> )	service life [years]	
Normal traffic								
New structure		T <sub>ref</sub> =100 years	6.99	4.30	6.99	4.79	_	
Existing structure	$t_0 = 30 \text{ years}$	T <sub>ref</sub> = 30 years	4,43	3,30	4,43	3,94	_	
Full replacement								
New structure		T <sub>ref</sub> =100 years	6.59	3.90	6.59	4.45	82	
Existing structure	$t_0 = 30 \text{ years}$	T <sub>ref</sub> = 30 years	4.01	2.85	4.01	3.60	9	
Gradual replacement								
New structure		T <sub>ref</sub> =100 years	6.99	4.15	6.99	4.65	93	
Existing structure	$t_0 = 30 \text{ years}$	$T_{ref} = 30 \text{ years}$	4.43	3.29	4.43	3.92	28	



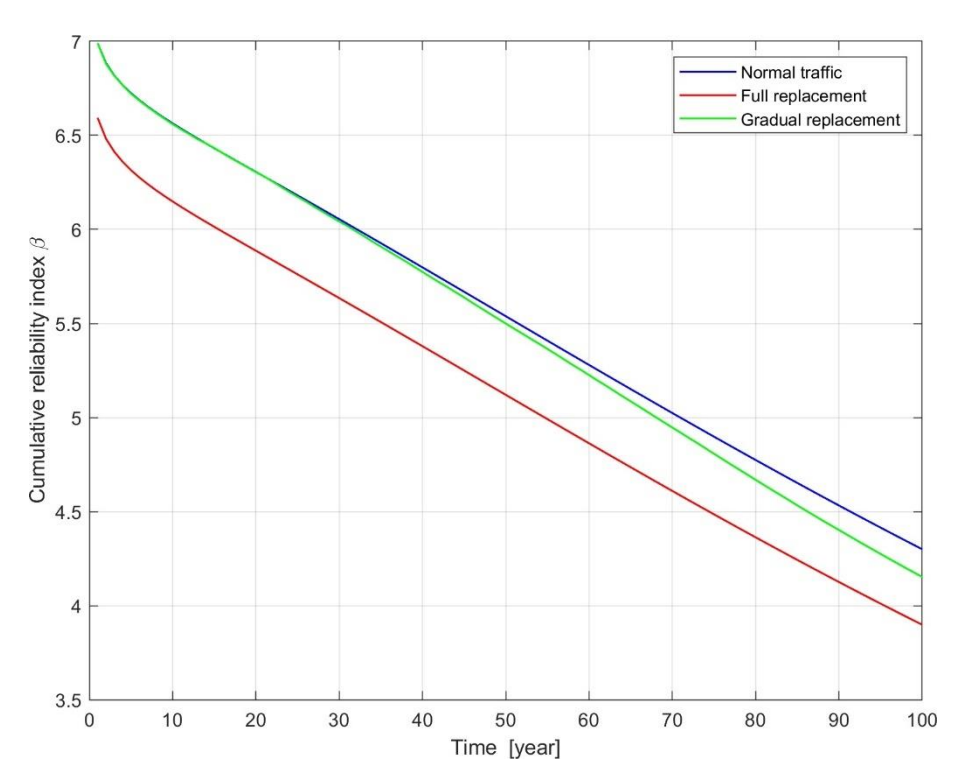


Figure 230: Comparison of cumulative reliability given different traffic scenarios for the new structure (steel structure, L = 50 m, simply-supported beam).

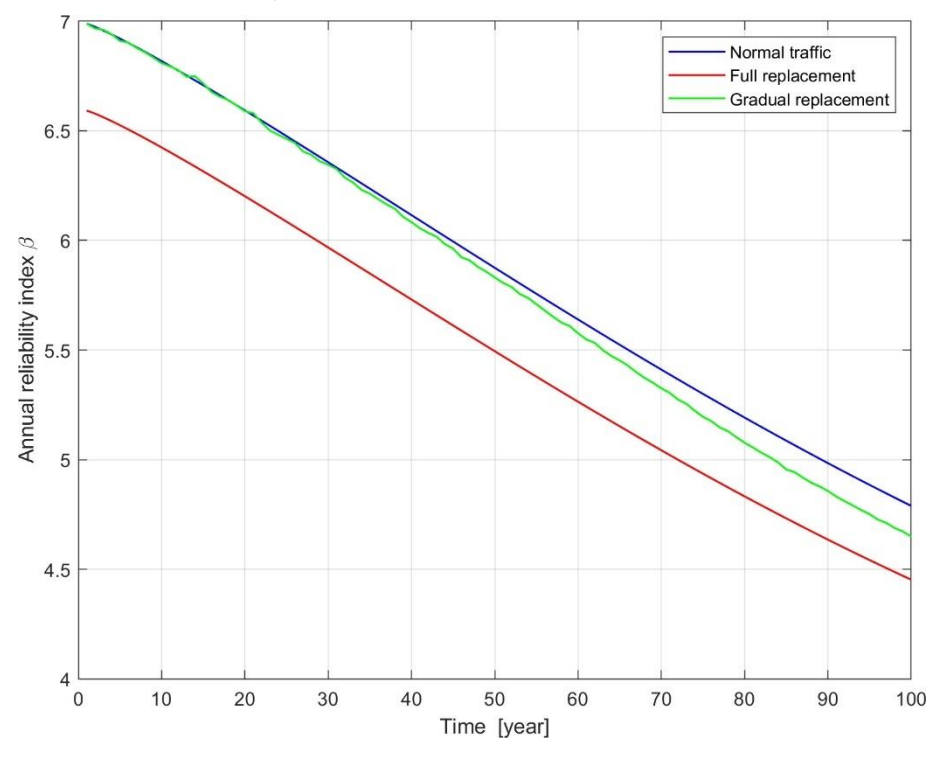


Figure 231: Comparison of annual reliability given different traffic scenarios for the new structure (steel structure, L = 50 m, simply-supported beam).



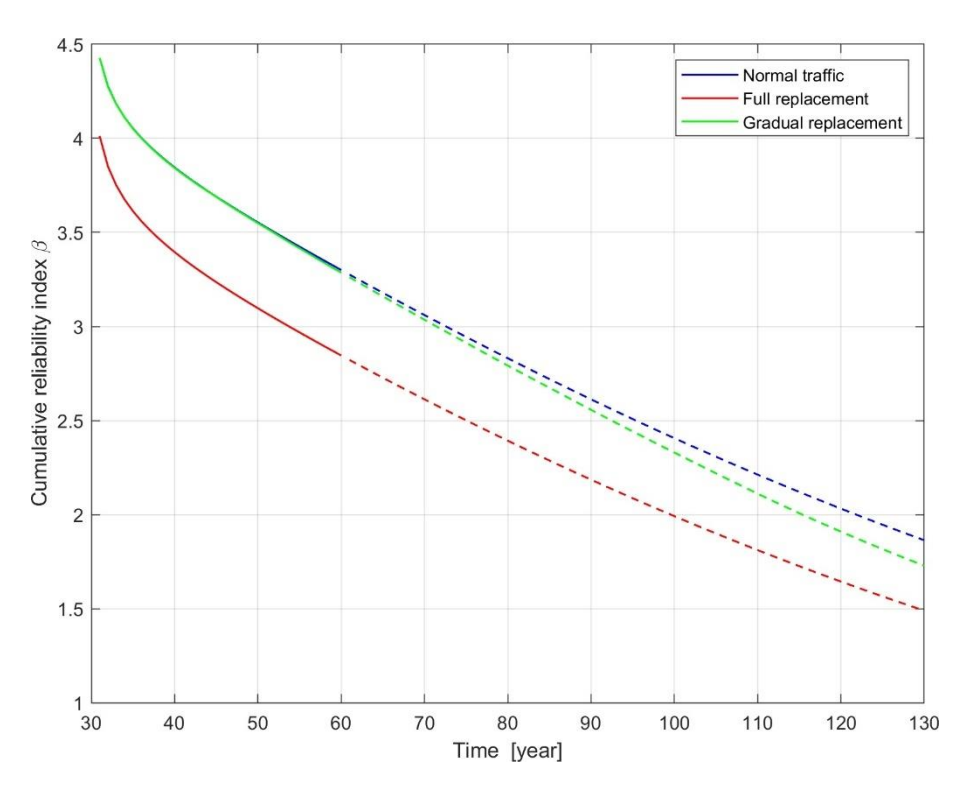


Figure 232: Comparison of cumulative reliability given different traffic scenarios for the existing structure (steel structure, elapsed 30 years, L = 50 m, simply-supported beam).

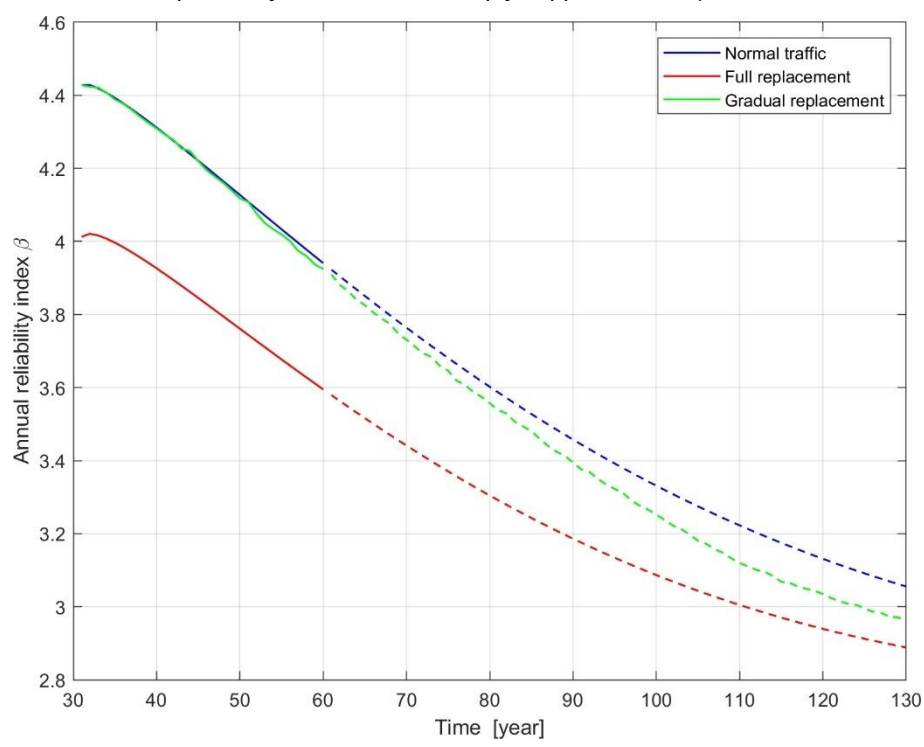


Figure 233: Comparison of annual reliability given different traffic scenarios for the existing structure (steel structure, elapsed 30 years, L = 50 m, simply-supported beam).



## APPENDIX 8 RESULTS STEEL BRIDGE (FATIGUE LIMIT STATE)

Table 34: Calibrated  $\alpha$  factors (span L = 100 m).

	α [-]
New structure	0,50
Existing structure, elapsed 30 years	0,69
Existing structure, elapsed 50 years	0,69
Existing structure, elapsed 70 years	0,69

Table 35: Calculated cumulative, annual reliability indices for a steel bridge (L = 100 m) under fatigue load conditions for new and existing structures. The results relate to the bending moment at midspan in a simply supported beam and to all three scenarios.

Structural system		Cumulative reliability $\beta$		Annual reliability β [-]		End of normative
		First year (t <sub>0</sub> )	Last year (t <sub>0</sub> +T <sub>ref</sub> )	First year (t₀)	Last year (t <sub>0</sub> +T <sub>ref</sub> )	service life [years]
Normal traffic scen	ario					
New structure	t <sub>0</sub> =0 years T <sub>ref</sub> =100 years	10,99	4.3	10.99	4.88	100
Existing structure	$t_0 = 30 \text{ years}$ $T_{ref} = 30 \text{ years}$	8.12	3,30	8.12	3.76	30
	$t_0 = 50 \text{ years}$ $T_{ref} = 30 \text{ years}$	8.12	3,30	8.12	3.76	30
	$t_0 = 70$ years $T_{ref} = 30$ years	8.12	3,30	8.12	3.76	30
Full replacement						
New structure	t <sub>0</sub> =0 years T <sub>ref</sub> =100 years	8.10	2.01	8.10	3,21	11
Existing structure	$t_0$ = 30 years $T_{ref}$ = 30 years	5.92	1.18	5.92	2.39	4
	$t_0 = 50 \text{ years}$ $T_{ref} = 30 \text{ years}$	5.92	1.18	5.92	2.39	4
	t <sub>0</sub> =70 years T <sub>ref</sub> = 30 years	5.92	1.18	5.92	2.39	4
Gradual replaceme	ent					
New structure	t <sub>0</sub> =0 years T <sub>ref</sub> =100 years	10,99	2.89	10,99	3.66	50
Existing structure	$t_0 = 30 \text{ years}$ $T_{ref} = 30 \text{ years}$	8.12	3.12	8.12	3.59	26
	$t_0 = 50 \text{ years}$ $T_{ref} = 30 \text{ years}$	8.12	3.12	8.12	3.59	26
	t <sub>0</sub> =70 years T <sub>ref</sub> = 30 years	8.12	3.12	8.12	3.59	26



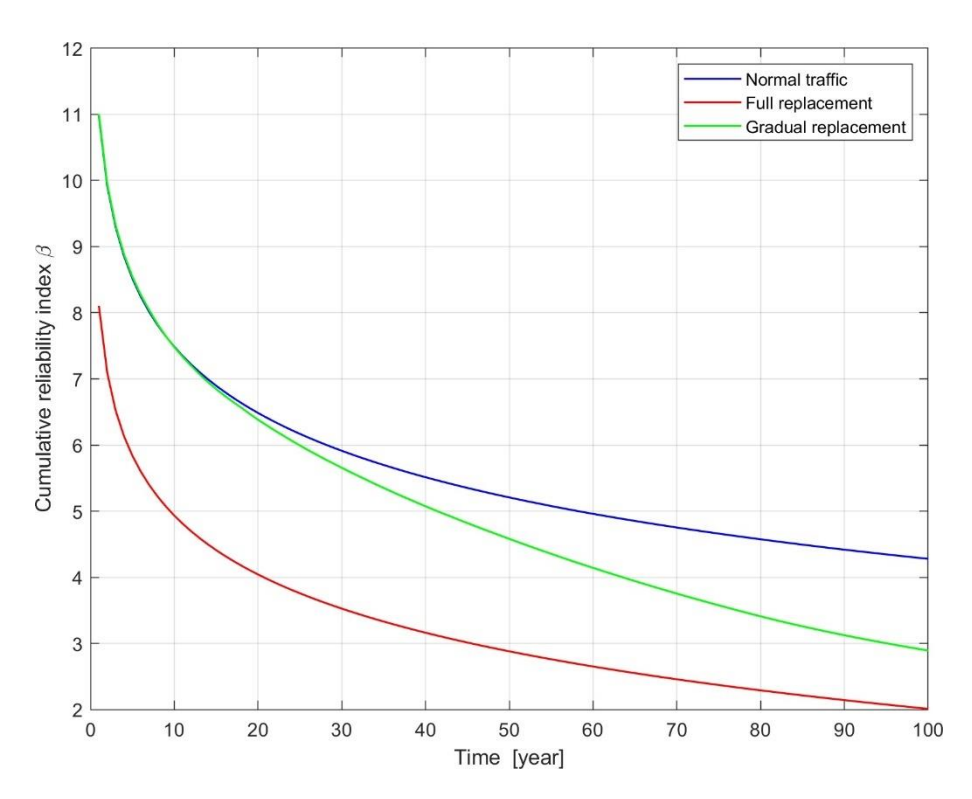


Figure 234: Cumulative reliability for the new structure (L = 100 m) with normal traffic conditions (blue), gradual replacement with SEC (green) and full replacement with SEC (red).

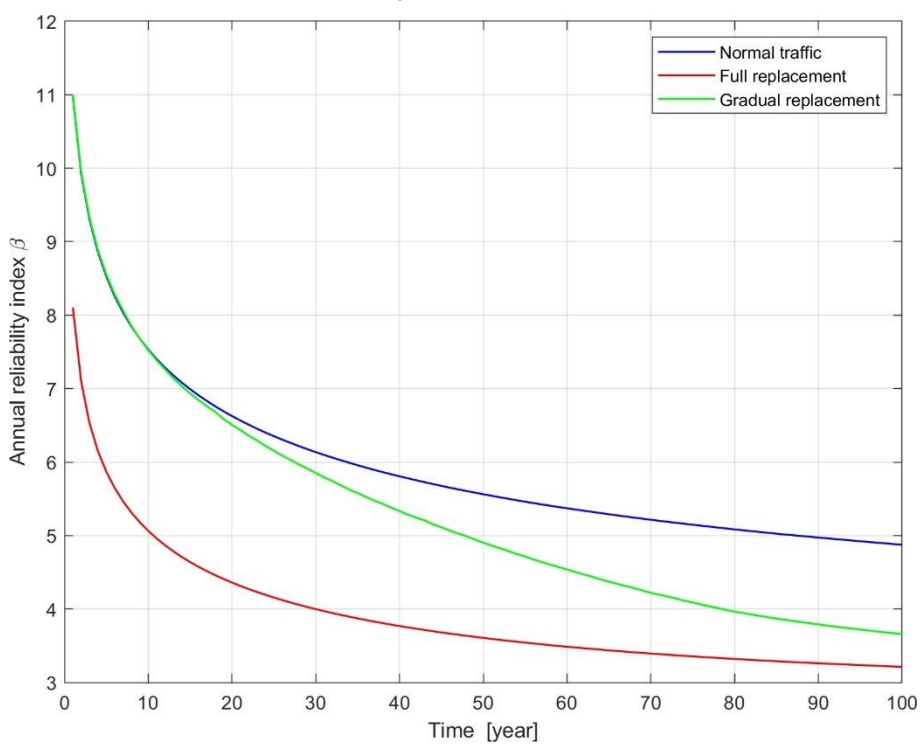


Figure 235: Annual reliability for the new structure (L = 100 m) with normal traffic conditions (blue), gradual replacement with SEC (green) and full replacement with SEC (red).



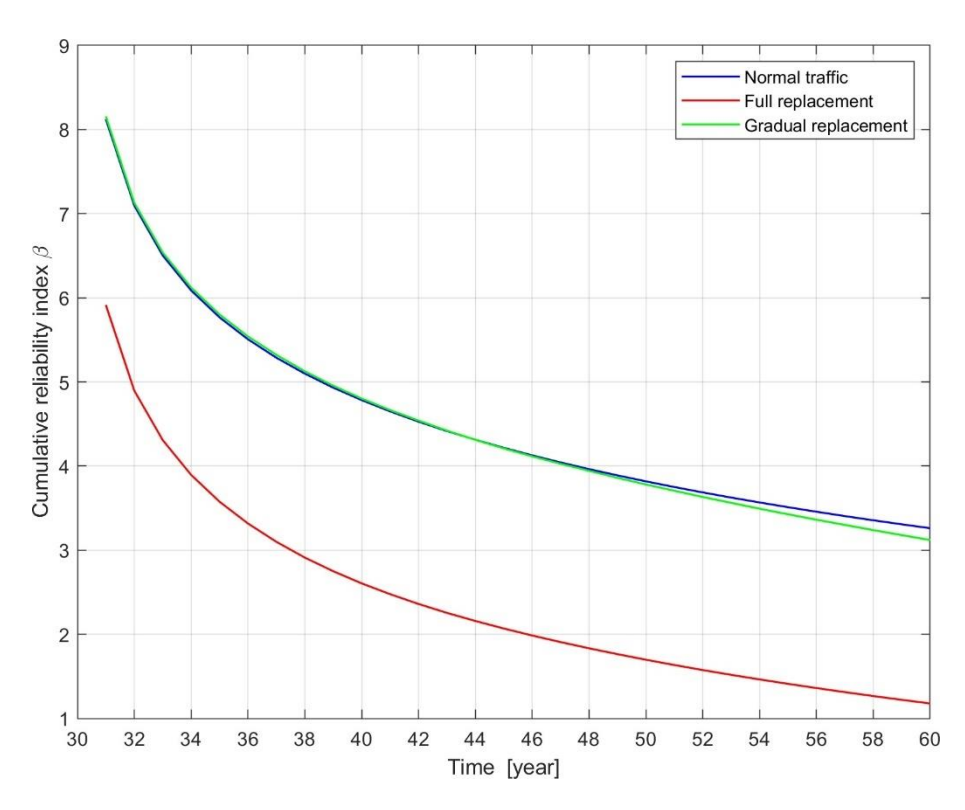


Figure 236: Cumulative reliability for the existing structure (L = 100 m) with elapsed service life 30 years with normal traffic conditions (blue), gradual replacement with SEC (green) and full replacement with SEC (red).

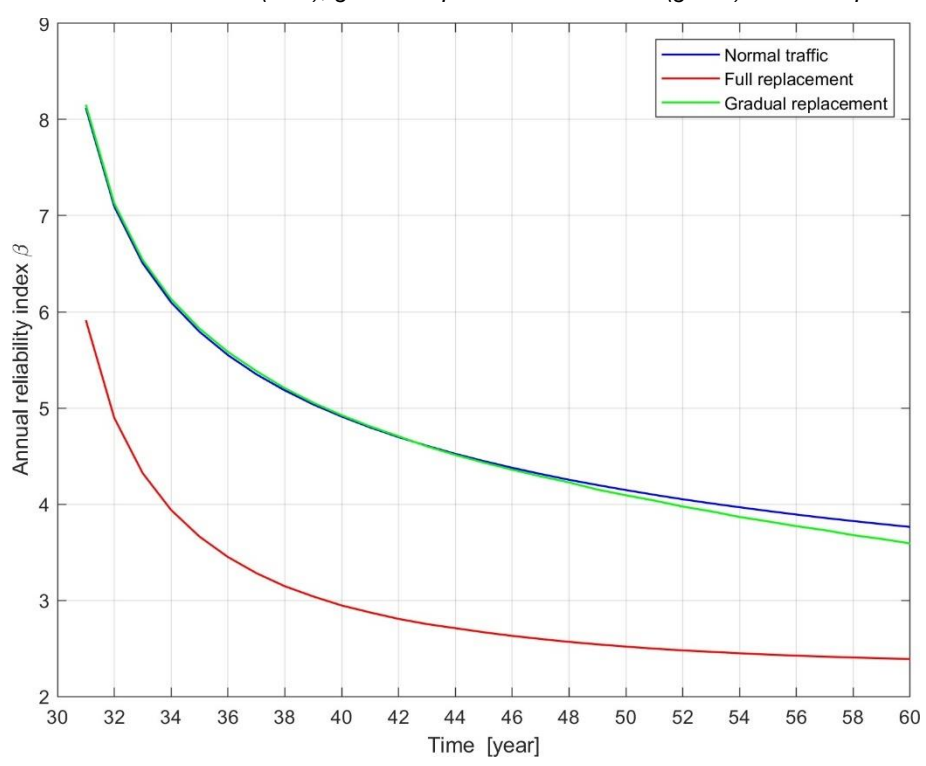


Figure 237: Annual reliability for the existing structure (L = 100 m) with elapsed service life 30 years with normal traffic conditions (blue), gradual replacement with SEC (green) and full replacement with SEC (red).



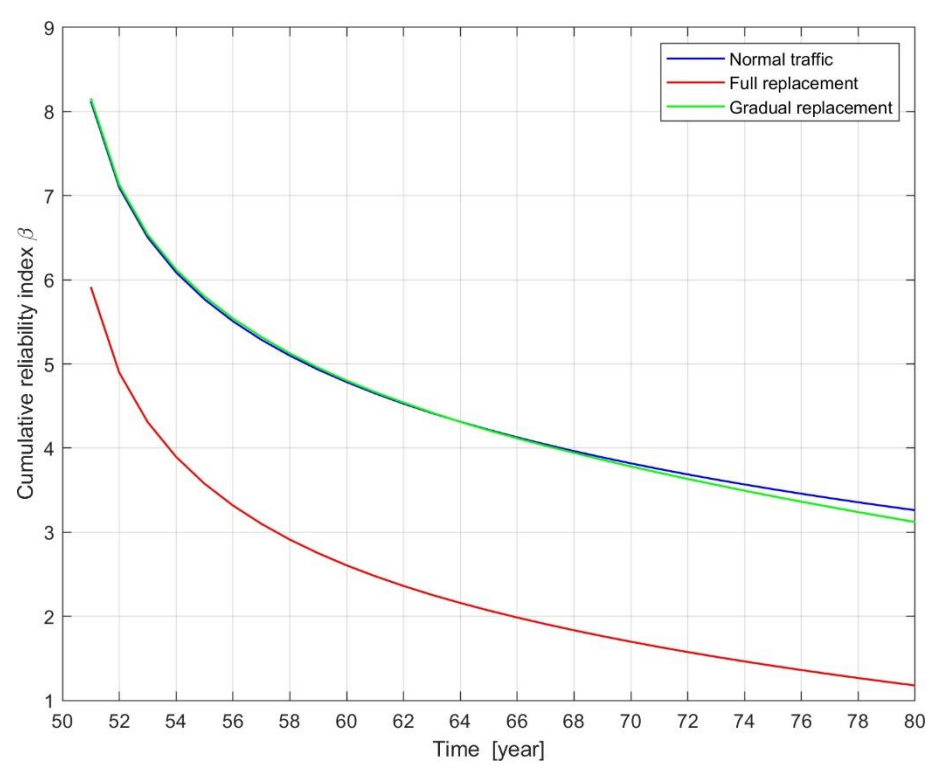


Figure 238: Cumulative reliability for the existing structure (L = 100 m) with elapsed service life 50 years with normal traffic conditions (blue) and full replacement with SEC (red).

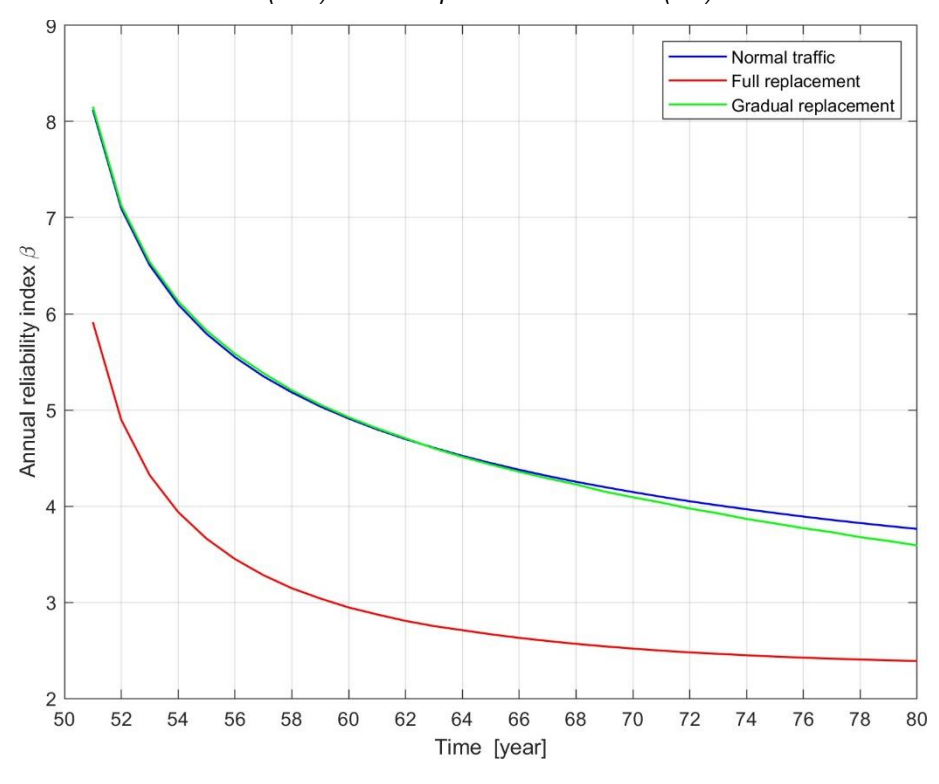


Figure 239: Annual reliability for the existing structure (L = 100 m) with elapsed service life 50 years with normal traffic conditions (blue) and full replacement with SEC (red).



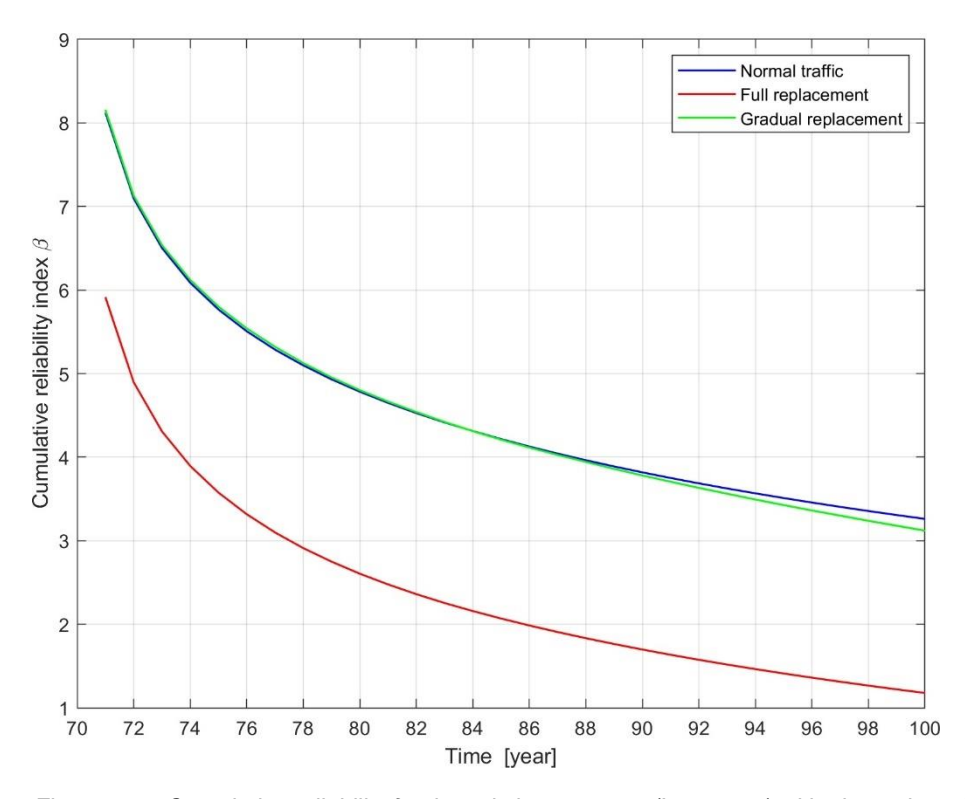


Figure 240: Cumulative reliability for the existing structure (L = 100 m) with elapsed service life 70 years with normal traffic conditions (blue) and full replacement with SEC (red).



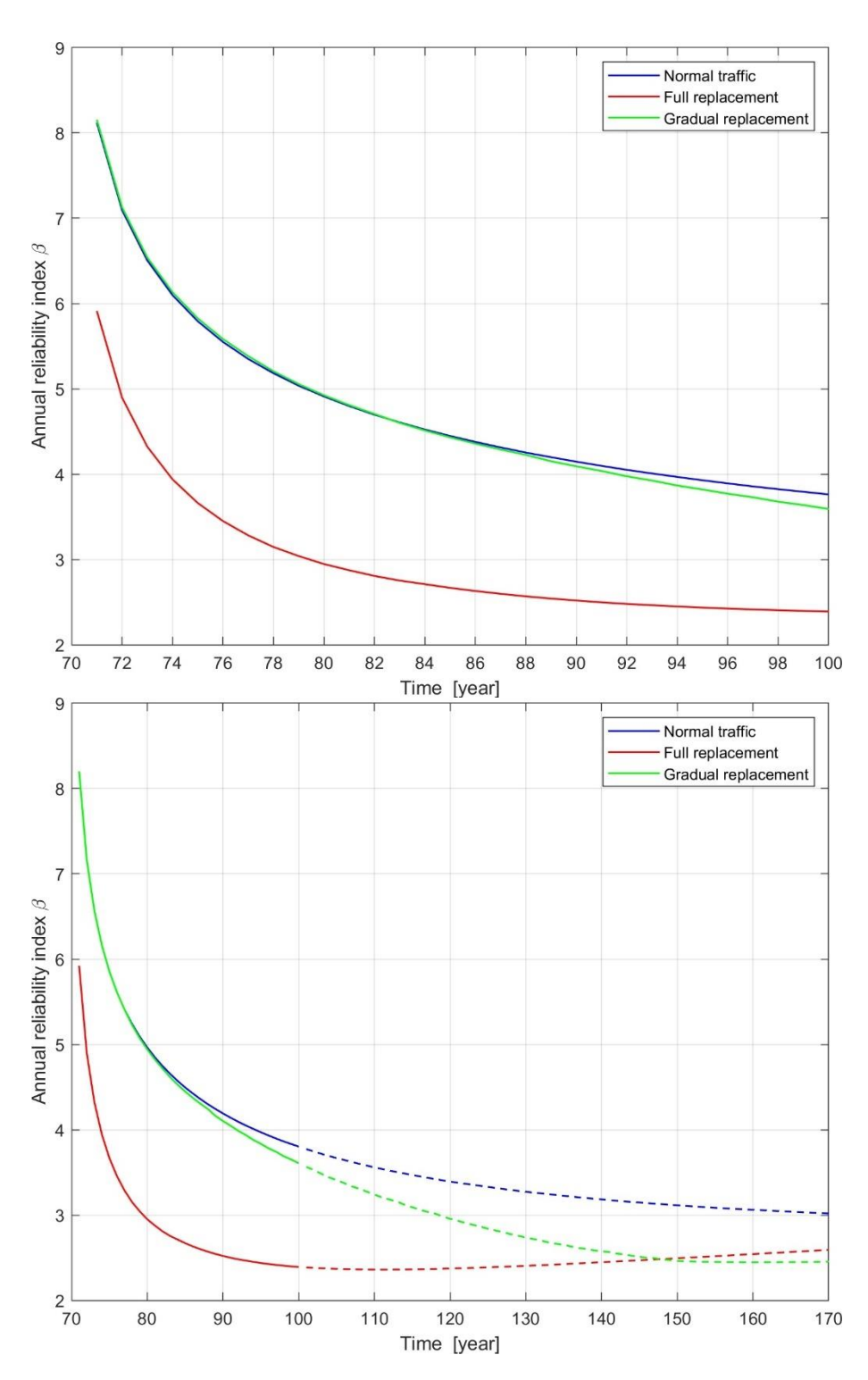


Figure 241: Annual reliability for the existing structure (L = 100 m) with elapsed service life 70 years with normal traffic conditions (blue) and full replacement with SEC (red).